DNA interaction and catalytic activity studies of some new transition metal complexes of Schiff bases derived from quinoxaline

Thesis Submitted to

Cochin University of Science and Technology

in partial fulfillment of the requirements

for the award of the degree of

Doctor of Philosophy

in

Chemistry

by

LEEJU P

DEPARTMENT OF APPLIED CHEMISTRY

COCHIN UNIVERSITY OF SCIENCE AND TECHNOLOGY

Kochi – 22

April 2011

Dedicated to

Kukoo…

Department of Applied Chemistry
Cochin University of Science and Technology
Kochi – 22

Certificate

This is to certify that the thesis entitled "**DNA interaction and catalytic activity studies of some new transition metal complexes of Schiff bases derived from quinoxaline"** is an authentic record of research work carried out by Ms. Leeju P under my supervision, in partial fulfillment of the requirements for the degree of Doctor of Philosophy in Chemistry from Department of Applied Chemistry, Cochin University of Science and Technology, and further that no part thereof has been presented before for any other degree.

Dr. K. K. Mohammed Yusuff
(Supervising guide)

Kochi-22
12th April, 2011

Declaration

I hereby declare that the work presented in this thesis entitled **"DNA interaction and catalytic activity studies of some new transition metal complexes of Schiff bases derived from quinoxaline"** is entirely original and was carried out by me independently under the supervision of **Dr. K. K. Mohammed Yusuff** (Emeritus Professor, Department of Applied Chemistry, Cochin University of Science and Technology) and has not been included in any other thesis submitted previously for the award of any degree.

Kochi -22 **Leeju P**

12th April, 2011

Acknowledgement

I am grateful to so many people who extended their help, in their own ways, for this research to be conducted. I extend my sincere gratitude to Prof. Dr. Mohammed Yusuff who provided me an opportunity to work in his group. I am thankful for his helpful discussions, his teaching skills and above all his endless fascination for chemistry. His guidance helped me at all moments of research and also in writing of this thesis. His truly scientific intuition has made him as a constant oasis of ideas. His passion for science exceptionally inspired and enriched my growth as a student, a researcher and would be a scientist. I am indebted to him in more than one way, more than what he is aware of.

I would like to express my deep gratitude and heartfelt thanks to Prof. Dr. K. Sreekumar, Head of the Department of Applied Chemistry and also former heads of the Department Prof. Dr. M. R.Prathapachandra Kurup and Prof. Dr.K.Girish Kumar for providing me the necessary facilities.

I am indebted to the help and practical advice offered by the faculty members, Dr. S. Sugunan, Dr. S. Prathapan, Dr. N. Manoj, Dr. P. V. Mohanan, Dr. P. A. Unnikrishnan, and Ms. P. M. Sabura Begum of this department.

I wish to express my warm and sincere thanks to Prof. Dr. Athappan, who gave me the opportunity to work with his group in the Department of Chemistry, Madurai Kamaraj University. I am grateful to Dr. Sarita Butt, (Department of Biotechnology, CUSAT) for her extensive discussions about my work and interesting suggestions in these studies which have been very helpful. I also wish to thank. Dr. Laksmi (Regional Cancer Centre, Thiruvanandapuram) for her kind support in my studies.

I am also grateful to my friends for having made the lab feel like a home. It was a wonderful feeling and i would like to specially thank Dr. Arun, who motivated

me to work in this speciality and also for his quiet and reassuring attitude, Dr. P. P Robinson, Dr. Annu Anna Varghese and Dr. Rani Ebraham, for clarifying the doubts. Special thanks to Dr. Manju Sebastian, Ms. G. Varsha and Ms. Digna Varghese for their immense support at different stages of my work. I recall with gratitude the critical suggestions and kind advice by the late Dr. Jose Matew. My special thanks to Mr.D. Gopinath for his interesting suggestions in the studies and Mr. Binoop (Indu photos, Kalamassery) for formatting the thesis.

I am greatly indebted to Mr. Rajasekaran and Mr. Prabhakaran (M.K.U), Ms. Helvin (Biotechnology, CUSAT) for their help while doing DNA studies. My Sincere thanks to all research scholars of this department especially Miss. Reni and Ms. Rose Philo for the friendship offered to me. I am thankful to Department of Science and technology, India for providing the instrumental facilities of Sophisticated Analytical Instrument Facility (SAIF) at the Sophisticated Analytical Instrumentation centre (STIC), Cochin University of Science and Technology, Cochin and IIT, Mumbai for the help in sample analyses. Many thanks for financial assistance from Cochin University whose support made this research possible.

But most of all, I would like to thank those whom I deeply love, respect and admire, and whom I am dedicating this thesis to my family, My parents, for the ease and beauty of their character, their solid trust and patience, and for the most precious thing they have given me their unconditional love. My sister and her family, for all good vibes and positive energy. My darling daughter Pooja, who never troubled me and seemed to understand that I was doing some serious work. Above all my hubby, for having held my hand throughout this journey over the past six years.

Above all my gratitude is due to God, who continues to look after me despite my flaws.

Leeju P

Preface

DNA is the primary target for many anticancer drugs. Thus the design of new anticancer drugs is based on the modification of DNA. A number of transition metal complexes especially those of platinum, palladium and copper are known to modify DNA structure and find application as chemotherapeutic drugs which regulate gene expression. Furthermore the presence of heterocyclic rings in the complexes facilitates them to bind with DNA through groove binding or intercalation. The complexes with this type of binding are known to be more active chemotherapeutic agents.

In this thesis we report the synthesis and characterisation of new transition metal complexes of Pd(II), Cu(II), Ru(III) and Ir(III) of Schiff bases derived from quinoxaline-2-carboxaldehyde/3-hydroxyquinoxaline-2-carboxaldehyde and 5-aminoindazole, 6-aminoindazole or 8-aminoquinoline. The complexes have been characterised by spectral and analytical data. Pd(II) and Cu(II) form square planar complexes and Ru(III) and Ir(III) form octahedral complexes with these Schiff bases.

The DNA binding properties of these synthesised complexes have been studied by various methods including electronic absorption spectroscopy, cyclic voltammetry, differential pulse voltammetry and circular dichroism spectra were used. Gel electrophoresis experiments were also performed to investigate the DNA cleavage of these complexes. Furthermore Ru(III) and Ir(III) complexes find application as oxidation and hydrogenation catalysts. The studies on catalytic activities has been presented. The metal complexes presented in this thesis assure significance as they contribute to the development of new DNA binding agents and antibacterial and anticancer drugs.

CONTENTS

.....ꕥ.....

Chapter 1

Introduction

Contents

Metal complexes play important and diversified roles in biological systems. The role of chlorophyll, haemoglobin, carbonic anhydrase, vitamin B_{12}, xanthine oxidase, and haemocyanin illustrates the intimate linkage between inorganic chemistry and biology. Studies of these types of metal complexes are now part of the highly expanding field, bio-inorganic chemistry.

Metal complexes find interesting applications not only in the field of biology, but also in a variety of fields like catalysis and medicine. The use of inorganic substance in medicine has its origin from the time of Hippocrates. He recommended the medicinal use of metallic salts. However, the logical bases for understanding the role of inorganic species in medicine have been established only after the advances in the field of bio-inorganic chemistry.

Metal complexes have been used as diagnostic and therapeutic agents. Studies on metal based anticancer drugs and antiarthritic agents are some currently active topics of investigation in bio-inorganic chemistry. Many metal complexes, especially those of Schiff bases, have been studied from the point of view of using them as antibacterial and anticancer drugs. In this

chapter a discussion of the Schiff bases, their metal complexes and their general application is presented.

1.1 Schiff base ligands

Schiff bases are important class of ligands due to their synthetic flexibility, their selectivity and sensitivity towards the central metal atom, structural similarities with natural biological substances. Schiff base ligands are considered as 'privileged ligands'(1) containing azomethine group (-HC=N-). They are formed by condensation of a primary amine and carbonyl compound. The azomethine group is particularly suited for binding to metal ions via the N atom lone pair. When the Schiff bases contain one or more donor atoms in addition to –C=N- group they act as polydentate chelating ligands or macrocycles. Both aldehydes and ketones form Schiff bases; however, the formation takes place less readily with ketone than with aldehyde. Because of the versatility of the Schiff bases very large number of complexes with interesting structures are being synthesised even now. Schiff bases derived from aliphatic aldehydes are unstable and are readily polymerizable (2) while those derived from aromatic aldehydes are more stable. The common Schiff bases are crystalline and feebly basic in nature.

Generally Schiff bases are prepared under acid or base catalysis or with heat. When two equivalents of salicylaldehyde are combined with a diamine, a particular chelating Schiff base is produced. The so-called Salen ligands, with four coordinating sites and two axial sites open to ancillary ligands, are very much like porphyrins, but can be more easily prepared. The term Salen was used only to describe the tetradentate Schiff bases derived from ethylenediamine (Figure 1.1). The more general term Salen-type is used in the literature (1) to describe the class of (O, N, N, O) tetradentate bis-Schiff base ligands (Figure 1.2).

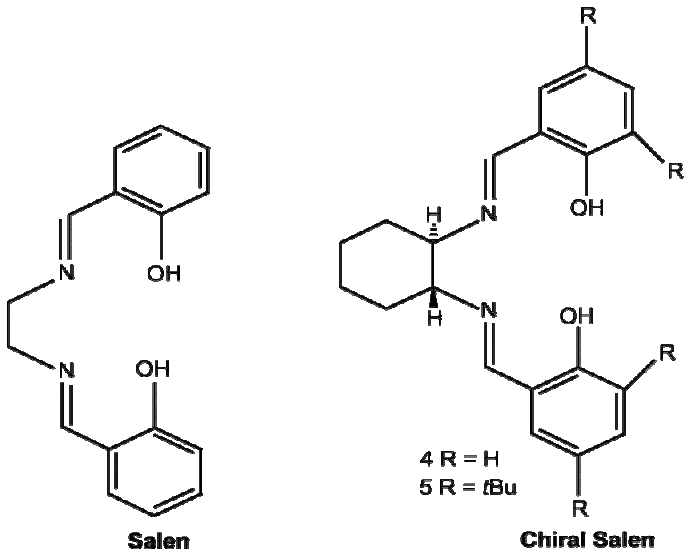

Figure 1.1. Different Salen ligands (Adopted from Ref. 1)

Chiral salen ligands have several attractive features that constitute the basis for their utility in asymmetric reactions. The Salicylaldehyde and the diamine components are synthetically accessible and their condensation to generate the salen ligand generally proceeds in nearly quantitative yield (3)

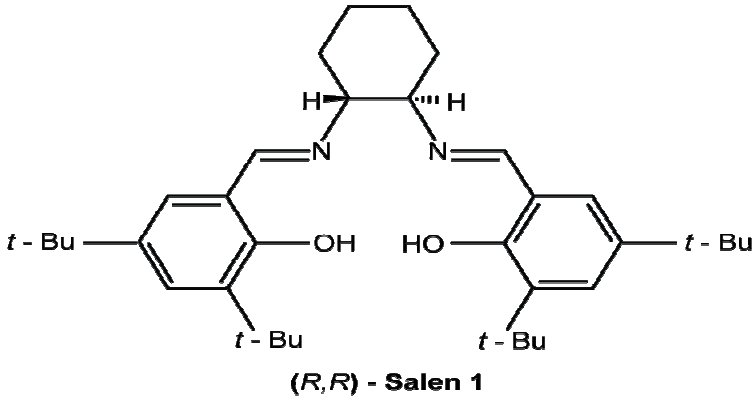

Figure 1.2. Salen Ligand (Adopted from Ref. 1)

Schiff bases have been widely used in many fields, e.g., in biological, inorganic, analytical and in drug synthesis. A large number of Schiff bases and their complexes have been studied for their interesting and important properties, e.g., catalytic activity and transfer of the amino group (4), photochromic behaviour (5)

and complexing ability towards some toxic metals (6). Some Schiff bases (Figure 1.3) are employed as fluorescent indicators by spectrofluorimetric monitoring of small changes of pH (7).

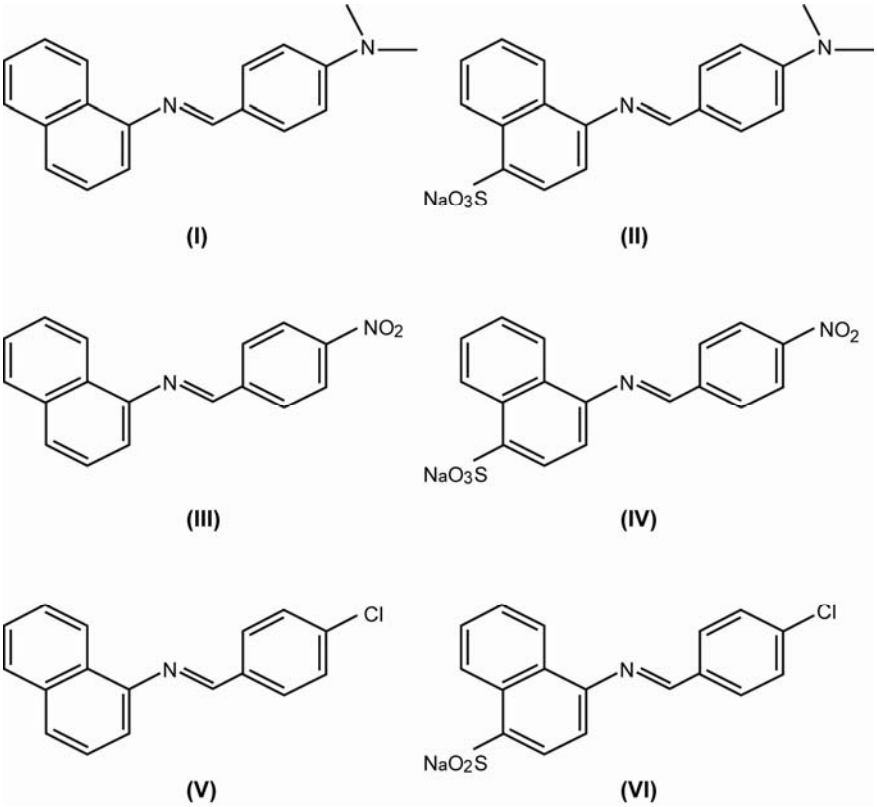

Figure 1.3. Structure of some fluorescent Schiff bases (Adopted from Ref. 7)

1.2 Schiff base metal complexes

Schiff base metal complexes are generally prepared by treating metal halides with Schiff base ligands under suitable experimental conditions. In special cases metal alkoxides, metal amides, metal alkyls or metal acetates have been used for the synthesis. There are numerous literature reviews on the synthesis and characterisation of Schiff base metal complexes (8-11).

Generally transition metal ions are used to prepare coordination complexes, as there is possibility of synthesising a variety of complexes with variable oxidation states, different coordination geometries and interesting physicochemical properties.

A large number of tetradendate Schiff base ligands and tridendate Schiff bases are reported in literature (12-14).

The -OH or -SH groups ortho to the azomethine moiety present in the Schiff bases can induce tautomerism in the compound and give rise to different structures.

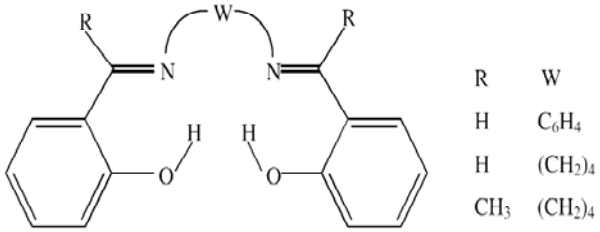

Fgure 1.4. Tetradendate Schiff base (Adopted from Ref. 40)

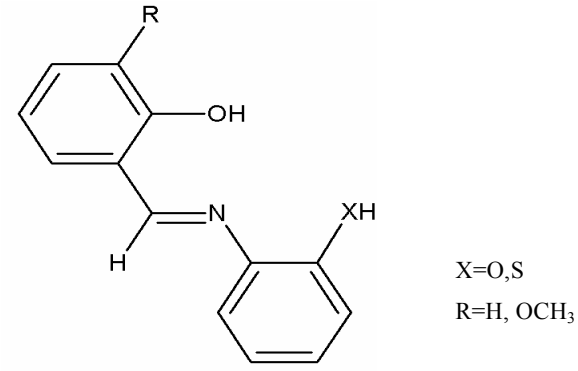

Fgure 1.5. Tridendate Schiff base (Adopted from Ref. 50)

A well known Schiff base complex, N,N'-bis(3,5-di-tert-butylsalicylidene)-1, 2-cyclohexanediaminomanganese(III) chloride, known as Jacobsen's catalyst (15) is used as an asymmetric catalyst in the epoxidation reaction. It can be prepared by separating 1, 2-diaminocyclohexane into its component enantiomers and then reacting with 3,5-di-tert-butyl-2-hydroxybenzaldehyde to form a Schiff base. Jacobsen's catalyst can be prepared from this ligand by treatment with manganese(II) acetate followed by oxidation with air, which may be isolated as the chloro derivative after the addition of lithium chloride.

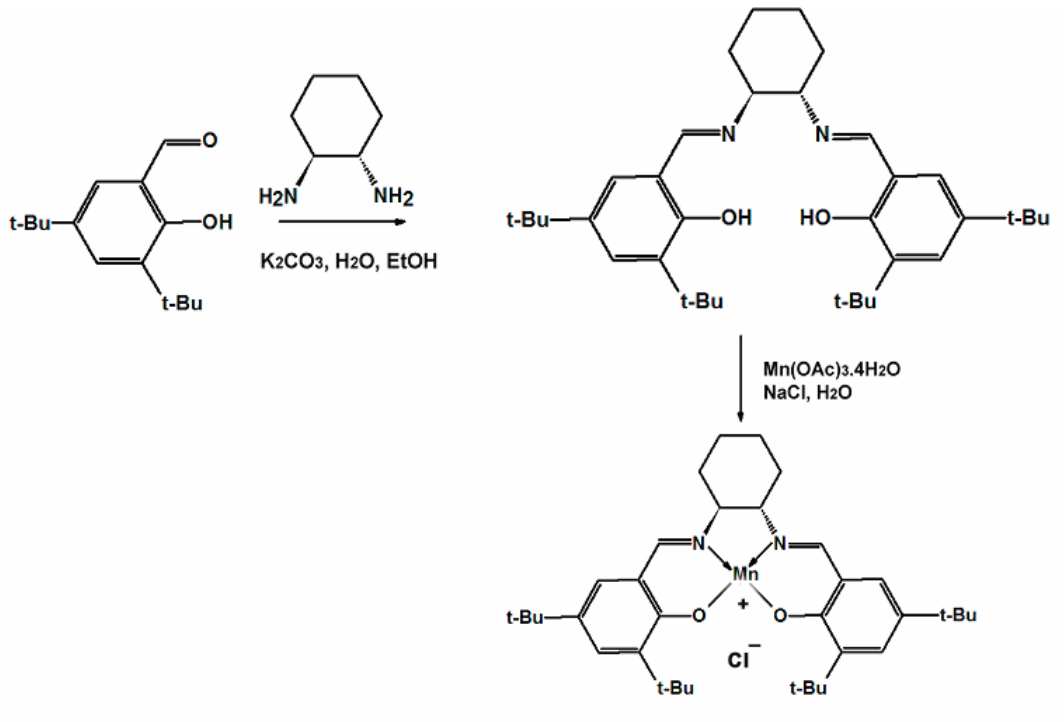

Figure 1.6. Synthesis of Jacobsen's catalyst

1.3 Transition metal complexes of quinoxaline Schiff base

Quinoxalines, also called a benzopyrazines, is a heterocyclic compound containing a ring complex made up of a benzene ring and a pyrazine ring containing two nitrogens in mutually para position. It is isomeric with quinazoline, phthalazine and cinnoline. Quinoxalines are used as dyes, pharmaceuticals and as antibiotics e.g echinomycin, levomycin and actinoleutin. Some studies were carried out in order to explore the antitumoral properties of quinoxaline compounds (16). Quinoxaline and its analogues have been investigated as the ligands for metal complex catalysts (17). These compounds have a wide range of applications in pharmacology, bacteriology and mycology (18-23). Most of the quinoxaline derivatives are synthesised by the condensation of 1,2-diamines with aliphatic or aromatic 1, 2-dicarbonyl compounds or benzilmonoxime using solid acid catalysts (24-27). Symmetrical and unsymmetrical 2, 3-disubstituted quinoxalines are formed by the palladium-catalyzed Suzuki-Miyaura coupling of 2,3-dichloroquinoxaline with various

boronic acids (28). Pyridine-substituted quinoxalines used as good bidentate ligands for the synthesis of metal complexes with Ru or Os (29)

Transition metal complexes of Schiff base formed by the reaction of quinoxaline-2-carboxaldehyde with orthophenylenediamine, o-aminophenol, 2-aminobenzimidazole were synthesised and characterised by Chittilappilly *et al.*(30). Various reports of quinoxaline-2-carboxaldehyde wth diamines show that quinoxaline containing transition metal complexes have lot of applications in different fields.

1.4 Applications of Schiff base metal complexes

Schiff base complexes are more selective in catalysing various reactions, such as hydroxylation, aldol condensation and epoxidation. They are also used as catalysts in various biological systems, polymers and dyes.

1.4.1 Schiff base metal complexes used as catalysts

Schiff base complexes have been widely used in both homogeneous and heterogeneous catalysed reactions and the activity depends on different factors such as nature of ligands, coordination sites and nature of metal ions. Metal complexes with vacant coordination site can act as catalysts for two reasons. Firstly, they can have several oxidation states and can take part in electron transfer reactions. Secondly, they can provide sites at which reactions can take place. This feature gives them a high probability to form the suitable intermediates required for preceding the catalytic reactions. They can show catalytic behaviour when dissolved in solutions or in solid state and act as homogeneous or heterogeneous catalysts. Literature reports reveal that a large number of Schiff base metal complexes exhibit catalytic activities including oxidations, aryl coupling reactions, aminations and carbonylations. The Schiff base complexes of platinum group metals Ru, Rh, Pd, Os, Ir, and Pt, are used for many of these transformations. As our studies are on the oxidation reaction catalysed by

Ru(III) complexes and hydrogenation reaction catalysed by Ir(III) Schiff base complexes, the discussion in the following section is limited to oxidation reaction and hydrogenation reaction.

1.4.1.1 Oxidation reactions

The oxidation of primary and secondary alcohols and hydrocarbons to the corresponding carbonyl compounds plays an important role in organic synthesis (31, 32). The use of oxidants such as *N*-methyl morpholine-*N*-oxide (NMO), hydrogen peroxide and inexpensive green oxidants, such as molecular oxygen or air for converting alcohols to carbonyl compounds on an industrial scale remains an important challenge in the development of industrial processes. The selective oxidation of phenol to catechol and hydroquinones is an industrially useful process and has been carried out using transition metal complexes. The oxidation of phenol in the presence of hydrogen peroxide is normally an activation process but accomplished in presence of transition metal catalysts (33-35).

The accessibility of higher oxidation states of ruthenium makes it as an excellent candidate as catalyst for oxidation reactions. Aerobic oxidation of primary alcohols catalyzed by ruthenium complexes and copper complexes has been reported (36-38). The oxidation of cyclic alcohols such as cyclopentanol, cyclohexanol, cycloheptanol and cyclooctanol to their corresponding ketones were accomplished efficiently up to 84% by the binuclear ruthenium(III) Schiff base complexes (39). Tetradedate Schiff base complexes of Ru have shown to be a good catalyst for oxidation reactions (40-43) (Figure 1.7).

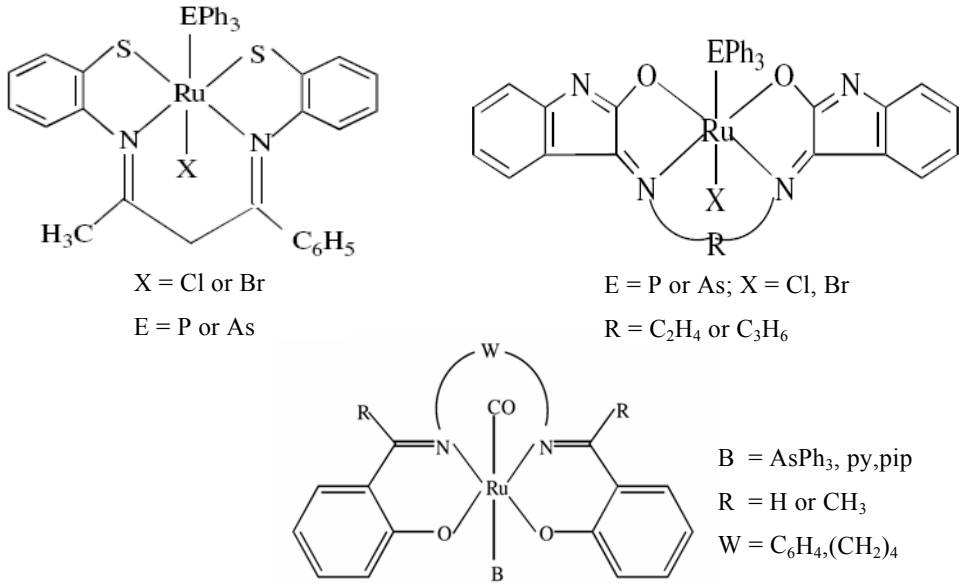

Figure 1.7. Tetradedate Ru(III) Schiff base complexes (Adopted from Ref. 81, 42, 40)

Transition metal complexes of tridentate Schiff base complexes have been successfully used in several catalytic oxidation reactions (44-45) (Figure 1.8).

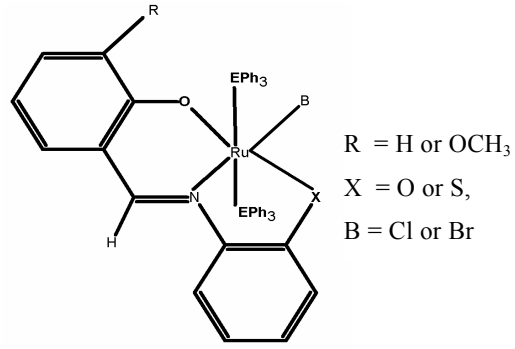

Figure 1.8. Tridentate Schiff base complexes (Adopted from Ref. 50)

Hexa-coordinated ruthenium (III) complexes, $[RuX(EPh_3)_2(L)]$ (where X = Cl or Br; L = dibasic tridentate Schiff base ligand; E = P or As) and $[RuX(EPh_3)(L)]$ **(**where L = dianion of the tetradentate Schiff base) are found to be good catalyst for the oxidation of benzyl alcohol and cyclohexanol in the presence of *N*-methylmorpholine-*N*-oxide (46,47). The relatively higher product yield obtained for the oxidation of benzyl alcohol than that for cyclohexanol was

due to the fact that the α-CH moiety of benzyl alcohol is more acidic than that of cyclohexanol (48). Ruthenium(II) Schiff base complexes containing triphenylphosphine/ triphenylarsine (49-51) and ruthenium(III) Schiff base complexes with bidentate N, O/S donor ligands exhibited catalytic activity for the oxidation of benzyl alchohol to benzaldehyde in presence of NMO (52). The complex $[Ru^{III}(amp)(bipy)(H_2O)]^+$ (where (H_2amp=*N*-(2-hydroxyphenyl) salicyldimine and bipy= 2,2′-bipyridyl) is found to be an effective catalyst in the oxidation of benzene to phenol by using *tert*-butylhydroperoxide (*t*-BuOOH) (53).

Triphenylphosphine complexes and chalconate complexes of Ru have been found to be efficient catalysts for the aerobic oxidation of alcohols (54,55). Ruthenium(III) Schiff base complexes have two N_2O_2 metal binding sites, which are linked to each other with a biphenyl bridge and acts as potential catalyst for oxidation of wide range of primary and secondary alcohols to corresponding aldehydes or ketones with moderate to high conversion in the presence of N-methylmorpholine-N-oxide (NMO) (56) (Figure 1.9).

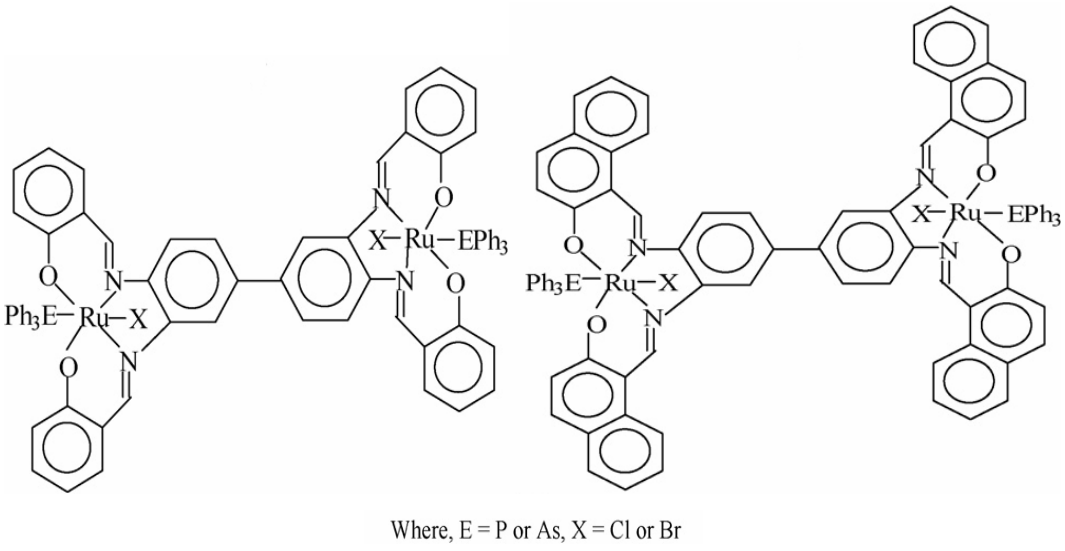

Figure 1.9. Structure of binuclear ruthenium(III) Schiff base complexes (Adopted from Ref. 56)

The complex, [Ru(CO)(EPh_3)(B)(L)] (E = P or As; B= PPh_3, $AsPh_3$, py or pip; L=dianion of the Schiff bases derived from thiosemicarbazone with acetoacetanilide, acetoacet-o-toluidide and o-chloro acetoacetanilide) is reported to have catalytic activity for the oxidation of benzyl alcohol and cyclohexanol in presence of NMO (51). Schiff base complexes of Palladium containing triphenylphosphine was found to be an efficient catalyst for the oxidation of alcohols (57). Schiff base complexes containing palladium was an effective catalyst in the direct oxygenation of unfunctionalized hydrocarbons and phenols (58-61).

Cobalt (II) Schiff base complex shows high catalytic activity for the aerobic oxidation of secondary alcohols to ketones (62). Iron(III) complex with tridentate Schiff base, acetylacetone and N-hydroxyphenyl-salicylideneamine was found to act as a homogeneous catalyst in the oxidation of sulfides (63). Manganese(III) Schiff-base complex act as a catalyst for oxidation of sulfides to sulfoxides using hydrogen peroxide (64).

There have been many attempts to anchor Schiff base metal complexes to polymer supports with a view to have the advantages of heterogeneous catalysts. Polymer-supported Schiff base complexes of metal ions show high catalytic activity in oxidation reactions (65). The polymer-anchored Schiff base complexes of Cu(II), Co(II), Ni(II), Mn(II) and Fe(III) exhibited good catalytic activity for the oxidation of cyclohexene (66).

1.4.1.2 Hydrogenation reaction

Ruthenium-based catalytic systems are found to be effective in the transfer hydrogenation of ketones and imines (67). Although the well known BINAP–Ru(II) complex as catalyst (BINAP = 2,20-bis (diphenylphosphine)-1, 10-binaphthyl) have proved to be extremely efficient for the asymmetric hydrogenation of functionalized ketones, it has been unable to hydrogenate simple ketones that lack hetero atoms anchoring the ruthenium metal (68). A ruthenium(II)

Schiff base complex system containing diphosphine and 1,2-diamine ligands in the presence of a base and 2-propanol was proved to be an efficient catalyst for the hydrogenation of ketones under mild conditions (69) Ru(II) Schiff base complexes were also found to act catalysts for the reduction of benzene (70).

The complex $[RuX(EPh_3)(L)_2]$ (where, E = P or As, X = Cl or Br and L = O, N donor Schiff bases was an efficient catalyst in the transfer hydrogenation of imines to amines (71) (Figure 1.10)

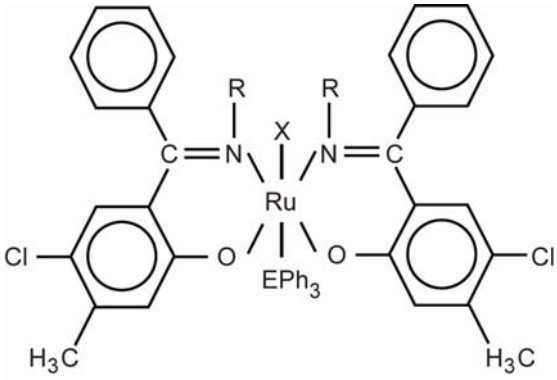

(Where, E=P, As E = P or As; X = Cl or Br; R = C_6H_5)

Figure 1.10. Structure of ruthenium(III) bis-bidentate Schiff base complexes (Adopted from Ref .71)

Mono and dinuclear Pd(II) complexes of Schiff bases having sterically constrained tertiary butyl groups on the salicyl ring exhibit very good catalytic activity towards hydrogenation of nitrobenzene and cyclohexene (72,73) The polymer-supported palladium(II) Schiff base complexes are found to be an efficient catalyst for hydrogenation reactions (74-76). Hydrogenation of a variety of ketones catalyzed by rhodium complexes was also reported (77). Au(III) Schiff base complex was effective for the hydrogenation of 1,3-butadiene into the butenes (78).

1.4.2 Biological Activities

Antimicrobial and antifungal studies of Schiff base ligands and their metal complexes are reported (79-82). The biological activity of Schiff bases either increase or decrease upon chelation with metal ions.

1.4.2.1 Antimicrobial activity

Ruthenium(II) carbonyl complexes of the type [$RuCl(CO)(PPh_3)(B)(L)$] (where B = PPh_3, pyridine, piperidine or morpholine; L= anion of bidentate Schiff bases) exhibit antibacterial activity against *S. aureus* and gram-negative *E. Coli.* (83). Cr(III) and Zn(II) Schiff base complexes containing ethyl2-((1-hydroxynaphthalen-2-yl)methyleneamino)-5,6-dihydro-4H-cyclopenta[b] thiopehene-3-carboxylate are reported to be active against pathogenic strains *Listeria monocytogenes* and *Staphylococcus aureus (84*). Co(II), Ni(II), Cu(II) and Zn(II) complexes of the Schiff base derived from vanillin and DL-α-aminobutyric acid found to exhibit higher antibacterial activity compared to the free Schiff bases (85). Cu, Ni, Fe and Zn Schiff base complexes derived from salicylaldehyde and o-amino benzoic acid shows good antibacterial activity against several pathogenic bacteria, such as *Pseudomonas aeruginosa*, *Proteus vulgaris, Proteus mirabilis, Klebsiella pneumonia* and *Staphylococcus aureus* (86). Zn(II), Cd(II), Ni(II) and Cu(II) complexes of furfurylidene diamine Schiff bases show antibacterial activities (87). N-5 chloro-salicylidiene tauriene Sciff bases and its Cu(II), Ni(II), complexes show antibacterial activities of *Colibacillus* and *Pseudomonas aeruginosa* (88).

Several mono and binuclear transition metal complexes of the Schiff bases derived from phenylaminoaceto hydrazide and dibenzoylmethane shows more potent bactericides and fungicides properties than those of the ligands (89). Platinum (IV) complexes [$Pt(L)_2Cl_2$] [where, L = benzyl-N-thiohydrazide, (benzyl-N-thio)-1, 3-propanediamine, benzaldehyde-benzyl-N-thiohydrazone and salicylaldehyde-benzyl-N-thiohydrazone] show antibacterial activity (90). Pd(II) complexes with N-substituted thiosemicarbazone show anti bacterial activity against *Escherichia coli, Staphylococcus aureus, Pseudomonas aeruginosa* and *Vibrio cholerae* (91). Various metal complexes in II^{nd} and IV^{th} oxidation states of Schiff bases derived from aniline show varying activities with different types of bacteria (92-94).

All the Schiff base ligands in the present study contain quinoxaline ring and quinoxaline compounds are known to have antibacterial proprties. Quinoxaline derivatives are fragments of many biologically active and pharmacologically important compounds, including riboflavin (vitamin B_2**),** flavoenzymes. Quinoxaline ring is a part of a number of synthetic medicines. The well known antibiotics echinomycin, leromycin, actinomycin and triostins are known to inhibit the growth of gram positive bactria and active against various tumours also (95-98). The structure of the quinoxaline ligand is recognized from a great number of natural compounds such as riboflavin and molybdopterines, and can be used as antibacterial, antiviral, anticancer and insecticidal agent (99). In addition, it adopts a planar conformation when chelates to a metal ion (100-102).

1.4.2.2 Antifungal activities

Schiff bases and their metal complexes formed between furan or furyl glycoxal with various amines shows anti fungal activities against *helminthosporium gramineum* (103). Cu(II), Ni(II), Co(II), Mn(II), Zn(II), VO(IV), Hg(II) and Cd(II) complexes of Schiff base derived from acetoacetanilido-4-aminoantipyrine with 2-aminobenzoic acid shows anti fungal activities against *Aspergillus niger, Aspergillus flavus, Rhizopus stolonifer, Candida albicans, Rhizoctonia bataicola and Trichoderma harizanum* (104). Diethylphthalate and benzidin with Cu(II) complex shows anti fungal activity against Aspergillus *niger, A. flavus, Trichoderma harizanum, T. Viridae and Rhizoctonia solani (105***).**

1.4.3 Other applications

The iridium(III) complexes containing 2,3-diphenylquinoxalines are highly efficient and pure-red emitting materials for electrophosphorescent organic light-emitting diodes (106). Organometallic complexes possessing a third-row transition-metal element are crucial for the fabrication of highly efficient organic light-emitting diodes (OLEDs). Schiff base complexes containing Zn(II) are now a days used as electroluminescent materials eg;bis[salicylidene(4-dimethylamino)aniline]zinc(II)

complex exhibits very good light emission and charge transporting performance in organic light emitting diodes (OLEDs).

A novel electroluminescent material, 6,7-dicyano-2,3-di-[4-(2,3,4, 5-tetraphenylphenyl)phenyl]quinoxaline (CPQ), which can be used as a multifunctional material in organic light-emitting diodes (OLEDs) (107) (Figure 1.11).

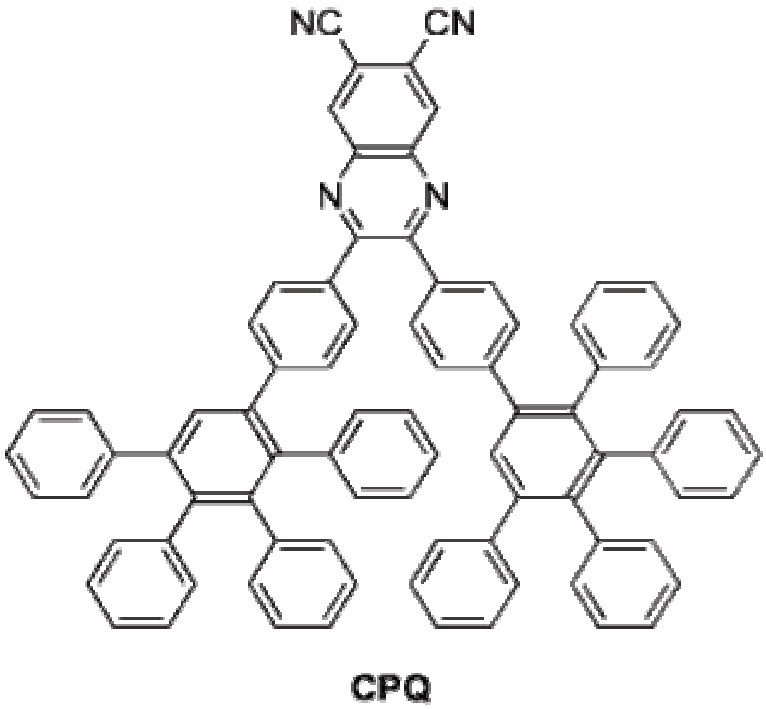

Figure 1.11. Structure of CPQ in OLEDs (Adopted from Ref. 107)

Metal complexes of Schiff bases have wide application in asymmetric epoxidation of unfunctionalised olefins (108,109), used in dye industry (110), antifertility and enzymatic agents (111) and used as catalysts for polymerisation reactions (112).

1.4.4 Antitumor and Cytotoxic activities

Interaction of DNA with transition metal complexes has gained considerable current interest due to its various applications in cancer research and nucleic acid chemistry (113-116). To understand clearly the binding

behaviour DNA with Schiff base metal complexes, a brief description about structure of DNA, nucleic acid and heredity, DNA binding modes and DNA cleavage is given below.

1.4.4.1 Structure of DNA

DNA, or deoxyribonucleic acid, is the hereditary material in humans and almost all other organisms. In a person's body each cell has the same DNA. Most of the DNA molecules located in the cell nucleus are called nuclear DNA but a small amount of DNA can also be found in the mitochondria as mtDNA). The information in DNA is stored as a code made up of four chemical bases: adenine (A), guanine (G), cytosine (C), and thymine (T). Human DNA consists of about 3 billion bases. More than 99 percent of these bases are the same in all people. The most widely accepted model for the structure of DNA molecule was proposed by Watson and Crick in 1953 for which he was awarded the Nobel Prize for Medicine in 1962. According to him the DNA molecule is a double helix (Figure.1.12). The molecule is formed by two antiparallel polynucleotide strands which are spirally coiled round each other in a right-handed helix. The two strands are held together by hydrogen bonds. The double stranded helical molecule has alternated major and minor grooves. Each strand is a long polynucleotide of deoxyribonucleotides. The two strands are complementary to each other with regards to the arrangement of the bases in the two strands. Thus, in the double helix, purines and pyrimidines exist in base pairs, i.e., (A and T) and (G and C). As a result, if the base sequence of one strand of DNA is known, the base sequence of its complementary strand can be easily deduced. The backbone of the strand is formed by alternately arranged deoxyribose sugar and phosphate molecules which are joined by the phosphodiester linkages.

The DNA molecule that Watson and Crick described was in B form. However DNA can exist in other forms also. A, B and C forms have right handed helix while Z form has left handed helix. B is the major form that is found in the cell.

The following table (1.1) summarises the features of the different forms of DNA and figure 1.13 shows different forms of DNA.

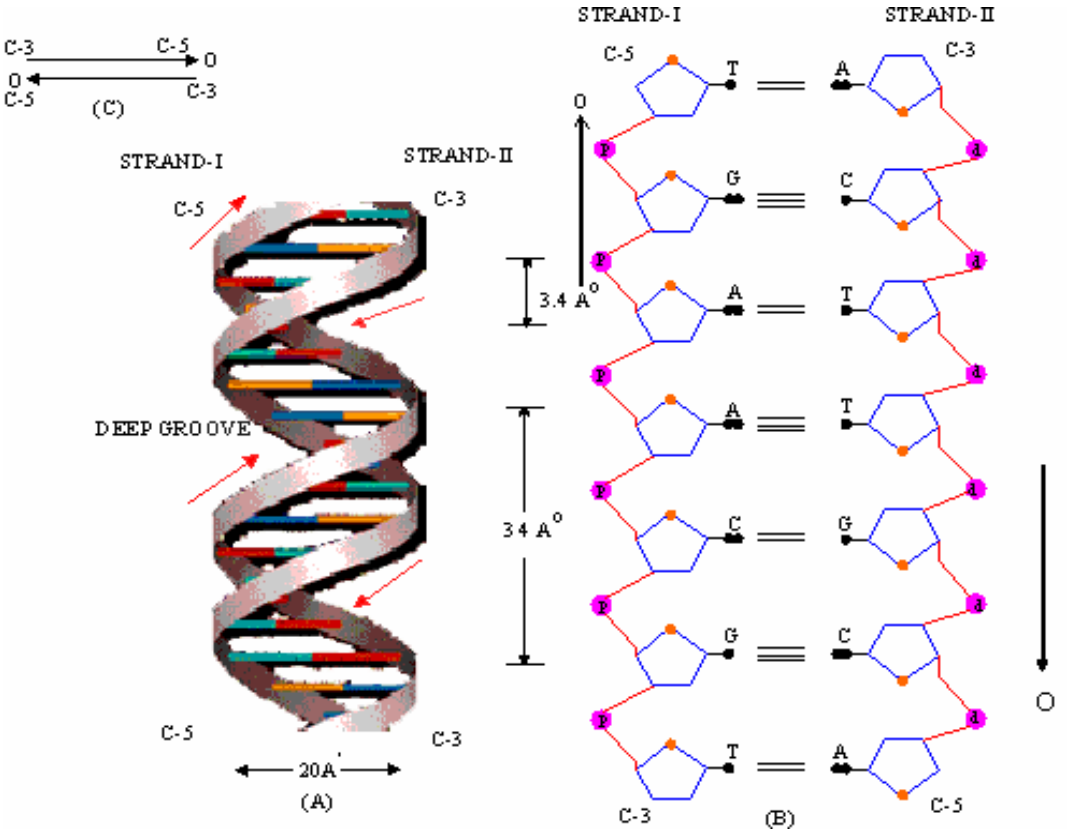

Figure 1.12. Structure of DNA.

Table 1.1. Some features of DNA Forms

Geometry attribute	A-form	B-form	Z-form
Helix sense	right-handed	right-handed	left-handed
Repeating unit	1 bp	1 bp	2 bp
bp/turn	11	10.5	12
Pitch/turn of helix	28.2 Å (2.82 nm)	33.2 Å (3.32 nm)	45.6 Å (4.56 nm)
Diameter	23 Å (2.3 nm)	20 Å (2.0 nm)	18 Å (1.8 nm)

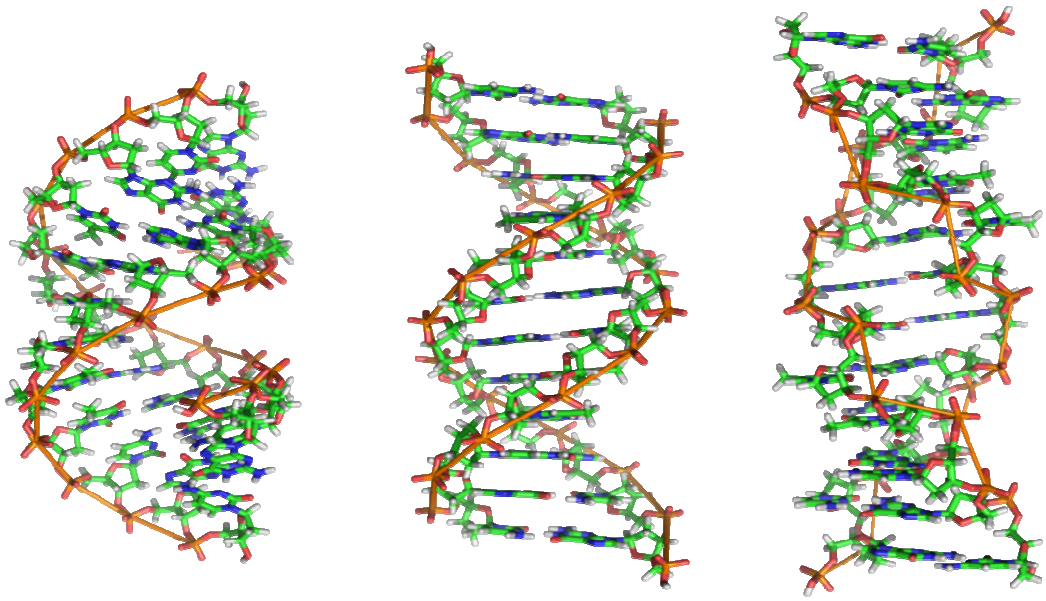

A form **B form** **Z form**

Figure 1.13. Different forms of DNA

1.4.4.2 Nucleic acids and heredity

DNA is the basis for the storage, transmission and expression of genetic-information, any reaction or damage caused to it will have important consequences. An organism's genetic information is stored as a sequence of deoxyribonuleotides stung together in the DNA chain. A mechanism exists for reading the DNA, for decoding the instructions contained therein, and for implementing those instructions to carry out the myriadd biochemical processes to sustain life.

Three fundamental processes take place in the transfer of genetic information:

(a) Replication is the process by which a replica or identical copy of DNA is made so that information can be preserved and handed down to offspring. This occurs when DNA double helix unwinds, complementary deoxyribonucleotidess line up in order, and two new DNA molecules are produced (Fig.16)

(b) Transcription is the process by which the genetic message contained in DNA are read or transcribed and carried out of nucleus to parts of the cells called ribosomes, where protein synthesis occurs. This occurs when a segment of the DNA double helix unwinds and ribonucleotides line up to produce messenger RNA [mRNA]

(c) Translation is the process by wich the genetic messages are decoded and used to build proteins. Each mRNA, which directs protein synthesis, has segments called codons along its chain. These codons are ribonclotide triads that are recognised by small amino acids carrying molecules of transfer RNA [tRNA], which then deliver the appropriate aminoacids needed for protein synthesis.

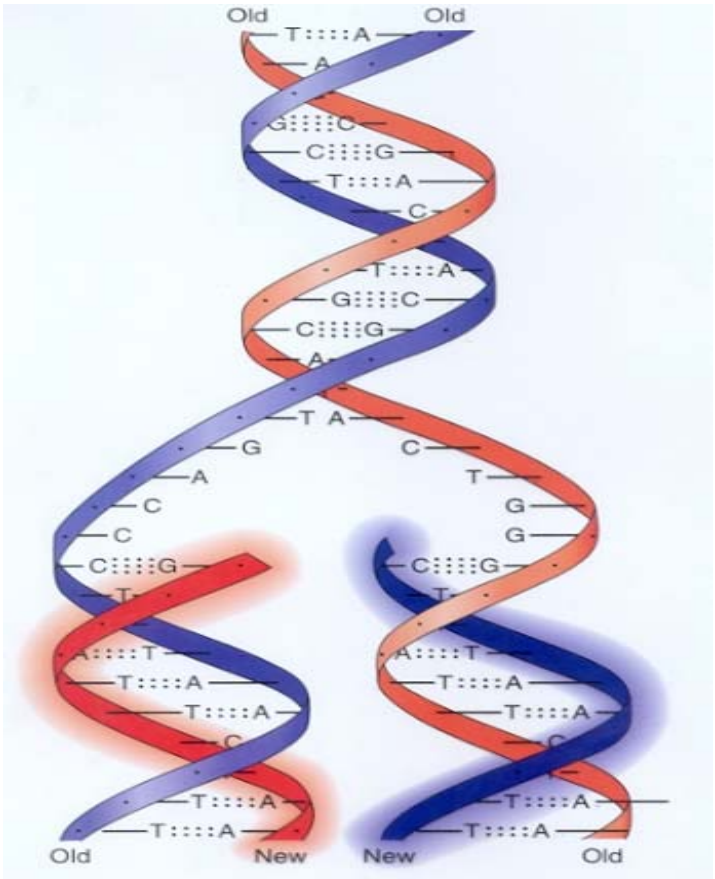

Figure. 1.14. DNA replication

1.4.4.3 DNA Binding Modes

DNA is an important genetic material in organisms and the basis of gene expression. Small molecules can interact with DNA (117-120) through intercalative binding, groove binding, electrostatic binding/external binding (figure 1.15).

Intercalative binding results when small molecules or the drug intercalate into the nonpolar interior of the DNA helix. Aromatic group is stacked between the base pairs in this type of binding and this happens when ligands of an appropriate size and chemical nature fit themselves in between base pairs of DNA. The ligands suitable for intercalation are mostly polycyclic, aromatic, and planar, and therefore often make good nucleic acid stains. There is a current interest in designing and synthesising DNA strand, as these molecules might function as chemotherapeutic agents.

Groove binding interactions involve direct interactions of the bound molecule with edges of base pairs in either of the major (G-C) or minor (A-T) grooves of the nucleic acids. The antibiotic netropsin is a model groove binder in which methyl groups prevents intercalation (121). Binding within the major groove of the double helix is rare for small molecules.

Electrostatic interaction happens in the case of positively charged molecules. They electrostatically interact with the negatively charged phosphates backbone of DNA chain. Electrostatic attraction is generally weak under physiological conditions. Cations such as Mg^{2+} usually interact in this way (122).

The two most common binding modes are intercalation into the base pair stack at the core of the double helix, and insertion into the minor groove. Intercalation is typically observed for cationic molecules having planar aromatic rings. The positive charge need not be part of the ring system, but rather could be on a substituent. This binding mode requires two adjacent base pairs to separate from one another to create a binding pocket for the ligand (123). Minor groove binders, on the other hand, usually have at least limited flexibility since this

allows the molecule to adjust its structure to follow the groove as it twists around the central axis of the helix (124,125). Binding in the minor groove requires substantially less distortion of the DNA compared with intercalative binding. The commonly used methods to provide insight into the binding modes of small molecules are spectroscopy, UV-vis spectroscopy, fluorescence spectroscopy circular dichroism (CD), and linear dichroism (LD).

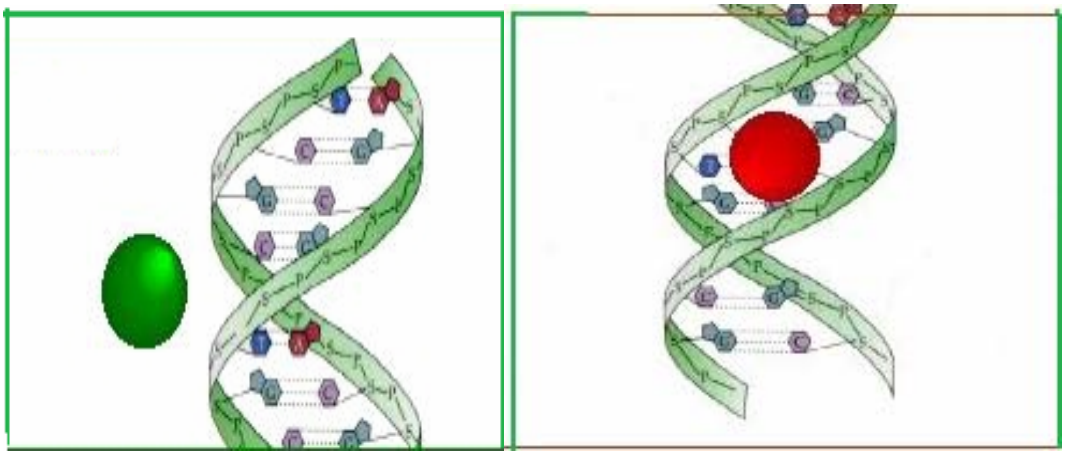

External binding **Groove binding**

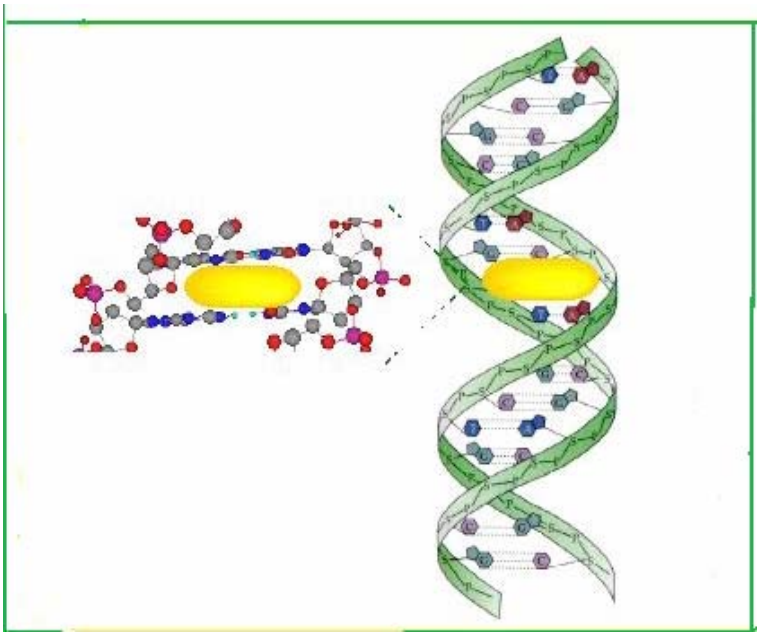

Intercalation

Figure 1.15. Binding modes of DNA

Binding to DNA will often cause a change in the absorption maximum or peak extinction coefficient. But this is insufficient to determine a binding mode, equilibrium binding constants can be determined based on the concentration dependence of any observed shifts. Fluorescent small molecules not only can exhibit changes in wavelength or quantum yield upon binding, but are often able to act as energy acceptors from the DNA bases. In these experiments, the DNA is excited with UV light and one looks for fluorescence from the ligand.

Circular dichroism measures the differential absorption of right- and left-handed circularly polarized light. Circular dichroism (CD) is a useful technique for an assessment of DNA-binding mode. When a ligand is bound to the chiral DNA, CD is induced (126,127). The actual sign and magnitude of the induced CD signal is complicated and depends on the binding mode, DNA sequence, and orientation of the transition dipole of the ligand. However, intercalators will often exhibit lower intensity CD spectra compared with groove binders and this is most likely due to the fact that a groove binder contacts a larger part of the helix, around 4–6 base pairs. In contrast, a simple intercalator only contacts two base pairs.

1.4.4.4 DNA Cleavage

DNA cleavage by metal complexes generally proceeds via two major pathways by oxidative pathway and hydrolytic pathway. The DNA cleavage activity of metal complexes can be targeted towards different constituents of DNA: the heterocyclic bases, deoxyribose sugar moiety and phosphodiester linkage. Oxidative cleavage of DNA takes place in the prescence of additives or photo-induced DNA cleavage. Photo-cleavers require the presence of a photo-sensitizer that can be activated on irradiation with UV or visible light.

Many metal complexes have been studied to understand their capability in the hydrolytic cleavage of DNA which involves hydrolysis of phosphodiester bond. Nucleophilic activation is required for hydrolytic cleavage of phosphodiester bond

due to unusual stability of the diester bond in DNA. Among several types of DNA cleavage reactions, those occurring under photoactivation are of particular importance in highly targeted chemotherapeutic applications. The reagents showing photo induced DNA cleavage have major advantage over chemical nucleases, as the latter requires a reducing agent and/ or H_2O_2 for its activity. The reagents cleaving DNA on photoactvation generally show localised effect as they are otherwise non toxic and such compounds should be useful in the photodynamic therapy (PDT), which has emerged as a promising tool against cancer. The FDA approved PDT drug photophrin, which is a mixture of hematoporphyrin derivatives and is currently used for the treatment of lung and oesophageal cancers.

1.5 Transition metal complexes as chemical probes for DNA

The design of molecules that exhibit strong binding affinity to DNA is a challenging area of research. Such molecules can act as excellent chemotherapeutic reagents that exert their biological activity through interactions with DNA (128-133). Interactions with DNA are not the only the factors that determine the biological activity of these molecules, but their reactivity and selectivity are often correlated with their mode of binding with DNA. Therefore a better understanding of the factors that govern the interactions of small molecules with DNA has an important role in the rational design of various DNA-targeted chemotherapeutic agents and molecular probes for DNA. Of these small molecules, the bifunctional derivatives that can undergo photo induced electron-transfer processes have attracted much attention in recent years for their use in DNA detection, analysis, and cleavage (134-139). Stable and inert complexes containing active metal centres are extremely valuable as probes of biological systems.

Gupta and co-workers reported DNA binding properties of a series of transition metal complexes having potential NNO-tridentate donor Schiff bases

derived from the condensation of 2, 6-dibenzoyl 4-methylphenol with diamines (140-145). Transition metal complexes, copper (146), ruthenium (147,148) and palladium complexes (149) are used now-a-days extensively to study metal complex–DNA interactions.

Pd(II) complexes with benzothiazole-2-thiolate and bipyridyl ligands found to interact with fish sperm DNA through intercalation (150). Tetra nuclear palladium(II) complex $[Pd_4(phen)_4(\mu\text{-}pydc)_4].10H_2O$ where, (phen=1, 10-phenanthroline, pydc = pyridine-3,4-dicarboxylate) binds with FS-DNA in an intercalative way (149). Octahedral polypyridyl ruthenium complexes have excellent DNA binding and DNA cleavage abilities as well as rich photophysical and photochemical propreties (151, 152). Lincoln and Norden studied the DNA binding studies for Ru(II) complexes containing 1, 10-phenanthroline (phen) and 2,2'-bipyridine as ligands (153). Lippard *et al*, established that square planar platinum(II) complexes containing an aromatic heterocyclic ligand could bind DNA by intercalation (154). Platinum(IV) complexes are widely applied in the treatment of various types of cancers such as testicular, ovarian and bladder carcinomas (155-159). Platinum (IV) complexes $[Pt(L)_2Cl_2]$ [where, L=benzyl-N-thiohydrazide, (benzyl-N-thio)-1, 3-propanediamine, benzaldehyde-benzyl-N-thiohydrazone and salicylaldehyde-benzyl-N-thiohydrazone] show cytotoxic activity (160). The Pt complex, [(5,6-dimethyl-1,10-phenanthroline) (1S,2S-diaminocyclohexane) platinum (II)]$^{2+}$ shows cytotoxicity 100-fold greater than that of cisplatin in the L1210 (murine leukemia) cell line (161).

Cu(II) complexes of this Schiff base interact with native calf thymus DNA by groove or intercalating binding mode (162). Binuclear copper(II) complexes having the Schiff base ligand, N,N'-bis(3,5-tert-butylsalicylidene-2- hydroxy)-1, 3-propanediamine, are found to be effective in the cleavage of plasmid DNA in the presence of hydrogen peroxide at pH = 7.2 and 37 °C. Cu(II) Schiff base

complexes derived from diethylenetriamine and 2-thiophene-carboxaldehyde/2-furaldehyde/2-pyrrole-2-carboxaldehyde are reported to interact with DNA through a simple mode of coordination (163). Some copper complexes of the Schiff base formed between benzaldehyde and alanine have shown the ability to suppress superoxide anion free radicals (O_2^-) which may cause inflammation or cancer in humans (164). Copper(II) complex of Schiff bases synthesised from salycylaldehyde,2,4dihydroxy-benzaldehyde and glycine possess antitumor activity (165). Complete cleavage of double stranded pUC19 DNA by the Cu(II) complex, $[Cu(dpq)_2(H_2O)](ClO_4)_2$ (where dpq= dipyridoquinoxaline) reported by Shanta Dhar *et al.*(166).

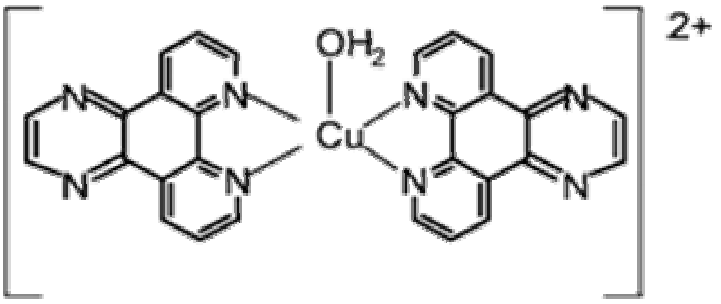

Figure 1.16. Cu(II) complex for the cleavage of pUC19 DNA (Adopted from Ref. 166)

Chromium(III) complexes derived from chiral binaphthyl Schiff base ligands (R- and S-2,2'-bis (salicylideneamino)1, 10-binaphthyl) are also interact with CT-DNA through groove binding (167). The interaction of chromium(III) Schiff base complexes, $[Cr(salen)(H_2O)_2]^+$ where salen = N,N'-ethylenebis (salicylideneimine) and $[Cr(salprn)(H_2O)_2]^+$ where salprn = N,N'- ropylenebis(salicylideneimine) with calf thymus DNA (CT-DNA) has been reported (168). 5-triethyl ammonium methyl salicylidene ortho-phenylendiimine ligand with Ni(II) strongly interacts with DNA (169). Various metal complexs of dppz, $[Co(phen)(qdppz)]^{3+}$ and $[Ni(phen)qdppz]^{2+}$ were found to be good intercalators of DNA due to the extensively π-conjugated and planar structure of this novel ligand (170). The cobalt(II) and nickel(II) complexes of salicylaldehyde-2-phenylquinoline-4-

carboylhydrazone interact with calf-thymus DNA through groove binding (171). The interaction between [Fe(salen)]Cl and calf thymus DNA through an electrostatic binding between the $Fe(Salen)^{+}$ cation and the phosphate groups of DNA (172). The Mn(II) complex, MnL (L=sodium(E)-3-(1-carboxyethylimino)methyl)-4-hydroxybenzenesulfonate), is also capable of intercalating into the double-stranded salmon sperm DNA (173).

1.6 Objectives and scope of the present work

The metal complexes of Schiff bases find interesting application in medicine, material science and catalysis. Hence there is a continuing interest in the synthesis of new Schiff bases and their complexes. It was therefore considered worthwhile to synthesise some new complexes of Schiff bases and study their physicochemical properties and application as oxidation catalyst hydrogenation catalyst and DNA cleaving agents.

The work presented in this thesis is mainly concerned with metal complexes of Schiff bases containing quinoxaline ring. These Schiff bases with an electron withdrawing heterocyclic system would be interesting, as their ligand field strengths are expected to be weaker than the Schiff bases derived from salycylaldehyde. Further the complexes of these ligands are expected to behave quite differently from the salen complexes in catalytic and DNA cleaving properties. Further it was expected that complexes containing heterocyclic ring, quinoxaline, quinoline and indazole could bind DNA by intercalation and might be more effective towards DNA cleavage. Most of the complexes reported efficiently for DNA cleaving were those of palladium(II) and copper(II). Therefore the complexes of Pd(II) and copper(II) were synthesised to study DNA cleaving properties. Ru(III) and Ir(III) complexes find application in catalysis, and therefore the complexes of these metals were also synthesised. Thus the work presented in this thesis was carried out with the following objectives

- To synthesise Schiff bases which contain heterocyclic rings and are capable of having electronic properties in their complexes different from those of salen ligand.
- To study the nature of coordination of such Schiff bases with metal ions like Pd(II), Cu(II), Ir(III) and Ru(III)
- To study the DNA binding and cleaving ability the complexes, particularly those of Pd(II) and Ir(III).
- To undertake a qualitative study of activity of the complexes as catalysts in oxidation and hydrogenation reaction.

The following ligands were selected for the study

a) quinoxaline-2-carboxalidine-5-aminoindazole (qc5in)

b) quinoxaline-2-carboxalidine-6-aminoindazole (qc6in)

c) 3-hydroxy-quinoxaline-2-carboxalidene-5-aminoindazole (hqc5in)

d) 3-hydroxy -quinoxaline-2-carboxalidene-6-aminoindazole (hqc6in)

e) 3-hydroxyquinoxaline-2-carboxalidine-8-aminoquinolidene (hqaqn)

New complexes of Pd(II), Ru(III), Ir(III) and Cu(II) with the above mentioned ligands were synthesised and characterised. Further their DNA binding and cleaving abilility and catalytic activity of the complexes in a typical oxidation and hydrogenation reaction were also studied. Details of these studies are embodied in this thesis.

1.7 References

[1] P. G. Cozzi, *Chem . Soc. Rev*, 33 (2004) 410

[2] Z. Li, K.R. Conser, E.N. Jacobsen, *J. Am. Chem. Soc*. 115 (1993) 5326.

[3] J. F. Larrow. E. N. Jacobsen, *Topics Organomet Chem.* 6 (2004) 123

[4] G.H. Olie, S. Olive, Springer, Berlin, 152 (1984).

[5] H. Dugas, C. Penney, *Bioorganic Chemistry*, Springer, New York, 435 (1981).

[6] K. Sancak, Mustafa. U. Yasemin, M. Yildirim, I. Degirmencioglu, *Transition Metal Chemistry* 32 (2007) 16.

[7] M.N. Ibrahim, S.E. A. Sharif, *E-Journal of Chemistry* 4 (2007) 531.

[8] P.G Cozzi. *Chemical Society Reviews* 33 (2004) 410.

[9] M. Kojima, H. Taguchi, M. Tsuchimoto, K. Nakajima. *Coordination Chemistry Reviews* 237 (2003) 183.

[10] A. Syamal, M.R. Maurya. *Coordination Chemistry Reviews* 95 (1989) 183.

[11] J. Costamagna, J. Vargas, R. Latorre, A. Alvarado, G. Mena. *Coordination Chemistry Reviews* 119 (1992) 67.

[12] P.A. Vigato, S.Tamburini, *Coord.Chem.Rev*. 248(2004)1717.

[13] A.A. Solimann,W. Linert, *Montash. Chem*. 138(2007) 175.

[14] E. Kim, E.E. Chufan, K. Kamraj, K.D. Karlin, *Chem.Rev*. 104 (2004) 1077.

[15] J.F. Larrow, E.N. Jacobsen, Org. *Synth*. 75 (1999) 1.

[16] J. Renault, M. Baron, P. Mailliet, *Eur. J. Med. Chem*, 16, 6 (1981) 545.

[17] X. Wu, A. E. V. Gorden. *J. Org. Chem.* 72 (2007) 8691.

[18] K.J. Schmidt, I. Hammann, Brit. Pat. 1, 60; *Chem. Abst*. 71 (1969), 113084Q.

[19] M.L. Davis, U.S. Pat. No. 3,852,443*; Chem. Abst*. 83 (1975), 48193.

[20] T. Nagishi, K. Tanaka, and H. Hikoya, *Chem. Pharm. Bull*, 28 (1980), 1347.

[21] T. Jerzy, J. Leon, Med. Dosw. *Mikrobiol*., 32 (1980), 221.

[22] F. Fabiopaul, S.A. Lang, Y. Lin, T. Cufcik and S. Andrew, *J. Med. Chem*, 23 (1980) 201.

[23] O. M. Junja, S. Sasamat, *J. Med. Chem*. 39 (1996) 3971.

[24] S. Ahmad, M. Ali. *Chinese Journal of Chemistry*, 25 (2007) 818.

[25] D.J. Brown, volume 61, John Wiley& Sons, Inc., Hoboken, New Jersey (2004).

[26] E. C. Taylor, Wipf, P., Eds.; John Wiley and Sons: New Jersey (2004).

[27] A.E.A. Porter, A.R. Katritsky, C.W. Rees, Eds.;Pergamon: Oxford, (1984)157.

[28] L. Mao, H. Sakurai, T Hirao. Synthesis, 15 (2004) 2535.

[29] M.A. Baldo, D.F. OBrien, Y. You, A. Shoustikov, S. Sibley, M.E. Thompson, S.R. Forrest, *Nature* 395 (1998) 151.

[30] P.S. Chitilappilly, K.K.M. Yusuff, *Indian Journal of Chemistry,* 47A (2008) 848.

[31] A. Dijksman, I.W.C.E. Arends, R.H. Sheldon, *Chem. Commun*. (1999)1591.

[32] R .I. Kureshy, N.H. Khan, S.H.R. Abdi, S.T. Patel, P. Iyer, J. Mol. 150 (1999) 175.

[33] S.Lin, Y.zhen, S.M.Wang, Y.M. Dai, *J.Mol.Catal.A* Chem.156 (2000)113.

[34] J.B. Berna, A.pazari, *J.Org.Chem.* 65 (2000) 2344.

[35] W.Adam,W.A.Hermann, *J.Org.Chem.* 39 (1994) 8281.

[36] D. Das, C.P. Cheng, *J. Chem. Soc., Dalton Trans*. (2000) 1081.

[37] W.K. Wong, X.P. Chen, J.P. Guo, Y.G. Chi, W.X. Pan, W.Y. Wong, *J. Chem. Soc., Dalton Trans*. (2002) 1139.

[38] J.W. Tsai, Y.H. Liu, S.M. Peng, S.T. Liu, *J. Organomet.* Chem. 690 (2005) 441.

[39] G. Venkatachalam, N. Raja, D. Pandiarajan, R. Ramesh, *Spectrochimica Acta Part A* 71 (2008) 884.

[40] R. Karvembu, K. Natarajan, *Inorganic Chemistry Communications* 6 (2003) 486.

[41] T. D. Thangadurai, K. Natarajan, *Transition Metal Chemistry* 25: (2000) 347.

[42] R. Ramesh, *Inorganic Chemistry Communications* 7 (2004) 274

[43] R. Prabhakaran, R. Huang, K. Natarajan, *Inorganica Chimica Acta* 359 (2006) 1114.

[44] G. Das, R. Shukla, S. Mandal, R. Singh, P.K. Bharadwaj, J.V. Hall, K.H. Whitmire, *Inorg. Chem*. 36 (1997) 323.

[45] D.J. Jones, V.C. Gibson, S.M. Green, P.J. Maddox, *Chem. Commun*. (2002) 1038.

[46] R. Prabhakaran, V. Krishnan, K. Pasumpon, D. Sukanya, E. Wendel, C. Jayabalakrishnan, H. Bertagnolli and K. Natarajan1 *Appl. Organometal. Chem.* 20 (2006) 203

[47] S. Manivannan, R. Prabhakaran, K. P. Balasubramanian1, V. Dhanabal, R. Karvembu, V. Chinnusamy and K. Natarajan, *Appl. Organometal. Chem.* 21 (2007) 952.

[48] B.N. Figgis. *Introduction to Ligand Field Theory*. Interscience: New York, 1966.

[49] R. Karvembu, K. Natarajan, *Transition Metal Chemistry* 29 (2004) 644.

[50] S. Priyarega, R. Prabhakaran, K. R. Aranganayagam1, R. Karvembu and K. Natarajan, *Appl. Organometal. Chem.* 21(2007) 788.

[51] P. Balasubramanian, R. Karvembu, R. Prabhakaran, V. Chinnusamy, K. Natarajan, *Spectrochimica Acta Part A 68 (2007) 50.*

[52] K.P. Balasubramanian, K. Parameswari, V. Chinnusamy, R. Prabhakaran, K. Natarajan, *Spectrochimica Acta Part A* 65 (2006) 678.

[53] D. Chatterjee**,** A. Mitra and S.Mukherjee**,** *Journal of Molecular Catalysis,* 165 (2001) 295.

[54] R. Karvembu, K. Natarajan*, Polyhedron* 21 (2002) 219.

[55] M.V. Kaveri, R. Prabhakaran, R. Karvembu, K. Natarajan *Spectrochimica Acta Part A 61 (2005) 2915.*

[56] G. Venkatachalam, N. Raja, D. Pandiarajan, R. Ramesh, *Spectrochimica Acta Part A* 71 (2008) 884.

[57] R. Dileep B.R. Bhat, *Applied Organometallic Chemistry* 24 (9) (2010) 663.

[58] B. Cabezon, A. Sastre, T. Torres, W. Schafer, J.J. Borras-Almenar, E.J. Coronado. *Journal of Chemical Society, Dalton Transactions*, (1995) 2305.

[59] R.C. Matthews, D.K. Howell, W.J. Peng, S.G. Train, W.D. Treleaven, G.G. Stanley, *Angewandte Chemie International Edition in English*, 35 (1996) 2253.

[60] N.O. Komatsuzaki, R. Katoh, Y. Himeda, H. Sugihara, H. Arakawa, K. Kasuga. *Bullettin of Chemical Society Japan*, 76 (2003) 977.

[61] E.K. Beuken, P.W.N.M. Leeuwen, P.H.M. Budzelaar, N. Veldman, A.L. Spek, B.L. Feringa, *Journal of Chemical Society, Dalton Transactions,* (1996) 3561.

[62] V.B Sharma, S.L.Jain, B. Sain, *Journal of Molecular Catalysis A: Chemical* 212 (1-2) (2004) 55.

[63] M. Bagherzadeh, L. Tahsini, R. Latifi, V. Amani, A. Ellern, L. Keith Woo *Inorganic Chemistry Communications* 12 (6), 476

[64] F. Hosseinpoor, H. Golchoubian, *Tetrahedron Letters* 47 (2006) 5195.

[65] K.C. Gupta, A. Kumar Sutar, C.C. Lin, *Coordination Chemistry Reviews* 253 (2009) 13.

[66] S.M. Islam, P. Mondal. K. Tuhina, A.S. Roy, D. Hossain, S. Mondal, *Transition Metal Chemistry* 35 (2010) 891.

[67] V. Cadierno, P. Crochet, J. Diez, J. Garcia-Alvarez, S.E. Garcia-Garrido, S. Gaxcia-Granda, J. Gimeno, M.A. Rodriguez, J. Chem. Soc., Dalton Trans. (2003) 3240.

[68] T. Ohkuma, H. Ooka, S. Harshiguchi, T. Ikariya, R. Noyori, *J. Am. Chem. Soc.* 117 (1995) 2675.

[69] R. Noyori, T. Ohkuma, *Angew. Chem., Int*. Ed. 40 (2001) 40.

[70] V. Arun, N. Sridevi, P.P. Robinson, S. Manju, K.K.M. Yusuff, *Journal of Molecular Catalysis A: Chemical* 304 (2009) 191.

[71] G. Venkatachalam, R. Ramesh, *Inorganic chemistry Communications* 9 (2006) 703.

[72] E. Tas, A. Kilic, M. Durgun, I. Yilmaz, I. Ozdemir, N. Gurbuz. *Journal of Organometallic Chemistry* 694 (2009) 446.

[73] V.T. Kasumov, E. Tas, F. Koksal, S. Ozalp-yaman, *Polyhedron* 24 (2005) 319.

[74] S. Alexander, V. Udayakumar, V. Gayathri, *Journal of Molecular Catalysis A: Chemical* 314 (1-2) (2009) 21.

[75] M.K. Dalal, R.N. Ram, *Studies in Surface Science and Catalysis* 130 D (2000) 3435.

[76] R. Antony, G.L. Tembre, M. Ravindranathan, R.N. Ram, *Journal of Applied Polymer Science* 90 (2003) 370.

[77] Y. Himeda, N. Onozawa-Komatsuzaki, H. Sugihara, H. Arakawa, K. Kasuga, *Journal of Molecular Catalysis A: Chemical* 195 (2003) 95.

[78] F.X. Llabrés i Xamena, A. Corma, *Journal of Catalysis* 265 (2009) 155.

[79] N. Raman, A. Kulandaisamy, K. Jeyasubramanian, *Synth. React. Inorg. Met.-Org. Chem*. 31 (2001) 1249.

[80] K.P. Balasubramanian, K. Parameswari, V. Chinnusamy, R. Prabhakaran,. K. Natarajan*, Spectrochim. Acta Part A* 65 (2006) 678.

[81] R. Prabhakaran, A. Geetha, M. Thilagavathi, R. Karvembu, V. Krishnan, H. Bertagnolli, K. Natarajan, *J. Inorg. Biochem.* 98 (2004) 2131

[82] S. Ren, R.Wang, K.Komatsu, P.Bonaz-Krause, Y. Zyrianov, C.E. McKenna, C.Csipke, Z.A. Tokes, E.J. Lien, *J. Med. Chem*. 45 (2002) 410.

[83] *K.N. Kumar, R. Ramesh, Spectrochimica Acta Part A. 60 (2004) 2913.*

[84] A. Altundas, N. Sarı, N. Colak H. Ogutcu *J. Med Chem Res.* 19 (2010) 576.

[85] M.S. Nair, R.S. Joseyphus. *Spectrochimica Acta Part A*, 70 (2008) 749.

[86] R. Johari, G. Kumar, D. Kumar, S. Singh, J. *Ind. Council Chem*, 26, 1 (2009) 23.

[87] M. Kumar, *Orient J. Chem* 18 (2002) 559.

[88] S. Zhang, Y. Jiang, M. Chen, *Chem Abstr,* 142 (2005) 347.

[89] A.S. El-Tabl, F.A. El-Saied, W. Plass, A.N. Al-Hakimi. *Spectrochimica Acta Part* A, 71 (2008) 90.

[90] A. K. Mishra, S. B. Mishra, N. Manav, D. Saluja, R. Chandra, N. K. Kaushika, *Bioorganic & Medicinal Chemistry* 14 (2006) 6333.

[91] R. Prabhakaran, S.V. Renukadevi, R. Karvembu, R. Huang, J. Mautz, G. Huttner, R. Subashkumar, K. N, *European Journal of Medicinal Chemistry* (2007) 1.

[92] T.D. Bharamagouclar, M.A. Pujar, A.R. Alagawadi, Curr Sci, 56 (1987) 889.

[93] F. Grums, P. Gurkah, Gunduz N, (FABAD) Farm Bilmer Derg,19 (1994) 5.

[94] M.D. Deshmukh, A.G. Doshi, *Orient J Chem*, 11(1995) 86.

[95] M.J. Waring, L.P.G Wakelin. Nature, 252 (1974) 653.

[96] M. J. Waring, L.P.G Wakelin. *Biochemical Journal*, 157 (1976) 721.

[97] A. K. J. Feigon, *Journal of Biochemistry*, 33 (1994) 12397.

[98] C. Bailly, S. Echepare, F. Gago, M. Waring, *Anti-Cancer Drug Design,* 14 (1999) 291.

[99] B. Zarranz, A. Jaso, I. Aldana, and A. Monge, *Bioorganic and Medicinal Chemistry*, 12, 13 (2004) 3711.

[100] Veroni, C. Makedonas, A. Rontoyianni, C. A. Mitsopoulou, *Journal of Organometallic Chemistry*, 691 (2006) 267.

[101] C. A. Mitsopoulou, C. E. Dagas, and C. Makedonas, *Journal of Inorganic Biochemistry*, 102 (2008) 77.

[102] C. A. Mitsopoulou, C. E. Dagas, and C. Makedonas, *Inorganica Chimica Acta*, 361 (2008) 1973.

[103] Dhakrey R and Saxena G, *J. Indian Chem Soc* 64 (1987) 685.

[104] N. Raman, A. Sakthivel, K. Rajasekaran, *Mycobiology* 35 (2007) 150.

[105] N. Raman, S. Parameswari, *Mycobiology* 35 (2007) 65.

[106] K. Tani, H. Fujii, L. Mao, H. Sakurai, T. Hirao. *Bulletin of the Chemical Society of Japan,* 80 (2007) 783.

[107] X. Xu, G.Yu, S. Chen, C. Di, Y. Liu, *J. Mater. Chem*, 18 (2008) 299.

[108] C.M. Che, J.S. Huang, *Coordination Chemistry Reviews,* 242 (2003) 97.

[109] V.R. de Souza, G.S. Nunes, R.C. Rocha, H.E. Toma*, Inorganica Chimica Acta,* 348 (2003) 50.

[110] K. Venkataraman, *Organic pigments, synthetic dyes,* Academic Press, Ins, New York, (1971) 427.

[111] R. Sing, N. Gupta, N. Fahmi, *Indian J Chem.* 38 (1999) 1150.

[112] M.A. Mekewi. *International Journal of Polymeric Materials*, 55 (2006) 219.

[113] H. M. Pinedo, J. M. Schornagel, *Platinum and Other Metal Coordination Compounds in Cancer Chemotherapy 2 (*Plenum Press, New York, 1996).

[114] L. R. Kelland, N. P. Farrell, *The Pathway to Oral Therapy* (Humana Press, Totowa, (2000) 299.

[115] Q.X. Wang, W. Li, F. Gao,S. Li, J. Ni, Z. Zheng, *Polyhedron* 29 (2010) 539.

[116] D.S. Sigman, D.R. Graham, V.D. Aurora, A.M. Stern, *J. Biol. Chem.* 254 (1979) 12269.

[117] W.D. Wilson In: G.M. Blackburn, M.J. Gait (eds) *Nucleic acids in chemistry and biology*. Oxford University Press, Oxford (1996) 329.

[118] J.A. Mountzouris, L.H.Hurley In: S.M. Hecht Ed, *Bioorganic chemistry:nucleic acids.* Oxford University Press, New York, (1996) 288.

[119] J.A. Cowan, *Curr. Opin. Chem. Biol*. 5 **(**2001) 634.

[120] L.N. Ji, X.H. Zou, J.G. Liu, *Coord. Chem. Rev*. 216 (2001) 513.

[121] H. Mei, J. Barton, *J. Am. Chem. Soc*. 108 (1986) 7414.

[122] J. Kelly, A.Tossi, D. McComell, *Nucl. Acids. Res*. 13 (1985) 6017.

[123] L.S. Lerman *J. Mol. Biol* 3 (1961) 18

[124] B.H. Geierstanger, D.E. Wemmer, R. Annu, *Biophys. Biomol. Struct*. 24 (1995) 463.

[125] B. A. Armitage, *Top Curr Chem*. 253 (2005) 55.

[126] R. Lyng, A. Rodger, B. Nordén, *Biopolymers* 31 (1991)1709.

[127] R. Lyng, A. Rodger, B. Nordén, *Biopolymers,* 32 (1992) 1201.

[128] L.S. Lerman,. *J. Mol. Biol.*, *3* (1961) 18.

[129] L. Pecq, J. B. M.L. Bret, J. Barbet, B. Roques, *Proc. Natl. Acad.Sci. U.S.A. 72* (1975) 2915.

[130] M.J. Waring, *Annu. Re*V. *Biochem. 50* (1981) 159.

[131] W.A. Denny, L.P.G. Wakelin,. *Anti-Cancer Drug Des. 5* (1990) 189.

[132] P.R. Reddy, A. Shilpa, *Indian Journal of Chemistry* 49 (2010) 1003.

[133] M. Demeunynck, C. Bailly, W.D. Wilson, Eds.; Wiley-VCH: Weinheim, Germany, *Small Molecule DNA and RNA Binders: From Synthesis to NucleicAcid Complexes*; 1, 2 (2002).

[134] E. Kuruvilla, J. Joseph, D. Ramaiah, *J. Phys. Chem. B*, *109* (2005) 21997.

[135] H. Morrison, Ed.; John Wiley andSons: New York, 1 (1990) 273.

[136] J.E. Rogers, T.P. Le, L.A. Kelly, *Photochem. Photobiol.73 (*2001) 223.

[137] J. Joseph, N.V. Eldho, D.J. Ramaiah, *Phys. Chem. B 107 (*2003) 4444.

[138] J. Joseph, N.V. Eldho, D. Ramaiah, *Chem. Eur. J. 9 (*2003) 5926.

[139] B. Akerman, E. Tuite, *Nucleic Acids Res.24 (*1996) 1080.

[140] S.K. Gupta, D.D. Agarwal, D. Raina. *Indian Journal of Chemistry Section A*: *Inorganic, Bioinorganic,Physical, Theoretical and Analytical Chemistry*, 35A (1996) 995.

[141] S.K. Gupta, D. Raina. Transition Metal Chemistry, 22 (1997) 372.

[142] S.K. Gupta, D. Raina. *Transition Metal Chemistry*, 22 (1997) 225.

[143] S.K. Gupta, K. Jain, Y.S. Kushwah. *Indian Journal of Chemistry Section A: Inorganic, Bioinorganic,Physical, Theoretical and Analytical Chemistry*, 38A (1999) 506.

[144] S.K. Gupta, Y.S. Kushwah. *Polyhedron* 20 (2001) 2019.

[145] S.K. Gupta, P.B. Hitchcock, Y.S. Kushwah, *Journal of Coordination Chemistry*, 55 (2002) 1401.

[146] A. Silvestri, G. Barone, G. Ruisi, D. Anselmo, S. Riela, V.T. Liveri. *Journal of Inorganic Biochemistry* 101 (2007) 841.

[147] Z.H. Xu, F.J. Chen, P.X. Xi, X.H. Liu, Z.Z. Zeng. *Journal of Photochemistry and Photobiology A*: Chemistry 196 (2008) 77.

[148] R. Vijayalakshmi, M. Kanthimathi, V. Subramanian, B.U Nair Biochimica et Biophysica Acta, 1475 (2000) 157.

[149] E.J. Gao, K.H. Wang, M.C. Zhu, L. Liu, *European Journal of Medicinal Chemistry* 45 (2010) 1034

[150] E.J. Gao, K.H. Wang, X.F. Gu, Y.Yu, Y.G. Sun, W.Z. Zhang, H. X Yin, Q. Wu, M.C.Zhu, X. Yan, *Journal of Inorganic Biochemistry* 101 (2007) 1404.

[151] X.H. Zou, B.H. Li, J.G. Liu, Y. Xiong, L.N.Ji,J. *Chem.Soc.,Dalton Trans.* (1999) 1423.

[152] H. Deng, J.W. Cai, H. Xu, Zhang, L.N. Ji, J. *Chem. Soc., Dalton trans,* (2003) 325

[153] P. Lincoln, B. Norden, *J. Phys. Chem*. B. 102 (1998) 9583.

[154] K.W. Jennette, S.J. Lippard, G.A. Vasssilades, W.R. Bauer, *Proc.Narl. Acad.Sci.* U.S.A. 71 (1974) 3839.

[155] Wheate, N. J. Collins, J. G. *Coord. Chem. Rev*.133 (2003) 241.

[156] C. Mqano, A. Treviasan, L. Giovagnini, D. Fregona, *Toxicol. In Vitro* 16 (2002) 413.

[157] B. Rosenberg, L. Van Camp,J.E. Trosko, V.H. Mansour, *Nature* 222 (1969) 385.

[158] L.H. Einhorn, J. Donohue, *J. Am. Intern. Med*. 87 (1977) 293.

[159] R.F. Ozols, R.C. Young, Semin. Oncol. 1984, 11, 251.

[160] A. K. Mishra et al. / *Bioorg. Med. Chem*. 14 (2006) 6333.

[161] Anwen M. Krause-Heuer et al, *J. Med. Chem.* 52 (2009) 5474.

[162] A. Silvestri, G. Barone, G. Ruisi, D. Anselmo, S. Riela, V.T. Liveri, *Journal of Inorganic Biochemistry* 101 (2007) 841.

[163] A.T. Chaviara, E.E. Kioseoglou, A.A. Pantazaki, A.C. Tsipis, P.A. Karipidis, D.A. Kyriakidis, C.A. Bolos. *Journal of Inorganic Biochemistry*, 102 (2008) 1749.

[164] X. Y. He, J. M. Wu, Z. H. Yan. Chinese *J. Inorg. Chem*., 11(1995) 302

[165] P. Lumme, E. Honnu, J. Jubani. *Inorg. Chim. Acta,* 92 (1984) 241

[166] S. Dhar, D. Senapati, P.A.N. Reddy, P. K. Das A.R. Chakravarty *Chem. Commun,* (2003) 2452.

[167] R. Vijayalakshmi, M. Kanthimathi, R. Parthasarathi, B.U. Nair, *Bioorganic and MedicinalChemistry* 14 (2006) 3300.

[168] R. Vijayalakshmi, M. Kanthimathi, V. Subramanian, B.U Nair. *Biochimica et Biophysica Acta,* 1475 (2000) 157.

[169] G. Barone, N. Gambino, A. Ruggirello, A. Silvestri, A. Terenzi, V.T. Liveri. *Journal of Inorganic Biochemistry*, 103 (2009) 731.

[170] C.V. Sastri, D.Eswaramoorthy, L.Giribabu, Bhaskar,G.Maiya, *J. Inorg. Biochem.* 94 (2003) 138.

[171] Z.H. Xu, F.J. Chen, P.X. Xi, X.H. Liu, Z.Z. Zeng. *Journal of Photochemistry and Photobiology A:Chemistry* 196 (2008) 77.

[172] A. Silvestri, G. Barone, G. Ruisi, M.T. Lo Giudice, S. Tumminello. *Journal of Inorganic Biochemistry* 98 (2004) 589.

[173] S. Niu, M. Zhao, R. Ren, S. Zhang. *Journal of Inorganic Biochemistry*, 103 (2009) 43.

.....ൠ.....

Chapter 2

Materials and experimental techniques: Synthesis and characterisation of the aldehydes and ligands:

Contents

2.1 Introduction

This chapter provides details of the reagents used, preparation of the aldehydes, preparation of new Schiff base ligands, various analytical and physico-chemical techniques employed in the characterisation of Schiff bases and their complexes, catalytic activity studies and DNA interaction studies. Procedural details regarding the synthesis of metal complexes are given in appropriate chapters.

2.2 Reagents

The metal salts used for the synthesis of Schiff base complexes are copper(II) chloride dihydrate (Merck), palladium(II) chloride (Sigma Aldrich), ruthenium(III) chloride trihydrate (Sigma Aldrich), iridium(III) chloride trihydrate (Sigma Aldrich).

The amines, 5-aminoindazole, 6-aminoindazole and 8-aminoquinoline were purchased from Sigma Aldrich Chemicals Private Limited, Bangalore. Orthophenylenediamine (Loba Chemie), D-glucose (SD Finechem Limited), sodium sulphate (Merck), sodium metaperiodate (Merck), calcium carbonate (Merck), glacial acetic acid (Qualigens),, hydrazine hydrate (Qualigens), sodium bicarbonate (Sisco Research Laboratories Limited), bromine (Merck) and sodium pyruvate (Sisco Research Laboratories Limited) were used.

Hydrogen peroxide (30 % w/v, Merck), benzene (Sisco Research Laboratories Limited), and 2-ethyl-1-hexanol (Spectrochem Private Limited, Mumbai) were used for the catalytic activity studies. Gas cylinders containing oxygen, nitrogen or hydrogen (Sterling gas Private Limited, Cochin) were used for this purpose.

The important reagents used for DNA binding studies were Tris-HCl buffer, (Tris-hydrochloride (197 mg, 5 mM) purchased from Himedia and sodium chloride (730 mg, 50 mM) were accurately weighed and made up to 250ml solution in a standard measuring flask using double distilled water. The pH of the solution was adjusted to 7.1 using 1mM sodium hydroxide solution with the help of pH meter (Eutech instrument, pH 510) before making up to the mark) Herring sperm DNA (Himedia) and pUC18 DNA (Genie Company, Bangalore). All other reagents were of analytical grade and the solvents employed were either 99% purity or purified by known laboratory procedures (1).

2.3 Synthesis of aldehydes

The aldehydes selected for the synthesis of Schiff bases were quinoxaline-2 -carboxaldehyde and 3-hydroxyquinoxaline-2-carboxaldehyde. The synthetic steps for the preparation of aldehydes are given below.

2.3.1 Synthesis of quinoxaline-2-carboxaldehyde

The following procedure reported by Ohle *et.al* (2) was used to synthesise quinoxaline-2-carboxaldehyde. Treatment of D-glucose (36 g, 0.2 mol) with

orthophenylenediamine (21.6 g, 0.2 mol) in the presence of hydrazine-hydrate (5 mL, 0.1 mol) and acetic acid (6 mL) on a boiling water bath under CO_2 atmosphere (provided by the addition of a pinch of sodium bicarbonate) gave the compound, 2(D-arabinoterahydroxybutyl)quinoxaline. The product was purified by recrystallisation from hot water and the purified compound was oxidised with sodium metaperiodate (13 g, 0.06 mol) in water in the presence of acetic acid at room temperature with controlled stirring for 16 hrs. It was then filtered and the filterate was neutralised with $NaHCO_3$. The neutral solution was then extracted with ether. The ether extract was dried with anhydrous sodium sulphate, filtered and evaporated to dryness. The resulting residue was recrystallized from petroleum ether to give pure quinoxaline-2-carboxaldehyde (figure 2.1) (Yield 60 %, M.P: 107 °C).

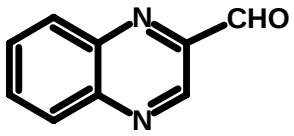

Figure 2.1. Quinoxaline-2-carboxaldehyde

2.3.2 Synthesis of 3-hydroxyquinoxaline-2-carboxaldehyde

3-Hydroxyquinoxaline-2-carboxaldehyde (Figure 2.2) was synthesised by adopting the following procedure (5). This procedure involves preparation of 3-hydroxy-2-dibromomethylquinoxaline form 3-hydroxy-2-methylquinoxaline and its conversion to the aldehyde. 3-Hydroxy-2-methylquinoxaline was prepared by the condensation of pyruvic acid with orthophenylenediamine (3, 4).

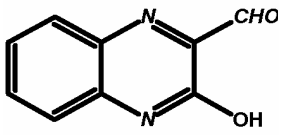

Figure 2.2. 3-hydroxy quinoxaline-2-carboxaldehyde

2.3.2.1 Preparation of 3-hydroxy-2-methylquinoxaline

Separate solutions of orthophenylenediamine (0.1 mol; 10.8 g) and sodium pyruvate (0.1 mol; 11.0 g) in 250 mL distilled water were prepared.

The sodium pyruvate solution was converted to pyruvic acid using concentrated HCl (8 mL). The pyruvic acid solution was taken in a 1 L beaker. To this solution, orthophenylenediamine was added drop by drop with constant stirring. The precipitated pale yellow compound (Scheme 1) was filtered, washed with water and dried over anhydrous calcium chloride. The crude sample was recrystallized from 50% absolute ethanol. (Yield: 90%; Colour: pale yellow. M.P:255 °C)

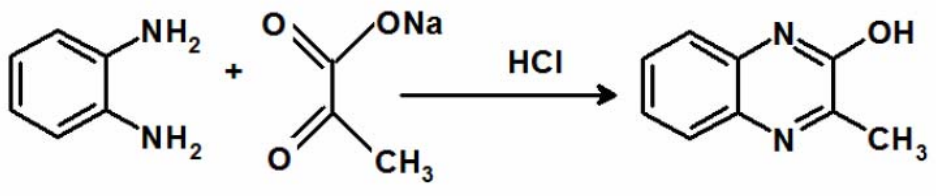

Scheme 1

2.3.2.2 Preparation of 3-hydroxy-2-dibromomethylquinoxaline

To a solution of 3-hydroxy-2-methylquinoxaline (0.1 mol, 16.2 g) in glacial acetic acid (200 mL), 10 % (v/v) bromine in glacial acetic acid (110 mL) was added with stirring. The mixture was then exposed to sunlight for 1 hr with occasional stirring. It was then diluted to 1 L with distilled water and the precipitated dibromo compound (Scheme 2) was filtered, washed with water and dried. The crude product was purified by recrystallisation from 50% absolute ethanol. Yield: 92%; Colour: pale yellow. The compound exhibits no sharp melting point, but decomposes within the range 210-222 °C.

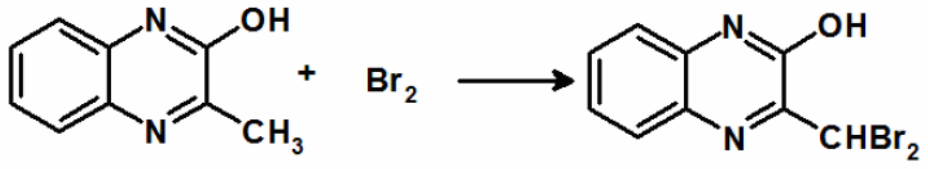

Scheme 2

2.3.2.3 Preparation of 3-hydroxyquinoxaline-2-carboxaldehyde

The dibromo compound (0.0157 mol, 5 g) was thoroughly mixed with precipitated calcium carbonate (20 g) using mortar and pestle. The mixture was

refluxed with distilled water (1.5 L) in a 3 L round bottom flask for 3 hrs with occasional shaking. The aldehyde formed (Scheme 3) remains in the solution and was collected by filtration. The yellow aqueous solution containing the aldehyde is very stable and can be used for the preparation of the Schiff bases.

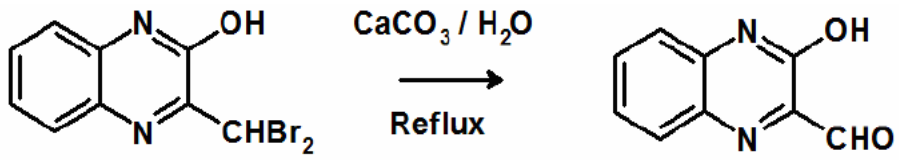

Scheme 3

2.4 Characterisation Techniques

A brief account of the physico-chemical methods employed for the characterization of the Schiff base ligands and their metal complexes and for the catalytic activity and DNA interaction studies is given below.

2.4.1 Elemental analyses

CHN analyses of all the synthesized ligands and compounds were done on an Elementar model Vario EL III CHNS analyser at Sophisticated Analytical Instrument Facility (SAIF) of Sophisticated Test and Instrumentation Centre (STIC), Kochi.

2.4.2 Estimation of metal ions

In all cases, the organic part of the complexes was completely eliminated before the estimation of metal ions. The following procedure was adopted for this purpose in the case of all the complexes. Accurately weighed sample of the metal complex (0.2-0.3 g) was treated with concentrated sulphuric acid (5 mL) followed by Concentrated nitric acid (20 mL). After the reaction subsided, perchloric acid (5 mL, 60 %) was added. The mixture was refluxed until the colour of the solution changes to that of the corresponding metal salt. The clear solution thus obtained was evaporated to dryness. After cooling, concentrated nitric acid was added and evaporated to dryness on a water bath. The residue was dissolved in water and this

neutral solution was used for the estimation of metals. The estimation of metals was carried out on a Thermo Electron Corporation, M series Atomic Absorption Spectrophotometer.

2.4.3 Estimation of Chloride

Chlorine present in the complexes was converted into soluble sodium chloride by the peroxide fusion. An intimate mixture of the complex (0.2 g), sodium carbonate (3 g) and sodium peroxide (2 g) was fused in a nickel crucible for nearly two hours. It was then treated with concentrated nitric acid. Chloride was then volumetrically estimated by Volhard's method (6). Chloride ion was precipitated as silver chloride by the addition of a known volume of standard silver nitrate solution. The excess silver nitrate was then titrated against standard ammonium thiocyanate solution using ferric alum as indicator.

2.4.4 Concentration of DNA

The stock solution of Herring sperm DNA was prepared in Tris-HCl buffer and its concentration was determined from the absorption intensity at 260 nm with a known ε value of 6600 $M^{-1}cm^{-1}$ (7). The Stock solutions were stored at 4 °C and were used within 4 days.

2.4.5 Magnetic susceptibility measurements

The magnetic susceptibility measurements were done at room temperature (28±2) on a simple Gouy type balance. The Gouy tube was standardised using $Hg[Co(SCN)_4]$ as standard as recommended by Figgis and Nyholm (8). The effective magnetic moments were calculated using the equation

$$\mu_{eff} = 2.84(\chi_m T)^{1/2} \text{ B.M.}$$

where T is the absolute temperature and χm is the molar susceptibility corrected for diamagnetism of all the atoms present in the complex using Pascals constants (9-11).

The magnetic susceptibility measurements were done on a Magway MSB Mk1 magnetic susceptibility balance.

2.4.6 Conductivity measurements

The molar conductivities of the complexes in dimethylsulphoxide (DMSO) solutions (10^{-3} M) at room temperature were measured using a direct reading conductivity meter (Systronic conductivity bridge type 305).

2.4.7 NMR spectra

^{1}H NMR spectra were recorded in $CDCl_3$ on a Bruker Avance DRX 300 FT- NMR spectrometer using TMS as the internal standard.

2.4.8 Infrared spectra

Room-temperature FT−IR spectra of the ligands and simple complexes were recorded as KBr pellets with a JASCO-8000 Fourier Transform Infrared Spectrophotometer in the 4000-400 cm^{-1} range.

2.4.9 Cyclic voltammetric studies

Cyclic voltammetric measurements of the all the synthesised ligands, complexes and the complexes after interaction with DNA were carried out on a Bio-Analytical System (BAS) model CV-50 W electrochemical analyser. The three-electrode cell consist of Ag/AgCl as reference electrode, platinum wire as counter electrode and glassy carbon as working electrode with surface area of 0.07 cm^2. Before each experiment, dissolved oxygen was removed by purging the solution with pure nitrogen for about 15 min. The purity of the supporting electrolyte and the solvent was checked by scanning the cyclic voltammogram for the blank solution.

2.4.10 Electronic spectra

Electronic spectra of the ligands and their complexes were recorded in DMSO on a Thermoelectron Nicolet evolution 300 UV-vis spectrophotometer.

Diffuse reflectance spectra of the complexes were recorded at room temperature in a Jasco V 570 UV-Vis spectrophotometer in the wavelength range 200-1800 nm. For the DNA binding studies elecronic spectra were recordrd in DMSO using JASCO V-550 UV-Vis spectrophotometer.

2.4.11 TG/ /DTG

TG- DTG analysis of the complexes were carried out in nitrogen atmosphere at a heating rate of 20 ºC min^{-1} using a Perkin Elmer Pyres Diamond thermogravimetric analyser.

2.4.12 EPR spectra

X-band EPR spectra of the complexes were recorded in DMSO at liquid nitrogen temperature (LNT) at Sophisticated Analytical Instrument Facility (SAIF), IIT, Mumbai. Tetracyanoethylene (TCNE) with a g value of 2.002 was used as the standard.

2.4.13 Gas Chromatography

For hydrogenation reaction the column used was Carbowax and nitrogen was used as the carrier gas. The GC-MS used was Varian 1200 L Single Quadrupole GC-MS at Sophisticated Analytical Instrument Facility (SAIF). The various components in the oxidation reaction were separated using an OV-17 or carbowax column.

2.4.14 Gel Electrophoresis

The cleavage of DNA by metal complexes was studied using agarose gel electrophoresis. To the 5 µl (50 mM) of supercoiled pUC18 plasmid DNA 3µl (3 mmol) of metal complex was added and incubated at 37 °C for 1h. Agarose (1%) gel was melted and prepared in 1X TAE (Tris-acetate-EDTA) buffer. The mixture was poured on to a platform fixed with a comb to form slots. The mould was prepared by sealing the edges of a clean, dry Plexiglas platform with adhesive

tapes. The gel was allowed to set. The comb and the tapes were removed, and immersed in the electrophoresis tank containing 1X TAE buffer. DNA samples were mixed with loading dye (0.25 % bromophenol blue, 0.25 % xylene cyanol, 30 % glycerol) and loaded into the slots of submerged gel and electrophoresis was carried out at 80V for 1hr. The gel was stained with ethidium bromide, (1.0 μg/mL) viewed under UV transilluminator (Bio-Rad UV Transilluminator 2000) and photographed. (12).

2.4.15 Circular Dichroism (CD)

CD spectra of the solutions of the DNA in the absence and presence of complexes at 25 °C were recorded on a JASCO-J-810 (200-900 nm) spectropolarimeter using a quartz cuvette of 1mm optical path length.

2.4.16 Single Crystal XRD

X-ray crystal structure determination was performed with a Bruker SMART APEX CCD X-ray diffractometer at Central Salt & Marine Chemicals Research Institute (CSMCRI), Bhavnagar, Gujrat using graphite monochromated MoKα radiation (λ=0.71073, φ and ω scans). The data was reduced using SAINTPLUS (13) and a multiscan absorption correction using SADABS (14) was performed. The structure was solved using SHELXS-97 and full matrix least squares refinement against F^2 was carried out using SHELXL-97 in anisotropic approximation for non-hydrogen atoms (15).

2.5 Preparation of Schiff bases

2.5.1 Synthesis of quinoxaline-2-carboxalidine-5-aminoindazole (qc5in*)*

A hot solution of 5-aminoindazole (1.4 g, 10 mmol) in ethanol (40 mL) was added slowly to a hot solution of quinoxaline-2-carboxaldehyde (1.6 g, 10 mmol) in ethanol (80 mL). On cooling at room temperature, pale green Schiff base was formed (Scheme 4), which was filtered, and recrystallised from ethanol. (Yield: 80 %, M.P: 225 °C)

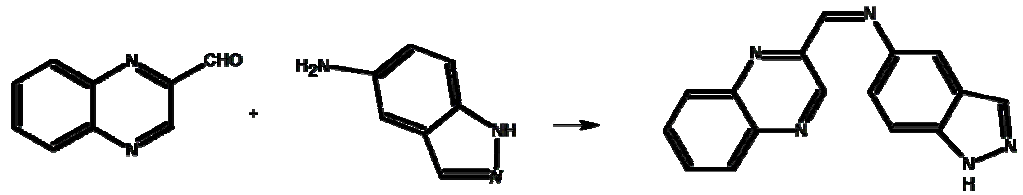

Scheme 4. Formation of qc5in

2.5.2 Synthesis of quinoxaline-2-carboxalidine-6-aminoindazole (qc6in)

A hot solution of 6-aminoindazole (1.3 g, 10 mmol) in ethanol (40 mL) was added slowly to a hot solution of quinoxaline-2-carboxaldehyde (1.6 g, 10 mmol) in ethanol (80 mL). The resulting mixture on cooling to room temperature yielded a yellow coloured Schiff base (Scheme 5). The compound was filtered, washed with ethanol and dried over anhydrous calcium chloride. (Yield: 70 %: M.P: 235 °C)

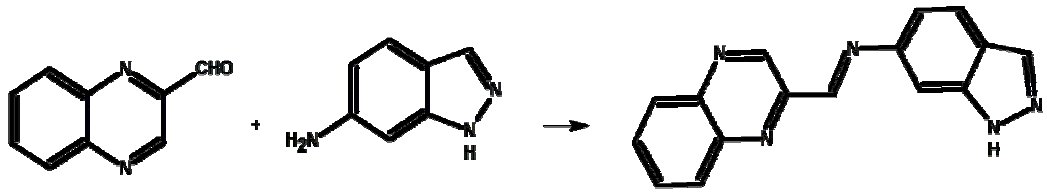

Scheme 5. Formation of qc6in

2.5.3 Synthesis of 3-hydroxy-quinoxaline-2-carboxalidene-5-aminoindazole (hqc5in)

To a solution of 3-hydroxyquinoxaline-2-carboxaldehyde (1.7 g, 10 mmol in 500 ml distilled water), 3 to 4 drops of Con.HCl was added. An alchoholic solution of 5-aminoindazole (1.4 g, 10 mmol) in ethanol (20 mL) was then added to this solution with constant stirring. Yellow coloured Schiff base precipitated (Scheme 6) was filtered washed with ethanol and dried over anhydrous calcium chloride in a desiccator. (Yield: 75 %. M.P: 220 °C)

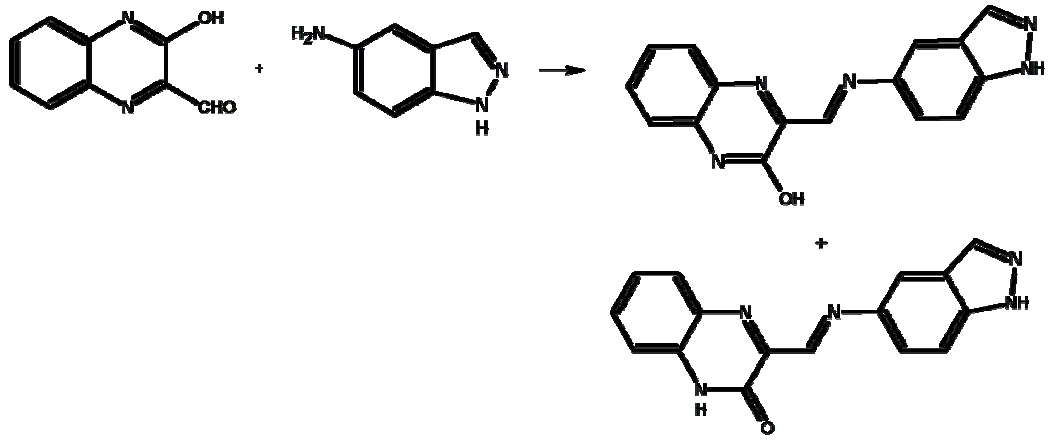

Scheme 6. The formation of tautomeric forms of hqc5in

2.5.4 Synthesis of 3-hydroxy -quinoxaline-2-carboxalidene-6-aminoindazole (hqc6in)

To a solution of 3-hydroxyquinoxaline-2-carboxaldehyde (1.7 g, 10 mmol, in 500 ml distilled water) 3 to 4 drops of con. HCl was added. An alchoholic solution of 6-aminoindazole (1.4 g in 10 mmol) in ethanol (20 mL) was added to this solution with constant stirring. Red coloured Schiff base formed (Scheme 7) was filtered, washed with water and dried over anhydrous calcium chloride. The crude product was recrystallised from absolute ethanol. (Yield: 65 %. M.P: 225 °C)

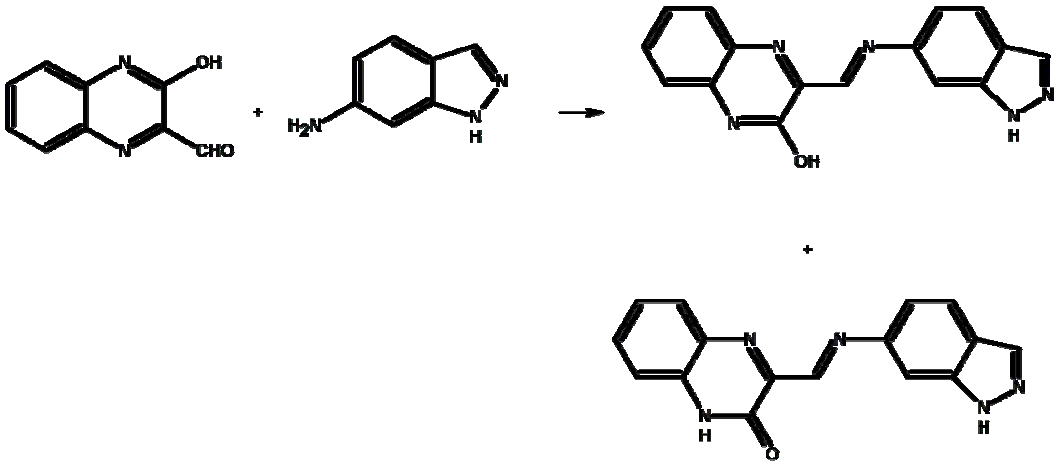

Scheme 7. The formation of tautomeric forms of hqc6in

2.5.5 Synthesis of 3-hydroxyquinoxaline-2-carboxalidine-8-aminoquinolidene (hqaqn)

To a solution of 3-hydroxyquinoxaline-2-carboxaldehyde (1.7 g, 10 mmol, in 500 ml distilled water), 3 to 4 drops of con.HCl was added. An alchoholic solution of 8-aminoquinoline (1.5 g, 10 mmol) in methanol (20 mL) was added to this solution with constant stirring. Dark yellow coloured Schiff base formed (Scheme 8) was filtered, washed with ethanol and dried over anhydrous calcium chloride. The crude product was recrystallised from absolute ethanol. (Yield: 75 %. M.P: 220 °C)

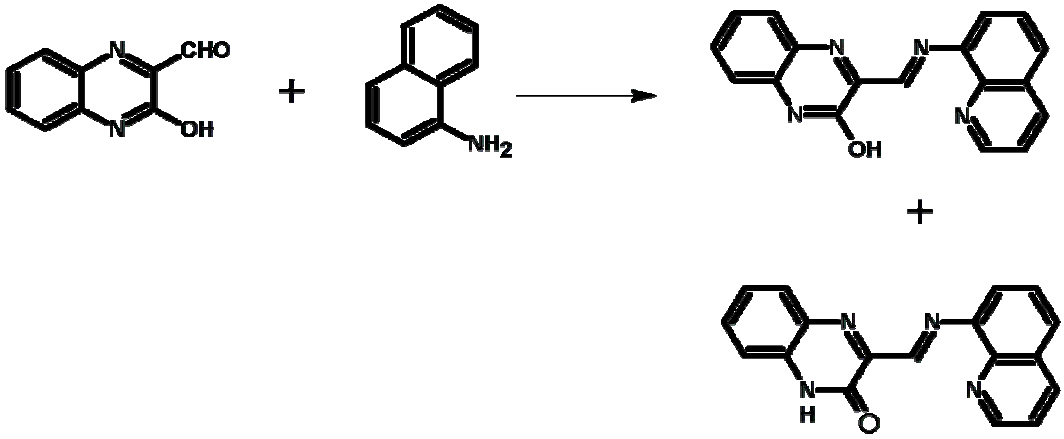

Scheme 8. The formation of tautomeric forms of hqaqn

2.6 Characterisation of the Schiff base ligands

The Schiff base ligands were characterised by elemental analysis, UV-visible spectra, FT-IR spectra and ^{1}H NMR spectra. The electrochemical behaviour of these Schiff bases was determined by cyclic voltammetry.

2.6.1 Elemental analyses

The analytical data of the Schiff base are given in Table 2.1. The data agree with the expected structure of the Schiff bases.

Table 2.1. Analytical data of the Schiff base ligands

Schiff base	Molecular Formula	Formula Weight	C (%)	H (%)	N (%)
qc5in	$C_{16}H_{11}N_5$	273.30	70.26 (70.32)	3.98 (4.06)	25.60 (25.63)
qc6in	$C_{16}H_{11}N_5$	273.30	70.16 (70.32)	4.12 (4.06)	25.58 (25.63)
hqc5in	$C_{16}H_{11}N_5O$	289.29	64.80 (66.43)	3.72 (3.83)	24.02 (24.21)
hqc6in	$C_{16}H_{11}N_5O$	289.29	66.38 (66.43)	3.80 (3.83)	24.18 (24.21)
hqaqn	$C_{18}H_{12}N_4O$	300.31	71.86 (71.99)	4.06 (4.03)	18.59 (18.66)

2.6.2 Electronic spectra

The electronic spectra of the Schiff bases in DMSO in the range 5000-10000 cm^{-1} are given in Figures 2.3-2.7 and in the Table 2.2.

Table 2.2. UV-visible spectral data of Schiff base ligands in DMSO (10^{-5}mol L^{-1})

Schiff bases	λmax, nm (cm^{-1}) in DMSO
qc5in	223 (44,840) 262 (38,170) 373 (26,810)
qc6in	220 (45,454) 263 (38,020) 353 (28,330)
hqc5in	219 (45,660) 291 (34,360) 332 (30,120) 412 (24,270)
hqc6in	220 (45,450) 285 (35,050) 351 (28,490) 426 (23,470)
hqaqn	263 (38,020) 342 (29,240) 420 (23,810) 476 (21,010)

The strong bands observed is due to $\pi \rightarrow \pi^*$ transitions of the aromatic ring and quinoxaline $\pi \rightarrow \pi^*$ (16). The bands in the region 21,010- 24,270 cm^{-1} is assigned to n- π^* of the azomethine group and ring C=N groups.

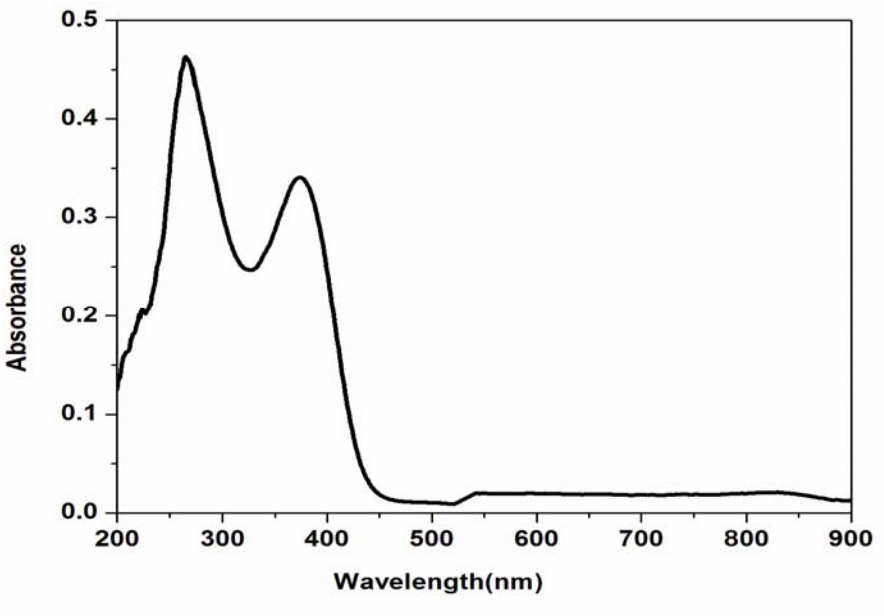

Figure 2.3. UV-Vis spectrum of qc5in

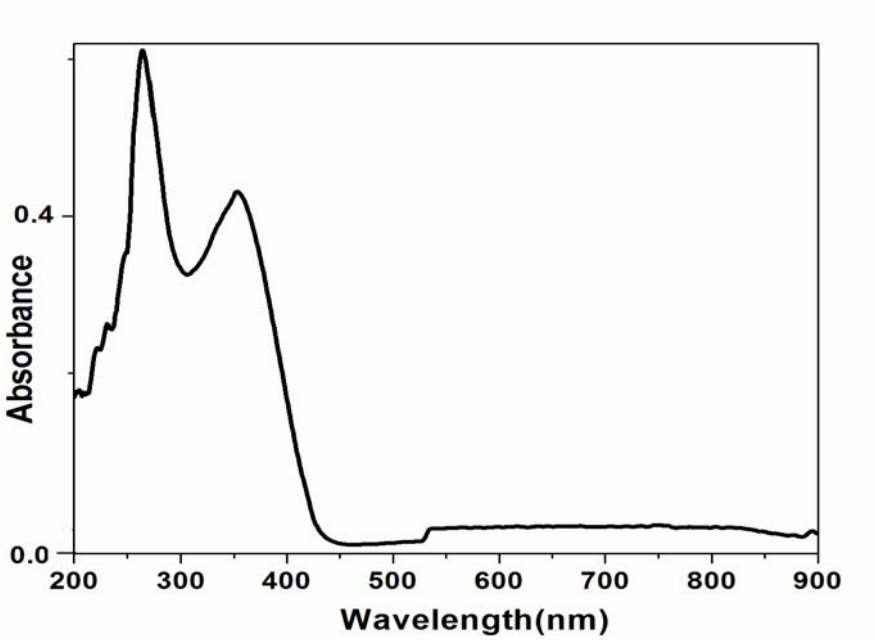

Figure 2.4. UV-Vis spectrum of qc6in

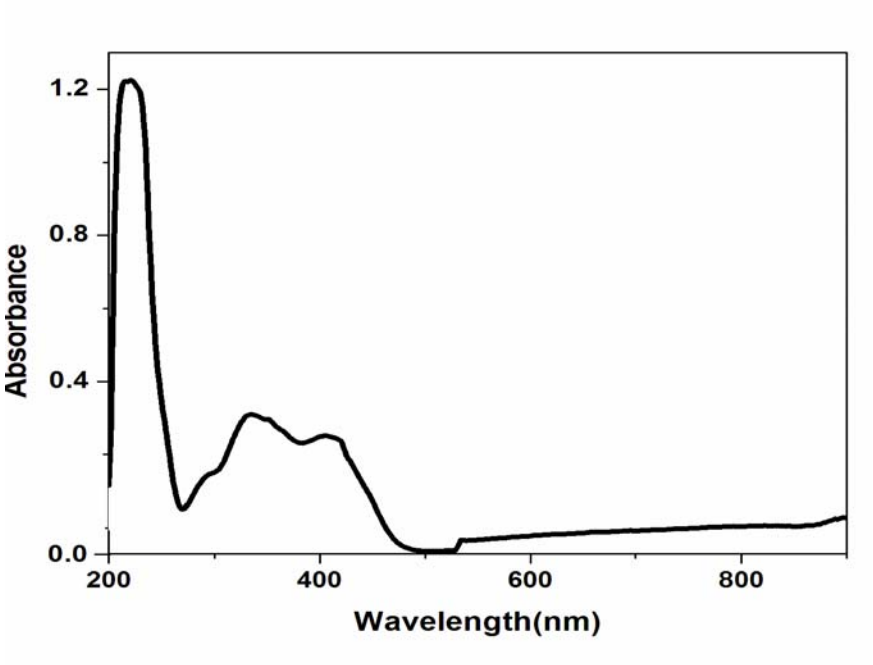

Figure 2.5. UV-Vis spectrum of hqc5in

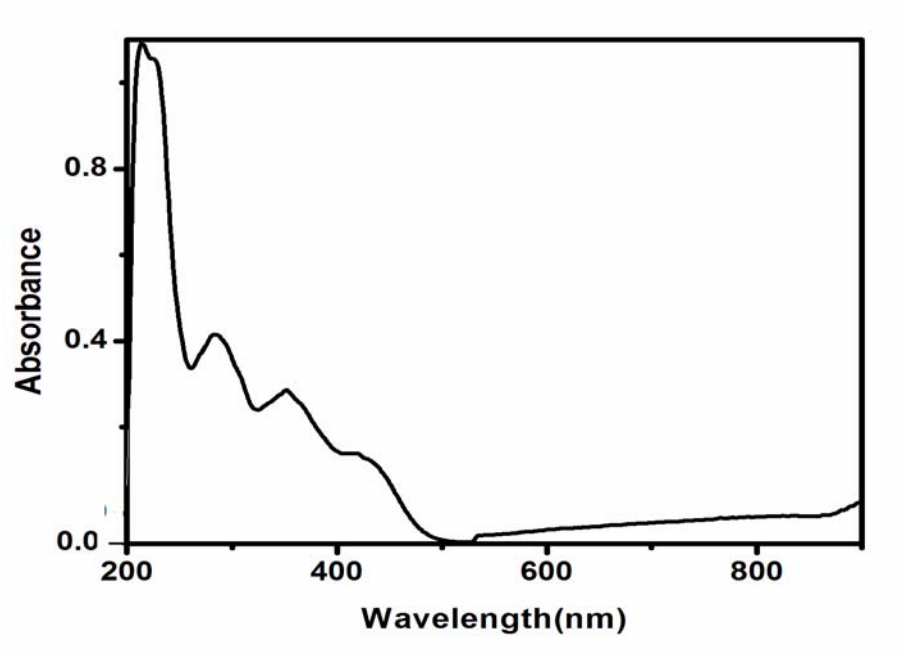

Figure 2.6. UV-Vis spectrum of hqc6in

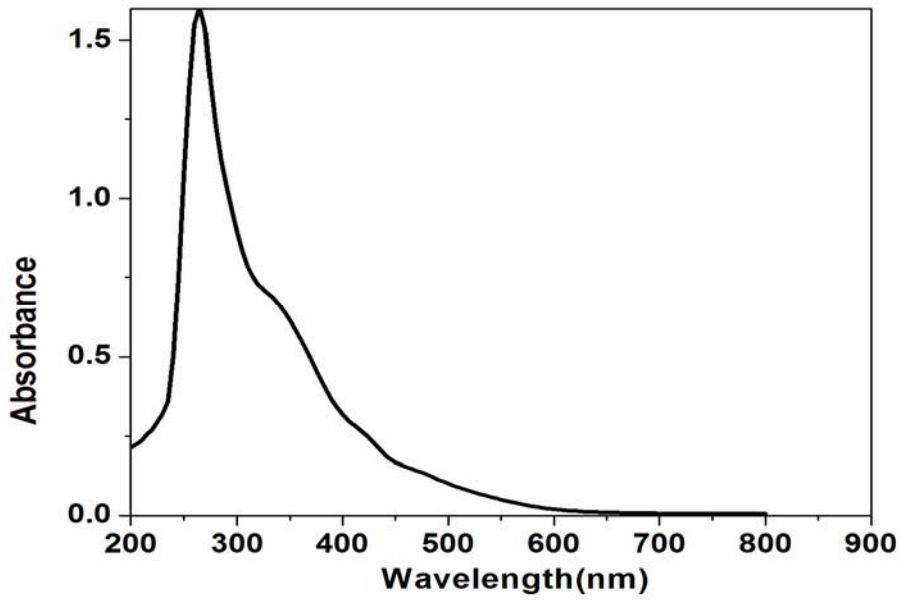

Figure 2.7. UV-Vis spectrum of hqaqn

2.6.3 Infrared spectra

Infrared spectroscopy is an invaluable tool for the identification of products obtained by the condensation of aldehyde and amines. The strong broad absorption band centered at 3437 cm^{-1} for qc5in and that at 3220 cm^{-1} for qc6in may be due to ν(NH). A strong broad absorption band is seen around 3372 cm^{-1} for hqc5in, 3400 cm^{-1} for hqc6in and 3380 cm^{-1} for hqaqn respectively, which may be due to hydrogen bonded ν(OH) in the iminol tautomer or ν(NH) in the amide tautomer. The medium intensity bands observed in the range 3170-2910 cm^{-1} correspond to asymmetric and symmetric stretching vibrations of the aromatic CH groups. The IR stretching frequencies of the C=O and C=N (quinoxaline ring) vary from compound to compound and it is difficult to assign a particular range for these two types of stretching frequencies particularly for tautomeric quinoxaline derivatives (17-26). In the amide tautomeric form, hqc5in, hqc6in and hqaqn contain ketonic carbonyl groups which are evidenced by the presence of strong bands in the range 1670-1680 cm^{-1} (27). The peaks that appear in the range 1610-1640 cm^{-1} may be due to stretching of the azomethine -CH=N group, whereas the bands in the

range 1500-1560 cm^{-1} could be due to the ν(C=N) of the quinoxaline ring (28). A group of bands observed in the range 1210-930 cm^{-1} may be due to the aromatic in-plane deformation vibrations and the fairly strong band near 820 cm^{-1} may be due to the =CH out-of-plane vibration.

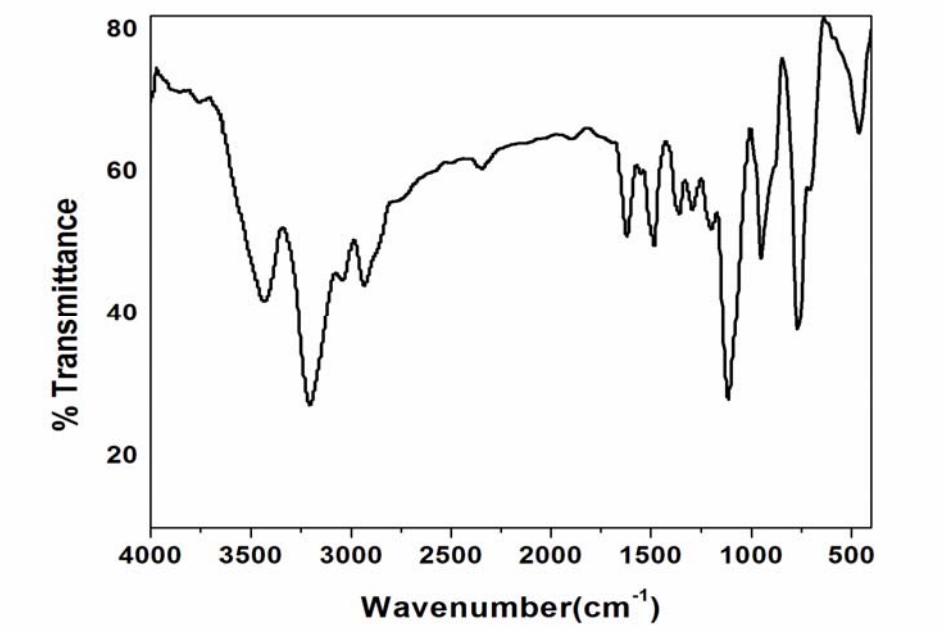

Figure 2.8. FTIR spectrum of qc5in

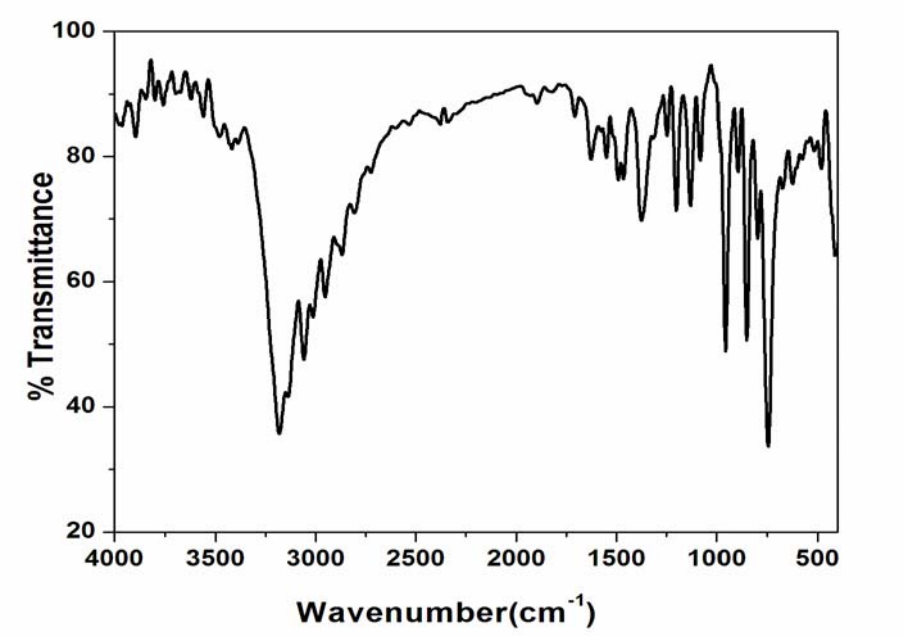

Figure 2.9. FTIR spectrum of qc6in

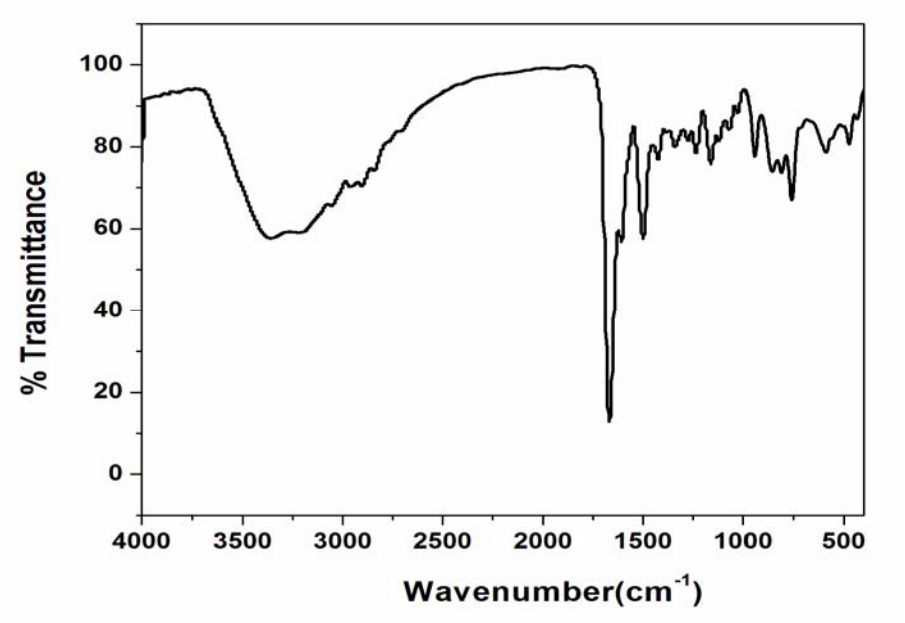

Figure 2.10. FTIR spectrum of hqc5in

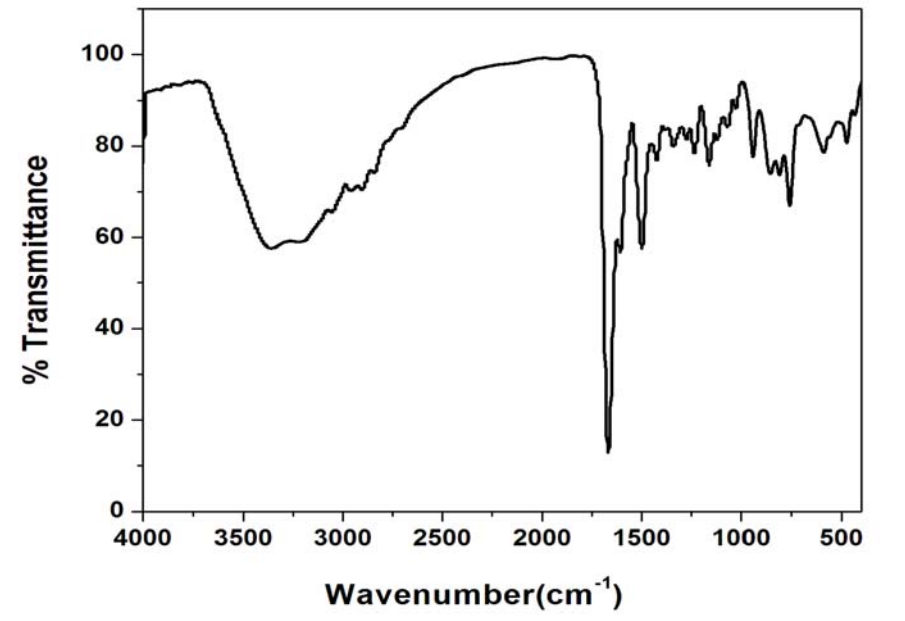

Figure 2.11. FTIR spectrum of hqc6in

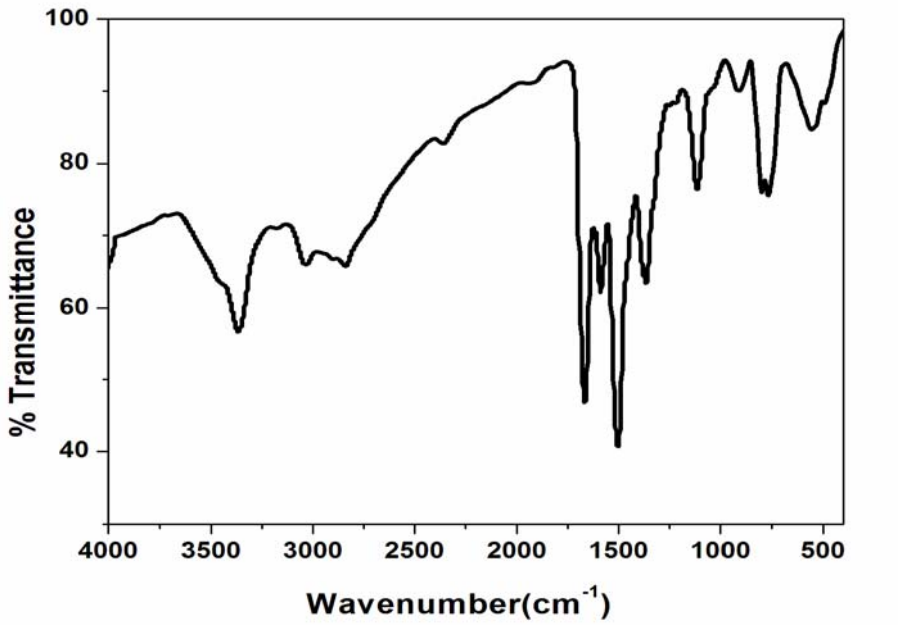

Figure 2.12. FTIR spectrum of hqaqn

2.6.4 NMR spectra

The azomethine protons of the Schiff bases appear in the range 7.1-9.9 ppm. Multiplet signals observed in the 6.4-8.1 ppm range are due to the aromatic protons of the Schiff bases. The ^{1}H NMR spectra of the Schiff bases hqc5in, hqc6in and hqaqn (Figure 12-16) shows signal in confirmity with the tautomeric structure. The peaks observed in the range 12.2-13.4 ppm in these Schiff bases are assignable to the N—H proton of the amide tautomer or O—H of the iminol form (29).

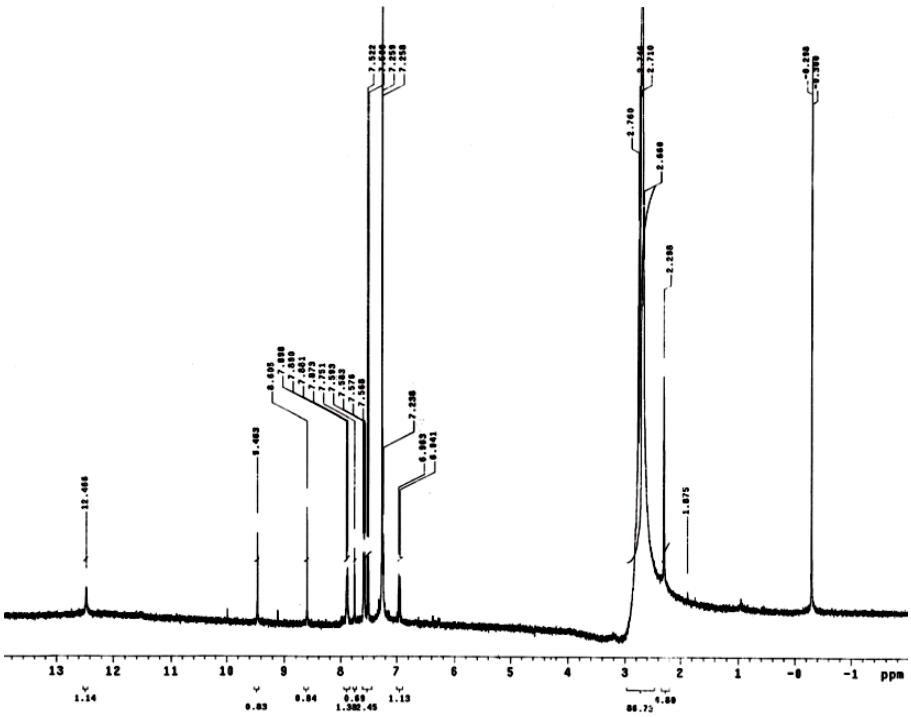

Figure 2.13. The ^{1}H NMR spectrum of qc5in in 500 MHz, $CDCl_3$, 298 K)

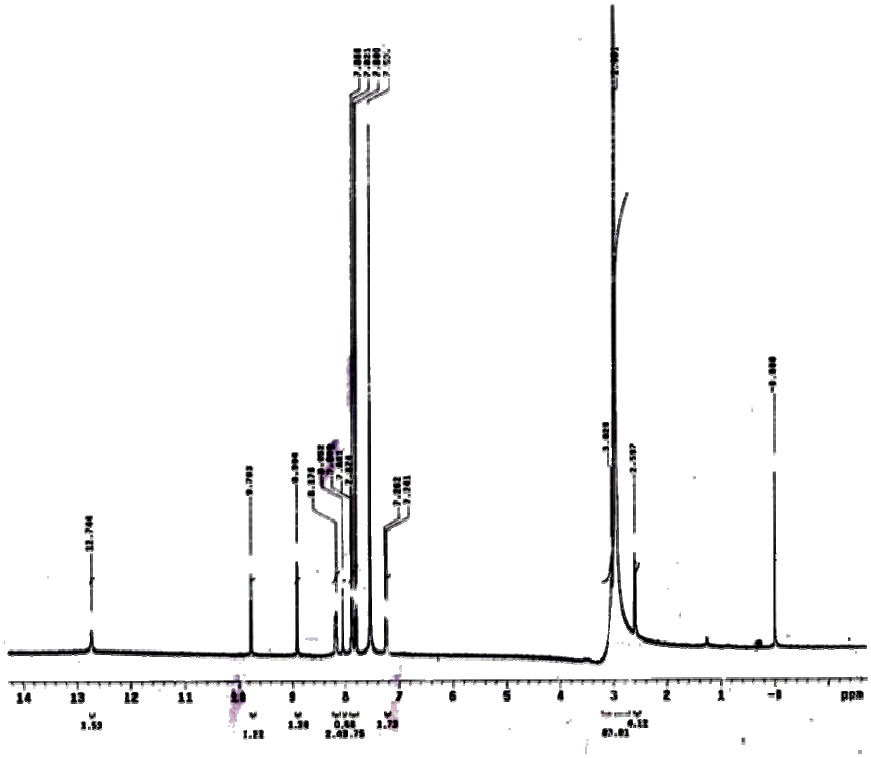

Figure 2.14. The 1 H NMR spectrum of qc6in in 500 MHz, $CDCl_3$, 298 K)

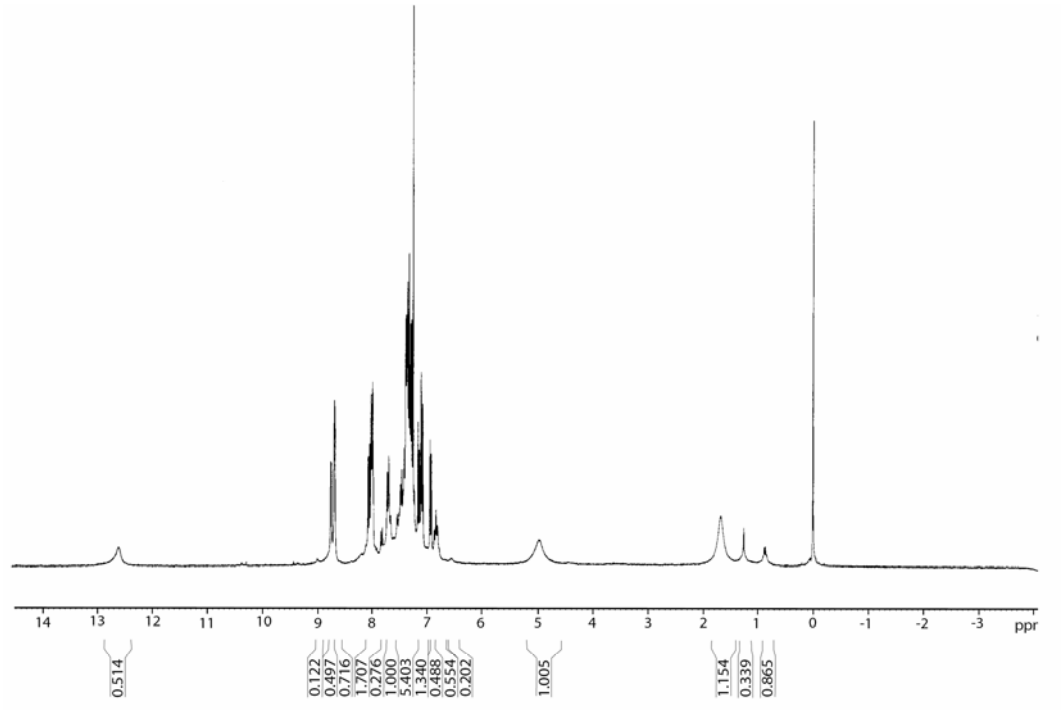

Figure 2.15. The ^{1}H NMR spectrum of hqc5in in 500 MHz, $CDCl_3$, 298 K)

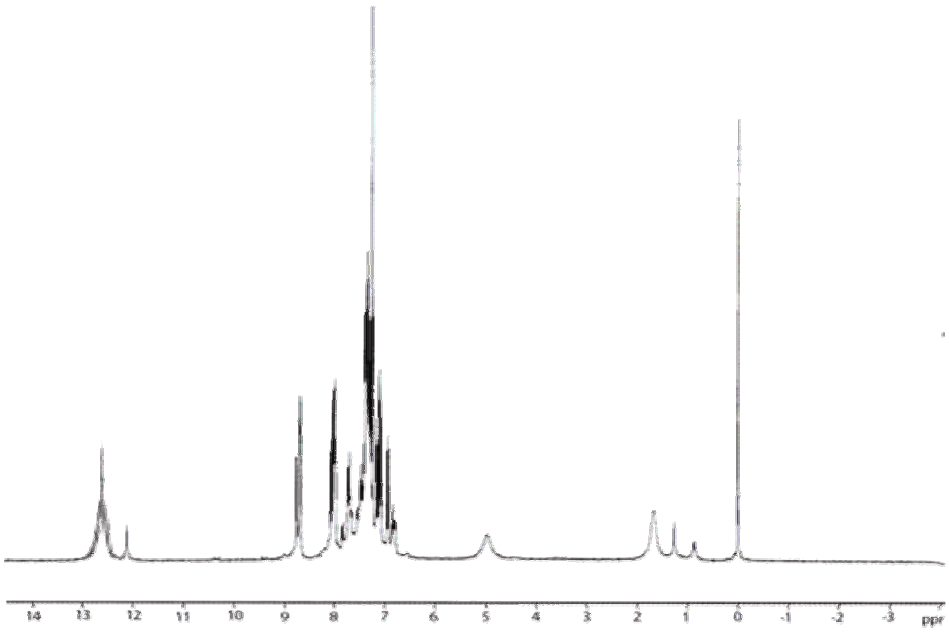

Figure 2.16. The ^{1}H NMR spectrum of hqc6in in 500 MHz, $CDCl_3$, 298 K)

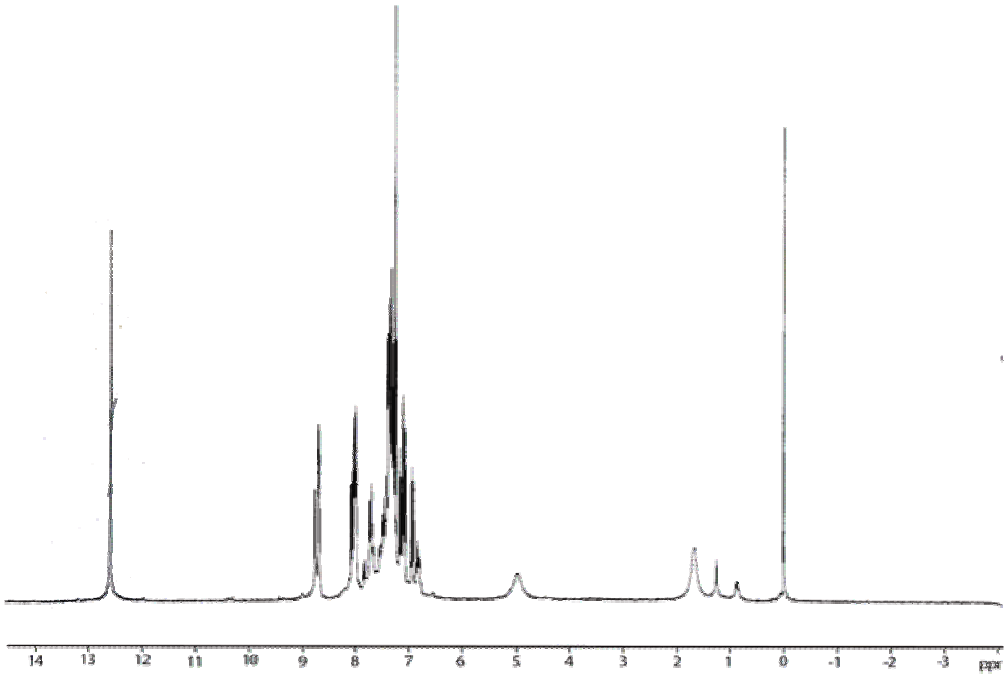

Figure 2.17. The ^{1}H NMR spectrum of hqaqn in 500 MHz, $CDCl_3$, 298 K)

2.6.5 Cyclic voltammetric studies

The cyclic voltammogram of Schiff bases in DMSO are given in Figures 2.18-2.22 and in Table 2.3. The studies were done with Schiff base solutions (5×10^{-5} mol L^{-1}) and tetra-n-butylammonium hexafluorophosphate (0.05 mol L^{-1}) as the supportimg electrolyte. The relatively less negative value of the reduction potential for these Schiff bases when compared to other pyrazine derivatives (30), could possibly be due to the presence of oxygen atoms bonded directly to the pyrazine ring of the ligand. The oxidation and reduction peaks appearing in the +1.5 to 0.0 V range in the cyclic voltammograms of all the Schiff bases are quasireversible and the $E_{1/2}$ value for this redox couple falls in the range of 0.12 to 0.23 V. One electron transfer during the redox process is evident from the I_{pc}/I_{pa} values lying in the range 1.0 to 1.4.

Table 2.3. Cyclic Votammetric data of Schiff bases

Schiff base	E_{pc} (V)	E_{pa} (V)	$E_{1/2}$ (V)	I_{pc} (μV)	I_{pa} (μV)	No. of electrons (I_{pc}/I_{pa})
qc5in	-1.24	0.723	.235	1.70	1.52	1.1
qc6in	-1.13	0.735	.197	1.07	.94	1.1
hqc5in	-1.03 -0.27	0.729	1.48	1.01	. 97	1.1
hqc6in	-0.636 -0.922	0.608	.157	2.76	2.05	1.3
hqaqn	-0.83 -0.53	0.30 -0.63	.123	.60	.53	1.2

E_{pc} = cathodic peak potential;
E_{pc} = anodic peak potential;
I_{pc} = cathodic peak current;
I_{pa} = anodic peak current;
$E_{1/2}$ = $0.5 \times (E_{pa} + E_{pc})$; scan rate 100 mV

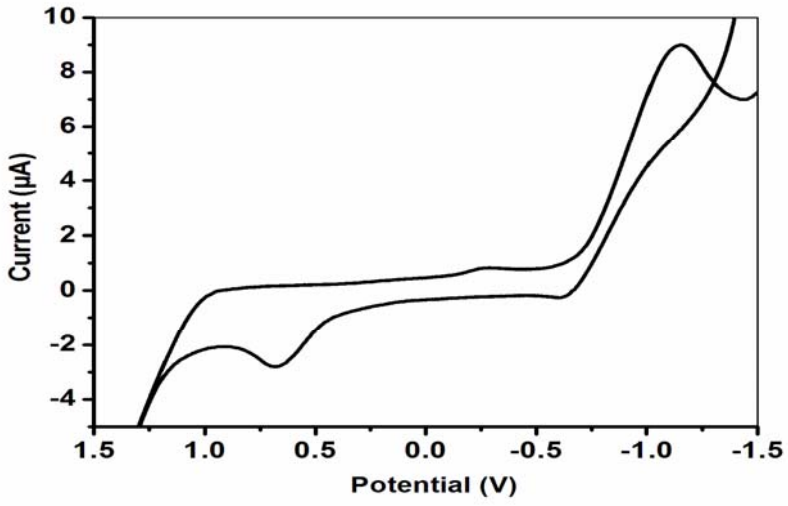

Figure 2.18. Cyclic voltammogram of qc5in

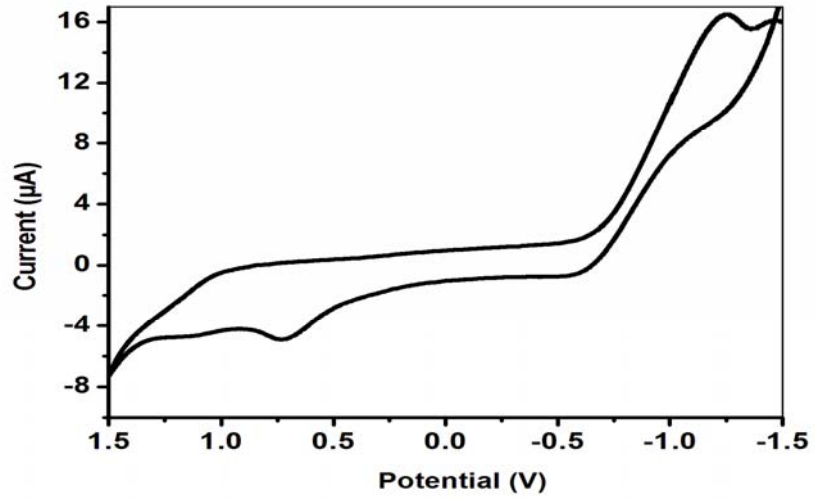

Figure 2.19. Cyclic voltammogram of qc6in

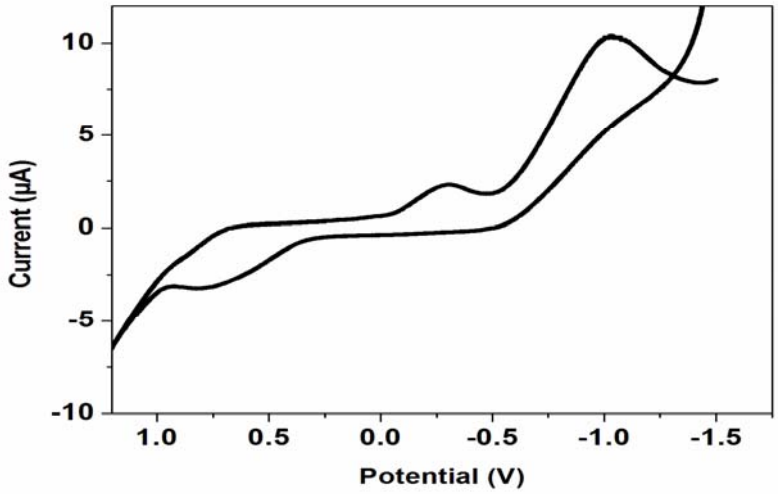

Figure 2.20. Cyclic voltammogram of hqc5in

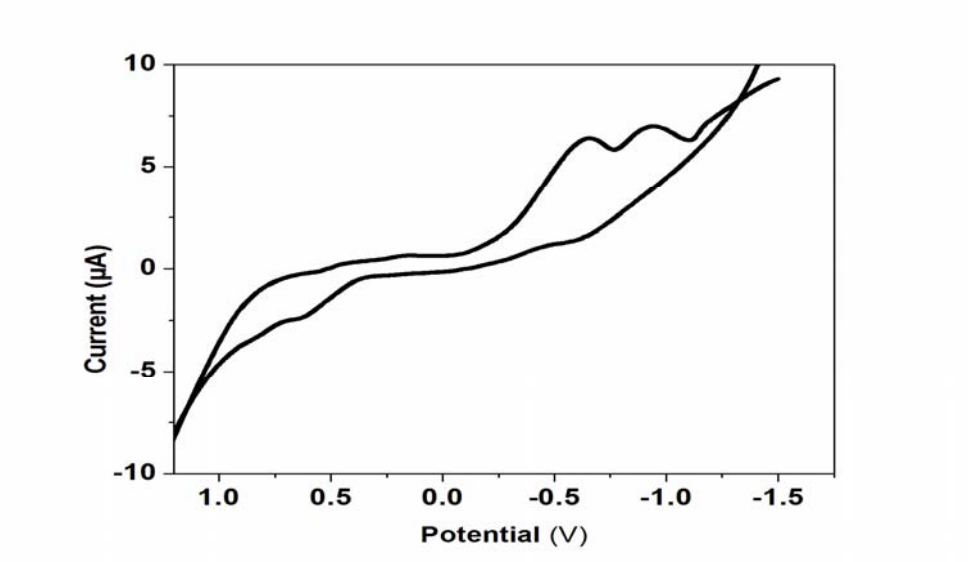

Figure 2.21. Cyclic voltammogram of hqc6in

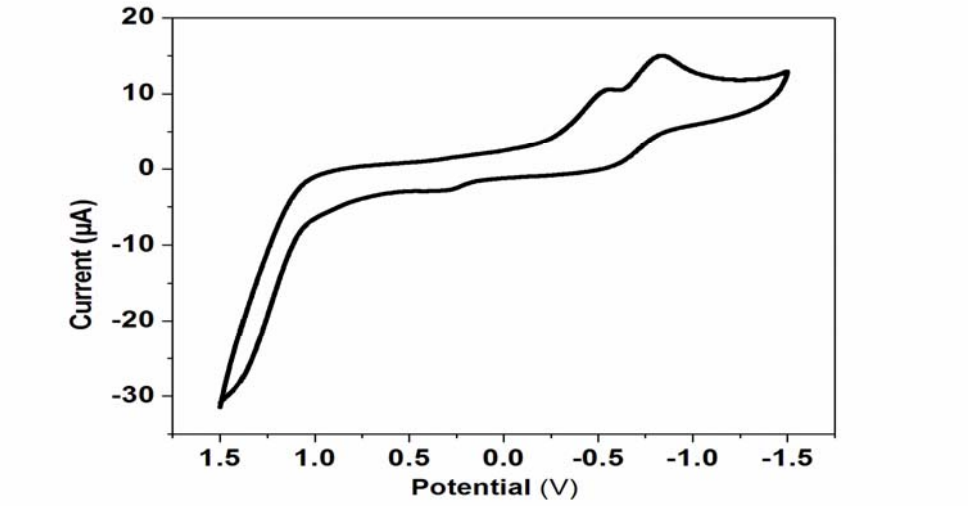

Figure 2.22. Cyclic voltammogram of hqaqn

2.7 Crystal structure analysis

The single crystal of the Schiff base, qc5in were obtained by the slow evaporation of ethanolic solution of the Schiff base (31). The crystal structure of the compound with numbering scheme is shown in figure 2.23. The quinoxaline ring and indazole ring are each approximately planar, with the maximum deviations of 0.0254 (4) and 0.0213 (4) Å from the least square planes, respectively. The compound is non-planar due to the twisting of rings with respect to azomethine group. In the crystal structure, molecules are held together by π–π stacking interactions and N—H···N intermolecular hydrogen bonding. The crystallographic data and structure refinement parameters are listed in Table.2.4. Selected hydrogen bonding parameters, important bond length (Å), and bond angles **(°)** are given in Table 2.5, Table 2.6 and Table 2.7 respectively.

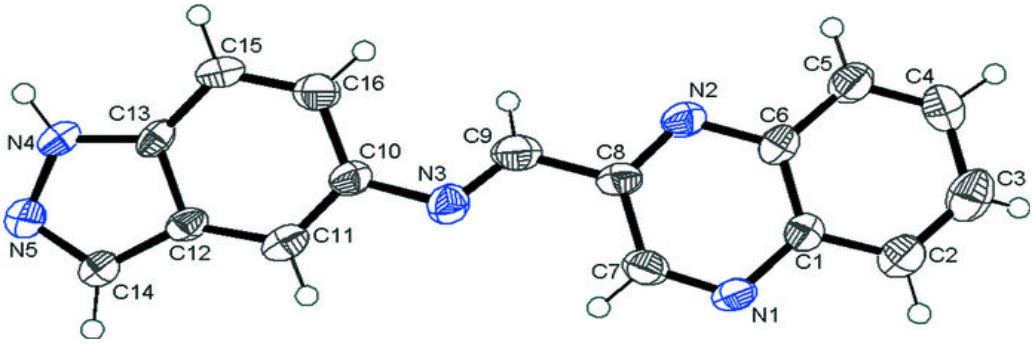

Figure 2.23. ORTEP diagram of qc5in showing the atom labelling scheme

Table 2.4. Crystal data summary for qc5in

Empirical formula	$C_{16}H_{11}N_5$
Formula weight	273.30
Crystal size(mm)	0.45× 0.27× 0.08
Wavelength(A)	0.71073
Crystal system	Monoclinic
Space group	$P2_1/c$
Cell constants:	
Unit cell and dimensions (Å)	
a (Å)	*7.7015 (6)*
b (Å)	*8.0330 (6)*
c (Å)	*20.6034 (16)*
β (º)	*96.882 (2)*
V (Å^3)	*1265.47 (17)*
Z	*4*
F(000)	568
θ range for data reflection (º)	2.6 to 29.8º
Absorption coefficient (mm^3)	0.09
*D*x (Mg m^{-3})	1.434
T (K)	298
Reflections collected/unique	16012/3597 [R(int) =0.024]
parameters	190
R[$F^2 > 2\ (F^2)$]	0.046
wR(F^2)	0.143
Goodness- of-fit-on F^2	1.03

Table 2.5. Hydrogen-bond geometry (Å, °) in the ligand

D—H---A	D—H	H----A	D---A	D-H---A
N4—H4---N1^{iii}	0.86	2.31	3.1050 (15)	153

Symmetry code: (iii) *x*, −*y*+1/2, *z*+1/2.

The bond distances, N3-C9 (1.2610 Å) and N3—C10 (1.4162 Å) correspond to C-N double, C-N single bonds and are comparable to those for the previously reported Schiff bases (32,33).

Table 2.6. The important bond length (Å) of qc5in

N1—C7	1.3053 (17)	C5—C6	1.4070 (19)
N1—C1	1.3670 (17)	C5—H5	0.9300
N2—C8	1.3136 (17)	C7—C8	1.4225 (17)
N2—C6	1.3668 (16)	C7—H7	0.9300
N3—C9	1.2610 (18)	C8—C9	1.4684 (17)
N3—C10	1.4162 (16)	C9—H9	0.9300
N4—C13	1.3568 (17)	C10—C11	1.3768 (18)
N4—N5	1.3576 (17)	C10—C16	1.4185 (17)
N4—H4	0.8600	C11—C12	1.3989 (17)
N5—C14	1.3169 (17)	C11—H11	0.9300
C1—C2	1.4094 (18)	C12—C13	1.4039 (16)
C1—C6	1.4167 (17)	C12—C14	1.4150 (19)
C2—C3	1.4167 (17)	C12—C14	1.4150 (19)
C2—C3	1.360 (2)	C13—C15	1.3941 (19)
C2—H2	0.9300	C14—H14	0.9300
C3—C4	1.402 (2)	C15—C16	1.3691 (18)
C3—H3	0.9300	C15—H15	0.9300
C4—C5	1.3605 (19)	C16—H16	0.9300

Table 2.7. The important bond angles (°) of qc5in

C7—N1—C1	116.38 (11)	N2—C8—C7	121.92 (12)
C8—N2—C6	116.81 (10)	N2—C8—C9	116.67 (11)
C9—N3—C10	121.52 (11)	C7—C8—C9	121.40 (12)
C13—N4—N5	112.15 (10)	N3—C9—C8	121.03 (12)
C13—N4—H4	123.9	N3—C9—H9	119.5
C14—N5—N4	105.65 (12)	C11—C10—N3	115.26 (11)
N1—C1—C2	119.81 (11)	C11—C10—C16	119.99 (12)
N1—C1—C6	121.24 (11)	N3—C10—C16	124.73 (12)
C2—C1—C6	118.94 (12)	C10—C11—C12	119.44 (11)
C3—C2—C1	119.78 (13)	C10—C11—H11	120.3
C3—C2—H2	120.1	C12—C11—H11	120.3
C1—C2—H2	120.1	C11—C12—C13	119.28 (12)
C2—C3—C4	121.20 (13)	C11—C12—C14	136.49 (12)
C2—C3—H3	119.4	C13—C12—C14	104.21 (11)
C4—C3—H3	119.4	N4—C13—C15	131.95 (11)
C5—C4—C3	120.49 (14)	N4—C13—C12	106.21 (12)
C5—C4—H4A	119.8	C15—C13—C12	121.83 (12)
C3—C4—H4A	119.8	N5—C14—C12	111.77 (12)
C4—C5—C6	119.80 (13)	N5—C14—H14	124.1
C4—C5—H5	120.1	C12—C14—H14	124.1
C6—C5—H5	120.1	C16—C15—C13	117.81 (11)
N2—C6—C5	119.47 (11)	C16—C15—H15	121.1
N2—C6—C1	120.78 (12)	C13—C15—H15	121.1
C5—C6—C1	119.75 (12)	C15—C16—C10	121.58 (13)
N1—C7—C8	122.85 (13)	C15—C16—H16	119.2
N1—C7—H7	118.6	C10—C16—H16	119.2
C8—C7—H7	118.6		

2.8 Conclusions

This chapter presents various experimental and characterization techniques. Information about the synthesis and characterization of the five new Schiff bases, quinoxaline-2-carboxalidine-5-aminoindazole (qc5in), quinoxaline-2-carboxalidine-6-aminoindazole (qc6in), 3-hydroxyquinoxaline-2-carboxalidene-5-aminoindazole (hqc5in), 3-hydroxyquinoxaline-2-carboxalidene-6-aminoindazole (hqc6in), and 3-hydroxyquinoxaline-2-carboxalidine-8-aminoquinolidene (hqaqn) is included in this chapter. These Schiff bases were characterised using elemental analysis and spectroscopic techniques such as FT-IR, UV-visible spectroscopy and NMR. Details on the techniques used for the DNA binding studies UV-Vis absorption spectra, cyclic voltammetry, circular dichroism spectra and gel electrophoresis experiments given in this chapter.

2.9 References

[1] D.D. Perrin, W.L.F Armarego, D.R. Perrin, *Purification of Laboratory Chemicals*, *Pergamon Press, New York*, 1980.

[2] H. Ohle, G. Noetzel, *Chemische Berichte*, 76B (1943) 624.

[3] O. Hinsberg, *Annales de Chimie*, 237 (1887) 340.

[4] M.A. Verity, R. Gallagher, W.J. Brown, *Biochemical Journal*, 103 (1967) 375.

[5] V. Arun, P.P. Robinson, S. Manju, P. Leeju, G. Varsha, V. Digna, K.K.M.Yusuff, *Dyes and Pigments*. 82 (2009) 268.

[6] A.T. Stuart, *J. Am. Chem. Soc*. 33 (1911) 1344.

[7] J. Marthur, *J. Mol. Biol*. 3 (1961) 208.

[8] B.N. Figgis, R.S. Nyholm, *J. Chem. Soc*.(1958) 4190.

[9] B.N. Figgis, J. Lewis, Modern Coordination chemistry, J. Lewis, R.G. Wilkins, *Edn., Interscience*, New York (1958).

[10] P.W. Selwood, Magnetochemistry, *Interscience*, New York (1958).

[11] B.N.Figgis, J. Lewis, *Progress in Inorganic Chemistry*, F.A. Cotton, Ed.,interscience, New York (1964).

[12] N. Raman, S. Sobha**,** A. Thamaraichelvan, *Spectrochimica Acta Part A*: 78 (2011) 888.

[13] SAINTPLUS, Bruker AXS Inc.,Madison, USA (2003).

[14] G.M. Sheldrick, SADABS, *Program for Empirical Absorption Correction* University of Gottingen, Germany (1997).

[15] G.M. Sheldrick, SHELX-97, *Programs for Crystal Structure Analysis*, University of Gottingen, Germany (1997).

[16] M.A. Neelakantan, S. S. Mariappan, J. Dharmaraja, T. Jayakumar, K. Muthukumaran, *Spectrochim. Acta A* 71 (2008) 628.

[17] R.M. Ramadan, M. S. A. Hamza, A. E. M. Salem, F. M. El-Zawawy, *Transition Metal Chemistry*, 24 (1999) 193.

[18] R. Touzani, T. B. Hadda, S. Elkadiri, A. Ramdani, O. Maury, H. L. Bozec, L. Toupet, P.H. Dixneuf, *New Journal of Chemistry* 25 (2001) 391.

[19] H. Gazit, G. App, J. McMahon, A. Chen, F.D. Levitzki, Bohmer, *Journal of Medicinal Chemistry*, 39 (1996) 2170.

[20] V.L. Gein, A.V. Kataeva, L.F. Gein, *Chemistry of Heterocyclic Compound,* 43 (2007) 1385.

[21] V.A. Mamedov, A.A. Kalinin, A.T. Gubaidullin, O.G. Isaikina, I.A. Litvinov, *Russian Journal of Organic Chemistry* 41 (2005) 599.

[22] K.S. Bozdyreva, Z.G. Aliev, A.N. Maslivets, *Russian Journal of Organic Chemistry* 44 (2008) 607.

[23] V.A. Mamedov, A.A. Kalinin, A.T. Gubaidullin, T.K. Rizvanov, A.V. Chernova, G.M.Doroshkina, I.A. Litvinov, Y.A. Levin, *Russian Journal of Organic Chemistry*, 39 (2003)131.

[24] V. Mashevskaya, I. A. Tolmacheva, E. V. Voronova, T. F. Odegova, G. A. Aleksandrova, A.F. Goleneva, S. V. Koltsova, A. N. Maslivets, *Pharmaceutical Chemistry Journal*, 36 (2002) 86.

[25] M. Barbasiewicz, A. Szadkowska, R. Bujok, K. Grela, *Organometallics*, 25 (2006) 3599.

[26] E. R. Kotb, M.A. Anwar, M.S. Soliman, M.A. Salama, *Phosphorus, Sulfur, and Silicon and the Related Elements*, 182 (2007) 1119.

[27] V.A. Mamedov, A.A. Kalinin, N.M. Azancheev, Y.A. Levin. *Russian Journal of OrganicChemistry*, 39 (2003) 125.

[28] K. Nakamotto, Infrared and Raman Spectra of Inorganic and Coordination compounds, 5th Edn, Part B, John Wiley & Sons, London (1997).

[29] V. A. Mamedov, D.F. Saifina, E.A. Berdnikov, I. Kh. Rizvanov, *Russian Chemical Bulletin*, 56 (2007) 2127.

[30] S.M. Molnar, K.R. Neville, G.E. Jensen, K.J. Brewer, *Inorganica Chimica Acta,* 206 (1993) 69.

[31] P. Leeju, V. Arun, M. Sebastian, G. Varsha, Digna Varghese, K. K. M. Yusuff , *Acta Cryst*. (2009). E65, o1981.

[32] D. Varghese, V. Arun, M. Sebastian, P. Leeju, G. Varsha, K.K.M Yusuff, *Acta Cryst* (2009) E65, o435.

[33] G. Varsha, V. Arun, M. Sebastian, P. Leeju, D. Varghese, K.K.M Yusuff, *Acta Cryst* (2009) E65, o919.

.....ooo.....

Chapter 3

Synthesis, characterisation and DNA interaction of palladium(II) complexes

Contents

3.1 Introduction

The chemotherapeutic activity of cisplatin (*cis*-diamminedichloroplatinum in the early 1960s generated a tremendous amount of research activity to understand the role of this drug in destroying cancer cells. Cisplatin coordinates to DNA and inhibits replication and transcription of DNA. It also leads to programmed cell death (called apoptosis). Cisplatin is used in the treatment of head and neck cancer, lung carcinoma, stomach carcinoma, and so on. Unfortunately, its use is limited by development of resistance in tumor cells and the significant side effects, including nephrotoxicity, neurotoxicity, ototoxicity and myelotoxicity. To find out more effective and less toxic antitumour drugs, with broader spectrum of activity, improved clinical efficacy and reduced toxicity, analogues of cisplatin were synthesised and tested. On the basis of the structural and thermodynamic analogy about platinum(II) complexes, many palladium(II) complexes were probed as antitumor drugs [1–10].

The interest in the use of palladium drugs arises from the fact that this metal is isoelectronic with platinum. Because of the similar coordination modes and chemical properties, palladium(II) easily form square planar complexes. Square planar palladium complexes have excellent DNA binding and DNA cleavage abilities

because they are coordinatively unsaturated and are labile to substitution (11-14). In comparison with other transition metal complexes, palladium complexes have many medicinal, chemical and industrial applications (15–21).

Details regarding the synthesis, characterisation and DNA binding and cleavage ability of Pd(II) complexes of Schiff base ligands, quinoxaline-2-carboxalidene-5-aminoindazole (qc5in), quinoxaline-2-carboxalidene-6-aminoindazole (qc6in), 3-hydroxyquinoxaline-2-carboxalidene-5-aminoindazole (hqc5in), 3-hydroxyquinoxaline-2-carboxalidene-6-aminoindazole (hqc6in), 3-hyodroxyquinoxaline-2-carboxalidene-8-aminquinoline (hqaqn) are presented in this chapter.

3.2 Experimental

3.2.1 Materials

The details of materials used for the syntheses of the Schiff base ligands are given in Chapter 2.

3.2.2 Synthesis of Schiff base ligands

The procedure for the synthesis of the Schiff base ligands are given in Chapter 2

3.2.3 Synthesis of complexes

$PdCl_2$ (0.89 g, 5 mmol) dissolved in ethanol (20 mL) was mixed with the Schiff base ligand qc5in (1.37 g, 5 mmol), qc6in (1.37 g, 5 mmol), hqc5in (1.45 g, 5 mmol), hqc6in (1.45 g, 5 mmol) or hqaqn (1.50 g, 5 mmol), in ethanol (100 mL) and the mixture was heated at 80 °C and stirred for 15 minutes. The complex separated out was filtered, washed with ethanol and dried in vacuo over P_4O_{10}. Yield: 52 %

3.3 Results and discussion

All the complexes are non-hygroscopic. Colour of the complex varies from golden yellow to brown. They are soluble in DMSO and are insoluble in benzene, ethanol and chloroform. The ligands hqc5in, hqc6in and hqaqn which exhibit keto-enol tautomerism, predominantly exists in the keto form in the solid state.

3.3.1 Elemental analyses

Analytical data and conductance data are given in Table 3.1. The data suggest that the all complexes are mononuclear in nature and have metal to Schiff base ratio of 1:1. The molar conductance values of the complexes in DMSO (10^{-3} mol) indicate non-electrolytic nature of the complexes (22). Thus the chloride ions in all these complexes are coordinated to the metal ion (23).

Table 3.1. Analytical data and conductance data of palladium(II) complexes

Complexes of	C (%)	H (%)	N (%)	Cl (%)	Pd (%)	Molar conductance ($ohm^{-1}cm^2\ mol^{-1}$)
qc5in	42.58 (42.65)	2.52 (2.46)	15.58 (15.54)	16.02 (15.74)	23.49 (23.62)	8.5
qc6in	41.92 (42.65)	2.30 (2.46)	15.69 (15.54)	14.78 (15.74)	23.67 (23.62)	12.6
hqc5in	40.96 (41.18)	2.42 (2.38)	15.32 (15.01)	15.08 (15.20)	22.12 (22.81)	10.5
hqc6in	42.00 (41.18)	2.86 (2.97)	12.28 (12.39)	15.62 (15.20)	22.68 (22.81)	5.7
hqaqn	45.18 (45.26)	3.00 (2.53)	11.68 (11.73)	14.72 (14.85)	22.20 (22.28)	14.6

Based on the analytical and molar conductance data, the complexes have been assigned the molecular formula $[Pd(qc5in)Cl_2]$, $[Pd(qc6in)Cl_2]$, $[Pd(hqc5in)Cl_2]$, $[Pd(hqc6in)Cl_2]$ and $[Pd(hqaqn)Cl_2]$.

3.3.2 Infrared spectra

Selected infrared vibrational stretching frequencies of the free Schiff base ligands and the palladium complexes, which are useful for determining the mode of coordination of the ligands, are given in Table 3.2. The FT-IR spectra of the Pd(II) complexes are given in Figures 3.1-3.5. The strong broad absorption band centered at 3292 cm^{-1} for $[Pd(qc5in)Cl_2]$ and that at 3305 cm^{-1} for $[Pd(qc6in)Cl_2]$ may be due to ν(NH). A strong broad absorption band is seen in the range 3350-3450 cm^{-1} for

[Pd(hqc5in)Cl_2], [Pd(hqc6in)Cl_2)] and [Pd(hqaqn)Cl_2] which may be due to hydrogen bonded ν(OH) in the iminol tautomer or ν(NH) in the amide tautomer. The participation of azomethine group of the Schiff bases in coordination is evidenced by decrease in its stretching frequency (24, 25). The bands centered at 1633 cm^{-1} for qc5in, at 1630 cm^{-1} for qc6in, at 1626 cm^{-1} for hqc5in, at 1612 cm^{-1} for hqc6in and hqaqn decreases to 1617 cm^{-1}, 1619 cm^{-1}, 1605 cm^{-1}, 1600 cm^{-1} and 1602 cm^{-1} respectively for their metal complexes. In addition, these complexes exhibit one strong band in the range 410-440 cm^{-1}, which may be due to ν(Pd—N) suggesting coordination of azomethine nitrogen atoms. The ν(C=N) of the quinoxaline ring which is observed in the range 1480 cm^{-1} to 1540 cm^{-1} was also seen to decrease on complexation indicating the participation of the nitrogen atom of the quinoxaline ring in bond formation. The band due to the ν(C═O) at 1670 cm^{-1} for hqc5in, 1680 cm^{-1} for hqc6in and 1673 cm^{-1} for hqaqn is shifted to 1647 cm^{-1}, 1654 cm^{-1}, 1661 cm^{-1} for the complexes, [Pd(hqc5in)Cl_2], [Pd(hqc6in)Cl_2], [Pd(hqaqn)Cl_2] respectively suggesting the involvement of the C=O group in coordination.

Table 3.2. The IR spectral data of Pd(II) complexes

Compound	ν(O—H)[a]	ν(C=N)[b]	ν(C=N)[c]	ν(C=O)	ν(M-O)	ν(M-N)
qc5in	3208	1633	1489	-	-	-
[Pd(qc5in)Cl_2]	3292	1617	1482	-	-	406
qc6in	3211	1630	1532	-	-	-
[Pd(qc6in)Cl_2]	3305	1619	1500	-	-	409
hqc5in	3372	1626	1507	1670	-	-
[Pd(hqc5in)Cl_2]	3362	1605	1507	1647	466	411
hqc6in	3400	1612	1497	1670		
[Pd(hqc6in)Cl_2]	3397	1600	1497	1654	463	409
hqaqn	3378	1612	1511	1680	-	-
[Pd(hqaqn)Cl_2]	3428	1602	1510	1661	482	409

[a] ν(N−H)/ ν(O−H) of the free Schiff base or;
[b] ν(CH=N) of azomethine group; [c] ν(C=N) of quinoxaline:

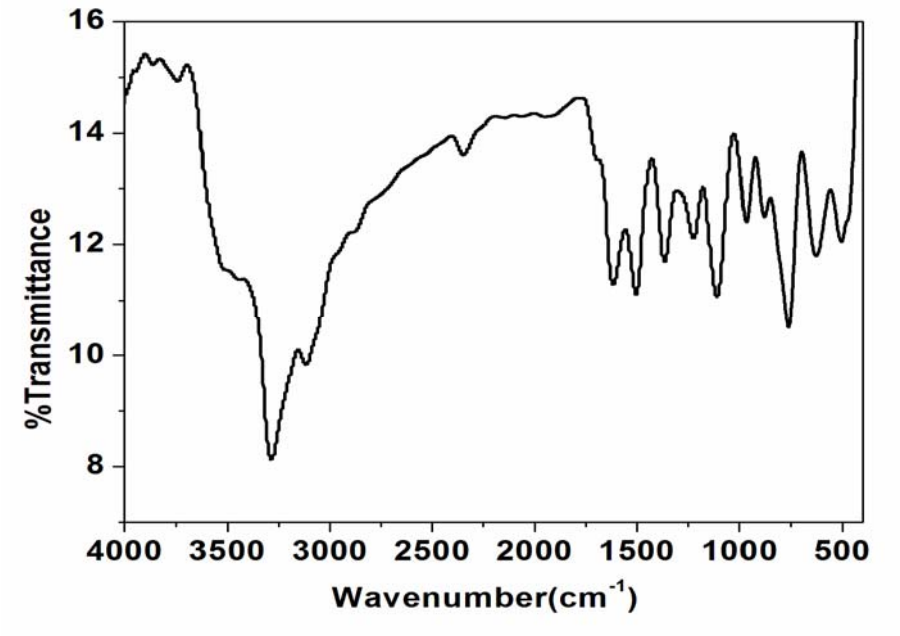

Figure 3.1. FTIR spectrum of [Pd(qc5in)Cl_2]

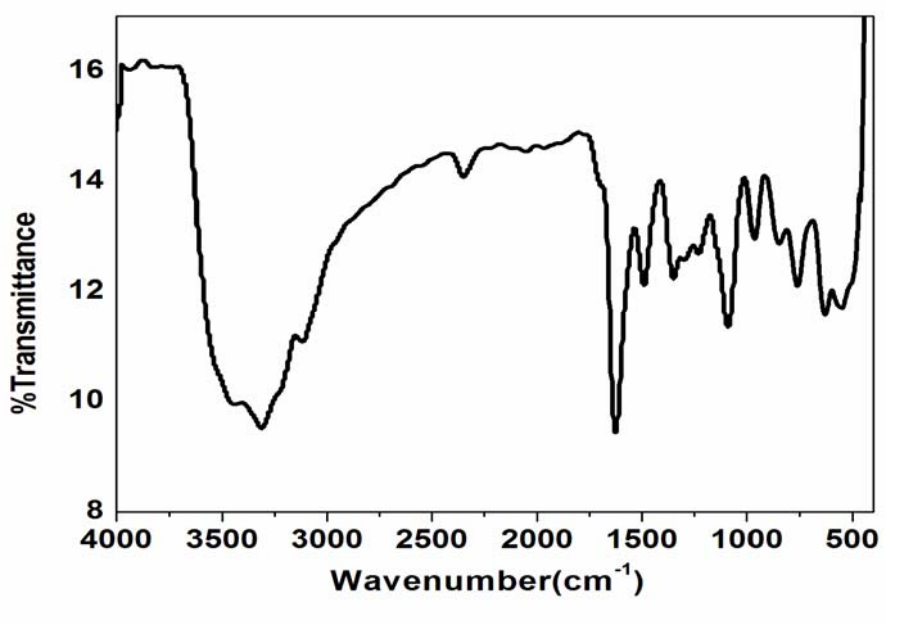

Figure 3.2. FTIR spectrum of [Pd(qc6in)Cl_2]

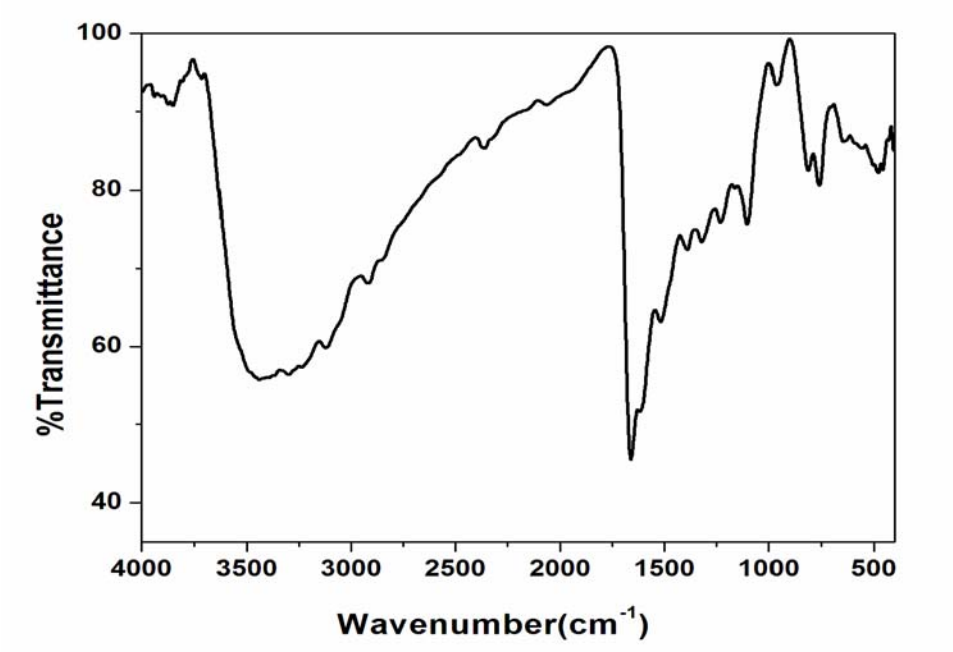

Figure 3.3. FTIR spectrum of [Pd(hqc5in)Cl_2]

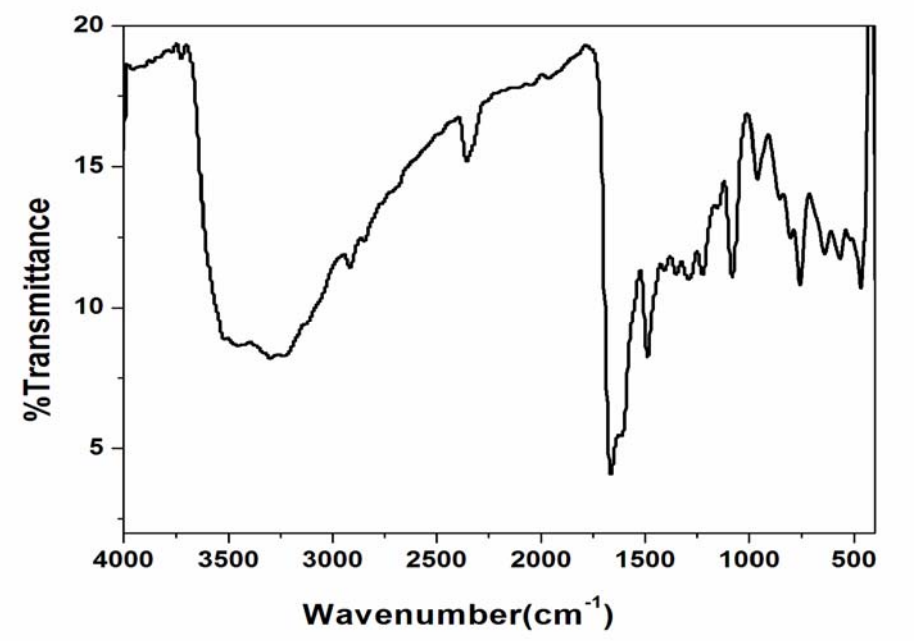

Figure 3.4. FTIR spectrum of [Pd(hqc6in)Cl_2]

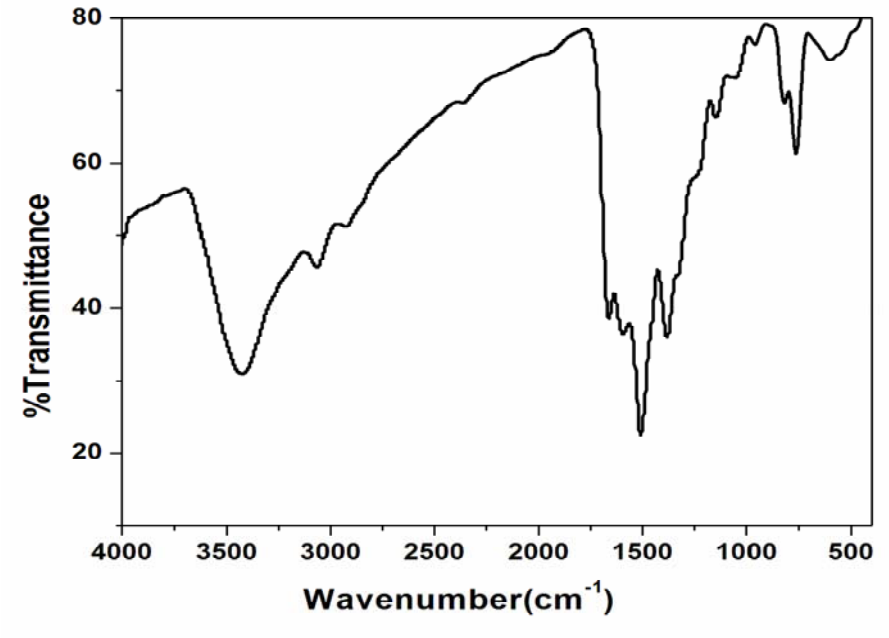

Figure 3.5. FTIR spectrum of [Pd(hqaqn)Cl_2]

3.3.3 Electronic spectra and magnetic moment data

All the Pd(II) complexes are diamagnetic. The Electronic spectral data of the complexes are given in Table 3.3 and spectra are shown in Figures 3.6-3.10.

Their electronic spectra show d-d spin- allowed transitions from the lower lying d levels to the empty $d_{x^2-y^2}$ orbital. The d^8 square planar palladium(II) complexes are expected to exhibit three spin-allowed d–d bands in their electronic spectra, corresponding to the $^1A_{1g}\rightarrow{}^1A_{2g}$, $^1A_{1g}\rightarrow{}^1B_{1g}$ and $^1A_{1g}\rightarrow{}^1E_g$ transitions. The transitions are assigned as a combinations of both $^1A_{1g}\rightarrow{}^1A_{2g}$ and $^1A_{1g}\rightarrow{}^1B_{1g}$ transitions as the difference in the energies of both b_{2g} (d_{xy}) and e_g (d_{xz},d_{yz}) levels is very low. The d-d transitions occur in these complexes in the range 19,010-31,550 cm^{-1} along with charge transfer bands. The nature of electronic spectra of these complexes suggest square planar geometry around Pd(II). Similar observations have been made in the case of square planar Pd(II) complexes (26-29).

Table 3.3. UV-visible spectral data of the complexes in DMSO

Complex	Electronic spectral bands:nm(cm^{-1})	Assignments
$[Pd(qc5in)Cl_2]$	231 (43,290)	CT
	264 (37,880)	CT
	386 (25,900)	$^1A_{1g} \rightarrow {}^1E_{2g}$
	556 (18,000)	$^1A_{1g} \rightarrow {}^1B_{1g}$
$[Pd(qc6in)Cl_2]$	216 (46,296)	Intra ligand transitions
	272 (36,760)	CT
	302 (33,110)	CT
	417 (23,980)	$^1A_{1g} \rightarrow {}^1A_{2g}$
$[Pd(hqc5in)Cl_2]$	224 (44,640)	Intra ligand transitions
	276 (36,230)	CT
	338 (29,590)	CT
	393 (25,450)	$^1A_{1g} \rightarrow {}^1E_{2g}$
	550 (18,180)	$^1A_{1g} \rightarrow {}^1B_{1g}$
	828 (12,080)	$^1A_{1g} \rightarrow {}^1A_{2g}$
$Pd(hqc6in)Cl_2]$	212 (47,170)	Intraligand transitions
	292 (34,250)	CT
	363 (27,550)	$^1A_{1g} \rightarrow {}^1E_{2g}$
	558 (17,920)	$^1A_{1g} \rightarrow {}^1B_{1g}$
	570 (17,540)	$^1A_{1g} \rightarrow {}^1A_{2g}$
$[Pd(hqaqn)Cl_2]$	232 (43,100)	CT
	255 (39,220)	CT
	354 (28,250)	$^1A_{1g} \rightarrow {}^1E_{2g}$
	410 (24,390)	$^1A_{1g} \rightarrow {}^1B_{1g}$
	526 (19,010)	$^1A_{1g} \rightarrow {}^1A_{2g}$

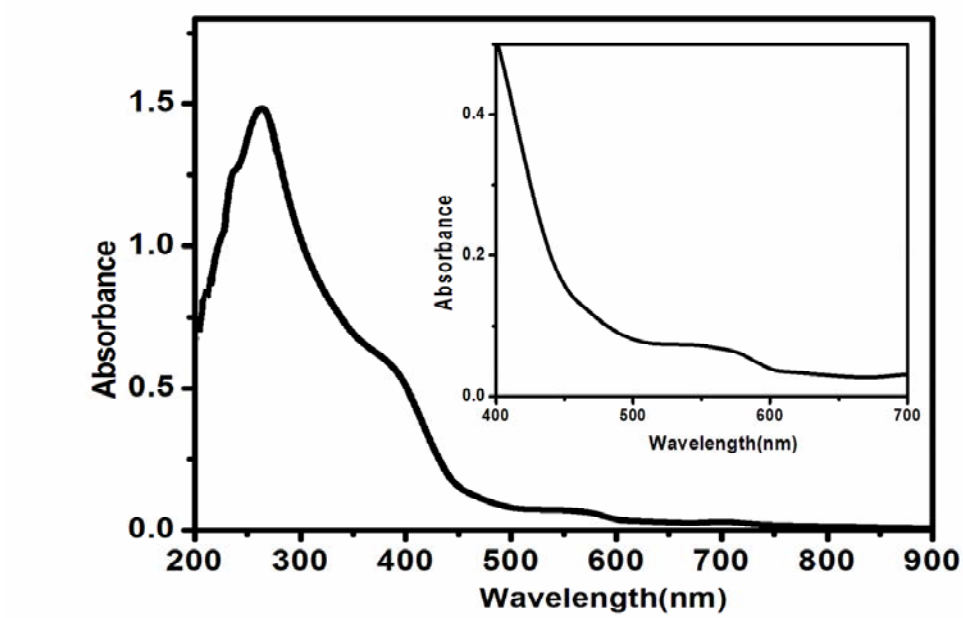

Figure 3.6. UV-Vis spectrum of [Pd(qc5in)Cl_2]

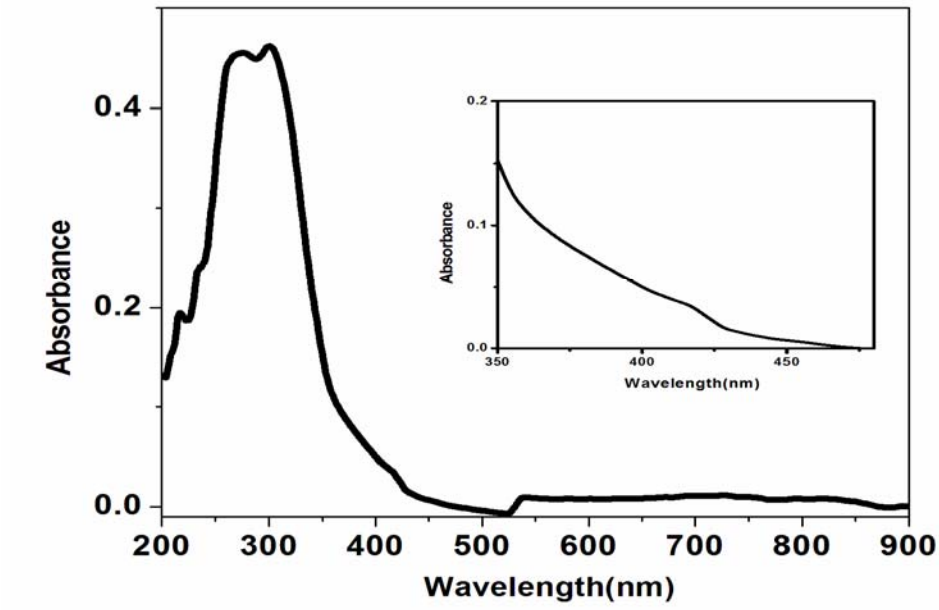

Figure 3.7. UV-Vis spectrum of [Pd(qc6in)Cl_2]

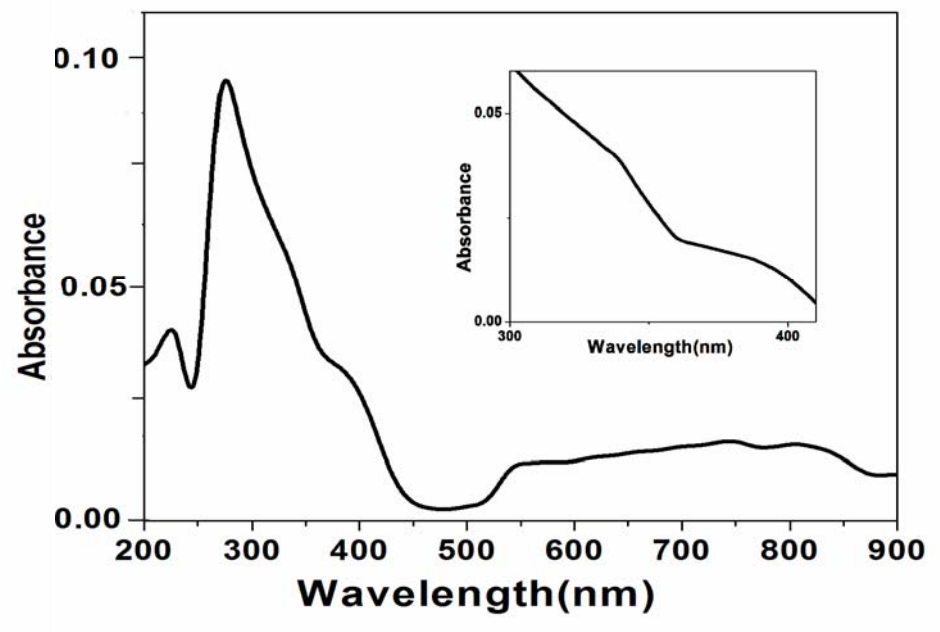

Figure 3.8. UV-Vis spectrum of [Pd(hqc5in)Cl_2]

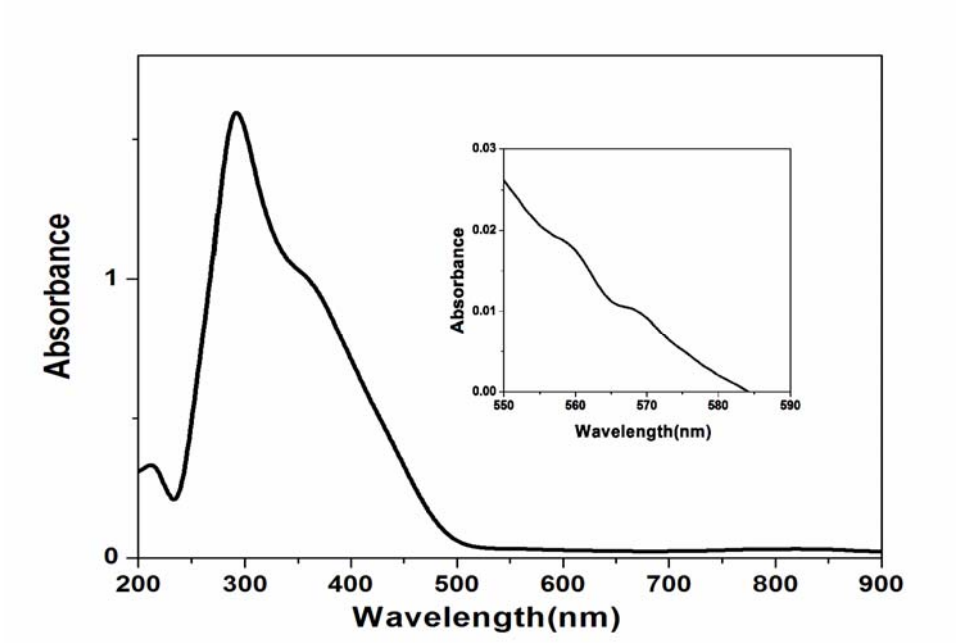

Figure 3.9. UV-Vis spectrum of of [Pd(hqc6in)Cl_2]

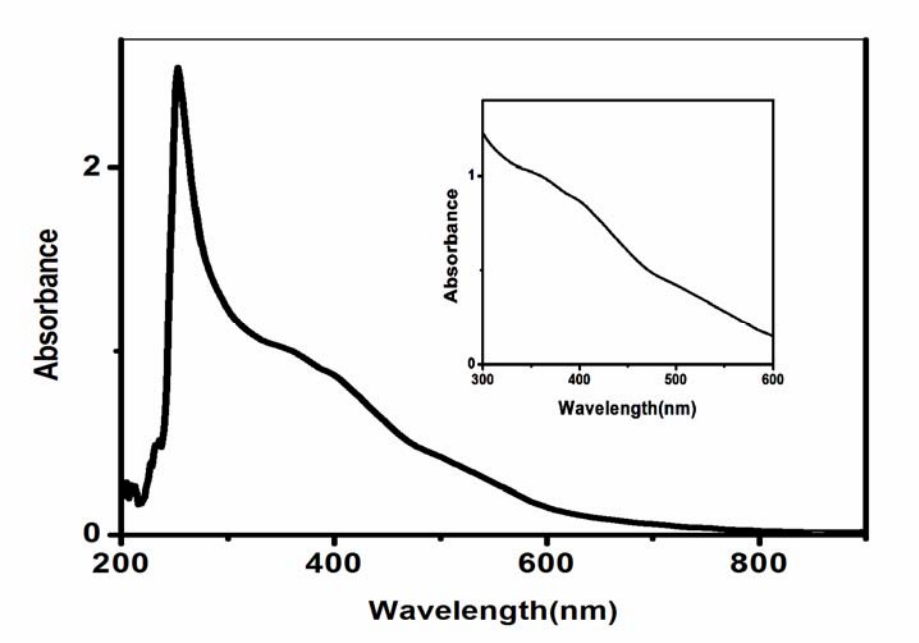

Figure 3.10. UV-Vis spectrum of of [Pd(hqaqn)Cl_2]

3.3.4 Cyclic voltammetry

The cyclic votammograms of mononuclear Pd complexes in DMSO show one well defined redox couple corresponding to $Pd^{II/I}$ and $Pd^{I/II}$. The data of Pd(II) complexes are given in Table 3.4 and Figures 3.11-3.15. The cathodic peak appears in the range -0.990 to -0.800 V for all the complexes corresponds to one electron reduction of Pd^{II} and the corresponding anodic peak appears in the range -0.610V to -0.580 V. The large ΔEp values of complexes (213-391 m V) indicate that these redox couples are quasi-reversibile (30). The reason for the quasi-reversibile electron transfer process may be due to slow electron transfer and the adsorption of the complex on the electrode surface (31). The ratio of the anodic and cathodic peak current is very smaller than unity for these two complexes implying quasi-reversible one electron transfer process. The variation in the redox potentials of the complexes might be due to electron donating ability of the ligands.

Table 3.4. Cyclic voltammetric data of Pd(II) complexes

Complex	E_{pc} (V)	E_{pa} (V)	$E_{1/2}$ (V)	I_{pc} (µA)	I_{pa} (µA)	No.of electrons (I_{pc}/I_{pa})
$[Pd(qc5in)Cl_2]$	-0.820	-0.606	-0.713	11.974	10.193	1.2
$[Pd(qc6in)Cl_2]$	-0.802	-0.589	-0.695	10.874	9.672	1.1
$[Pd(hqc5in)Cl_2]$	-0.816	-0.606	-0.711	5.677	5.768	1.0
$Pd(hqc6in)Cl_2]$	-0.996	-0.605	-0.800	4.021	3.440	1.2
$[Pd(hqaqn)Cl_2]$	-0.972	-0.591	-0.781	5.450	4.434	1.2

E_{pc} = cathodic peak potential; E_{pa} = anodic peak potential; I_{pc} =cathodic peak current; I_{pa} = anodic peak current; $E_{1/2} = 0.5 \times (E_{pa} + E_{pc})$; scan rate 100 mV (ΔEp=213mv to 391mV)

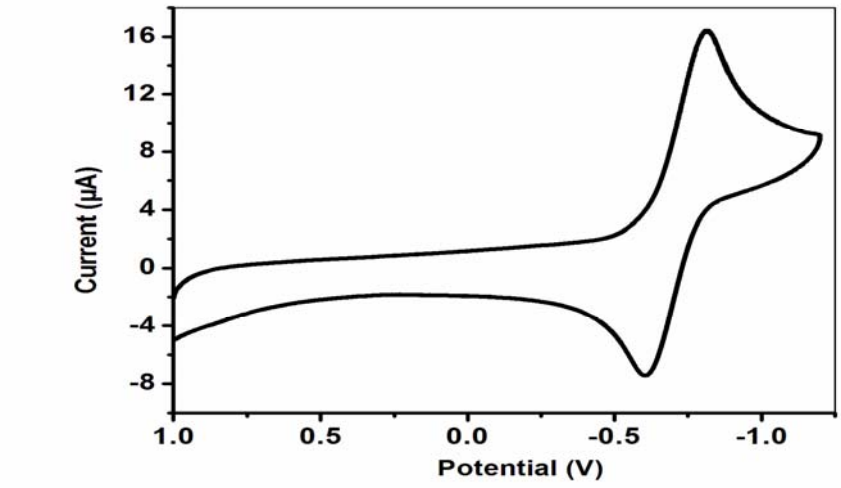

Figure 3.11. Cyclic votammogram of $[Pd(qc5in)Cl_2]$

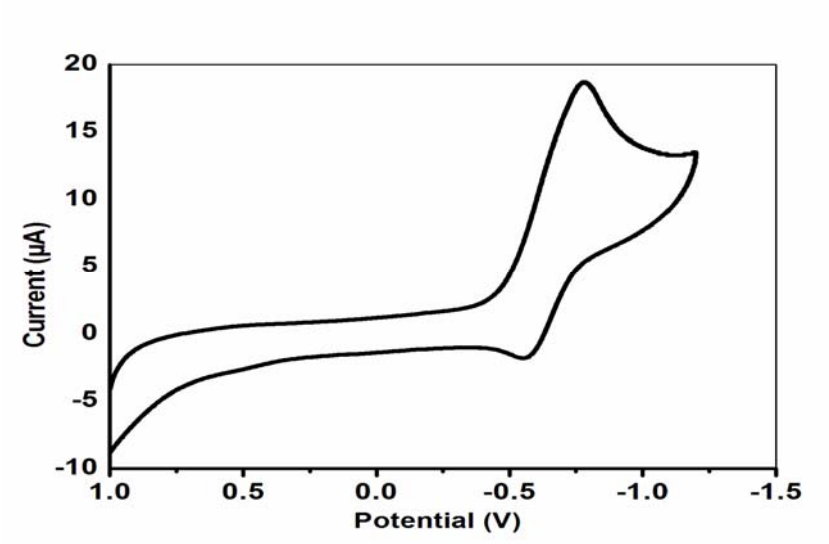

Figure 3.12. Cyclic votammogram of [Pd(qc6in)Cl_2]

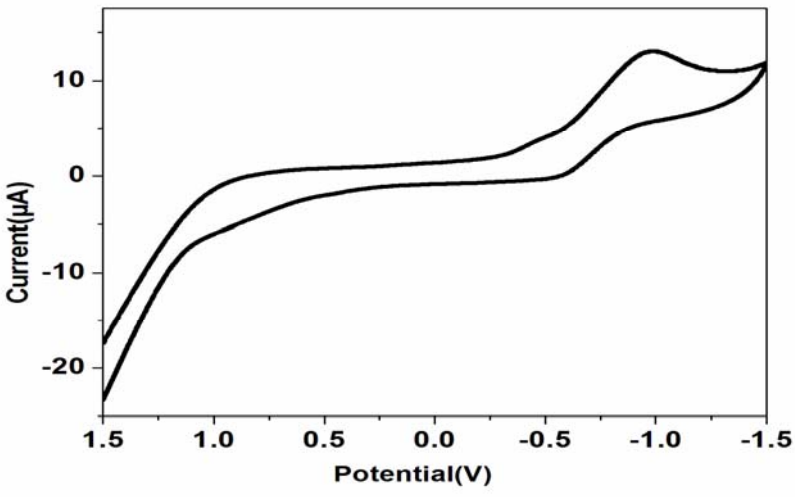

Figure 3.13. Cyclic votammogram of [Pd(hqc5in)Cl_2]

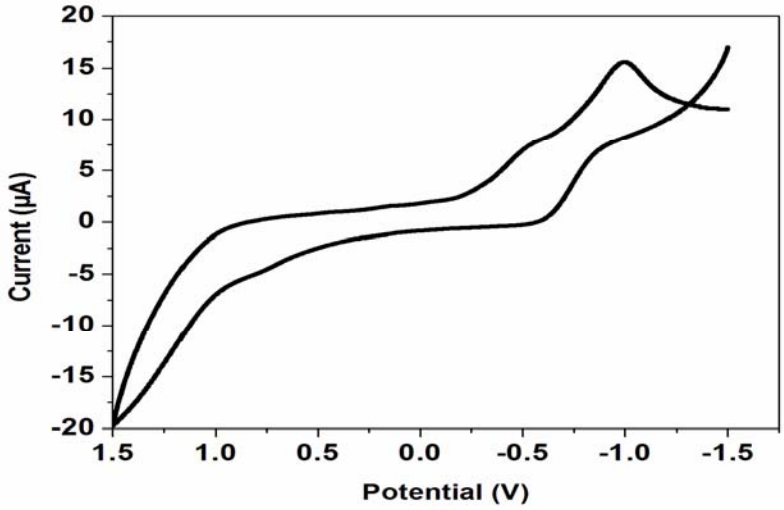

Figure 3.14. Cyclic votammogram of [Pd(hqc6in)Cl_2]

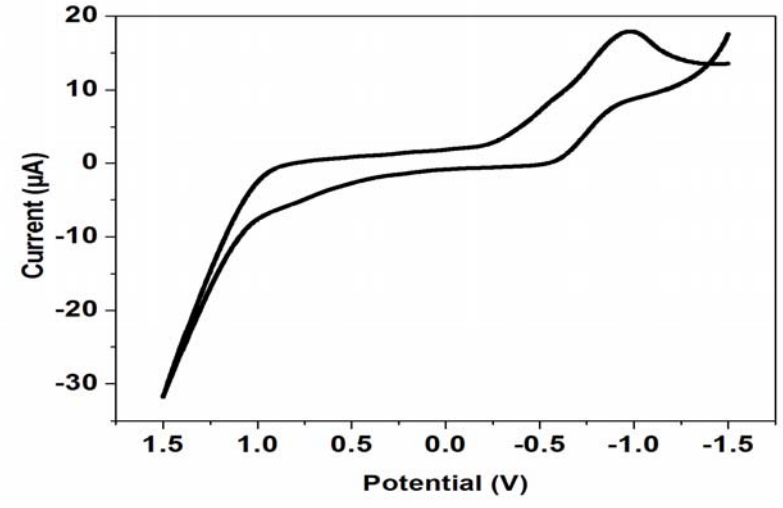

Figure 3.15. Cyclic votammogram of [Pd(hqaqn)Cl_2]

3.3.5 Geometry of the complexes

Based on the above studies square planar structure (Figure 3.16) has been assigned for the Pd(II) complexes, $[Pd(qc5in)Cl_2]$, $[Pd(qc6in)Cl_2]$, $[Pd(hqc5in)Cl_2]$, $[Pd(hqc6in)Cl_2]$, $[Pd(hqaqn)Cl_2]$.

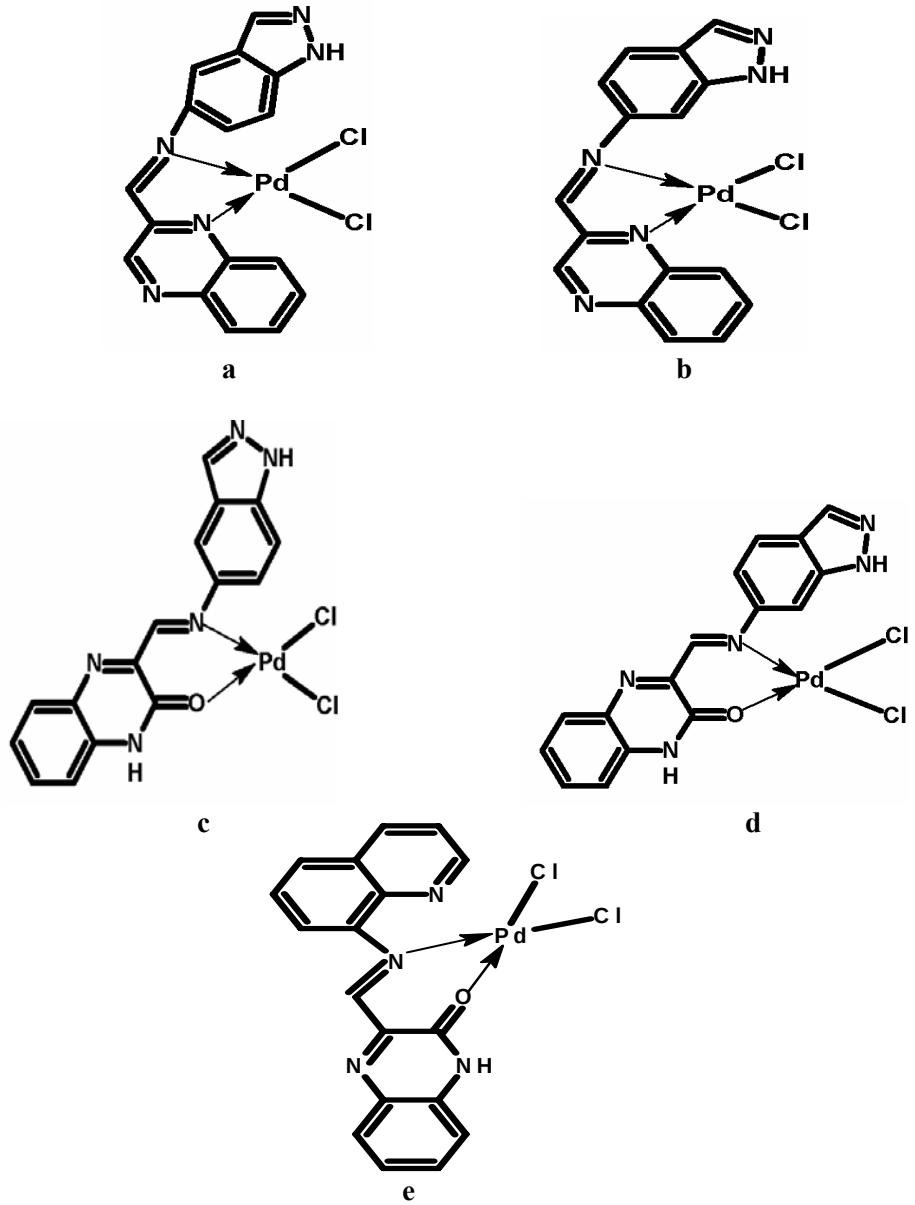

Figure 3.16. The Proposed geometry of Pd(II) complexes
here a= $[Pd(qc5in)Cl_2]$, b= $[Pd(qc6in)Cl_2]$, c=$[Pd(hqc5in)Cl_2]$, d=$[Pd(hqc6in)Cl_2]$, e=$[Pd(hqaqn)Cl_2]$,

3.4 DNA binding studies

There has been considerable interest in studying the affinity and selectivity in binding of metal complexes to DNA. The results of such studies may find application in chemotherapy and in the development of tools for biotechnology. Much work has been carried out to understand the noncovalent interactions of DNA by metal complexes. We have studied the interaction of the palladium complexes with DNA using absorption spectral studies, electrochemical studies and CD spectral studies. The results are presented in this section.

3.4.1 Absorption spectral studies

Electronic absorption spectroscopy is one of the powerful techniques for probing metal ion DNA interactions (32-34). The 'hyperchromic' effect and 'hypochromic' effect are spectral features of DNA concerning its double helix structure. 'Hypochromism' results from the concentration of DNA in the helix axis as well as from the change in conformation on DNA, while 'hyperchromism' results from the structural damage of DNA (35, 36). The extent of hyperchromism suggests the strength of intercalative binding; on the other hand either hyperchromism or hypochromism may result with metal complexes which bind non- intercalatively or electrostatically with DNA (37, 38).

Palladium(II) complexes do not give any intense d-d or charge transfer band to monitor their interaction with DNA. So the absorption band is used to monitor the changes. The electronic absorption titration of the complexes bas been carried out at a fixed concentration of the complexes (100 μM) in DMSO at 25 °C, varying the concentration of DNA and are illustrated in Figures 3.15-3.19. Palladium complexes in DMSO-buffer mixtures show bands in the region 290-370 nm and are assigned to ligand to metal charge transfer (LMCT) transitions. When the amount of DNA is increased, the intensity of the charge transfer band is also changed, due to either hypochromism or hyperchromism. The

complexes [Pd(qc5in)Cl_2], [Pd(qc6in)Cl_2] and [Pd(hqaqn)Cl_2] in the presence of DNA shows hyperchromism with slight red shift. A similar hyperchromic effect has been observed for certain metal complexes when interacted DNA (39-41). The complexes [Pd(hqc5in)Cl_2] and [Pd(hqc6in)Cl_2] show hyperchromism without any shift.

For comparing the binding strength of metal complexes the intrinsic binding constant, K_b was determined from a plot of the [DNA]/(ε_A–ε_F) versus [DNA] equation (42)

$$[DNA]/(\varepsilon_a–\varepsilon_f) = [DNA]/(\varepsilon_b–\varepsilon_f) + 1/K_b\ (\varepsilon_b–\varepsilon_f), \quad \text{where}$$

[DNA] = Concentration of DNA in base pairs,

ε_a = the apparent extinction coefficient = (A_{obsd}/[Complex]

ε_f = the extinction coefficient for free metal complex

ε_b = the extinction coefficient for free metal complex in the fully bound form

From the plot of [DNA]/ ε_a–ε_f versus [DNA], Kb was measured from the ratio of slope to intercept of the plot. The absorption spectra along with the plots are given in Figures 3.17-3.21 and the values of the binding constants are given in Table 3.7. The order of the K_b values are in the following order [Pd(hqaqn)Cl_2] > [Pd(qc5in)Cl_2] > [Pd(qc6in)Cl_2] > [Pd(hqc6in)Cl_2] > [Pd(hqc6in)Cl_2]. The K_b values show that the interaction is very strong between the complexes and Herring sperm (HS) DNA. The binding constants for qc5in, qc6in and hqaqn complexes are greater than those observed for other known DNA-intercalative complexes, such as $Ru(bpy)_2MPPIP]^{2+}$ (where bpy = 2,2′-bipyridine, MPPIP=2-(3′-phenoxyphenyl) imidazo[4,5-f]-1,10] phenanthroline) ($Kb=4.44\times10^4\ M^{-1}$) (43) [$Cu_2Cl_4$ $(phen)_2$] ($Kb=4.8\times10^4\ M^{-1}$) (44), [$Pd_2(\mu\text{-bzta})_4$] 1.5DMSO (where bzta = benzothiazole-2-thiolate) ($Kb=1.2\times10^4$) (45). All these results show that the present Pd(II) complexes have high DNA affinity.

Table 3.7. Binding constant of palladium complexes

Complex	Binding Constant(Kb) M^{-1}
$[Pd(qc5in)Cl_2]$	4.9×10^5
$[Pd(qc6in)Cl_2]$	3.1×10^5
$[Pd(hqc5in)Cl_2]$	2.1×10^3
$[Pd(hqc6in)Cl_2]$	3.2×10^3
$[Pd(hqaqn)Cl_2]$	5.5×10^5

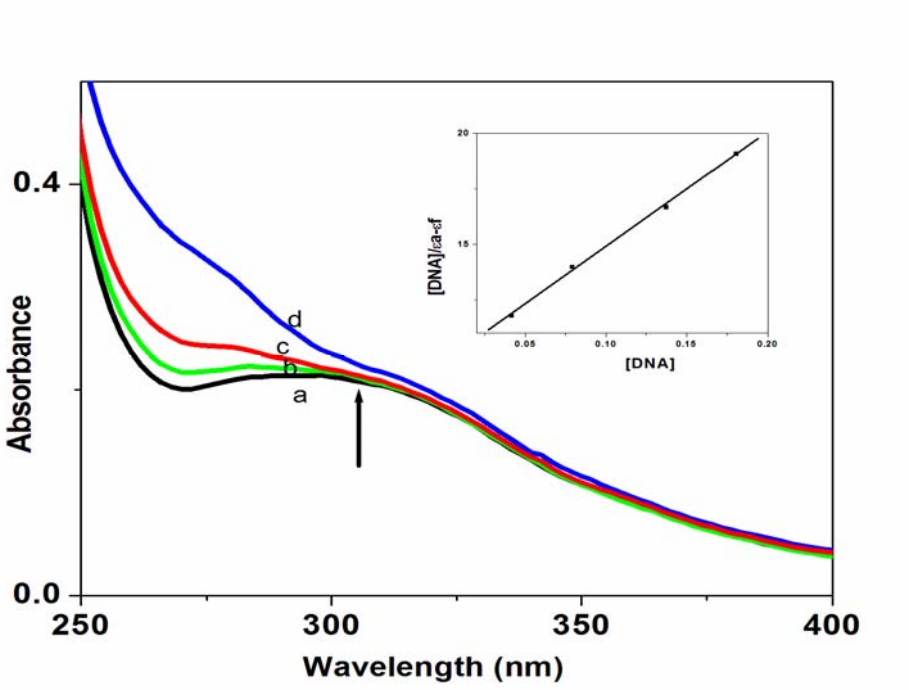

Figure 3.17. Absorption spectra of $Pd(qc5in)Cl_2$ in 5mM Tris-HCl buffer at pH 7.1 in the absence (a) and presence (b, c and d) of increasing amounts of HS DNA. Arrow indicate the absorption changes upon increasing the DNA Conc.(Inset: A plot of [DNA]/[DNA]/εa-εf)

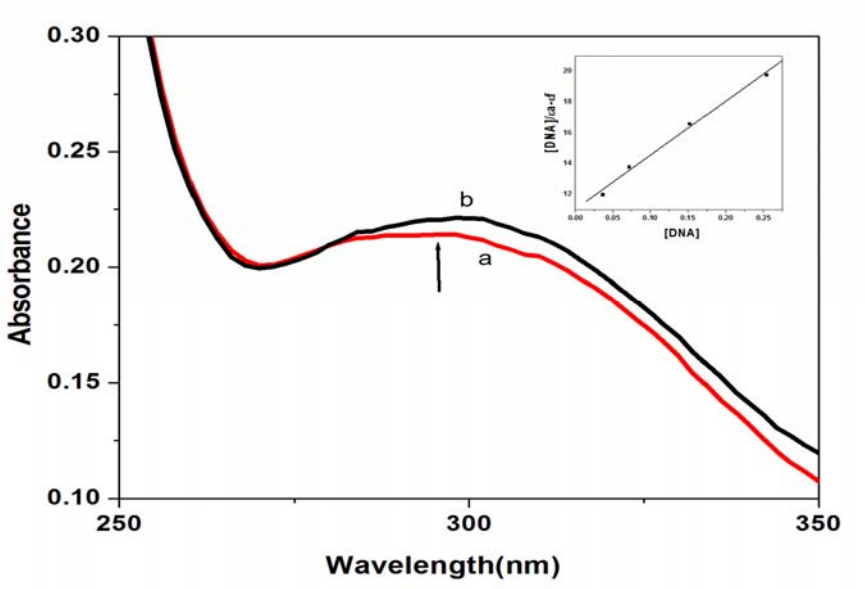

Figure 3.18. Absorption spectra of Pd(qc6in)Cl_2 in the absence(a) and presence (b) of HS DNA. Arrow indicate the absorption changes upon increasing the DNA Conc.(Inset: A plot of [DNA]/[DNA]/εa-εf)

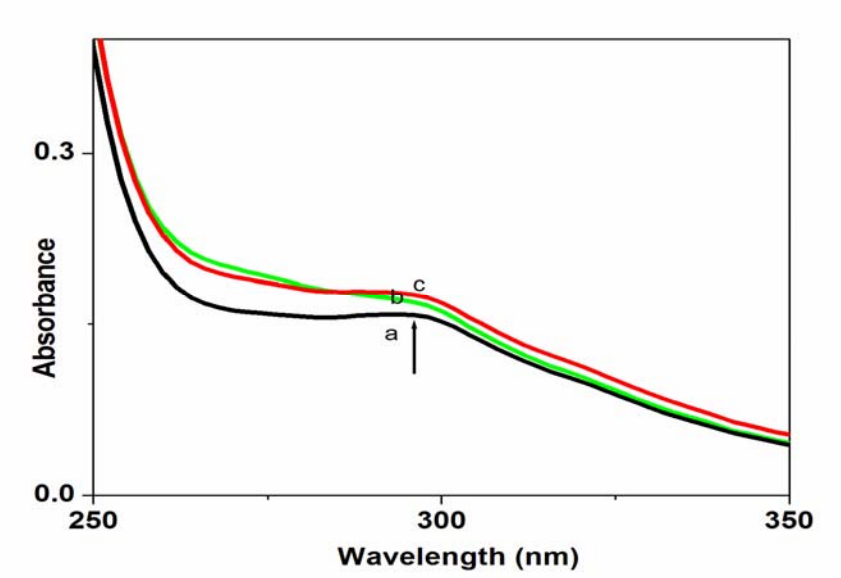

Figure 3.19. Absorption spectra of Pd(hqc6in)Cl_2 in 5mM Tris-HCl buffer at pH 7.1 in the absence (a) and presence (b and c) of increasing amounts of HS DNA. Arrow indicate the absorption changes upon increasing the DNA Conc.

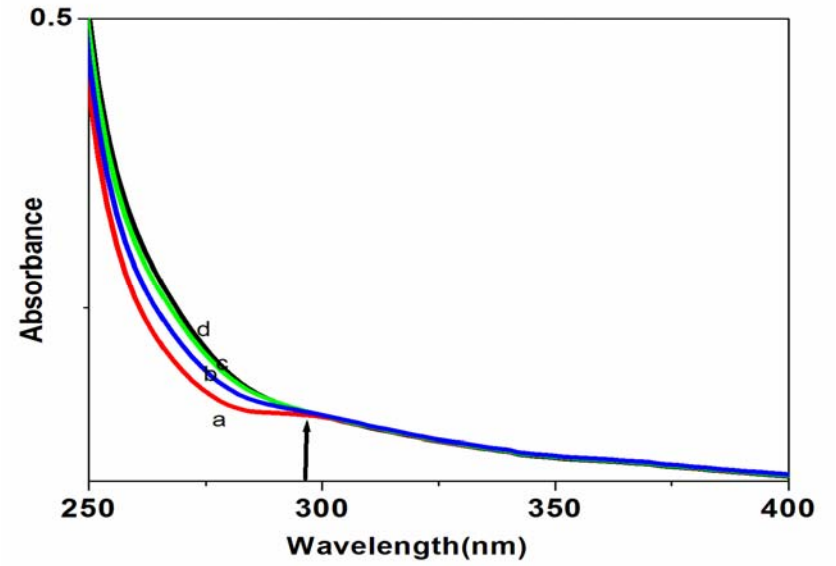

Figure 3.20. Absorption spectra of Pd(hqc6in)Cl_2 in the absence(a) and presence (b, c and d) of HS DNA. Arrow indicate the absorption changes upon increasing the DNA Conc.

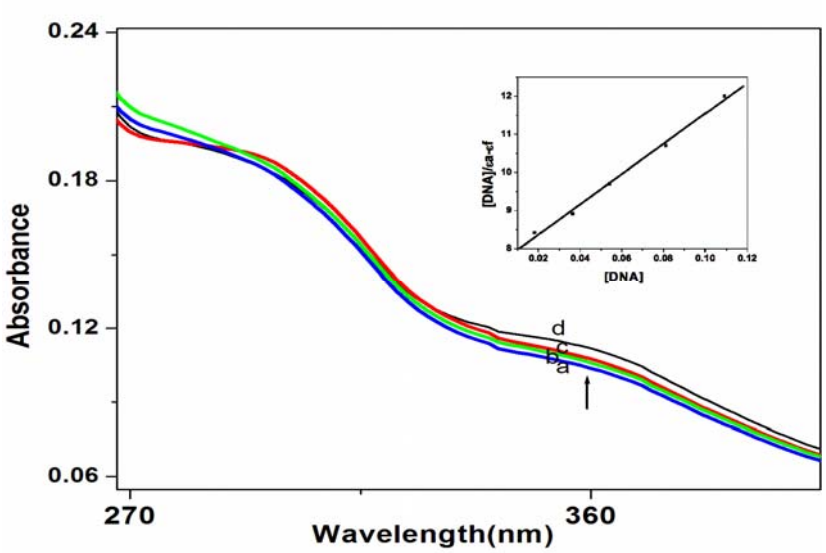

Figure 3.21. Absorption spectra of Pd(hqaqn)Cl_2 in the absence (a) and presence (b, c and d) of HS DNA. Arrow indicate the absorption changes upon increasing the DNA Conc.(Inset: A plot of [DNA]/[DNA]/εa-εf)

3.4.2 Electrochemistry

Cyclic voltammetric (CV) studies have been carried to probe the binding of the present complexes to DNA in buffer solution, and the voltammetric data are reported in Table 3.6. and voltammogram given in Figure 3.22. The complex, [Pd(qc5in)Cl_2], shows both cathodic and anodic peak potentials. On increasing the concentration of DNA the E_{pc} values undergo a positive shift of potential (shifts to less negative values). This shift might be due to the interaction of the reduced form of the complexes with DNA. The obvious shift of peak potential indicates the strong association of the complex with DNA [46]. It is reported by Bard *et.al.* that interaction will be intercalation or groove binding if the peak potential is shifted positively [*47*].

It is clear from the Table 4.6 and figure 3.22, the peak potential shift occurs positively for [Pd(qc5in)Cl_2] , so the mode of binding is intercalation or groove. The formal potential $E_{1/2}$ is taken as the average of Epc and $E_{pa.}$ The half wave potential $E_{1/2}$ of this complex undergoes a positive shift from -0.699 to -0.630 V (nearly 70 mV). This high shift after the addition of HS-DNA suggests high-binding affinity of [Pd(qc5in)Cl_2]. In addition to changes in the formal potential, the voltammetric currents decrease up on addition of DNA to the complex. This decrease in current is due to diffusion of an equilibrium mixture of free complex and DNA- bound complex to the electrode surface (48). All the observations point towards the fact that the complex, [Pd(qc5in)Cl_2], interact HS-DNA either in an intercalating way or through grooves.

Table 3.6. Cyclic voltammetric data of [Pd(qc5in)Cl_2] in the presence of different concentrations of DNA in Tris-HCl (5mM) buffer pH=7.1

Complex	R	E_{pc}/V	E_{pa}/V	ΔEp (V)	I_{pc}	I_{pa}	I_{pc}/I_{pa}	$E_{1/2}$ (V)	$\Delta E_{1/2}$ (mV)
[Pd(qc5in)Cl_2]	0	-0.807	-0.592	.214	7.69	7.52	1.02	-.699	
	0.2	-0.780	-0.557	.222	6.45	6.09	1.05	-.669	30
	0.4	-0.778	-0.553	.224	5.43	5.42	1.00	-.666	33

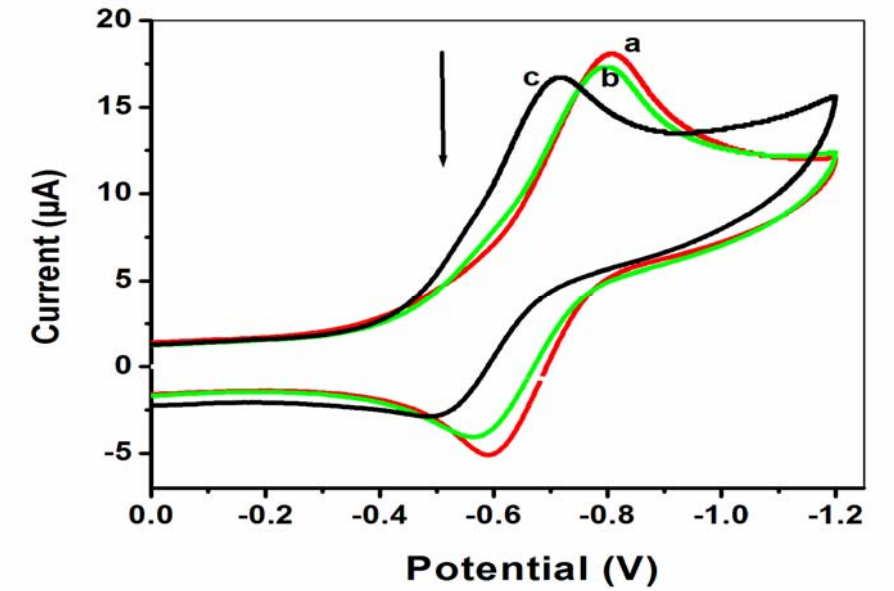

Figure 3.22. Cyclic voltammogram of the [Pd(qc5in)Cl_2] in the absence(a) (R=0) and presence (b and c) (R=0.2-0.4) of different concentrations of of DNA at the scan rate of 100mVs^{-1}.

As the anodic peak potential (E_{pa}) could not identified for complexes [Pd(qc6in)Cl_2], [Pd(hqc5in)Cl_2], [Pd(hqc6in)Cl_2] and [Pd(hqaqn)Cl_2] differential pulse voltametry (DPV) was conducted to observe the changes in the formal potential and current. Cyclic voltammograms of these complexes are shown in Figures 3.23-3.24. $E_{1/2}$ values of these complexes were calculated from DPV (Figures 3.25-3.28) and are given in table 3.7. For complexes, [Pd(qc6in)Cl_2] and [Pd(hqaqn)Cl_2], at different concentrations of DNA the peak current decreases and E_{pc} shifts to more positive potential. But for complexes, [Pd(hqc5in)Cl_2] and [Pd(hqc6in)Cl_2], E_{pc} shifts to negative potential.

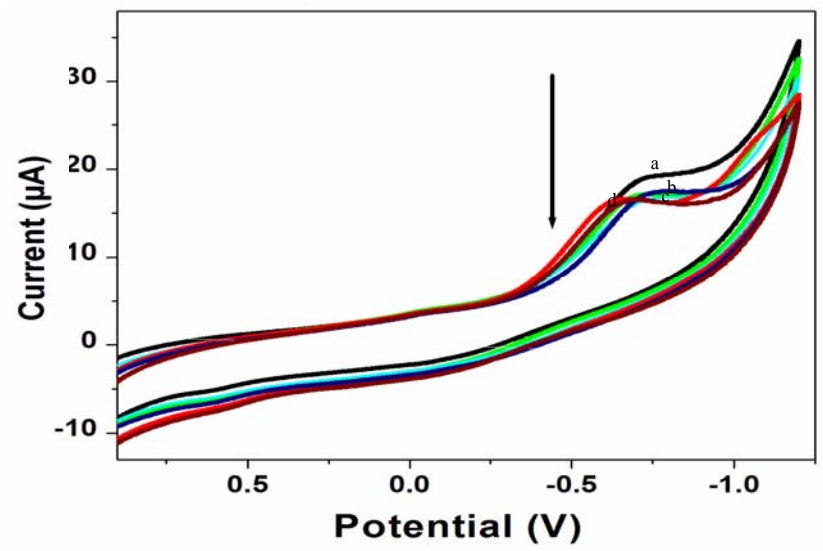

Figure 3.23. Cyclic voltammogram of the [Pd(qc6in)Cl_2] complex in the absence (a) and presence (b, c and d) of different concentrations of DNA in Tris-HCl (5mM) buffer pH=7.1

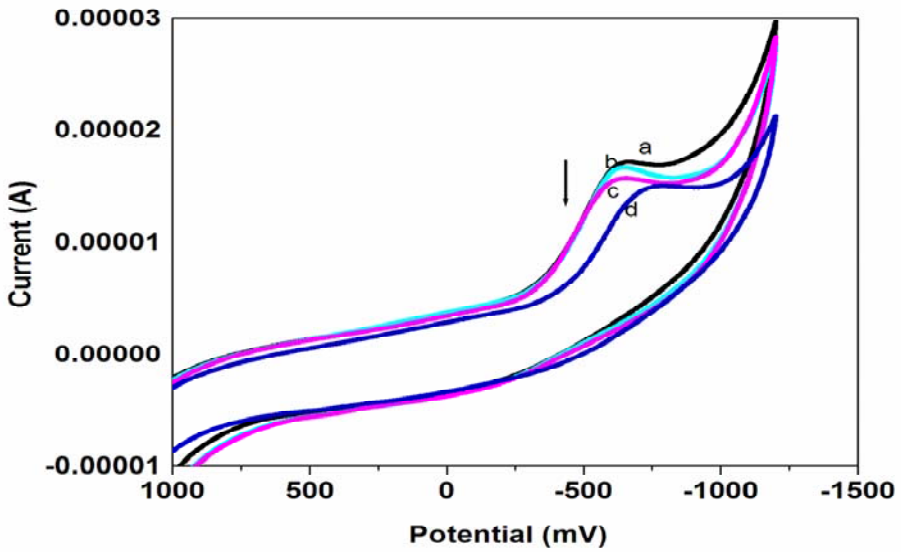

Figure 3.24. Cyclic voltammogram of the [Pd(hqaqn)Cl_2] complex in the absence (a) and presence (b, c and d) of different concentrations of DNA in Tris-HCl (5mM) buffer pH=7.1

Table 3.7. Differential Pulse voltammetric data of Palladium complexes in the presence of different concentrations of DNA in Tris-HCl buffer pH=7.1

Complex	R	E_{pc}/V	$E^{1/2}$(V)	$\Delta E^{1/2}$(mV)
[Pd(qc6in)Cl_2]	0	-0.628	-0.653	
	0.2	-0.587	-0.612	41
	0.4	-0.533	-0.558	95
	0.6	-0.528	-0.553	100
[Pd(hqc5in)Cl_2]	0	-0.525	-0.550	
	0.2	-0.540	-0.565	-15
	0.4	-0.544	-0.569	-19
	0.6	-0.588	- 0.613	-63
[Pd(hqc6in)Cl_2]	0	-0.653	-0.678	
	0.2	-0.669	-0.694	-16
	0.4	-0.673	-0.698	-20
	0.6	-0.684	-0.709	-31
[Pd(hqaqn)Cl_2]	0	-0.628	-0.653	
	0.2	-0.622	-0.647	6
	0.4	-0.591	-0.616	37
	0.6	-0.590	.0.615	38

$E_{1/2}$= Ep+ΔE/2 where $E_{1/2}$ is equivalent to the average of E_{pc} and E_{pa} in CV measurements and ΔE is the pulse amplitude (50 mV)

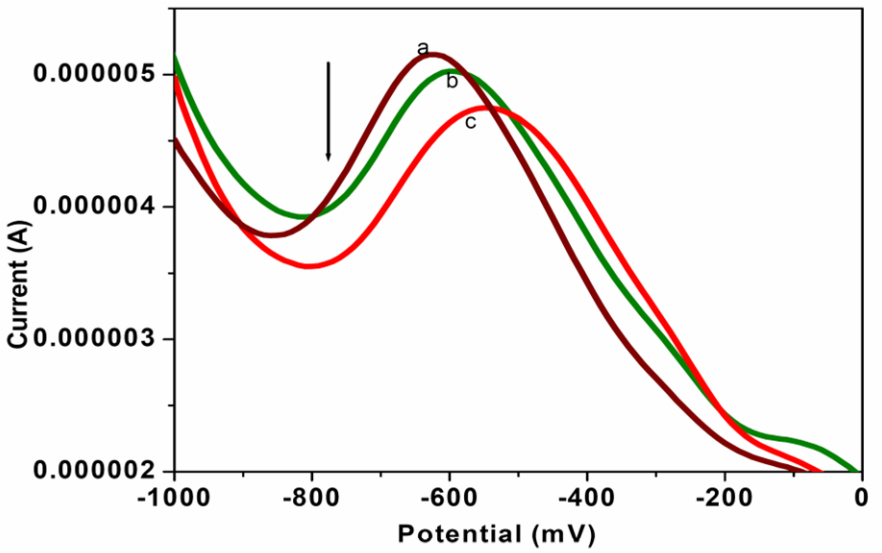

Figure 3.25. Differential pulse voltammogram of the [Pd(qc6in)Cl_2] complex in the absence (a) and presence (b and c) of different concentrations of DNA

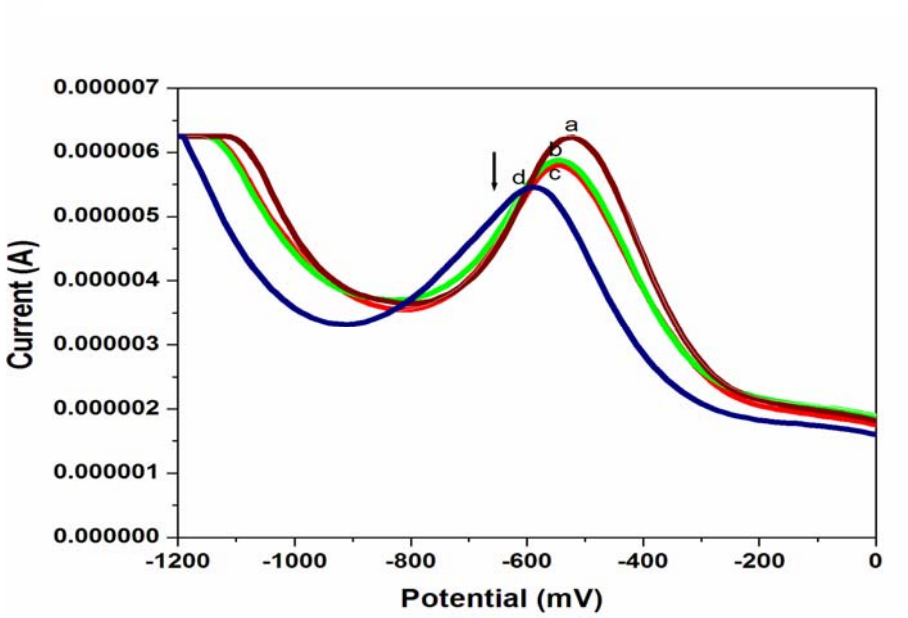

Figure 3.26. Differential pulse voltammogram of the [Pd(hqc5in)Cl_2] complex in the absence(a) and presence (b, c and d) of different concentrations of DNA in Tris-HCl buffer pH=7.1

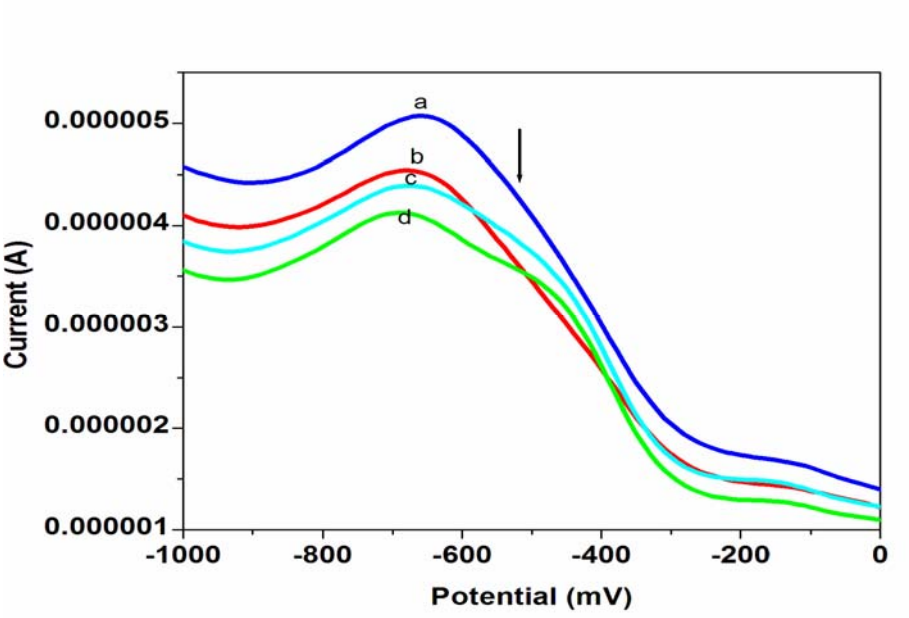

Figure 3.27. Differential pulse voltammogram of the [Pd(hqc6in)Cl_2] complex in the absence(a) and presence (b, c and d) of different concentrations of DNA in Tris-HClbuffer pH=7.1

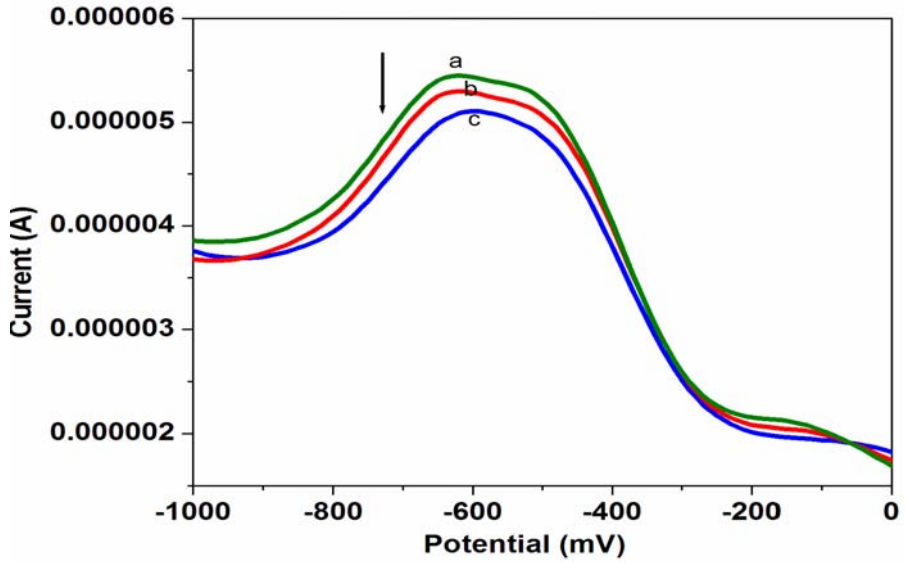

Figure 3.28. Differential pulse voltammogram of the [Pd(hqaqn)Cl_2] complex in the absence(a) and presence (b and c) of different concentrations of DNA in Tris-HCl (5mM) buffer pH=7.1

In the light of the results from the Bard's group, complexes [Pd(qc6in)Cl_2] and [Pd(hqaqn)Cl_2] interact with DNA through groove binding mode in contrast to [Pd(hqc5in)Cl_2] and [Pd(hqc5in)Cl_2], whose interaction mode is electrostatic in natures

3.4.3 CD spectral titration

Additional evidence for the interaction of DNA and Pd(II) complexes were obtained by CD measurements. The changes in intrinsic CD of chiral molecules reflect the binding geometry and binding mode of the complex with DNA bases (49).

The chirality of DNA double helix originates from the DNA geometry, the coupling of bases, phosphate backbone and chiral sugar units. The perturbed CD spectrum of DNA suggest the conformational changes brought about by the interacting guest molecules. Thus simple groove binding and electrostatic interaction of a small molecules with DNA show less or no perturbations on the

base stacking and helicity bands, while intercalation enhances the intensities of both the bands (50). If the spectrum changes both in shape and intensity, it may be attributed to a number of factors which include:

a) occupancy of more than one binding site with increase of concentration of the complex
b) ligand – ligand interaction and
c) changes in the DNA conformation.

In the present study each sample solution was scanned in the range 22-320 nm regions. The titration curves for each of the complexes are presented in Fig.4.9-4.11 and the data are given in Table 4.5. The observed CD spectrum of HS- DNA consists of a positive band at 275 nm due to base stacking and a negative band at 245 nm due to helicity, which are characteristic of B form of DNA (51)

When HS- DNA was allowed to interact with the complexes, the bands were modified. On increasing the concentration of $[Pd(qc5in)Cl_2]$ or $[Pd(qc6in)Cl_2]$ the positive band at 275 nm and negative band at 245 nm show an increase in the molar ellipticity. Furthermore a slight red shift (1-3nm) was observed without any change in the zero crossover at 258nm. The enhancement of molar ellipticity in the positive band has been assigned to an increase in the winding angle of the DNA helix with a concomitant decrease in the number of base pairs per helical turn (52).

The small increase in the molar ellipticity of the positive band and negative band of the CD spectrum of DNA observed for $[Pd(qc5in)Cl_2]$ and $[Pd(qc6in)Cl_2]$ indicates that the interaction between the metal complexes and DNA induces only slight modifications of the native conformation of DNA. This phenomenon could be due to groove binding. The CD spectral data did not indicate any change in the conformation of HS-DNA and therefore B form of the DNA is stabilised in these cases.

Table 3.8. CD parameters for the interaction of HS-DNA with Pd(II) complexes

samples	1/R	Positive band		Negative band	
		λ_{max} (nm)	CD (mdeg)	λ_{max} (nm)	CD (mdeg)
DNA	0	275	2.605	245	-2.174
[Pd(qc5in)Cl_2]	0.2	279	3.324	247	-2.242
[Pd(qc6in)Cl_2]	0.4	276	3.112	247	-2.292
	0.6	276	3.290	247	-2. 447
	0.8	278	3.343	247	-2.439
[Pd(hqc5in)Cl_2]	0.4	276	2.531	245	-1.762
[Pd(hqc6in)Cl_2]	0.2				
	0.4	276	2.598	245	-2.168
	0.6	275	2.594	246	-2.170
[Pd(hqaqn)Cl_2]	0.4	279	2.781	247	-2.220
	0.6	277	2.981	247	-2.482
		277	2.997	248	-2.478

Measurements made at1/R value of 0.2-0.6
where 1/R=[Complex]/[DNA]
Cell path length=1mm

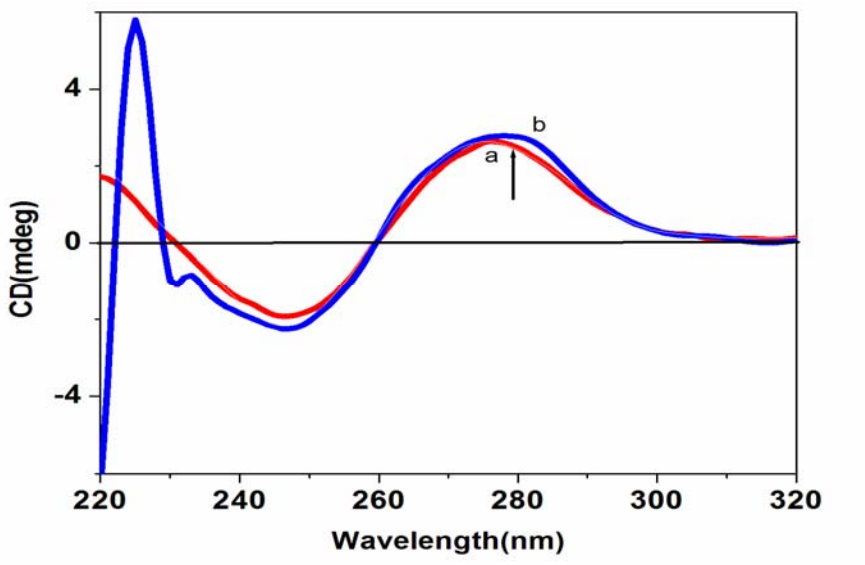

Figure 3.29. CD spectra of DNA in the absence (a) and presence (b) of complex [Pd(qc5in)Cl_2] in Tris HCl buffer pH 7.1.

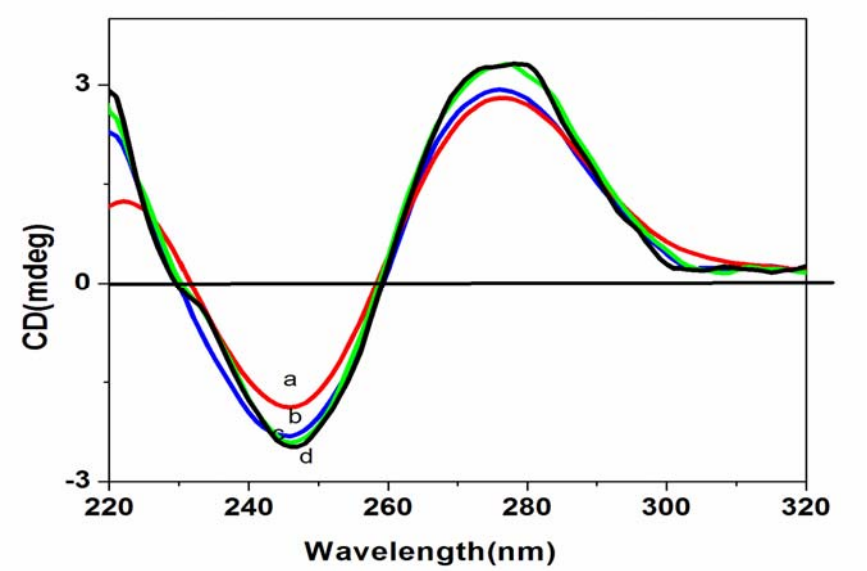

Figure 3.30. CD spectra of DNA in the absence (a) and presence (b, c and d) of complex, [Pd(qc6in)Cl_2] in Tris HCl buffer pH 7.1.

In the case of [Pd(hqc5in)Cl_2] and [Pd(hqc6in)Cl_2], the intensity of the negative ellipticity band decreases almost similar to that for the positive ellipticity. This suggests that the DNA binding of the complexes do not affect the conformations of DNA.

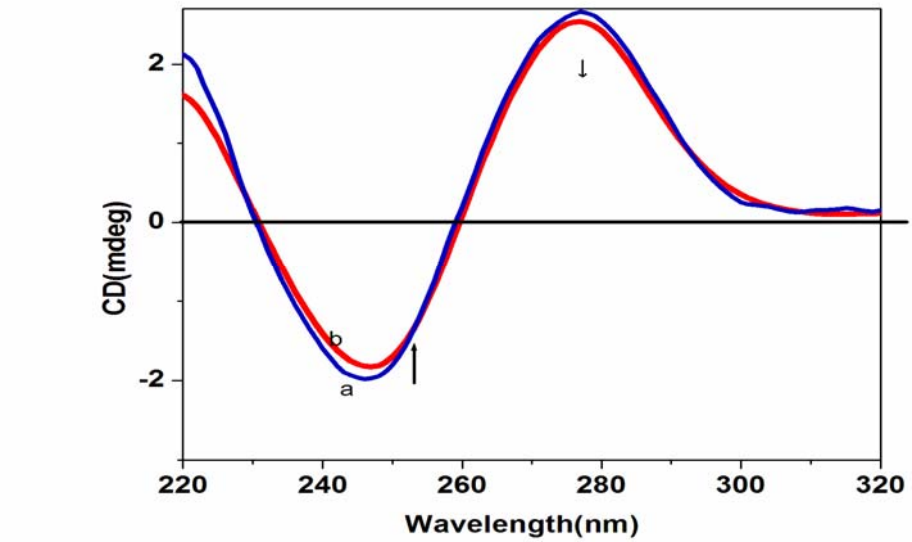

Figure 3.31. CD spectra of DNA in the absence (a) and presence (b) of complex, [Pd(hqc5in)Cl_2] in Tris HCl buffer pH 7.1.

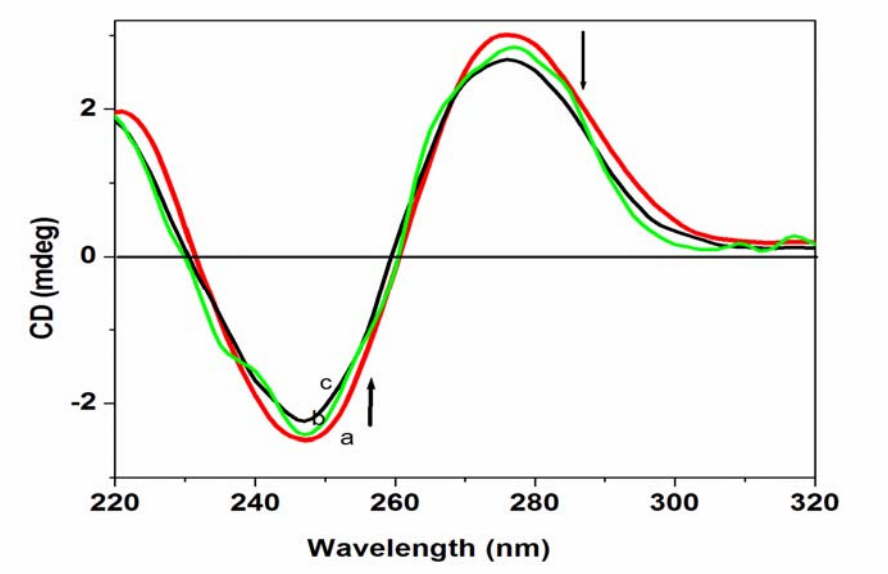

Figure 3.32. CD spectra of DNA in the and absence (a) presence (b and c) of complex, [Pd(hqc6in)Cl_2] in Tris HCl buffer pH 7.1.

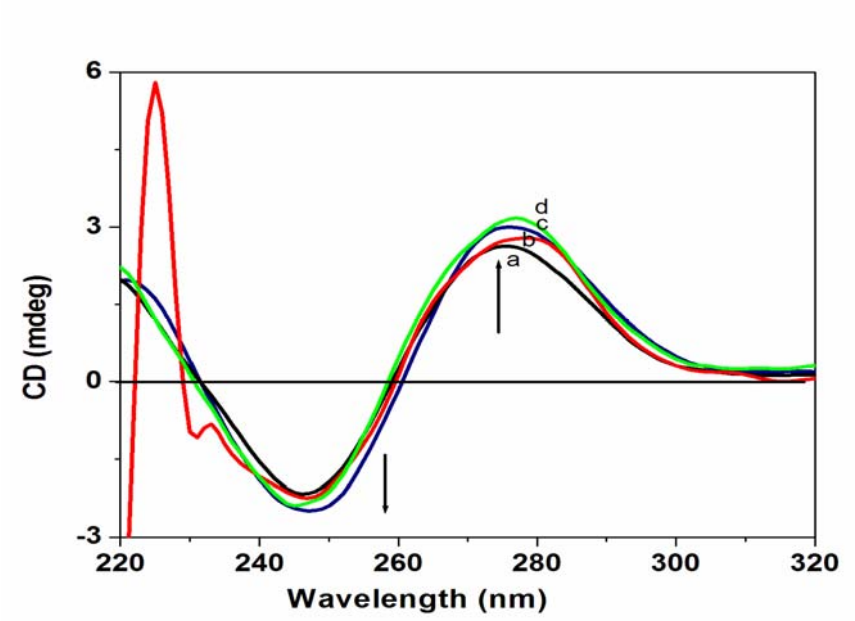

Figure 3.33. CD spectra of DNA in the absence(a) and presence (b, c and d) of complex, [Pd(hqaqn)Cl_2] in Tris HCl buffer pH 7.1.

For the complex, [Pd(hqaqn)Cl_2] the molar ellipticity of both positive and negative bands was seen to be increased. A slight red shift was also observed. These spectral changes may be due to DNA becomes A like on interaction with the complex (53). This indicates that the DNA is unwound upon interaction with this complex and suggest groove binding to DNA (54).

Eventhough the UV spectral and CV studies suggest the intercalative or groove binding for [Pd(qc5in)Cl_2], the CD studies suggest only groove binding for this complex. Thus the studies clearly reveal that binding of DNA with the complexes [Pd(qc5in)Cl_2], [Pd(qc6in)Cl_2] and [Pd(hqaqn)Cl_2] is through groove binding and that with the complexes [Pd(hqc5in)Cl_2] and [Pd(hqc6in)Cl_2] is electrostatic in nature.

3.5 DNA cleavage studies of the palladium complexes by gel electrophoresis method

The ability of the complexes to perform DNA cleavage is generally monitored by gel electrophoresis employing plasmid DNA like pUC19, pBR322 and pUC18 (55-58). In our study pUC18 plasmid DNA was used. On agarose gel, pUC18 shows two distinct bands corresponding to open circular and supercoiled forms. When circular plasmid DNA is subjected to electrophoresis, the fastest migration will be observed for the supercoiled form (Form I). If one strand is cleaved, the supercoil form will relax to produce a slower-moving nicked circular form (Form II). Agarose gel electrophoresis experiments using pUC18 plasmid DNA in the presence of the complex were carried out and the diagrams are shown in the Figures 3.34 and 3.35.

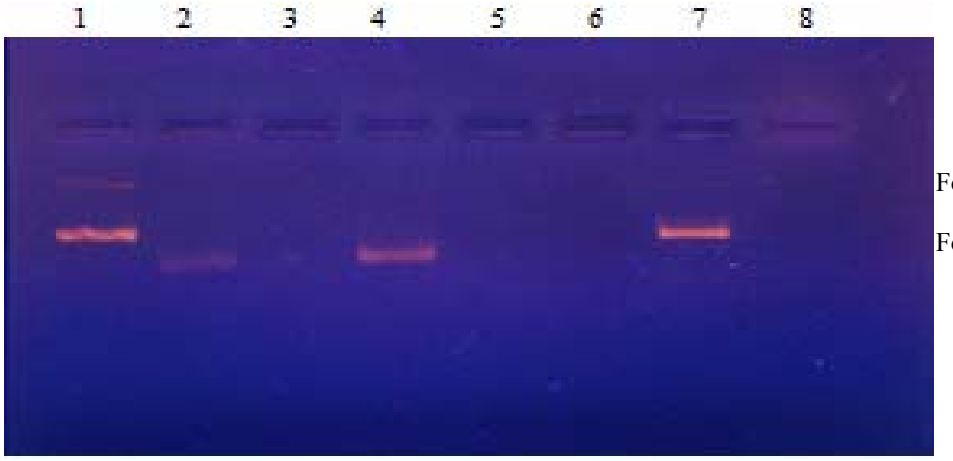

Lane 1 : pUC18 DNA
Lane 2 : pUC 18 DNA + [Pd(qc5in)Cl_2]
Lane 4 : pUC 18 DNA + [Pd(qc6in)Cl_2]
Lane 7 : pUC 18 DNA + [Pd(hqc5in)Cl_2]

Figure 3.34. Cleavage of pUC 18 DNA in the presence of Pd(II) complexes

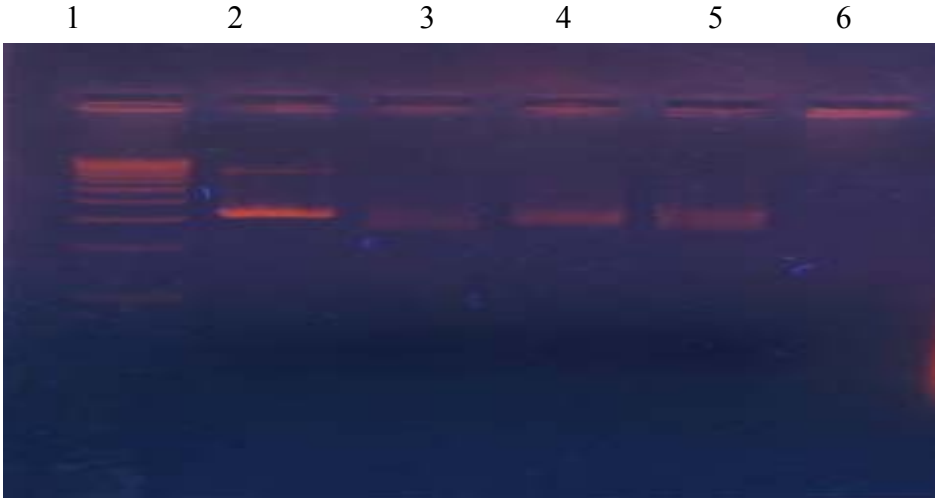

Lane 1 : 500 bp DNA marker
Lane 2 : pUC 18 DNA
Lane 3 : pUC 18 DNA + [Pd(qc6in)Cl_2
Lane 4 : pUC 18 DNA + [Pd(hqc6in)Cl_2
Lane 5 : pUC 18 DNA + [Pd(hqaqn)Cl_2

Figure 3.35. Cleavage of pUC 18 DNA in the presence of Pd(II) complexes

Two bands were observed for pUC18 DNA (Lane 1) which corresponds to the open circular (Form II) and supercoiled form (Form I) see figure 3.34. In the presence of complexes, [Pd(qc5in)Cl_2] (lane 2), [Pd(qc6in)Cl_2] (lane 4)

[Pd(hqc5in)Cl_2] (lane 7), only one form of plasmid pUC18 was visible which corresponds to supercoiled DNA (Form I). In these cases other open circular form is not visible. These complexes have good ability to cleave DNA.

A marker is used to identify the lanes of pUC18 plasmid DNA (Figure 3.35). Only one form of plasmid pUC18 is visible (lane 3 – 6) which corresponds to supercoiled DNA (Form I) and other open circular form is not visible. Thus it could be concluded that the binding of the metal complexes resulting in the conformational changes in DNA by degrading the whole open circular DNA (Form II) and also diminishing in the intensity of the supercoiled form (Form I) by degrading it. The complexes Pd(qc6in)Cl_2, Pd(hqc6in)Cl_2 and [Pd(hqaqn)Cl_2 show efficient DNA cleavage activity. Similar observations for the reported Pd(II) complexes (59, 60).

3.6 Conclusion

All the Pd(II) complexes are square planar and diamagnetic in nature. The DNA binding behaviour of these complexes was studied by UV-Vis spectra, CV, DPV and CD spectral studies. Upon electronic absorption spectral titration, the complexes, [Pd(qc5in)Cl_2], [Pd(qc6in)Cl_2]and [Pd(hqaqn)Cl_2] show hyperchromism with slight red shift and complexes [Pd(hqc5in)Cl_2], and [Pd(hqc5in)Cl_2] show hyperchromism with no shift. From CV and CD the results clearly reveal that binding of DNA with the complexes [Pd(qc5in)Cl_2], [Pd(qc6in)Cl_2] and [Pd(hqaqn)Cl_2] is through groove binding, the complexes [Pd(hqc5in)Cl_2], and [Pd(hqc5in)Cl_2], electrostatically binds with DNA. The binding constant (K_b) for th complexes is in the order [Pd(hqaqn)Cl_2]> Pd(qc5in)Cl_2]> [Pd(qc6in)Cl_2]> [Pd(hqc6in)Cl_2] > [Pd(hqc6in)Cl_2]. The capability of cleavage of pUC18 DNA by the complexes indicates that the complex exhibits an efficient DNA-cleavage.

3.7 References

[1] E.J. Gao, Y.G. Sun, Q.T. Liu, L.Y. Duan, *J. Coord. Chem*. 59 (2006) 1295

[2] E.J. Gao, S.M. Zhao, Q.T. Liu, *Russ J Coord Chem*. 33 (2007) 120

[3] J.L. Butour, S. Wimmer, F. Wimmer, P. Castan, *Chem. Biol. Inter* 104 (1997) 165.

[4] R. Jose, L. Julia, V. Consuelo, L. Gregorio, M.L. Jose, M. Miguel, X.A. Francesc, B. Delia, M. Virtudes, *J. Inorg. Chem* 47 (2008) 6990.

[5] R. Jose, D.V. Marıa, C. Natalia, L. Gregorio, H. Concepcion de, B. Delia, M. Virtudes, V. Laura, *J. Inorg. Chem* 47 (2008) 4490.

[6] R. Guddneppanavar, J.R. Choudhury, A.R. Kheradi, B.D. Steen, G. Saluta, G.L. Kucera, C.S. Day, U. Bierbach, *J. Med. Chem* 50 (2007) 2259.

[7] R. Jose, L. Julia, S. Laura, C. Natalia, V. Consuelo, D.V. Marıa, X.A. Francesc, L. Gregorio, M. Virtudes, P. Jose, B. Delia, *J. Inorg. Chem* 45 (2006) 6347.

[8] W. Micklitz, W.S. Sheldrick and B. Lippert, *Inorg. Chem.* 29 (1990) 211.

[9] E. Budzisz, M. Miernicka, I. P. Lorenz, P. Mayer, R.A. Kwiecien, P. Paneth, U. Krajewska, M. Rozalski, *Inorg. Chem.* 45 (2006) 9688.

[10] H. Baruah, C.G. Barry, U. Bierbach, *Curr. Top. Med. Chem* 4 (2004) 1537.

[11] M. Sonmez, M. Çelebi**,** Y. Yardım**,** Z. Şenturk**,** *European Journal of Medicinal Chemistry 45 (2010) 4215*

[12] E.J. Gao, M. C. Zhu, Y. Huang, L. Liu, H.Y. Liu, F.C. Liu, S. Ma, C.Y. Shi, *European Journal of Medicinal Chemistry* 45 (2010) 1034.

[13] M. Yodoshi, N. Okbe, *Chem. Pharm. Bull*. 56 (2008) 908.

[14] E.J. Gao, M.C. Zhu, H.X. Yin, L. Liu, Q. Wu, Y.G. Sun, *J. Inorg. Biochem*. 102 (2008) 1958.

[15] R. Mital, G.M. Shan, T.S. Srivastava, R.K. Bjattacharya, *Life Sci.* 50(1992) 781.

[16] N. Nikolis, C. Methenitis, G. Pneumatikakis, M.M.L. Fiallo, *J. Inorg. Biochem*. 89 (2002) 131.

[17] N. Nikolis, C. Methenitis, G. Pneumatikakis, *J. Inorg. Biochem*. 95 (2003) 177.

[18] A.G. Quirogen, J.M. Perez, I. L. Solera, E.I. Montero, J.R. Masagure, C. Alonso, C. N. Ranninger, *J. Inorg. Biochem*. 69(1998) 275.

[19] E. Budzisz, M. Malecka, I.P. Lorenz, P. Mayer, R.A. Kwiecien, P. Paneth, U. Krajewska, M. Rozalski, *Inorg. Chem*. 45 (2006) 9688.

[20] A.G. Quirogen, J.M. Perez, E.I. Montero, J.R. Masagure, C. Alonso, C. N. Ranninger, *J. Inorg. Biochem*. 70 (1998) 117.

[21] A.G. Quirogen, J.M. Perez, E.I. Montero, D.X. West, C. Alonso, C. Navarro-Ranninger, *J. Inorg. Biochem*. 75 (1999) 293–301.

[22] P.G. Ramappa and K.G. Somashekharappa, *Indian J.Chem*, 33A (1994) 67.

[23] P.G. Ramappa, K.G. Somashekharappa, *Indian J.Chem*, 5 (1993) 41.

[24] L.J. Baucher, *J. Inorg. Nucl. Chem*. 36 (1974) 531.

[25] J. Uttamachandani, R.N. Kapoor, *Trans. Met. Chem* 3 (1978) 79.

[26] A.M. Khattab, M. S. Soliman, *Transition Met. Chem.* 8 (1983) 285

[27] M.A. Ali, A. H. Mirza See, T.W. Keng, *Transition Metal Chemistry* 28 (2003) 241.

[28] R. K. Agarwal, S.Prasad, *Turk J. Chem* 29 (2005) 289.

[29] E. Kwiatkowski, M. Kwiatkowski, *Inorg. Chim. Acta* 117 (1986) 145-(1986) 149.

[30] Koca, H.A. Dincer, M.B. Kocak, A. Gul *Russian Journal of Electrochemistry,* 42 (2006) 31–37.

[31] A.W. Wallace, W.R. Murphy, J.D. Peterson, *Inorg. Chim. Acta,* 166 (1989) 47.

[32] Q.Wang, Z.Y.Yang, G.F. Qi, D.D. Qin, *Eur. J. Med. Chem.* 44 (2009) 2425.

[33] Q.L. Zhang, J.G. Liu, J.Z. Liu, H. Li, Y. Yang, H. Xu, H. Chao, L.N.Ji, *Inorg. Chim. Acta* .339 (2002) 34.

[34] X.H. Zou, B.H. Ye, H. Li, J.G. Liu, Y. Xiong, L.N. Ji, J. *Chem. Soc.,Dalton Trans.* (1999) 1423.

[35] F.Q. Liu, Q.X. Wang, K. Jiao, F.F. Jian, G.Y. Liu, R.X. Li, *Inorg. Chim. Acta*. 359 (2006) 1524.

[36] D. Lawrence, V.G. Vaidyanathan, B. Unni Nair, *J. Inorg. Biochem*. 100 (2006) 1244.

[37] E.C. Long, J.K. Barton, *Acc. Chem. Res*. 23 (1990) 271.

[38] S. Tabassum, I.U.H. Bhat, *Chem. Pharm. Bull.* 58 (2010) 318.

[39] M. Chauhan, K. Banerjee, F.Arjmand, *Journal of Inorganic Chemistry*. 46 (2007) 3072.

[40] F. Arjmand, B. Mohani, S. Parveen, *Bioinorganic Chemistry and Applications* (2006) 1

[41] J. Chen, X. Wang, Y. Shao, J. Zhu, Y. Li, Q. Xu, Z. Guo, *Inorg. Chem*. 46 (2007) 3306

[42] Wolfe, G.H. Shimer, T. Meehan, *Biochemistry* 26 (1987) 6392.

[43] L.F. Tan**,** X.H. Liu**,** H. Chao**,** L.N. Ji**,** *Jornal of Inorganic biochemistry* 101 (2007) 56.

[44] Q.Q. Zhang, F. Zhang, W.G. Wang, X.L. Wang, *J. Inorg. Biochem.* 100 (2006) 1344.

[45] E.J. Gao, K. H. Wang, X.F. Gu, Y. Yu, Y.G. Sun, W.Z. Zhang, H. X. Yin, Q.Wu, M. C. Zhu, X.M. Yan, *Journal of Inorganic Biochemistry* 101 (2007) 1404–1409

[46] J. Sun, D.K.Y.Solaiman, *J.Inorg.Biochem*.40 (1990) 271.

[47] M. T. Carter, A. J. Bard, *J. Am. Chem. Soc.* 111 (1989) 8901.

[48] R. Indumathy, S. Radhika, M. Kanthimathy, T. Weyhermuller, B. Unni Nair, *J. Inorg. Biochem.*101 (2007) 434.

[49] R. Vijayalakshmi, M. Kanthimathi, R. Parthasarathi, B.U. Nair, *Bioorg. Med. Chem.* 14 (2006) 3300.

[50] J.G. Collins, T.P. Shields, J.K. Barton, *J. Am. Chem. Soc.* 116 (1994) 9840.

[51] P. Uma Maheswari, V. Rajendiran, M.Palaniandavar, R. Thomas, G.U. Kulkarni, *Inorg.Chim. Acta*. 359 (2006) 4601.

[52] R.D. Sheardy, D. Suh, R.Kurzinsky, *J. Inorg.Biochem*. 101 (2007) 233.

[53] B. Selvakumar, V.Rajendran, P. Uma Maheswari, H.S. Evans, M.Palaniandavar, *J. Inrg.Biochem.* 100 (2006) 316.

[54] A.K. Patra, M. Nethaji, A.R. Chakravarthy, *J.Inorg.Biochem*.101(2007) 233.

[55] J. Sambrook, E. Fritsch, and I. Maniatis, "Molecular Cloning, A laboratory manual." (C.S.H.Laboratory, Ed), 3rd edition (2000).

[56] R.G.M. Moreno, M.V. Alipazaga, O.F. Gomes, E. Linares, M. H.G. Medeiros, N. Coichev, *J. Inorg. Biochem*. 101 (2007) 866.

[57] B. Macıas, M.V. Villa, B. Gomez, J. Borras, G. Alzuet, M. G.A lvarez, A. Castieiras, *J. Inorg. Biochem*. 101 (2007) 444.

[58] Ghosh, A.C. Barve, A.A. Kumbhar, A.S. Kumbhar, V.G. Puranik, P.A. Datar, U.B. Sonawane, R.R. Joshi, *J. Inorg. Biochem*. 100 (2006) 331.

[59] E. Gao**,** L. Wang**,** M.C. Zhu**,** L.Liu**,** W.Z. Zhang**,** *European Journal of Medicinal Chemistry* 45 (2010) 311.

[60] E.J. Gao, Y.G. Sun, Q.T. Liu and L.Y. Duan, *J. Coord. Chem.* 59 (2006) 1230

.....ꕥ.....

Chapter 4

Synthesis, characterisation and DNA interaction of iridium(III) complexes

Contents

The chemistry of iridium complexes has been receiving considerable current attention, because of the interesting biological properties exhibited by these complexes. Iridium complexes have useful applications in the biological field (1-6). Several iridium complexes of multidentate ligands containing O and N donor sites were used for catalysis (7). In comparison with other transition metal complexes, iridium complexes also have many chemical and industrial applications (8).

The DNA binding and in vitro cytotoxicity of the dinuclear Ir(III) polypyridyl complexes containing quinoxaline and 4,4'-bipyridine ligands show cytotoxicity against HT-29 (colon carcinoma) cells (9). Cyclometalated iridium compounds act as photoactivated agents in redox reactions with DNA (10). Anticancer studies of iridium(III) Schiff base complexes are relatively rare in the literature. So our study was mainly focused on DNA interaction of iridium(III) Schiff base complexes.

4.2 Experimental

4.2.1 Materials

The details of materials used for the syntheses of the Schiff base ligands are given in Chapter 2.

4.2.2 Synthesis of Schiff base ligands

The procedure for the synthesis of the Schiff base ligands are given in Chapter 2

4.2.3 Synthesis of complexes

$IrCl_3.3H_2O$ (1.80 g, 5 mmol) dissolved in ethanol (40 mL) was mixed with the Schiff base ligand qc5in (1.37 g, 5 mmol,), qc6in (1.37 g, 5 mmol), hqc5in (1.45 g, 5 mmol), hqc6in (1.45 g, 5 mmol) or hqaqn (1.5 g, 5 mmol) in ethanol (100 mL) in a molar ratio 1:1 and refluxing in an inert atmosphere for 3 hours. The complex separated out was isolated, washed with ethanol and dried in vacuo over P_4O_{10}. Yield: 52%.

4.3 Results and discussion

All the complexes are black and non-hygroscopic. They are soluble in DMSO and are insoluble in benzene, ethanol and chloroform.

4.3.1 Elemental analyses

Analytical data and conductance data are given in Table 4.1. The analytical data suggest that all the complexes are mononuclear and have metal to Schiff base ratio of 1:1. The molar conductance values of the complexes in DMSO (10^{-3} mol) indicate non-electrolytic nature.

Table 4.1. Analytical data a of the iridium(III) complexes

Complex of	C (%)	H (%)	N (%)	Cl (%)	Ir (%)	Molar conductance (ohm^{-1} cm^2 mol^{-1})
qc5in	32.52 (32.58)	2.22 (2.32)	11.82 (11.87)	17.86 (18.03)	32.48 (32.59)	16.6
qc6in	32.50 (32.58)	2.18 (2.32)	11.76 (11.87)	17.92 (18.03)	31.98 (32.59)	14.5
hqc5in	32.51 (32.60)	2.66 (2.74)	11.86 (11.88)	11.86 (12.03)	32.54 (32.61)	12.8
hqc6in	32.51 (32.60)	2.70 (2.74)	11.80 (11.88)	11.97 (12.03)	32.50 (32.61)	11.4
hqaqn	35.96 (36.00)	2.70 (2.85)	9.20 (9.33)	11.68 (11.81)	31.88 (32.00)	10.0

4.3.2 Thermal Analysis

Thermal analysis was mainly used to know information about the metal chelates and decide whether the water molecules in the complex are lattice held or coordinated. The first stage of decomposition occurs in the range 110-130 °C for qc5in and qc6in complexes can be attributed to the loss of one lattice water molecule. Whereas for hqc5in, hqc6in and hqaqn complexes the mass loss occurs in the range 130-230 °C corresponds to the loss of one coordinated water molecule. Decomposition of occurs at higher temperature. Although thermal degradation of the ligand part could not be approximated, the complete decomposition of the ligand occur above 600 °C in the complexes. The end product was stable metal oxide of Ir_2O_3.

From the elemental analysis,molar conductance and TG datas the molar formula of qc5in, qc6in, hqc5in, hqc6in, hqaqn complexes are $Ir(qc5in)Cl_3H_2O]H_2O$, $[Ir(qc6in)Cl_3H_2O]H_2O$, $[Ir(hqc5in)Cl_3H_2O]$, $[Ir(qc5in)Cl_3H_2O]$ and $Ir(hqaqn)Cl_3H_2O]$ respectively.

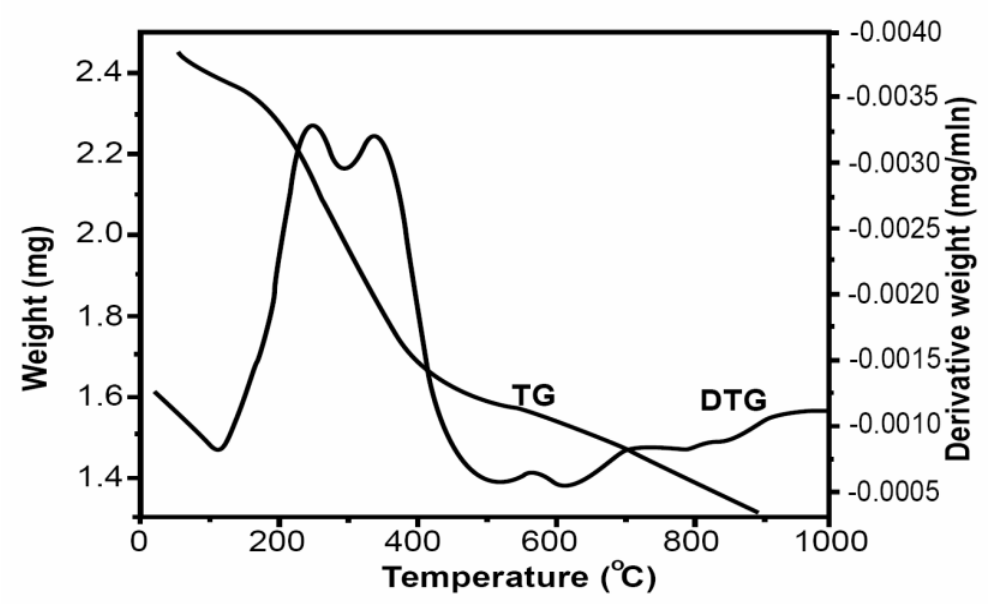

Figure 4.1. TG of [Ir(qc5in)Cl_3H_2O] H_2O

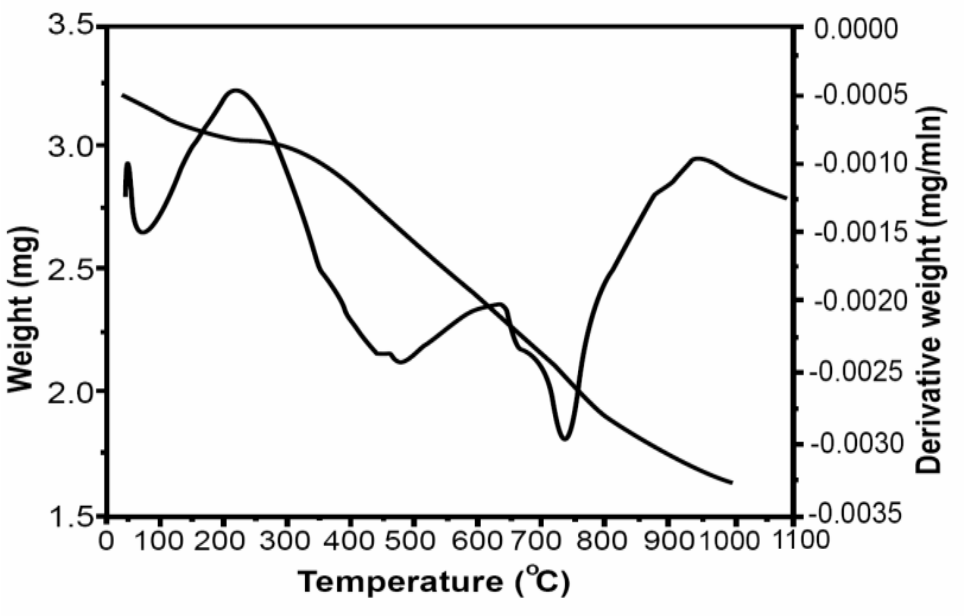

Figure 4.2. TG of [Ir(qc6in)Cl_3H_2O] H_2O

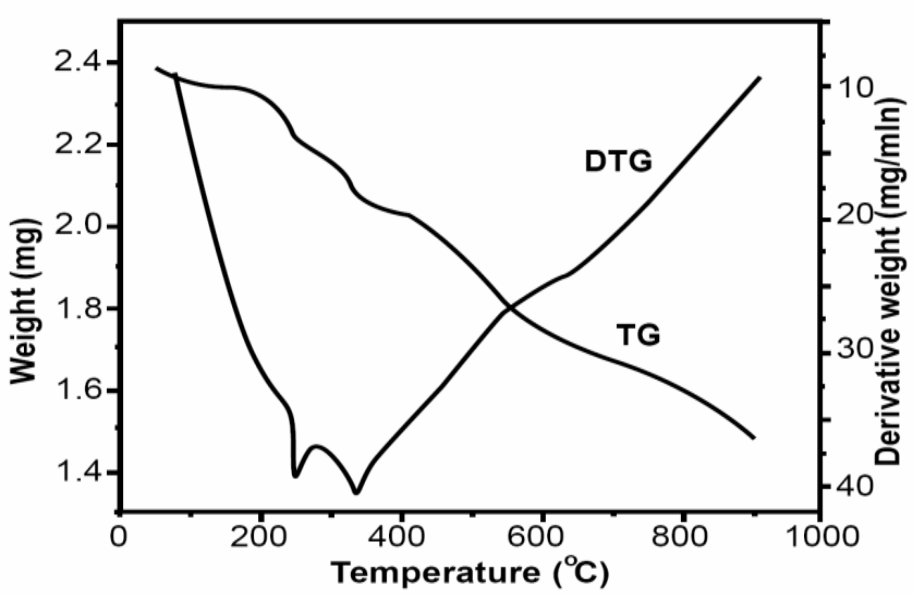

Figure 4.3. TG of [Ir(hqc5in)$Cl_3(H_2O)$]

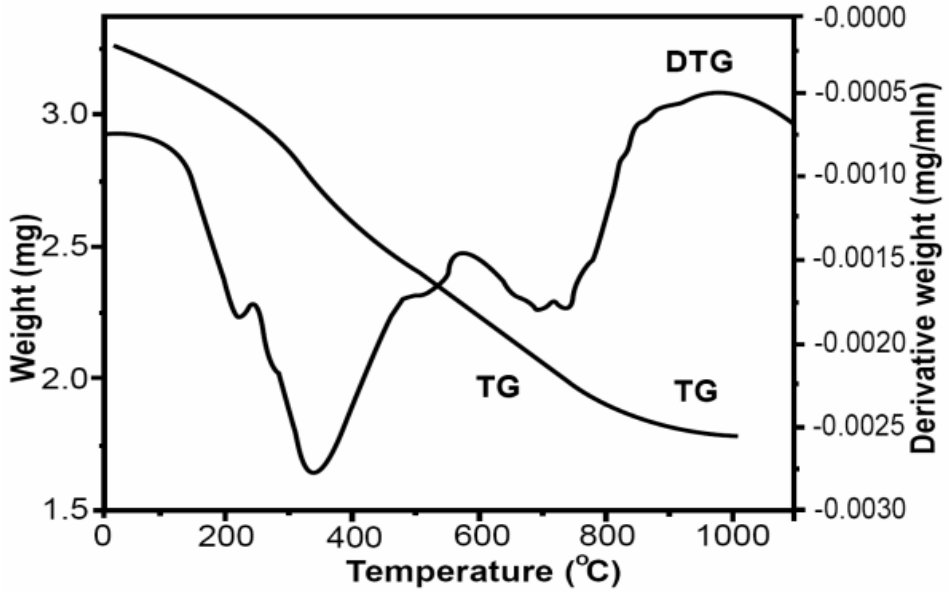

Figure 4.4. TG of [Ir(hqc6in)$Cl_3(H_2O)$]

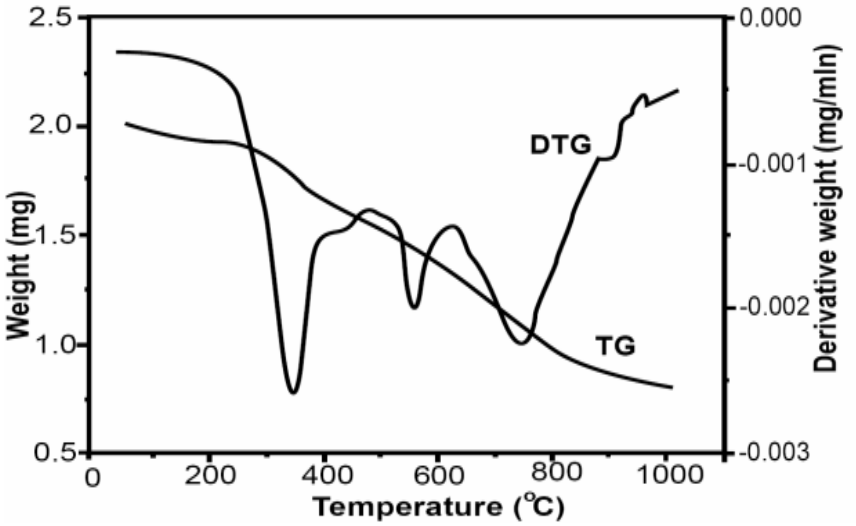

Figure 4.5. TG of [Ir(hqaqn)$Cl_3(H_2O)$]

4.3.3 Infrared spectra

The infrared absorption frequencies of the ligands and their metal complexes along with their assignments are listed in Table 4. 2. The FT-IR spectra of the Ir(III) complexes are given in Figures 4.6- 4.10. In all these spectra there is a broad band in the range 3040 - 3432 cm^{-1} assignable to coordinated water or uncoordinated water molecules associated with the complex. This fact is also indicated by the results of elemental analyses and TG-DTG of these complexes. The strong broad absorption band centered at 3229 cm^{-1} for [Ir(qc5in)Cl_3H_2O]H_2O and that at 3460 cm^{-1} for [Ir(qc6in)Cl_3H_2O] H_2O may be due to ν(NH). A strong broad absorption band is seen in the range 3210-3440 cm^{-1} for [Ir(hqc5in)$Cl_3(H_2O)$], [Ir(hqc6in)$Cl_3(H_2O)$] and [Ir(hqaqn)$Cl_3(H_2O)$] which may be due to hydrogen bonded ν(OH) in the iminol tautomer or ν(NH) in the amide tautomer. The bands centered at 1633 cm^{-1} for qc5in, at 1630 cm^{-1} for qc6in, at 1626 cm^{-1} for hqc5in, at 1612 cm^{-1} for hqc6in and hqaqn, which can be attributed to the azomethine stretching frequency decreases to 1612 cm^{-1},1610, 1598, 1602 and 1570 cm^{-1} respectively for their metal complexes suggesting the coordination of azomethine nitrogen to the metal (11, 12). The ν(C=N) of the quinoxaline ring in the spectra of qc5in and qc6in undergoes a

decrease in stretching frequency on complexation suggesting the coordination of the ring nitrogen to the metal in their complexes. However this band for the ligands hqc5in, hqc6in and hqaqn remains unchanged on complexation suggesting nonparticipation of quinoxaline ring nitrogen in bonding to Ir(III). The ν(C=O) band at 1675 cm^{-1} for hqc5in, shifts to lower frequency suggesting the involvement of the C=O group in coordination.

Table 4.2. The IR spectral data of Ir(III) complexes

Compound	ν(O—H)[a/b]	ν(C=N)[c]	ν(C=N)[d]	ν(C=O)	ν(M-O)	ν(M-N)
qc5in	3208	1633	1489	-	-	-
$[Ir(qc5in)Cl_3H_2O]H_2O$	3229	1612	1479	-	-	406
qc6in	3211	1630	1532	-	-	-
$[Ir(qc6in)Cl_3H_2O]H_2O$	3060	1610	1500	-	-	436
hqc5in	3372	1626	1507	1675	-	-
$[Ir(hqc5in)Cl_3(H_2O]$	3215	1598	1506	1661	466	411
hqc6in	3400	1612	1497	1670	--	--
$[Ir(hqc6in)Cl_3(H_2O]$	3305	1602	1497	1632	463	409
hqaqn	3378	1612	1511	1680	-	-
$[Ir(hqc6in)Cl_3(H_2O)]$	3432	1570	1511	1626	482	409

[a] ν(N−H)/ ν(O−H) of the free Schiff base or
[b] ν(O—H) of coordinated water molecule
[c] ν(−CH=N) of azomethine group; [d] ν(C=N) of quinoxaline

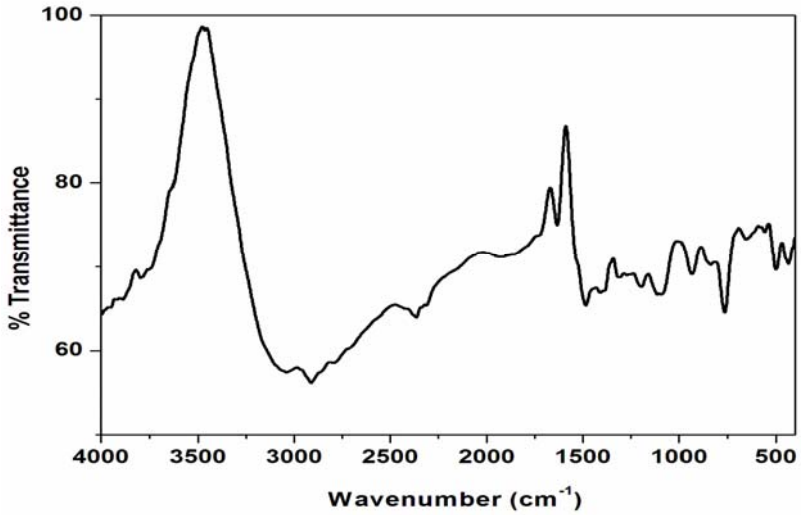

Figure 4.6. FTIR spectrum of $[Ir(qc5in)Cl_3H_2O].H_2O$

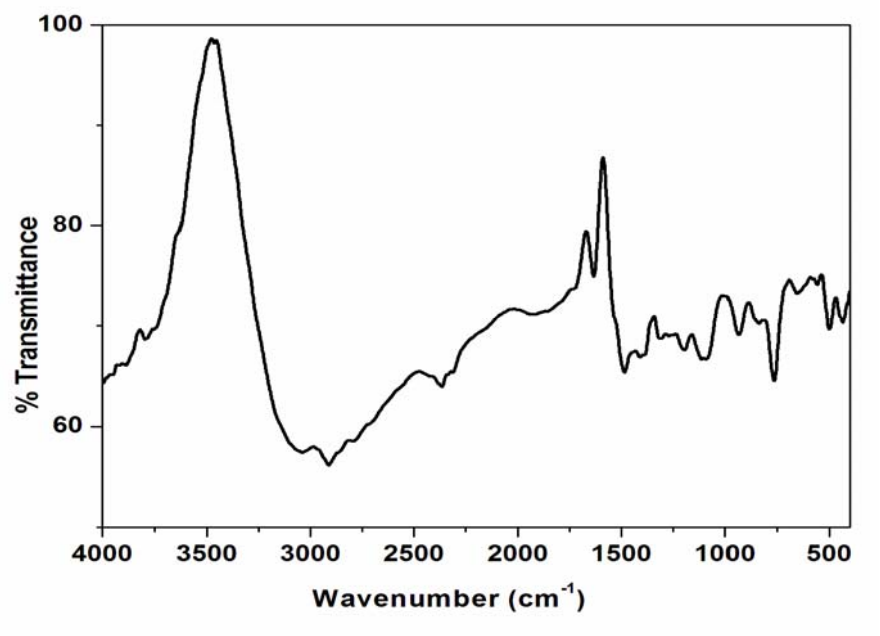

Figure 4.7. FTIR spectrum of [Ir(qc6in)Cl_3H_2O].H_2O

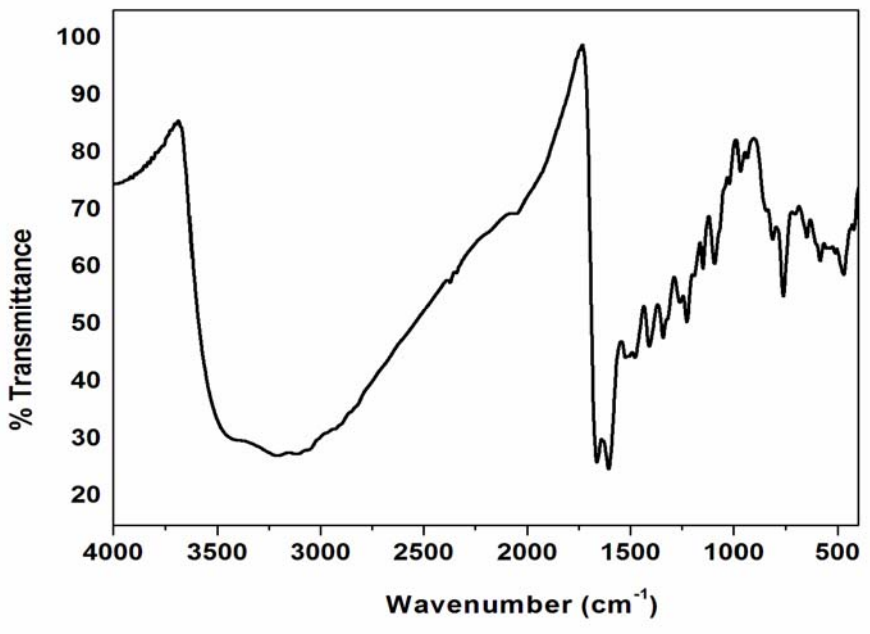

Figure 4.8. FTIR spectrum of [Ir(hqc5in)$Cl_3(H_2O)$]

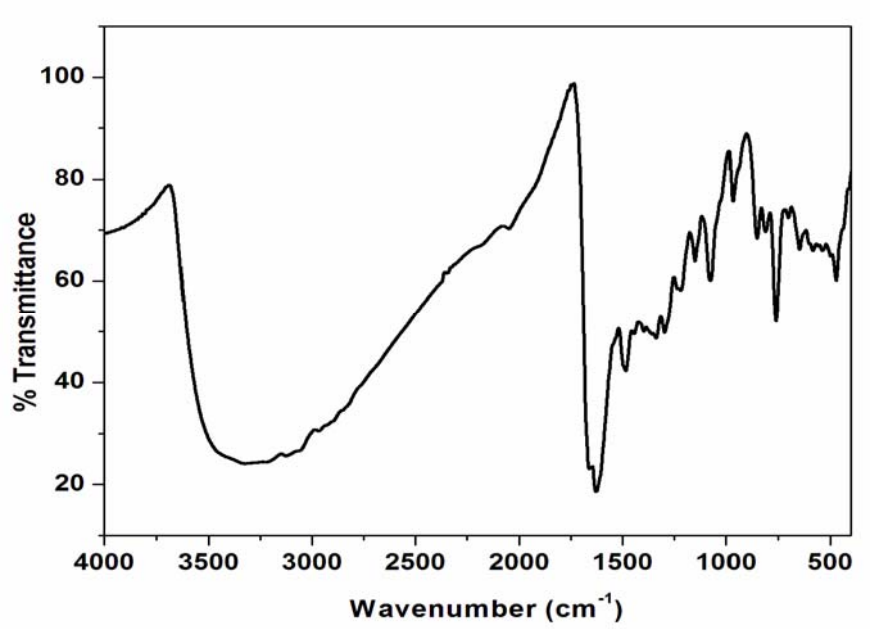

Figure 4.9. FTIR spectrum of [Ir(hqc6in)Cl_3(H_2O)]

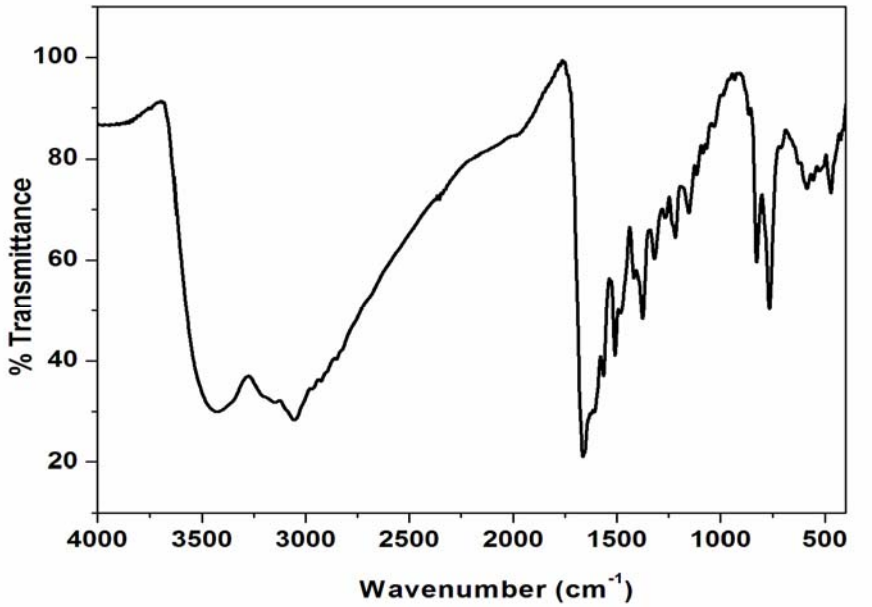

Figure 4.10. FTIR spectrum of [Ir(hqaqn)Cl_3(H_2O)]

4.3.4 Electronic spectra and magnetic moment data

All the Ir(III) complexes are diamagnetic. The Electronic spectral data of the complexes are given in Table 4.3 and spectra are shown in Figures 4.11-4.15. The electronic spectra of Ir(III) complexes show three d-d spin-allowed transitions. The ground state is ^1A_1g. The spectra of the Ir(III)complexes displayed bands in the region 17,700 – 18,400 cm^{-1}, 21,320 – 25,980 cm^{-1} and 29,070–30,680 cm^{-1}, assigned to $^1A_1g \rightarrow {}^1T_2g$, $^1A_1g \rightarrow {}^1T_1g$ and $^1A_1g \rightarrow {}^3T_1g$ transitions, respectively increasing order of energy. The bands above 30,680 cm^{-1} may be due to charge transfer transitions. This pattern of the spectra indicates octahedral geometry around the metal ion. Similar observations have been made in the case of octahedral Ir(III) complexes (13,14,15).

Table 4.3. UV-visible spectral data of the complexes in DMSO

Complex	Electronic spectral bands:nm(cm^{-1})	Assignments
$[Ir(qc5in)Cl_3H_2O]\ H_2O$	260 (38,461)	CT
	285 (35,890)	CT
	555 (18,018)	$^1A_1g \rightarrow {}^1T_1g$
$[Ir(qc6in)Cl_3H_2O]\ H_2O$	260 (38,461)	CT
	333 (30,030)	$^1A_1g \rightarrow {}^1T_2g$
	393 (25,445)	$^1A_1g \rightarrow {}^1T_1g$
$[Ir(hqc5in)Cl_3(H_2O)]$	263 (38,022)	CT
	565 (17,700)	$^1A_1g \rightarrow {}^1T_1g$
$[Ir(hqc6in)Cl_3(H_2O]]$	260 (38,461)	CT
	344 (29.069)	$^1A_1g \rightarrow {}^1T_2g$
	385 (25,974)	$^1A_1g \rightarrow {}^1T_1g$
$[Ir(hqaqn)Cl_3(H_2O)]$	270 (37,037)	CT
	326 (30,674)	$^1A_1g \rightarrow {}^1T_2g$
	469 (21,321)	$^1A_1g \rightarrow {}^1T_1g$
	544 (18,382)	$^1A_1g \rightarrow {}^3T_1g$

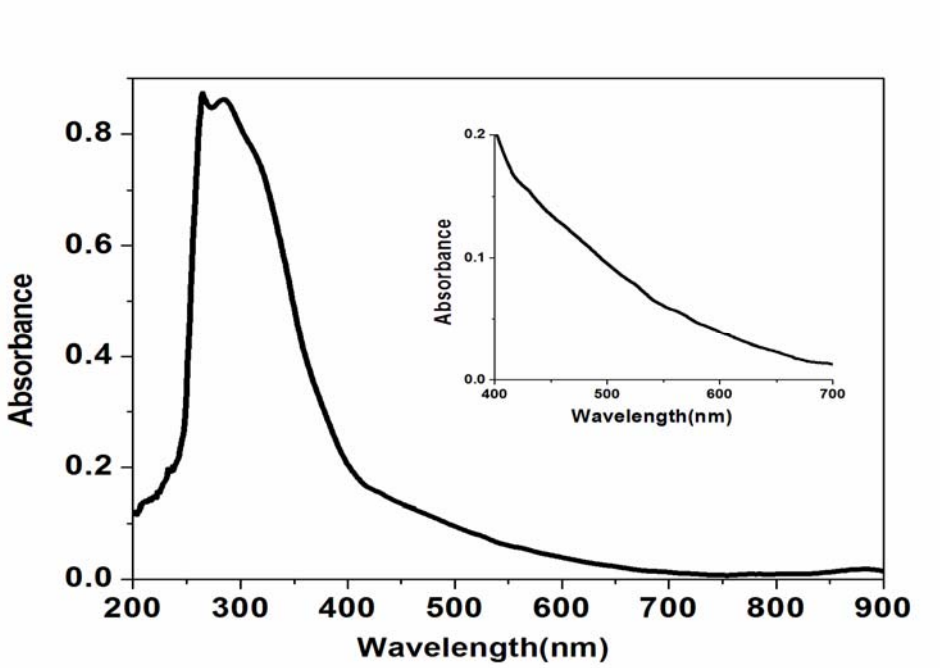

Fgure 4.11. Electronic spectrum of [Ir(qc5in)Cl_3H_2O] H_2O

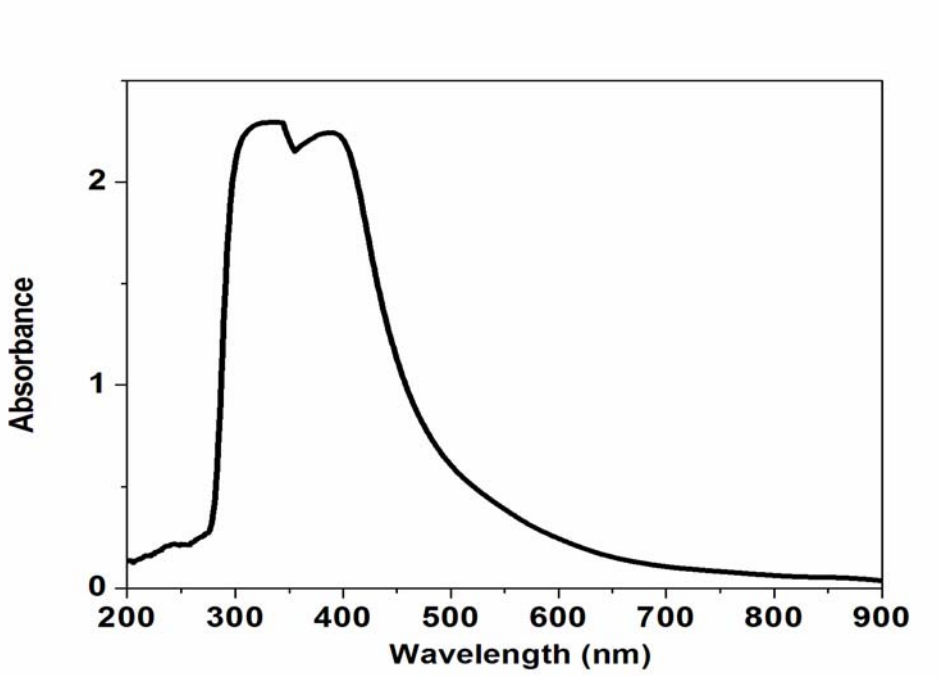

Fgure 4.12. Uv-Vis spectrum of [Ir(qc6in)Cl_3H_2O]. H_2O

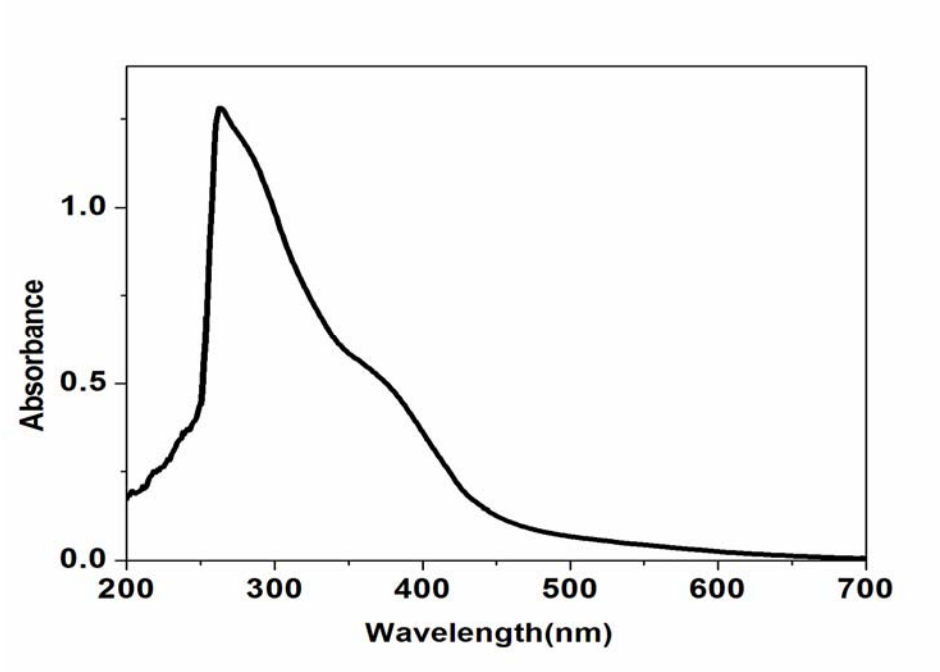

Fgure 4.13. Uv-Vis spectrum of [Ir(hqc5in)$Cl_3(H_2O)$]

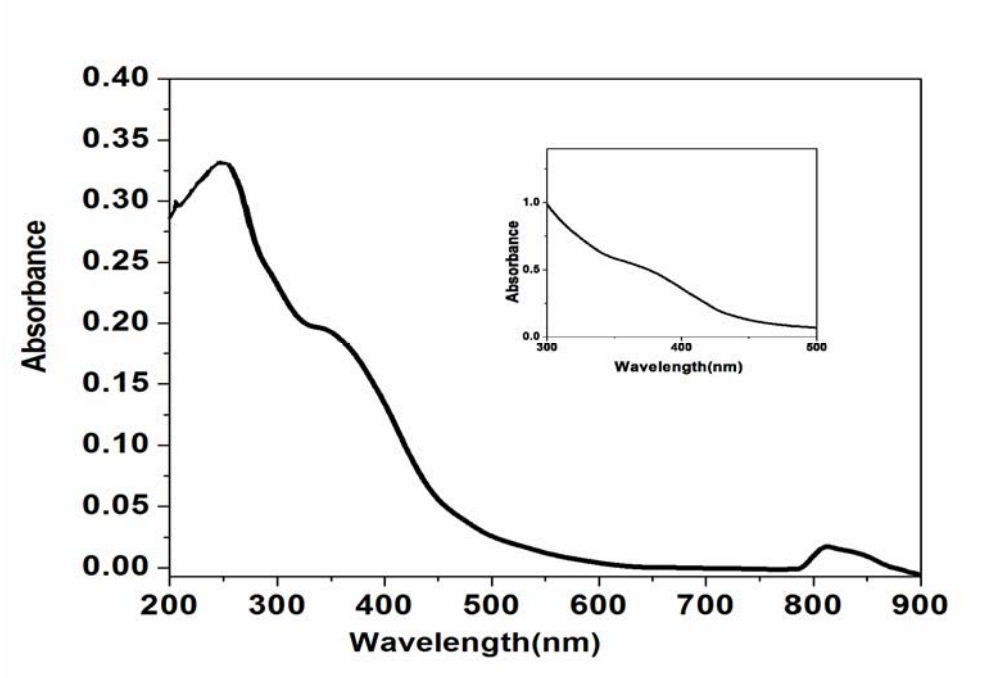

Fgure 4.14. Uv-Vis spectrum of [Ir(hqc6in)$Cl_3(H_2O)$]

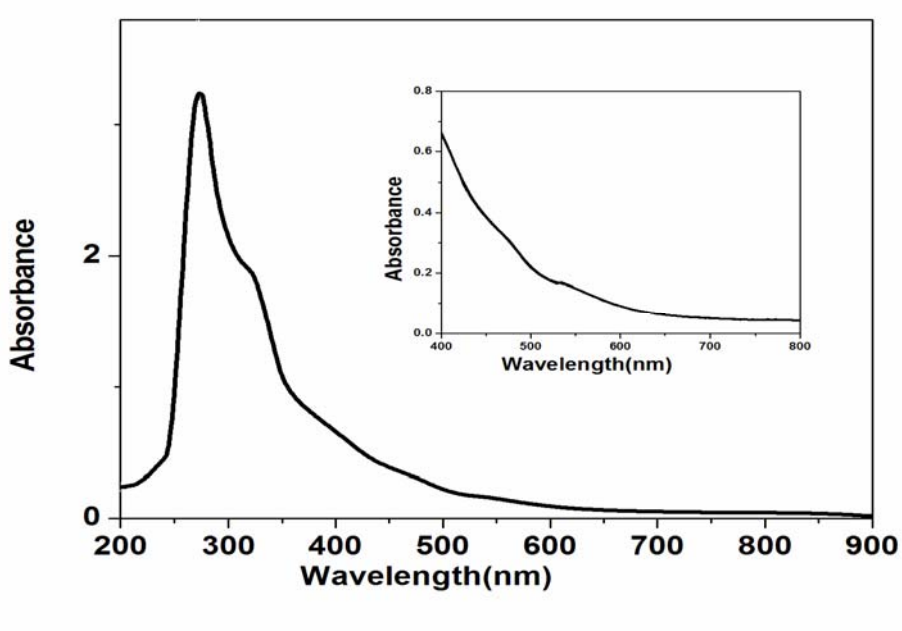

Figure 4.15. Uv-Vis spectrum of [Ir(hqaqn)$Cl_3(H_2O)$]

4.3.5 Cyclic voltammetry

The cyclic voltammogram of mononuclear Ir(III) complexes in DMSO (Figures 4.16-4.20) shows one well defined redox couple corresponding to $Ir^{III/II}$ and $Ir^{II/III}$. The CV data for the Ir(III) complexes are given in Table 4.4.The cathodic peak appearing in the potential range -630 to -840 mV, corresponds to the one electron reduction of Ir(III) and the corresponding anodic peak appears in the potential range -0.570 to -0.620. The ΔEp values of complexes indicate that these redox couples are quasi-reversibile. The ratio of the cathodic and anodic peak current is nearly unity and indicates one electron transfer in this redox process.

Table 4.4. Cyclic voltammetric data of Ir(III) complexes

Complex	E_{pc} (V)	E_{pa} (V)	$E_{1/2}$ (V)	I_{pc} (μA)	I_{pa} (μA)	No. of electrons (I_{pc}/I_{pa})
$[Ir(qc5in)Cl_3H_2O]\ H_2O$	-0.626	-0.579	-0.602	2.70	3.00	.82
$[Ir(qc6in)Cl_3H_2O]\ H_2O$	-0.658	-0.568	-0.613	3.12	2.98	1.0
$[Ir(hqc5in)Cl_3(H_2O)]$	-0.977	-0.570	-0.773	4.65	3.86	1.2
$Ir(hqc6in)Cl_3(H_2O)]$	-0.761	-0.584	-0.672	4.85	3.92	1.2
$[Ir(hqaqn)Cl_3(H_2O)]$	-0.836	-0.617	-0.726	5.02	3.80	1.3

E_{pc} = cathodic peak potential;
E_{pa} = anodic peak potential;
I_{pc} = cathodic peak current;
I_{pa} = anodic peak current;
$E_{1/2}$ = 0.5 × (E_{pa} + E_{pc}); scan rate 100 mV (ΔEp=47 mv to 407 mV)

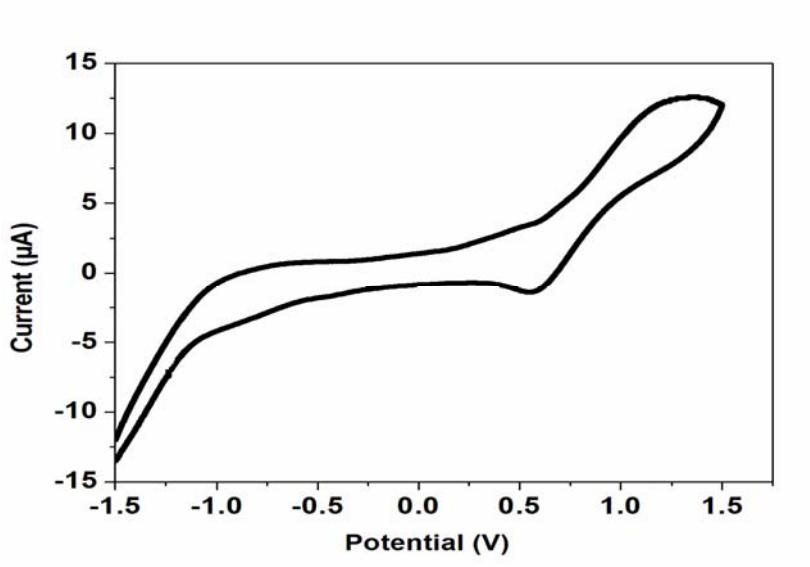

Figure 4.16. Cyclic voltammogram of $[Ir(qc5in)Cl_3H_2O].\ H_2O$

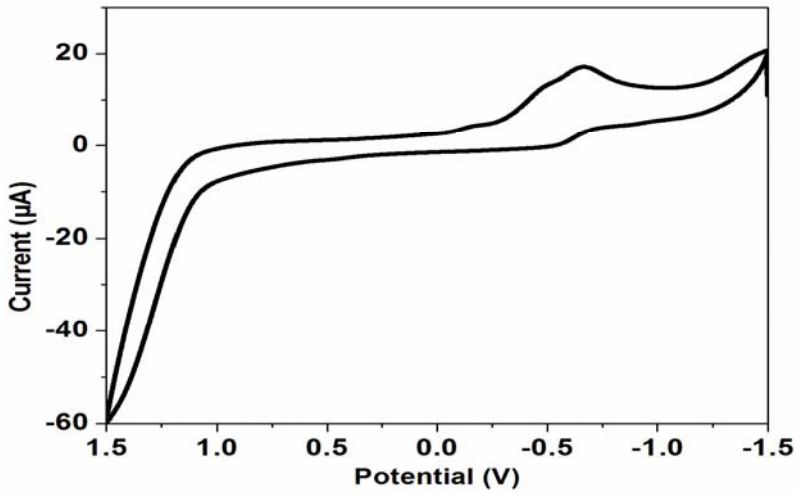

Figure 4.17. Cyclic voltammogram of [Ir(qc6in)Cl_3H_2O].H_2O

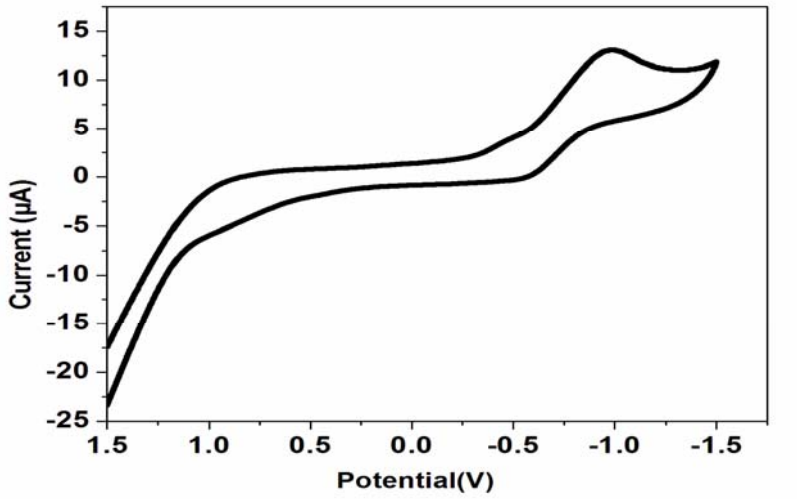

Figure 4.18. Cyclic voltammogram of [Ir(hqc5in)$Cl_3(H_2O)$]

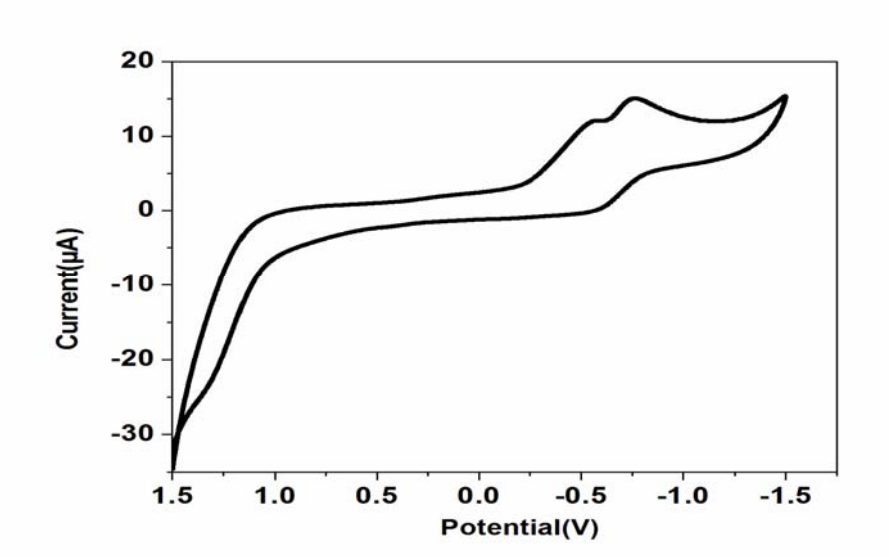

Figure 4.19. Cyclic voltammogram of [Ir(hqc6in)$Cl_3(H_2O)$]

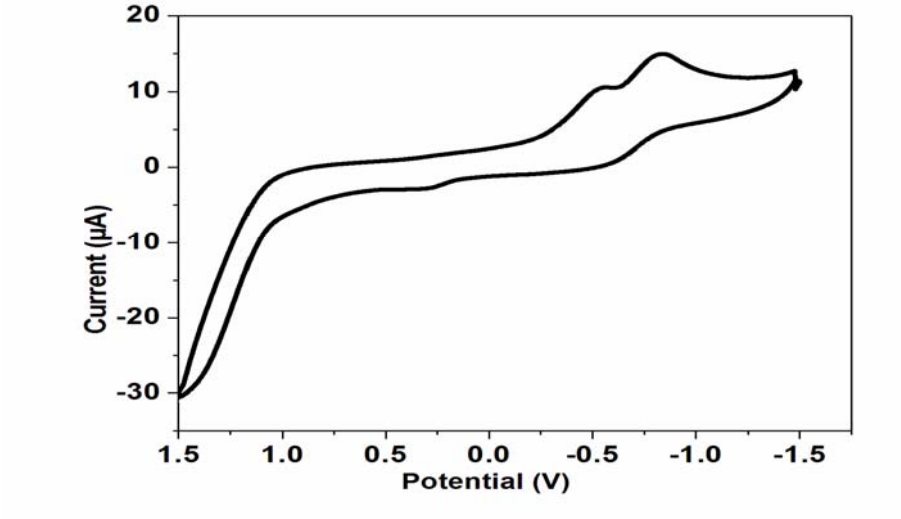

Figure 4.20. Cyclic voltammogram of [Ir(hqaqn)$Cl_3(H_2O)$]

4.3.6 Geometry of the complexes

Based on the above studies an octahedral structure (Figure 4.21) has been assigned for the Ir(III) complexes $[Ir(qc5in)Cl_3H_2O].\ H_2O$, $[Ir(qc6in)Cl_3H_2O].\ H_2O$, $[Ir(hqc5in)Cl_3(H_2O)]$, $[Ir(hqc65in)Cl_3(H_2O)]$ and $[Ir(hqaqn)Cl_3(H_2O)]$.

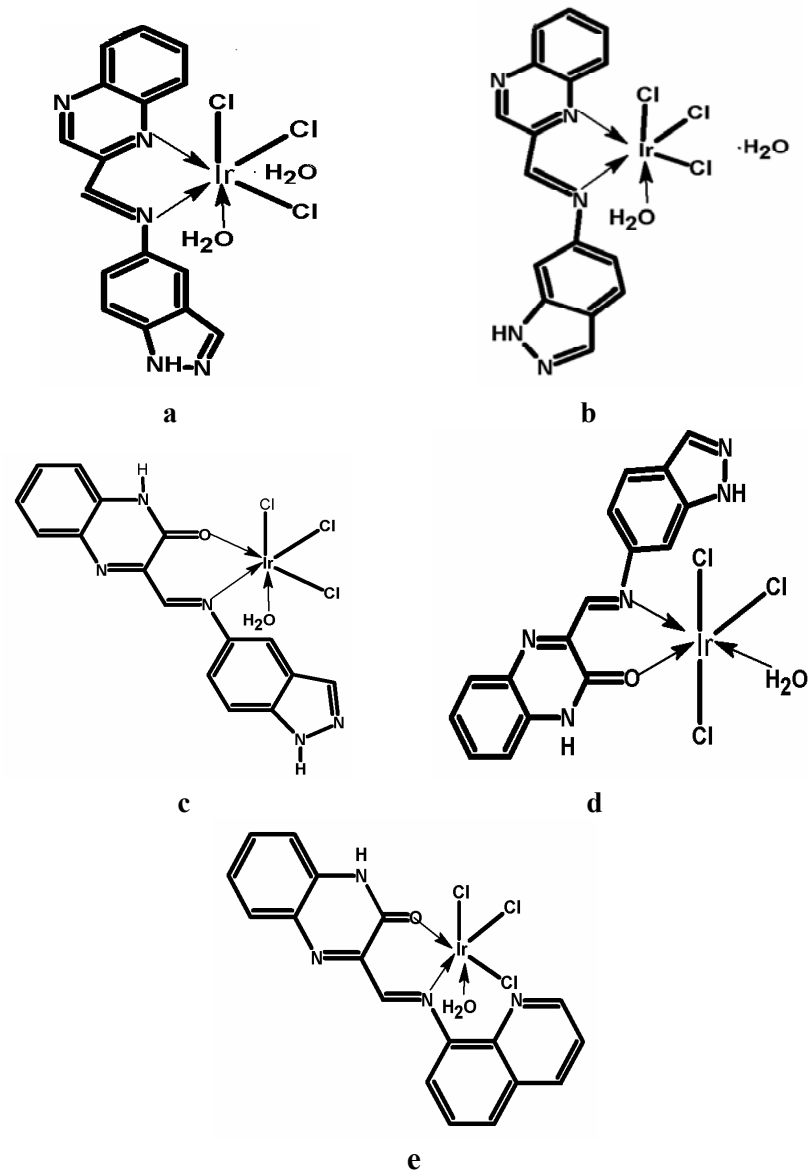

Figure 4.21. The Proposed geometry of Ir(III) complexes

Where a=$[Ir(qc5in)Cl_3H_2O].\ H_2O$], b=$[Ir(qc6in)Cl_3H_2O].\ H_2O$

c = $[Ir(hqc5in)Cl_3(H_2O)]$ d= $[Ir(hqc6in)Cl_3H_2O]$ e= $[Ir(hqaqn)Cl_3(H_2O)]$

4.4 DNA binding and Cleavage studies

The DNA binding behaviour of these complexes was studied by UV-Vis spectra, CV, DPV and CD spectral techniques. Upon electronic absorption titration, all the complexes, exhibit hyperhromism with blue shift. The Kb values for $[Ir(qc5in)Cl_3H_2O].H_2O$, $[Ir(qc6in)Cl_3H_2O].H_2O$, $[Ir(hqc5in)Cl_3(H_2O]$, $[Ir(hqc6in)Cl_3(H_2O]$ and $[Ir(hqaqn)Cl_3(H_2O]$ found to be $3.1\times10^5\ M^{-1}$, $2.3\times10^5\ M^{-1}$, $2.0\times10^5\ M^{-1}$, $1.2\times10^5\ M^{-1}$, $4.5\times10^6\ M^{-1}$ respectively. Addition of increasing amounts of DNA result in a reduction in the intensity of the absorption band and the slight blue shift observed for the complexes suggests a strong stacking interaction between aromatic group and the base pairs of DNA.

The mode and the extent of binding of complexes to DNA can be determined by various techniques such as absorption spectroscopy, CV, DPV and CD.

4.4.1 Electronic Absorption titration

The electronic absorption titration of iridium complexes has been carried out at a fixed concentration of the complexes (100 μM) in DMSO at 25°C by varying the concentration of DNA are shown in Figures 4.22-4.26. When the amount of DNA is increased the intensity of the charge transfer band is also changed. The bands appearing in the region 290-380 nm are assigned to ligand to metal charge transfer (LMCT) transitions. The "hyperchromic effect" observed on the addition of herring sperm DNA to the complexes reflects the structural damage to the secondary structure of DNA duplex as a consequence of strong binding of the complexes (16).

The slight blue shift (2-3 nm) and increase in the absorption intensity observed with the increase of concentration of DNA observed for all the complexes suggest a strong binding involving the aromatic group and the base pairs of DNA. These results indicate that these complexes interact with DNA through groove binding.

The intrinsic binding constants (K_b) calculated and is in the following order $[Ir(hqaqn)Cl_3(H_2O)]$ > $[Ir(qc5in)Cl_3H_2O]H_2O$ > $[Ir(qc6in)Cl_3(H_2O)]$ H_2O > $[Ir(hqc5in)\ Cl_3H_2O]$ > **[**$Ir(hqc6in)Cl_3(H_2O)]$

Table 4.5. Binding constant of Iridium complexes

Complex	Binding Constant (kb) M^{-1}
$[Ir(qc5in)Cl_3H_2O]\ H_2O$	3.1×10^5
$[Ir(qc6in)Cl_3H_2O]\ H_2O$	2.3×10^5
$[Ir(hqc5in)Cl_3(H_2O)]$	2.0×10^5
$[Ir(hqc6in)Cl_3(H_2O)]$	1.2×10^5
$[Ir(hqaqn)Cl_3(H_2O)]$	4.5×10^5

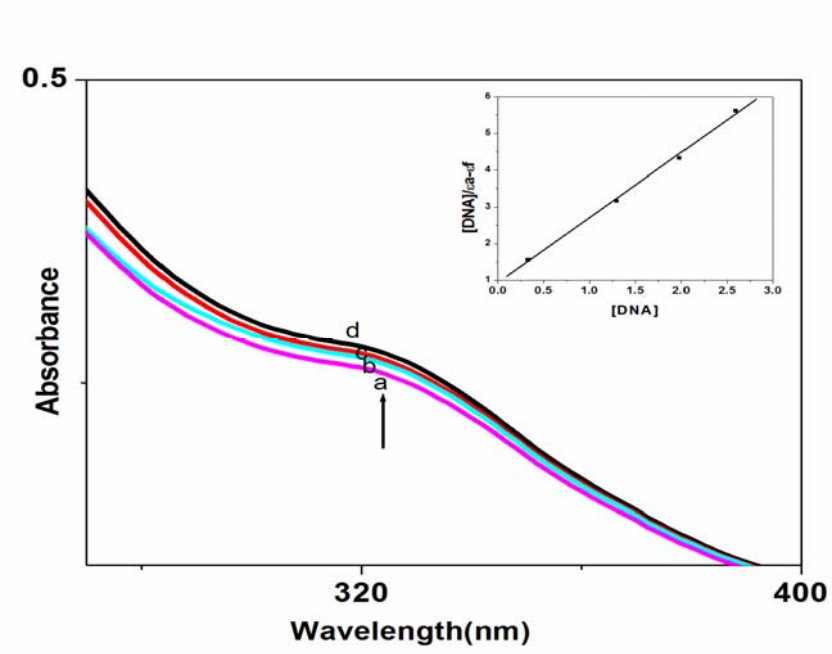

Figure 4.22. Absorption spectra of $[Ir(qc5in)Cl_3H_2O]H_2O$ in 5mM Tris-HCl buffer at pH 7.1 in the absence (a) and presence (b, c and d) of increasing amounts of HS DNA. Arrow indicate the absorption changes upon increasing the DNA Conc. (Inset: A plot of [DNA]/[DNA]/εa-εf)

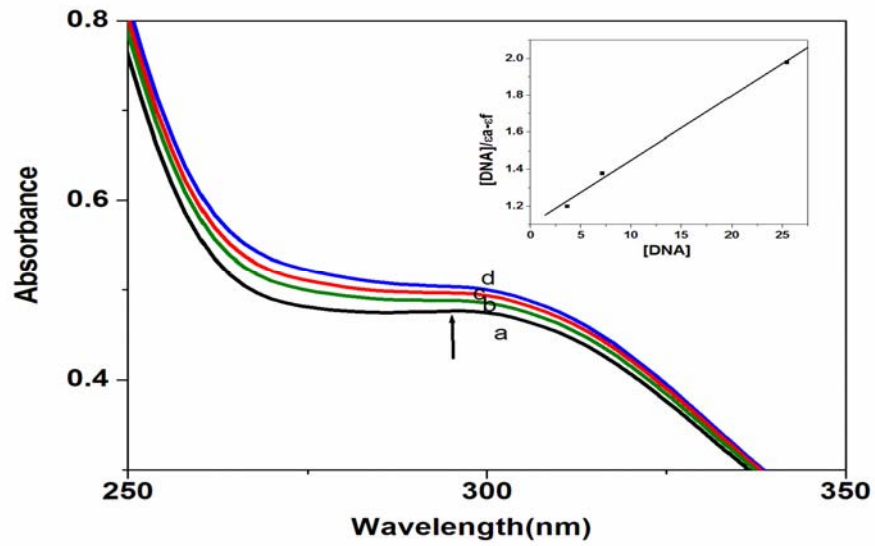

Figure 4.23. Absorption spectra of[Ir(qc6in)Cl_3H_2O]H_2O in 5mM Tris-HCl buffer at pH 7.1 in the absence (a) and presence (b, c and d) of increasing amounts of HS DNA. Arrow indicate the absorption changes upon increasing the DNA Conc. (Inset: A plot of [DNA]/[DNA]/εa-εf)

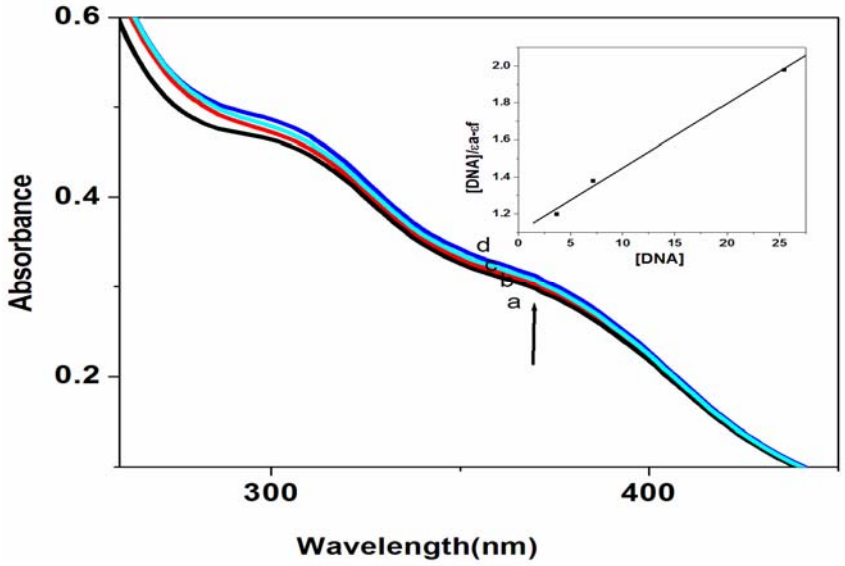

Figure 4.24. Absorption spectra of[Ir(hqc5in)Cl_3H_2O] in 5mM Tris-HCl buffer at pH 7.1 in the absence (a) and presence (b, c and d) of increasing amounts of HS DNA. Arrow indicate the absorption changes upon increasing the DNA Conc. (Inset: A plot of [DNA]/[DNA]/εa-εf)

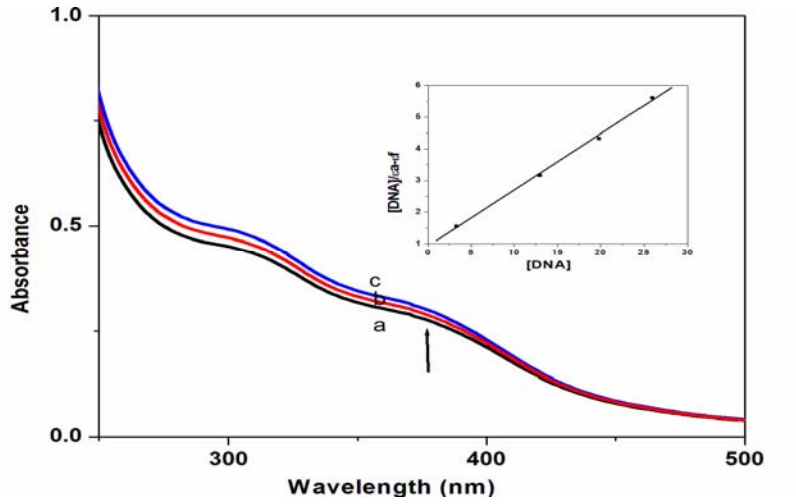

Figure 4.25. Absorption spectra of[Ir(hqc6in)Cl_3H_2O] H_2O in 5mM Tris-HCl buffer at pH 7.1 in the absence (a) and presence (b and c) of increasing amounts of HS DNA. Arrow indicate the absorption changes upon increasing the DNA Conc.(Inset: A plot of [DNA]/[DNA]/εa-εf)

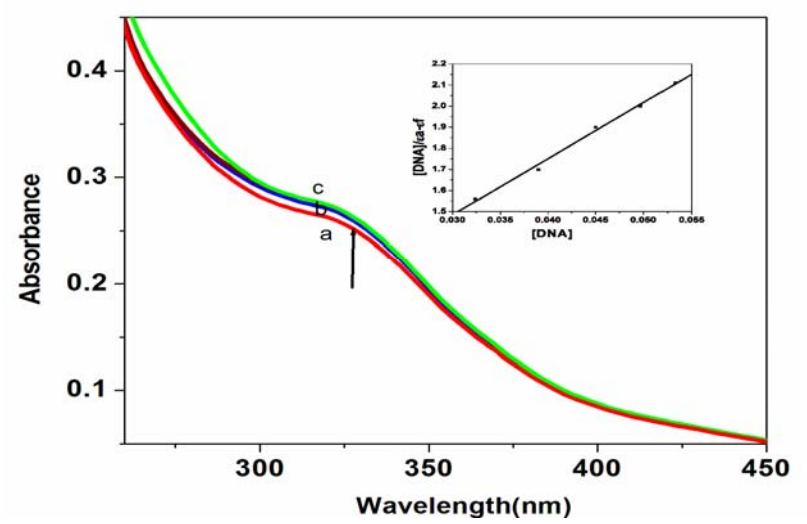

Figure 4.26. Absorption spectra of [Ir(hqaqn)Cl_3H_2O] in 5mM Tris-HCl buffer at pH 7.1 in the absence (a) and presence (b) and (c) of increasing amounts of HS DNA. Arrow indicate the absorption changes upon increasing the DNA Conc. (Inset: A plot of [DNA]/[DNA]/εa-εf)

4.4.2 Electrochemistry

Electrochemical methods are widely used to study the interaction of DNA with metal chelates. Cyclic voltammetric behaviour of complexes in the absence and

presence of DNA is shown in Figure 4.13. Complex $[Ir(qc5in)Cl_3H_2O].H_2O$ shows cathodic and anodic peak potentials. The ratio of cathodic to anodic peak current I_{pc}/I_{pa} is less than unity indicating quasi- reversible redox process. The formal potential $E_{1/2}$ in the absence of DNA for the complex $[Ir(qc5in)Cl_3H_2O]H_2O$ is-0.772 V. On increasing the concentration of DNA undergoes a positive shift of peak potential. The obivious shift of peak potential indicates strong association of the complex with DNA. Furthermore the voltammetric currents decrease up on addition of DNA to the complex. This decrease in current is due to diffusion of an equilibrium mixture of free DNA bound complex to electrode surface. Thus the results of CV studies are in favour of intercalation or groove binding (17).

For complexes, $[Ir(qc6in)Cl_3H_2O]H_2O$, $[Ir(hqc5in)Cl_3(H_2O)]$, $[Ir(hqc6in)\ Cl_3(H_2O)]$, $[Ir(hqaqn)Cl_3(H_2O)]$ we have investigated the interaction with DNA using DPV because the anodic peak potential could not be identified. Curve 'a' is the absence of DNA in Tris-HCl buffer, while curve 'b', 'c' and 'd' is in the presence of DNA. In the case of complexes $[Ir(qc6in)Cl_3H_2O].H_2O$, $Ir(hqc5in)Cl_3(H_2O)]$, $Ir(hqaqn)Cl_3(H_2O)]$ and at different concentrations of DNA the peak current is decreased and E_{pc} shifted to more positive potential. But E_{pc} value shifted to negative potential in the case of $[Ir(hqc5in)Cl_3(H_2O)]$. In the light of Bard's report the complexes $[Ir(qc6in)Cl_3H_2O]H_2O$, $[Ir(hqc5in)Cl_3(H_2O)]$, $[Ir(hqc6in)Cl_3(H_2O)]$ interact with DNA through groove binding mode in contrast to $[Ir(hqaqn)Cl_3(H_2O)]$ whose interaction mode is intercalative.

Table 4.6. Cyclic voltammetric data of $[Ir(qc5in)Cl_3H_2O]H_2O$ in the presence of different concentrations of DNA in Tris-HCl(5mM) buffer pH=7.1

Complex	R	E_{pc}/V	E_{pa}/V	ΔEp (V)	I_{pc}	I_{pa}	I_{pc}/I_{pa}	$E_{1/2}$ (V)	$\Delta E_{1/2}$ (mV)
$[Ir(qc5in)Cl_3H_2O]H_2O$	0	-0.772	-0.575	0.197	7.69	7.52	1.02	0.673	
	0.2	-0.776	-0.560	0.216	6.45	6.09	1.05	0.668	5
	0.4	-0.708	-0.510	0.198	5.43	5.42	1.00	0.609	64

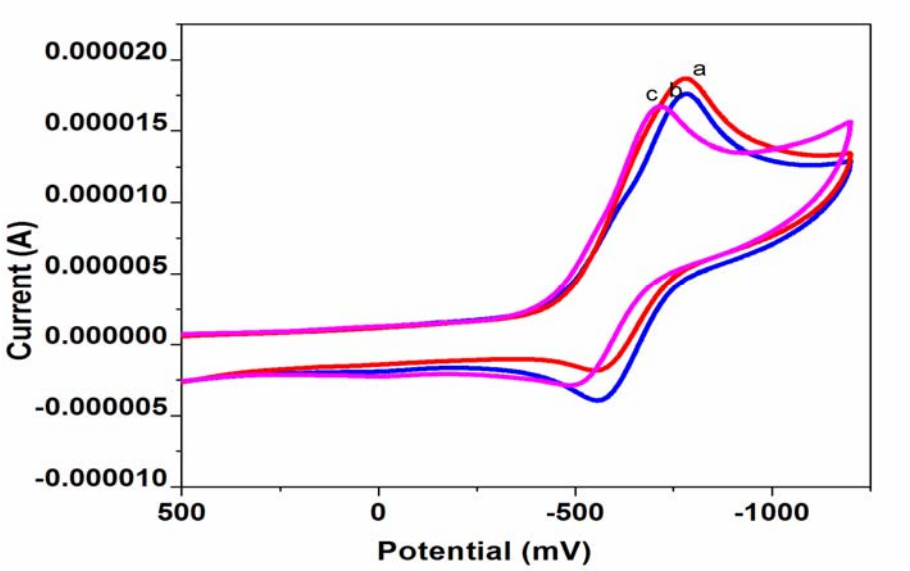

Figure 4.27. Cyclic voltammogram of [Ir(qc5in)Cl_3H_2O].H_2O in the absence (a) and presence (b and c) of different concentrations of DNA in Tris-HCl (5mM) buffer pH=7.1

Table 4.7 Differential Pulse voltammetric data of iridium complexes in the presence of different concentrations of DNA in Tris-HCl buffer pH=7.1

Complex	R	E_{pc}/V	$E^{1/2}$(V)	$\Delta E^{1/2}$(mV)
[Ir(qc6in)Cl_3H_2O]H_2O]	0	-0.566	-0.591	
	0.2	-0.571	-0.596	5
	0.4	-0.558	-0.583	8
	0.6	-0.551	-0.576	15
[Ir(hqc5in)Cl_3H_2O]	0	-0.728	-0.653	
	0.2	-0.622	-0.647	6
	0.4	-0.520	-0.616	37
[Ir(hqc6in)Cl_3H_2O]	0	-0.630	-0.655	
	0.2	-0.585	-0. 605	50
	0.4	-0.542	-0.567	88
[Ir(hqaqn)Cl_3H_2O]	0	-0.720	-0.745	
	0.2	-0.600	-0.625	120
	0.4	-0.520	-0.545	200

$E_{1/2}$= Ep+ΔE/2 where $E_{1/2}$ is equivalent to the average of E_{pc} and E_{pa} in CV measurements and ΔE is the pulse amplitude (50 mV)

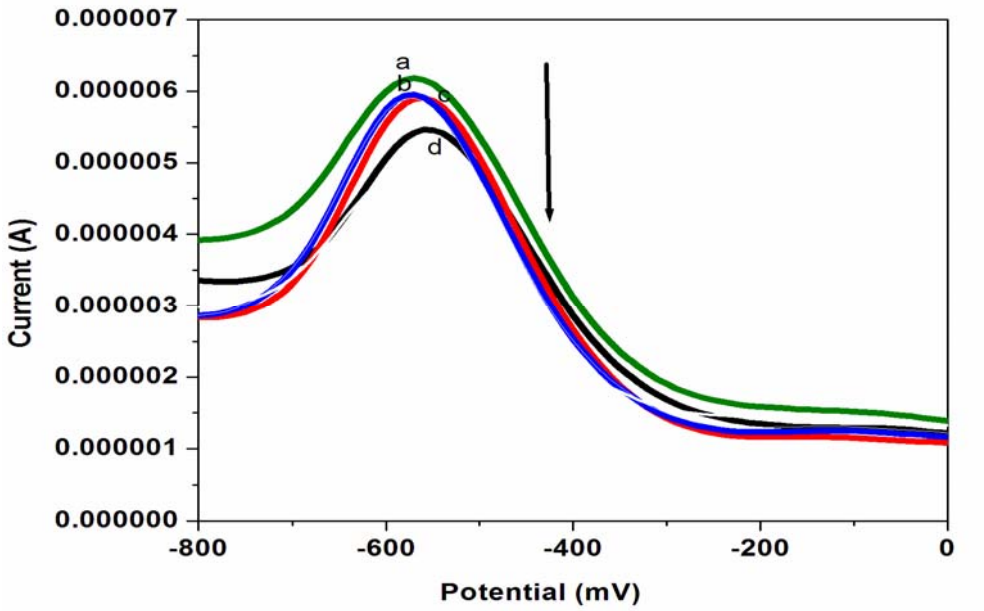

Figure 4.28. Differential pulse voltammogram of the complex $[Ir(qc6in)Cl_3H_2O].H_2O$ in the absence(a) and presence (b, c and d) of different concentrations of DNA in Tris-HCl(5mM) pH=7.1

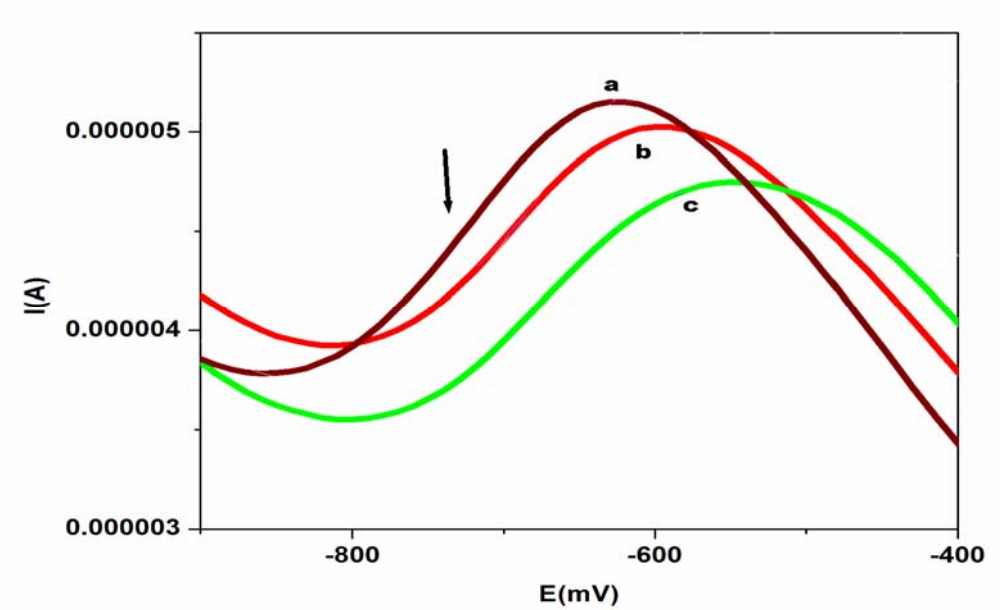

Figure 4.29. Differential pulse voltammogram of the complex $[Ir(hqc5in)Cl_3(H_2O)]$ in the absence (a) and presence (b and c) of different concentrations of DNA in Tris-HCl (5mM)) buffer pH=7.1

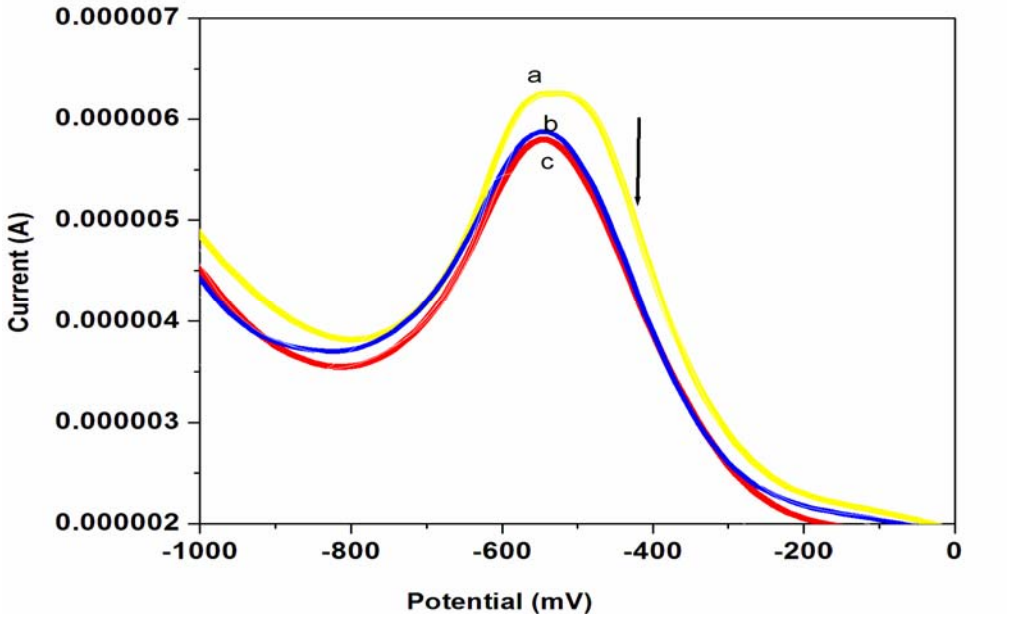

Figure 4.30. Differential pulse voltammogram of the complex [Ir(hqc6in)$Cl_3(H_2O)$] in the absence (a) and presence (b and c) of different concentrations of DNA in Tris-HCl (5mM) buffer pH=7.1

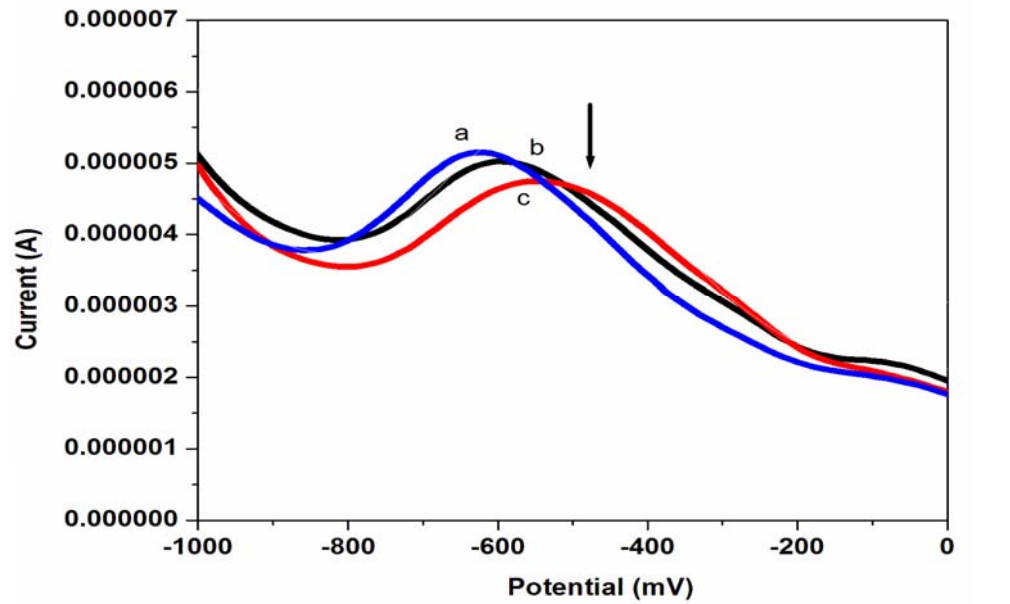

Figure 4.31. Differential pulse voltammogram of the complex [Ir(hqaqn)$Cl_3(H_2O)$] in the absence (a) and presence (b and c) of different concentrations of DNA in Tris-HCl(5mM) buffer pH=7.1

4.4.3 CD spectral titration

CD spectra of DNA in the presence and absence of complexes were recorded. The spectra are presented in Figures 4.32-4.36 and the data are given in Table 4.8. Initial CD is consistent with B-type DNA, with a positive peak at 275nm, a negative peak at 245nm, zero cross over point at 258 nm. On the addition of complexes, $[Ir(qc5in)Cl_3H_2O]H_2O$, $[Ir(qc6in)Cl_3H_2O]H_2O$, $[Ir(hqc5in)Cl_3H_2O]$ and $[Ir(hqc6in)Cl_3H_2O]$ to the DNA solution, the positive band at 275 nm shows a slight red shift (1-3 nm) and an increase in the molar ellipticity suggesting that there exist interaction between aromatic rings of the complex and base pairs of DNA. But on the addition of $[Ir(hqaqn)Cl_3H_2O]$, to the DNA solution, both bands show a slight red shift (1-3 nm) and a large increase in the molar ellipticity suggesting intercalative mode of binding. Furthermore these spectral changes suggest that the DNA becomes more A-like upon interaction with these complexes.

These observations clearly indicate that the DNA is unwound upon interaction with this complex and suggest groove binding to DNA. This kind of B to A transition has already been reported on the interaction with certain multinuclear Pt(II) complexes. Patra et al, reported if the positive band 278 nm showed increase in molar ellipticity with a minor red shift of the band maximum along with an increase in intensity upon addition of the copper complexes to DNA the phenomenon could be due to groove binding that stabilises the right-handed B form of DNA (18).

All the results clearly reveal that binding of DNA with the complexes $[Ir(qc5in)Cl_3H_2O]H_2O$, $[Ir(qc6in)Cl_3H_2O]H_2O$, $[Ir(hqc5in)Cl_3H_2O]$ and $[Ir(hqc6in)Cl_3H_2O]$ through groove binding and $[Ir(hqaqn)Cl_3H_2O]$ intercalatively bind with DNA.

Table 4.8. CD parameters for the interaction of HS-DNA with Ir(III) complexes

samples		Positive band		Negative band	
	1/R	λ_{max} (nm)	CD (mdeg)	λ_{max} (nm)	CD (mdeg)
DNA	0	275	3.287	245	-2.559
$[Ir(qc5in)Cl_3H_2O]H_2O$	0.6	279	3.324	248	-2.652
	0.8	278	3.850	249	-2.867
$[Ir(qc6in)Cl_3H_2O]H_2O$	0.4	277	3.312	247	-2.678
	0.6	277	3.426	247	-2. 774
$[Ir(hqc5in)Cl_3H_2O]$	0.6	277	3.816	247	-2.845
$[Ir(hqc6in)Cl_3H_2O]$	0.6	277	3.797	245	-2.904
$[Ir(hqaqn)Cl_3H_2O]$	0.6	276	20.700	247	-19.61
	0.8	277	22.940	247	-20. 39

Measurements made at1/R value of 0.2-0.8,
where 1/R=[Complex]/[DNA]
Cell path length=1mm

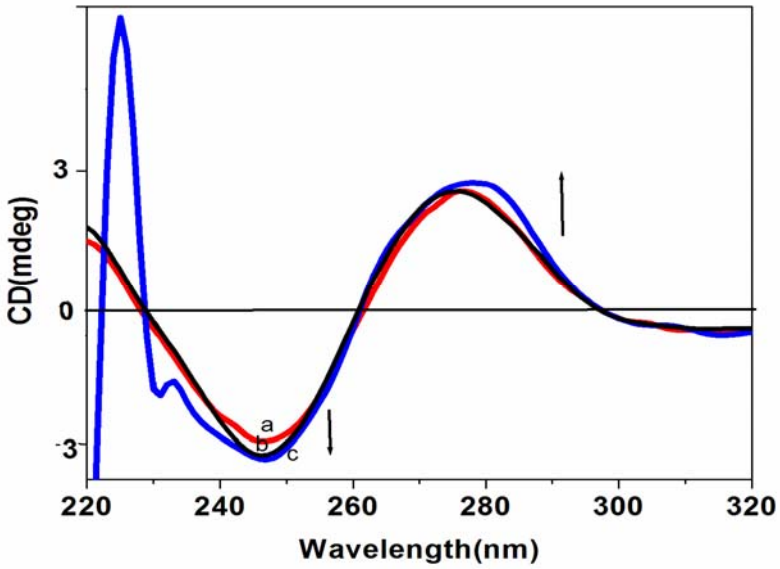

Figure 4.32. CD spectra of DNA in the absence (a) of complex [Ir(qc5in) $Cl_3H_2O]H_2O$ and presence (b and c) of complex in Tris HCl buffer pH 7.1.

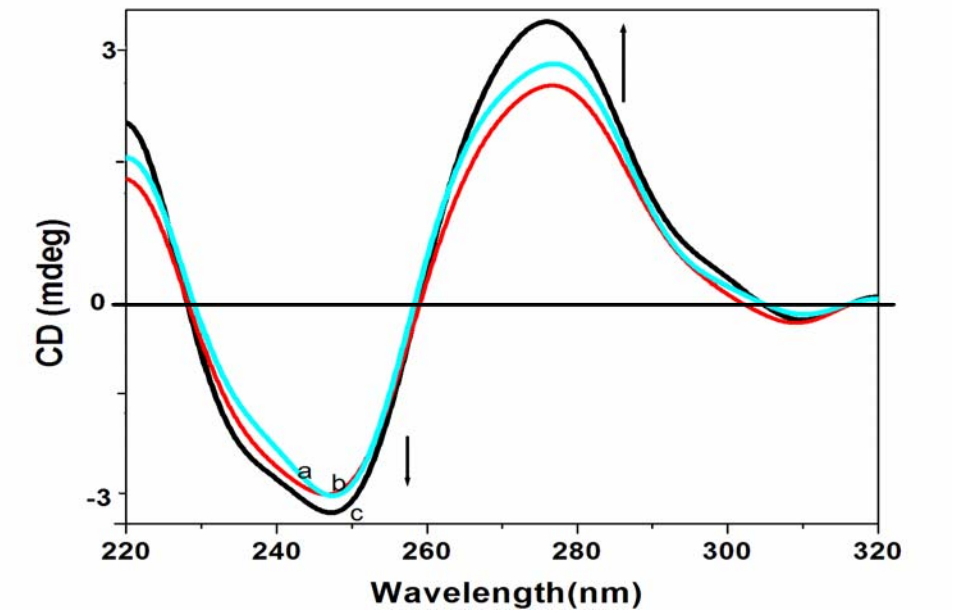

Figure 4.33. CD spectra of DNA in the absence (a) of complex [Ir(qc6in) Cl_3H_2O]H_2O and presence (b and c) of complex in Tris HCl buffer pH 7.1.

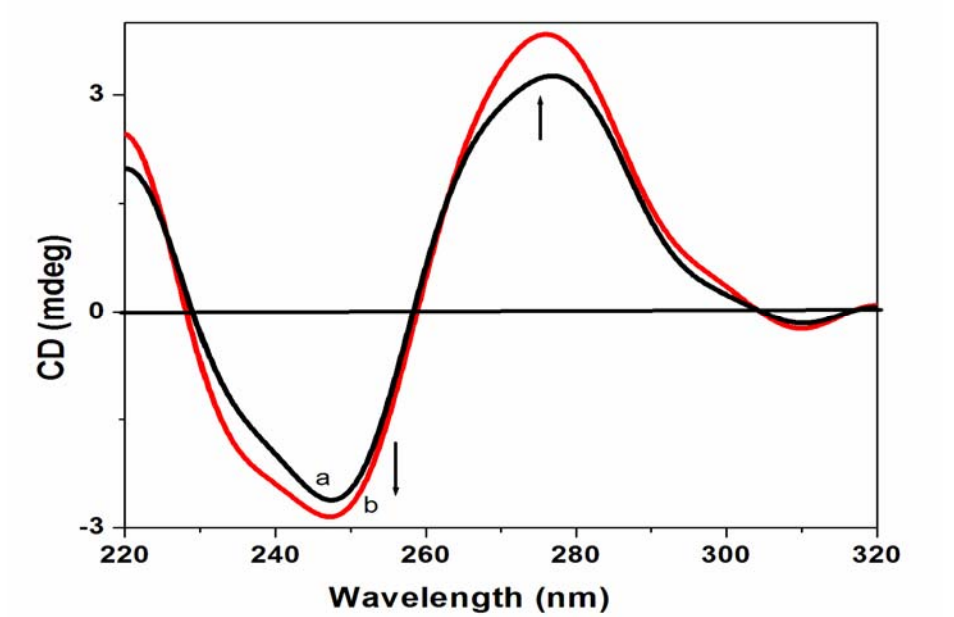

Figure 4.34. CD spectra of DNA in the absence (a) of complex [Ir(hqc5in) Cl_3H_2O] and presence (b) of complex in Tris HCl buffer pH 7.1.

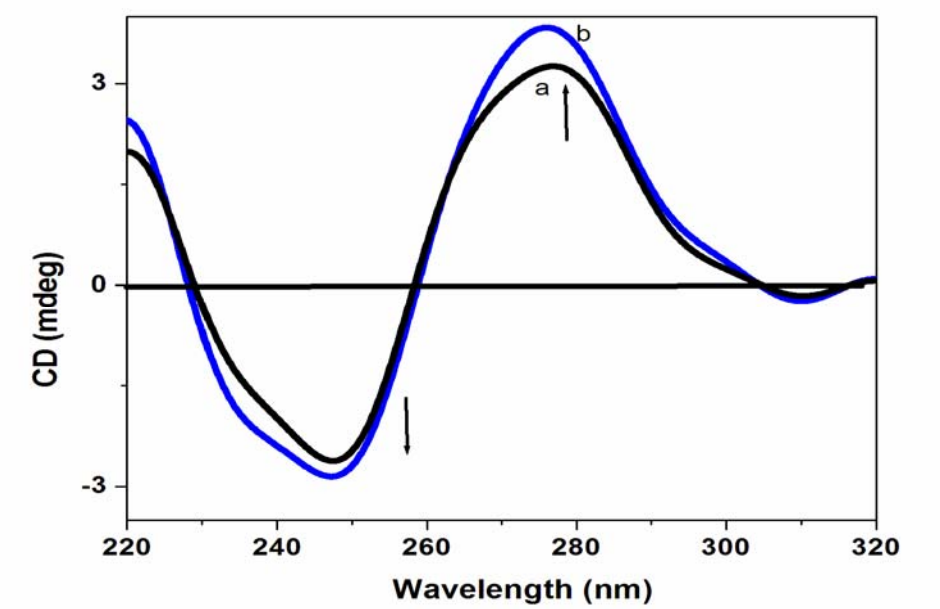

Figure 4.35. CD spectra of DNA in the absence (a) of complex [Ir(hqc6in) Cl_3H_2O] and presence (b) of complex in Tris HCl buffer pH 7.1.

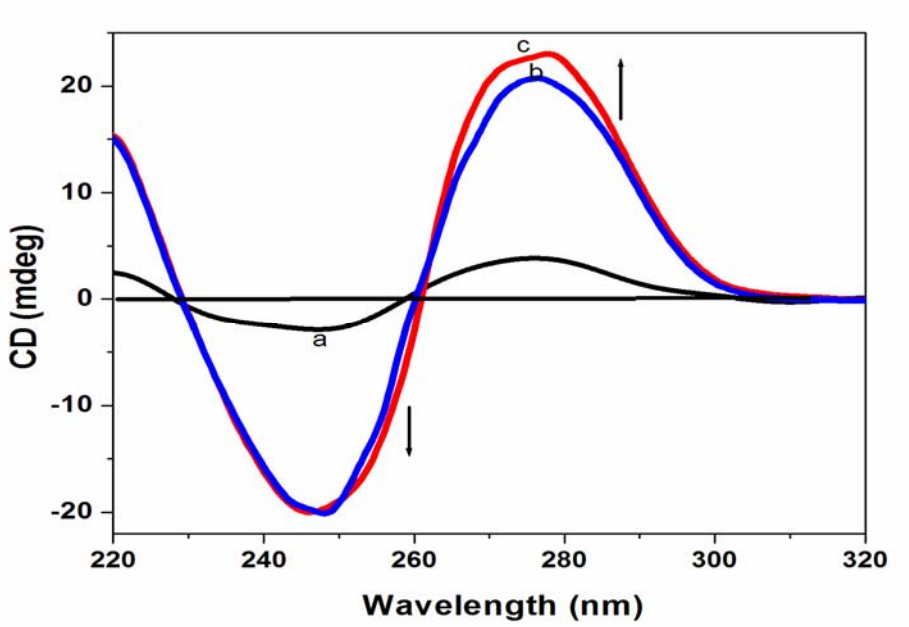

Figure 4.36. CD spectra of DNA in the absence of complex (a) [Ir(hqaqn) Cl_3H_2O] and presence (b and c) of complex in Tris HCl buffer pH 7.1.

4.5 DNA cleavage studies of the Iridium complexes by gel electrophoresis method

On agarose gel, pUC18 DNA shows three distinct bands corresponding to the two different conformations of the plasmid, namely, open circular and supercoiled forms. Agarose gel electrophoresis using pUC18 plasmid DNA in the presence of the complex was carried out and is shown in the figure. In the gel diagram two bands are visible for pUC18 DNA (Lane 2) which corresponds to the open circular and supercoiled form of DNA. In the presence of Ir(III) complexes only one form of plasmid pUC18 was visible (Lane 3, 4, 5, 6 and 7) which corresponds to supercoiled DNA (Form I) and other open circular form is not visible. The binding of the metal complexes cause the shift in conformation of DNA by degrading the whole open circular DNA (Form II).

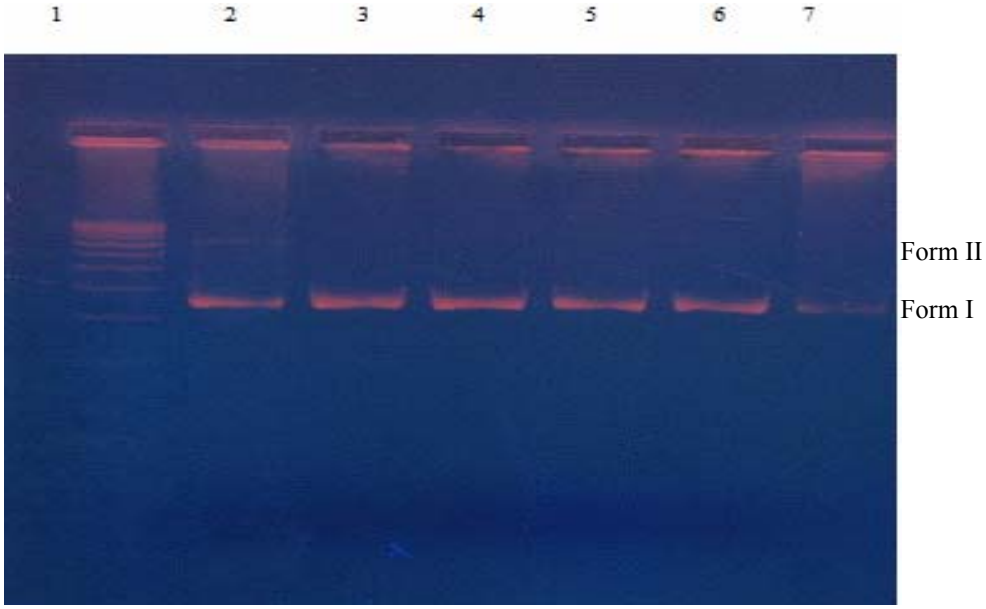

Lane 1 : 500 bp DNA marker
Lane 2 : pUC 18 DNA
Lane 3 : pUC 18 DNA + [Ir(qc5in)Cl_3H_2O] H_2O
Lane 4 : pUC 18 DNA + [Ir(qc6in)Cl_3H_2O] H_2O
Lane 5 : pUC 18 DNA + Ir (hqc5in)$C1_3(H_2O)$
Lane 6 : pUC 18 DNA + Ir (hqc6in)$C1_3(H_2O)$
Lane 7 : pUC 18 DNA + Ir (hqaqn)$C1_3(H_2O)$

Figure 4.36. Cleavage of pUC 18 DNA in the presence of Ir(III) complexes

4.6 Conclusion

All the Ir(III) complexes are octahedral and diamagnetic in nature. The molar conductance values suggest non electrolytic nature of these complexes. The complexes show quasi reversible oxidation and reduction. The I_{pc}/I_{pa} ratio for the complexes indicates one electron transfer in this redox process. The DNA binding behaviour of these complexes was studied by UV-Vis spectra, CV, DPV and CD spectral studies. The complexes in the decreasing order of binding constants (K_b) are as follows. $[Ir(hqaqn)Cl_3H_2O] > [Ir(qc5in)Cl_3H_2O]H_2O > [Ir(hqc5in)Cl_3H_2O] > [Ir(qc5in)Cl_3H_2O]H_2O > [Ir(hqc6in)\ Cl_3H_2O]$. Agarose gel electrophoresis assay indicate that these complexes have the ability to cleave the pUC18 plasmid DNA.

4.7 References

[1] S. Sakaguchi, T. Yamaga, Y. Ishii, *J. Org. Chem. 66 (2000) 4710*.

[2] J.P. Genet, A. Marinetti, R.V. Virginie, *Pure Appl. Chem.* 73 (2001) 299;

[3] K.K. Lo, D.C. Ng, C.K. Chung, *Organometallics 20* (2001) 4999.

[4] K.K. Lo, C.K. Chung, T.K. Lee, L. Lui, K.H. Tsang, N. Zhu, *Inorg. Chem. 42* (2003) 6886.

[5] K.K. Lo, C.K. Chung, N. Zhu, *Chem. Eur. J. 12 (*2006) 1500

[6] F. Shao, B. Elias, W.Lu, J. K. Barton, Inorganic Chemistry 46 (2007) 10187

[7] R. Wepf, M. Amrein, U. Burkli, H. Gross, *J. Microsc.* 163(1991) 51.

[8] J. H. Palmer, A. C. Durrell, Z. Gross, J. R. Winkler, H. B. Gray, *J. Am. Chem. Soc*, 132 (2010) 9230.

[9] M. A. Nazif, J.A. Bangert, I. Ott, R. Gust, R. Stoll, W. S. Sheldrick, *J. Inorg. Biochem.* 103 (2009) 1405

[10] F. Shao, B. Elias , W. Lu , J. K. Barton , *Inorg. Chem*. 46 (2007) 10187.

[11] R. Ramesh, N. Dharmaraj, R. Karvembru, K. Natarajan, *Indian J. Chem.* 39A (2000) 1079

[12] V. K. Sharma, O. P. Pandey, S. K. Sengupta, D. M. Halepoto, *Transition Met. Chem.* 14 (1989) 263

[13] J. Lewis, B. N. Figgis, *Prog. Inorg. Chem.* 6 (1964) 105)

[14] V.K. Sharma, A. Srivastava , S. Srivastava, *J. Serb. Chem. Soc. 71* (2006) 917.

[15] V. K. Sharma, A. Srivastava, S. Srivastava, *Indian Journal of chemistry* 46 (2007)1963.

[16] F. Arjmand, M. Chauhan, *Chim. Acta*, 88 (2005) 2413.

[17] M. T. Carter, A. J. Bard, *J. Am. Chem. Soc.* 111 (1989) 890

[18] A.K. Patra, M. Nethaji, A.R. Chakravarthy, *J.Inorg.Biochem*.101(2007) 233.

.....ꕥ.....

Chapter 5

Synthesis, characterisation and DNA cleavage of ruthenium(III) complexes

Contents

5.1 Introduction

The chemistry of ruthenium is currently receiving a lot of attention, because of their use in catalytic reactions like oxidation (1-6) and hydrogenation (7-8) and also due to their biocidal activity (9-19). Ruthenium offers a wide range of oxidation states and the reactivity of the ruthenium complexes depends on the stability and interconvertibility of these oxidation states (20-22). Steric and electronic effects around the Ru core can be finely tuned by an appropriate electron withdrawing or electron donating substituents attached to the Schiff bases.

With a view to study the catalytic activity in oxidation reactions we have synthesised new ruthenium(III) complexes by the reaction of the Schiff base ligands, quinoxaline-2-carboxalidene-5-aminoindazole (qc5in), quinoxaline-2-carboxalidene-6-aminoindazole (qc6in), 3-hydroxyquinoxaline-2-carboxalidene-5-aminoindazole (hqc5in), 3-hydroxyquinoxaline-2-carboxalidene-6-aminoindazole (hqc6in), 3-hyodroxyquinoxaline-2-carboxalidene-8-aminquinoline (hqaqn) with Ru(III) chloride. The results of studies on the synthesis and characterisation are

presented in this chapter. The details of the catalytic activity are presented in chapter VII.

5.2 Experimental

5.2.1 Materials

The details of materials used for the synthesis of the Schiff base ligands are given in Chapter 2.

5.2.2 Synthesis of Schiff base ligands

The procedure for the synthesis of the Schiff base ligands are given in Chapter 2

5.2.3 Synthesis of complexes

All the ruthenium(III) complexes were prepared by mixing an ethanolic solution (10 mL) of $RuCl_3.3H_2O$ (1.30 g, 5 mmol) with an ethanolic solution (100 mL) of the ligand, qc5in (1.36 g, 5 mmol), qc6in (1.36 g, 5 mmol), hqc5in (1.45 g, 5 mmol), hqc6in (1.45 g, 5 mmol) or hqaqn (1.50 g, 5 mmol) in a molar ratio of 1:1 and refluxing for 3hours. The complex separated out was washed with ethanol and then with petroleum ether and dried over anhydrous calcium chloride in a desiccator.

5.3 Results and discussion

All the complexes are black and non-hygroscopic. They are soluble in DMSO but are insoluble in benzene, ethanol and chloroform.

5.3.1 Elemental analyses

Analytical data and conductance data are given in Table 5.1. The data suggest a metal to Schiff base ratio of 1:1 for all the complexes. The molar conductance values of the complexes in DMSO (10^{-3} mol) indicate non-electrolytic nature of the complexes [23].

Table 5.1. Analytical and conductance data of the ruthenium(III) complexes

Complexes of	C (%)	H (%)	N (%)	Cl (%)	Ru (%)	Molar conductance ($ohm^{-1}cm^2\ mol^{-1}$)
qc5in	37.12 (37.19)	2.86 (2.93)	13.46 (13.55)	19.40 (20.58)	20.02 (19.56)	5.6
qc6in	37.24 (37.19)	2.92 (2.93)	13.46 (13.55)	19.26 (20.58)	19.46 (19.56)	6.0
hqc5in	37.28 (37.33	2.20 (2.55)	13.70 (13.61)	18.62 (20.66)	19.52 (19.64)	5.4
hqc6in	37.26 (37.33)	2.96 (2.55)	13.56 (13.61)	21.82 (20.66)	18.98 (19.64)	5.8
hqaqn	42.00 (41.15)	3.20 (3.26)	10.68 (10.67)	13.28 (13.50)	18.14 (19.24)	6.2

5.3.2 Thermal Analysis

Thermal stability of the complexes were investigated using TG at a heating rate of 20 ºC /min in nitrogen over a temperature range of 40-1000 ºC. TG curves of the complexes are given in Figures 5.1-5.5. The initial weight loss below 130 °C observed for all the complexes is attributed to the removal of lattice water molecules associated with the complex. Loss of coordinated water occurs in the range 130-250 ºC. This is followed by two or three stages of decompositions leading to the removal of other ligands. In nitrogen atmosphere the decomposition was incomplete even after 1000 ºC.

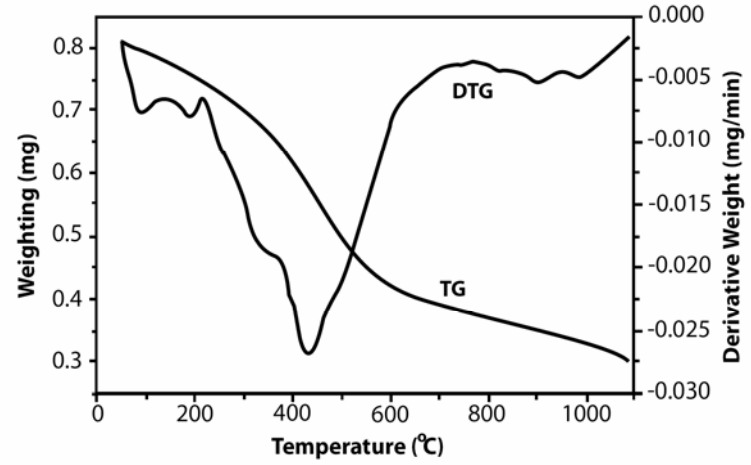

Figure 5.1. TG-DTG of $[Ru(qc5in)Cl_3H_2O].H_2O$

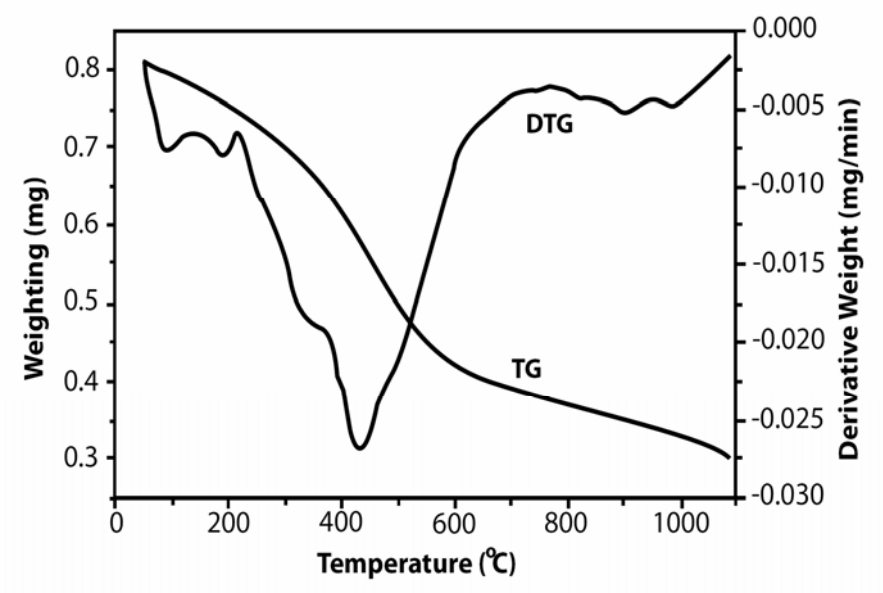

Figure 5.2. TG-DTG of [Ru(qc6in)$Cl_3$$H_2O$].$H_2O$

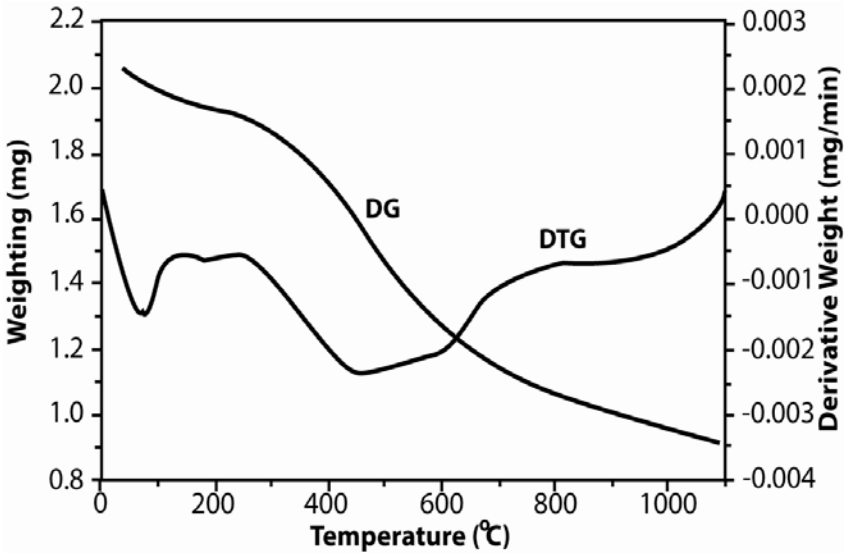

Figure 5.3. TG-DTG of [Ru(hqc5in)Cl_3(H_2O)].H_2O

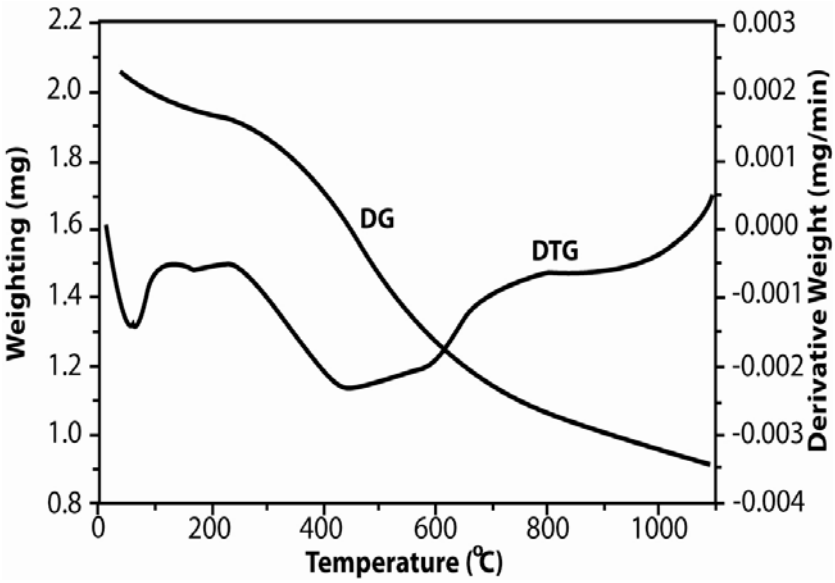

Figure 5.4. TG-DTG of [Ru(hqc6in)$Cl_3(H_2O)]H_2O$

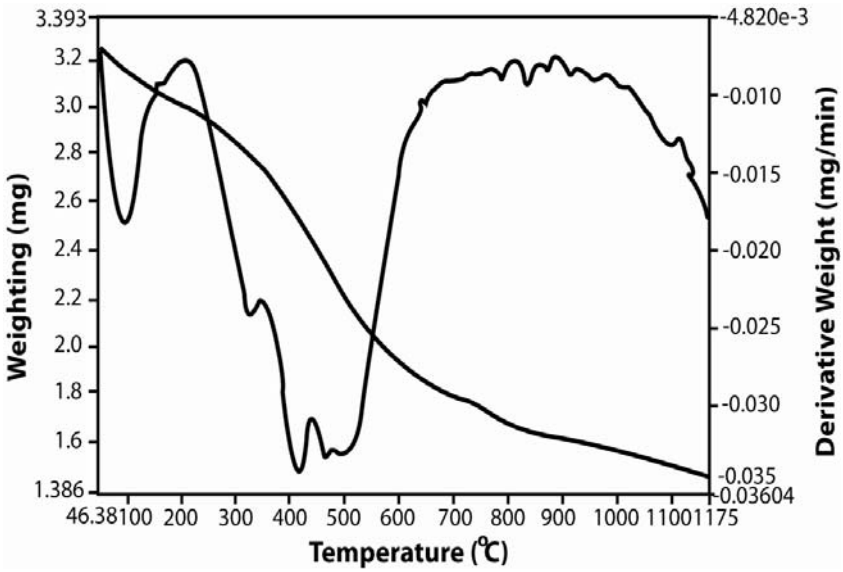

Figure 5.5. TG-DTG of [Ru(hqaqn)$Cl_3(H_2O)]H_2O$

Based on the analytical, molar conductance and TG data, the following molecular formula have been assigned for the complexes [Ru(qc5in) Cl_3H_2O].H_2O, [Ru(qc6in)Cl_3H_2O].H_2O, [Ru(hqc5in)$Cl_3(H_2O)$].H_2O, Ru(hqc6in) $Cl_3(H_2O)$].H_2O and Ru(hqaqn)$Cl_3(H_2O)$].H_2O

5.3.3 Infrared spectra

Selected vibrational stretching frequencies of the free Schiff base ligands and those ruthenium complexes, which are useful for determining the mode of coordination of the ligands, are given in Table 5.3. The FT-IR spectra of the ruthenium(III) complexes are given in Figures 5.6-5.10. In all these spectra there is a broad band in the range 3355-3432 cm^{-1} assignable to coordinated water or uncoordinated water molecules (24). This fact is also indicated by the results of elemental analyses and TG-DTG of these complexes (25). The participation of azomethine nitrogen atom of the Schiff bases in coordination is evidenced by decrease in their stretching frequency. The bands entered at 1633 cm^{-1} for qc5in, at 1630 cm^{-1} for qc6in, at 1626 cm^{-1} for hqc5in, at 1612 cm^{-1} for hqc6in and hqaqn decreases to 1619 cm^{-1}, 1612, 1600, 1598 and 1528 cm^{-1} respectively in the spectra of their metal complexes. The ν(C=N) of the quinoxaline ring in the spectra of qc5in and qc6in undergoes a decrease in stretching frequency on complexation suggesting the coordination of the ring nitrogen to the metal in their complexes. However this band for the ligands hqc5in, hqc6in and hqaqn remains unchanged on complexation suggesting the noninvolment of quinoxaline ring nitrogen in coordination to ruthenium. In addition, these complexes exhibit bands in the range 410-440 cm^{-1}, which may be due to ν(Ru—N) (26). The bands in the range 1670-1680 cm^{-1} due to the C═O group of the hqc5in and hqc6in, hqaqn shifted to lower frequency indicating the involvement of this group in coordination.

Table 5.3. The IR spectral data of Ru(III) complexes

Compound	ν(O—H)[a/b]	ν(C=N)[c]	ν(C=N)[d]	ν(C=O)	ν(M-O)	ν(M-N)
qc5in	3208	1633	1489	-	-	-
$[Ru(qc5in)Cl_3H_2O]H_2O$	3418	1619	1500	-	-	406
qc6in	3211	1630	1532	-	-	-
$[Ru(qc6in)Cl_3H_2O]H_2O$	3432	1612	1514	-	-	436
hqc5in	3372	1626	1497	1670	-	-
$[Ru(hqc5in)Cl_3(H_2O)]H_2O$	3412	1600	1497	1654	478	411
hqc6in	3376	1612	1493	1670	-----	-----
$[Ru(hqc6in)Cl_3(H_2O)]H_2O$	3418	1598	1493	1658	485	409
hqaqn	3378	1585	1511	1675	-	-
$[Ru(hqaqn)Cl_3(H_2O)]H_2O$	3432	1528	1510	1633	455	409

[a] ν(N−H)/ ν(O−H) of the free Schiff base or
[b] ν(O—H) of coordinated water molecule
[c] ν(CH=N)of azomethine group; [d] ν(C=N) of quinoxaline

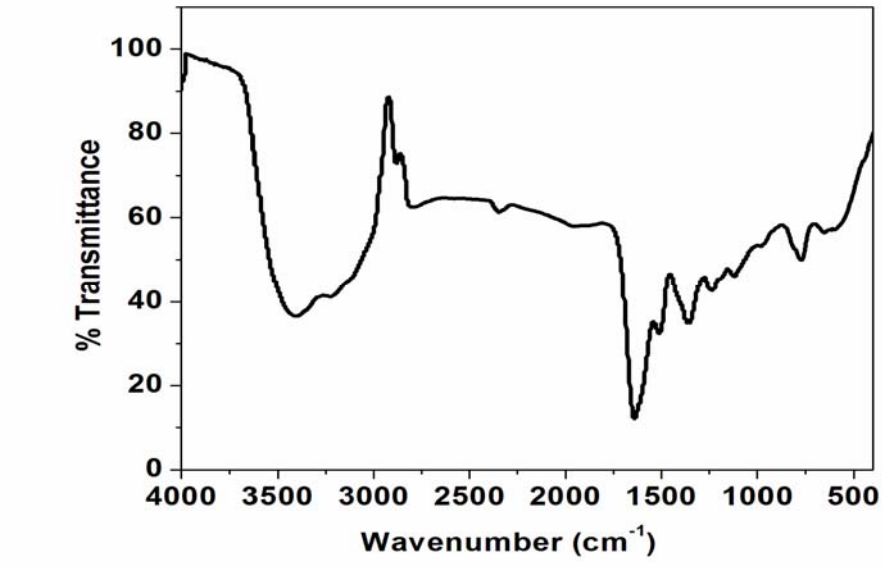

Figure 5.6. FTIR spectrum of $[Ru(qc5in)Cl_3H_2O]H_2O$

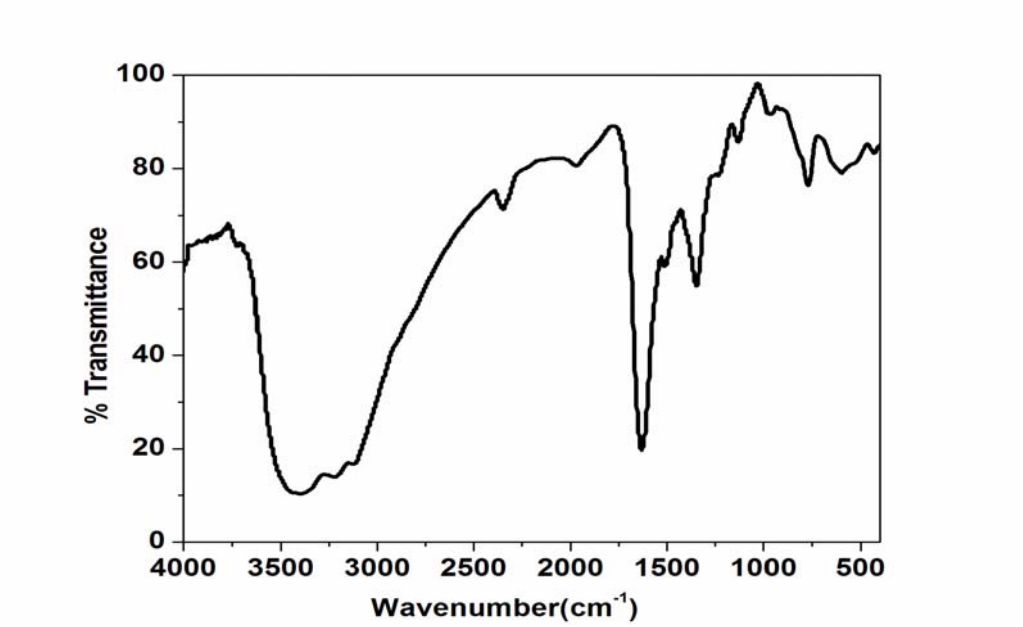

Figure 5.7. FTIR spectrum of [Ru(qc6in)Cl_3H_2O]H_2O

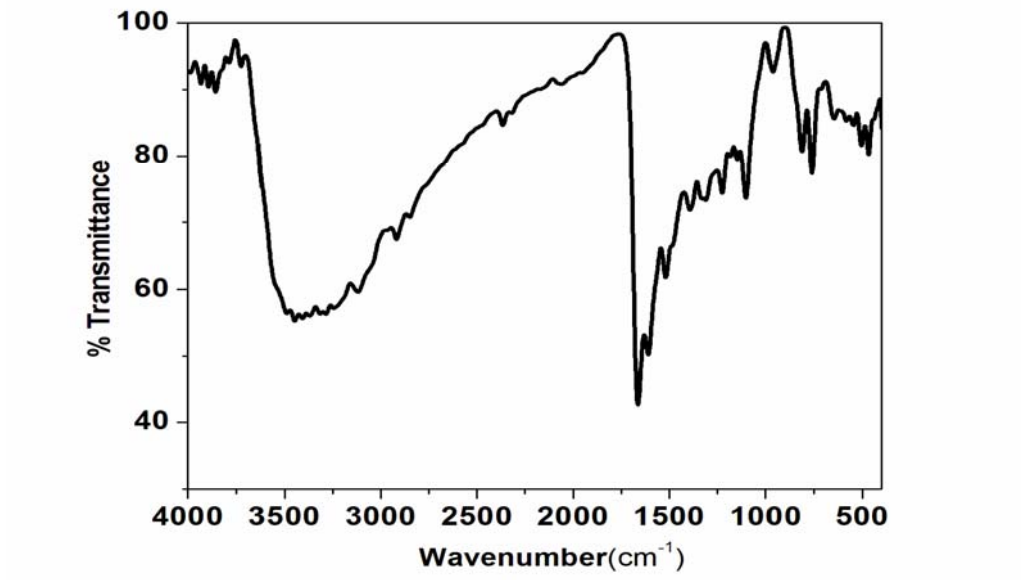

Figure 5.8. FTIR spectrum of [Ru(hqc5in)$Cl_3(H_2O)$] H_2O

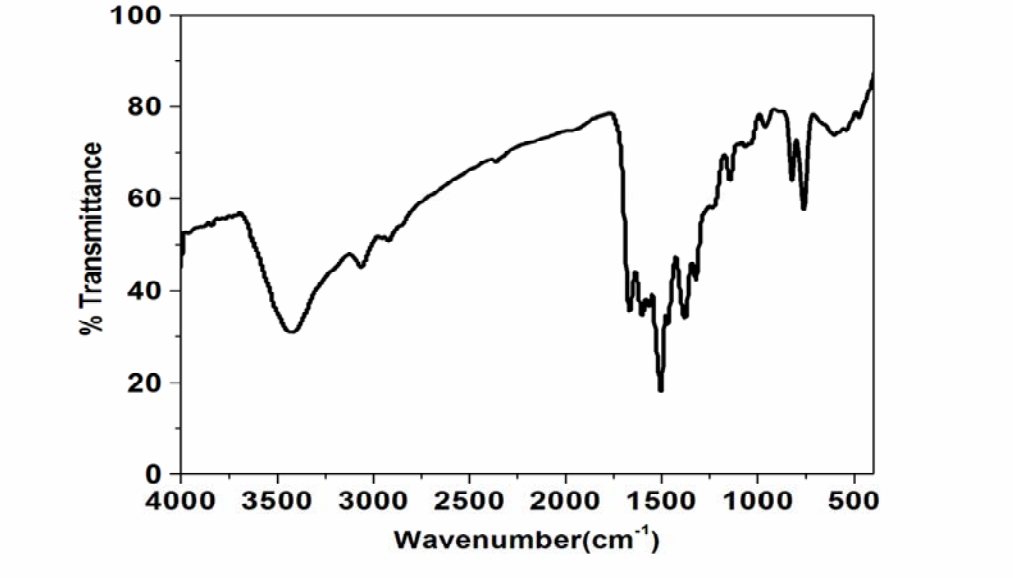

Figure 5.9. FTIR spectrum of [Ru(hqc6in)$Cl_3(H_2O)$] H_2O

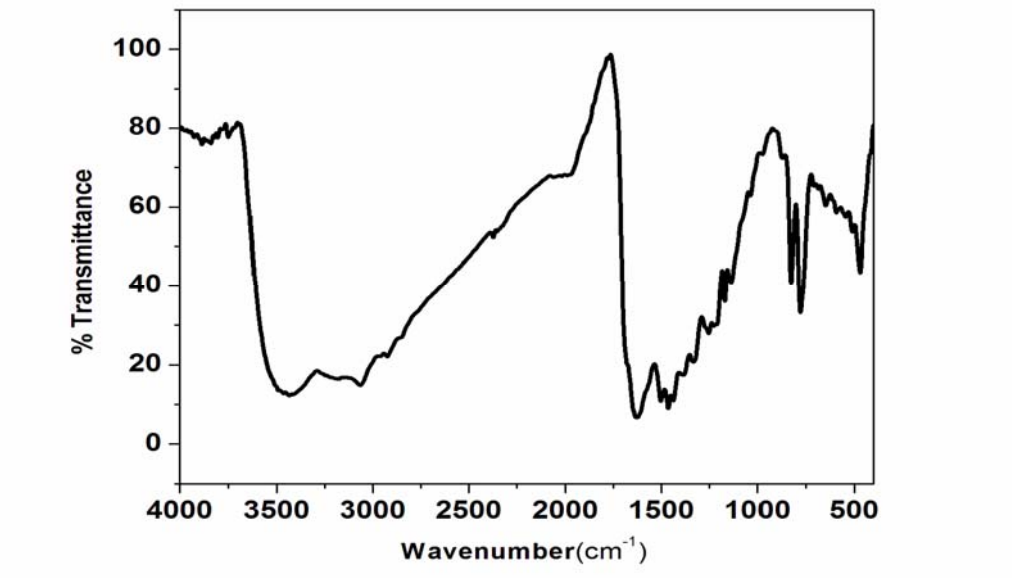

Figure 5.10. FTIR spectrum of [Ru(hqaqn)$Cl_3(H_2O)$] H_2O

5.3.4 Electronic spectra and magnetic moment data.

The electronic spectra of all the complexes were recorded in DMSO solution (see Table 5.4 and Figures 5.11-5.15). The ground state of ruthenium(III) is $^2T_{2g}$ and the first excited doublet levels in the order of increasing energy are

$^2A_{2g}$ and $^2T_{1g}$ which arises from the $t_{2g}^4eg^1$ configuration. In most of the ruthenium(III) complexes, the UV–vis spectra show only charge transfer bands. As ruthenium(III) in its complexes has relatively high oxidizing ability, ligand to metal the charge transfer bands become prominent in the low energy region and obscure the weaker bands due to d–d transition (27). Therefore it becomes difficult to assign conclusively the bands of ruthenium(III) complexes which appear in the visible region. However, the bands observed in the region 502-580 nm might be due to d-d transitions. Similar observations have been made for other ruthenium(III) octahedral complexes (28-32). The electronic spectral data of the complexes are given in Table 5.4 and in Figures 5.11-5.15

Table 5.4. Electronic spectral and magnetic moment data of Ru(III) complexes

Complex	Electronic spectral bands:nm(cm^{-1})	Assignments	μ_{eff} (BM)
$[Ru(qc5in)Cl_3H_2O]H_2O$	265 (37,740) 313 (31,950) 613 (16,310)	Intraligand transitions CT $^2T_{2g}\rightarrow{}^4T_{1g}$	1.76
$[Ru(qc6in)Cl_3H_2O]H_2O$	230(43,480) 260(38,460) 322(31,060) 635(15,750)	Intraligand transitions CT CT $^2T_{2g}\rightarrow{}^4T_{1g}$	1.72
$[Ru(hqc5in)Cl_3(H_2O)]H_2O$	221 (45,250) 272 (36,760) 314 (31,850) 430 (23,255) 518 (19,310)[s] 641 (15,600)[s]	CT CT CT $^2T_{2g}\rightarrow{}^2A_{2g}, {}^2T_{1g}$ $^2T_{2g}\rightarrow{}^2T_{1g}$ $^2T_{2g}\rightarrow{}^2A_{2g}$	1.64
$[Ru(hqc6in)Cl_3(H_2O)]H_2O$	264 (37,880) 309 (32,360)[a] 384 (26,040)[a] 521 (19,200) 583 (17,150)[s]	Intraligand transitions CT $^2T_{2g}\rightarrow{}^2A_{2g}, {}^2T_{1g}$ $^2T_{2g}\rightarrow{}^4T_{2g}$ $^2T_{2g}\rightarrow{}^4T_{1g}$	1.82
$Ru(hqaqn)Cl_3(H_2O)]H_2O$	300(33,330) 371(26,960) 550(18,180)	Intraligand transitions $^2T_{2g}\rightarrow{}^2A_{2g}, {}^2T_{1g}$ $^2T_{2g}\rightarrow{}^4T_{2g}$	1.62

All the complexes were found to be paramagnetic in nature. The magnetic moment values lie between 1.64-1.76 indicating the presence of one unpaired electron and +3 oxidation states for ruthenium (33).

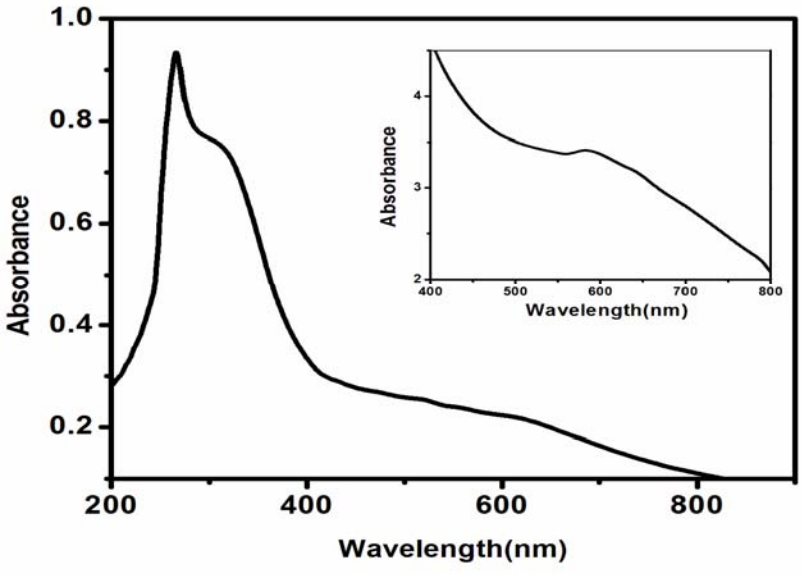

Figure 5.11. The UV-Vis spectrum of [Ru(qc5in)Cl_3H_2O]H_2O

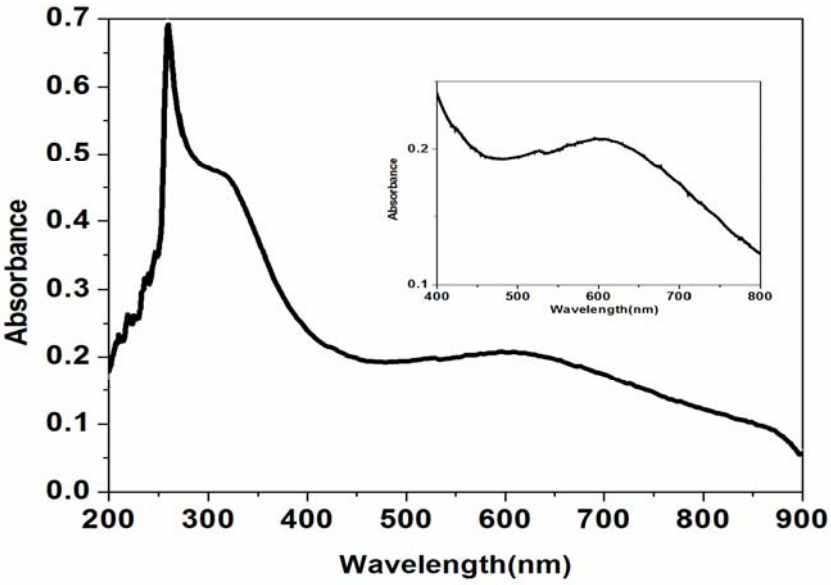

Figure 5.12. The UV-Vis spectrum of [Ru(qc6in)Cl_3H_2O]H_2O

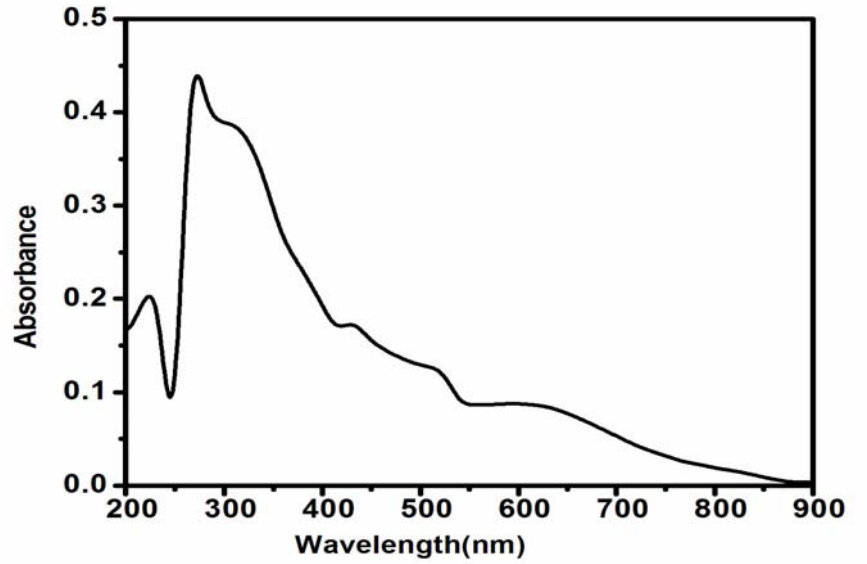

Figure 5.13. The UV-Vis spectrum of of [Ru(hqc5in)$Cl_3(H_2O)$] H_2O

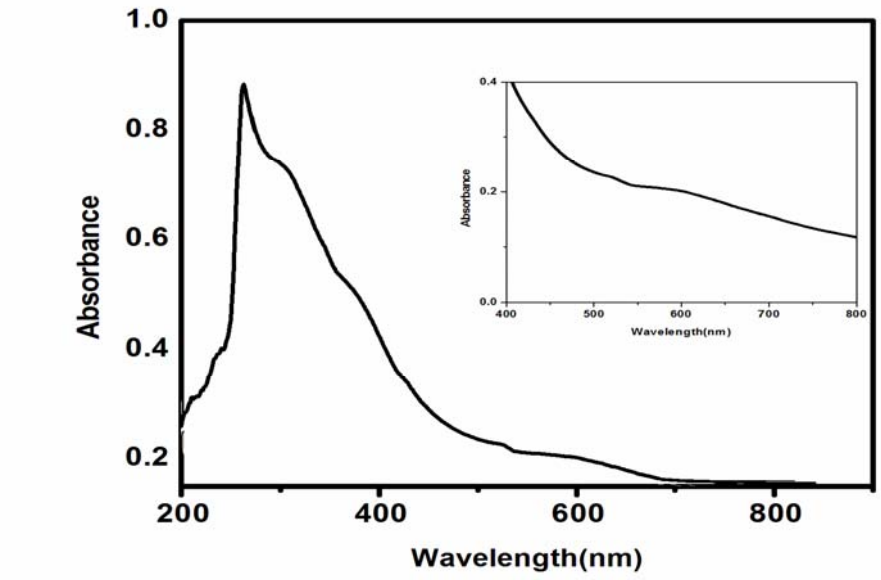

Figure 5.14. The UV-Vis spectrum of [Ru(hqc6in)$Cl_2(H_2O)_2$] H_2O

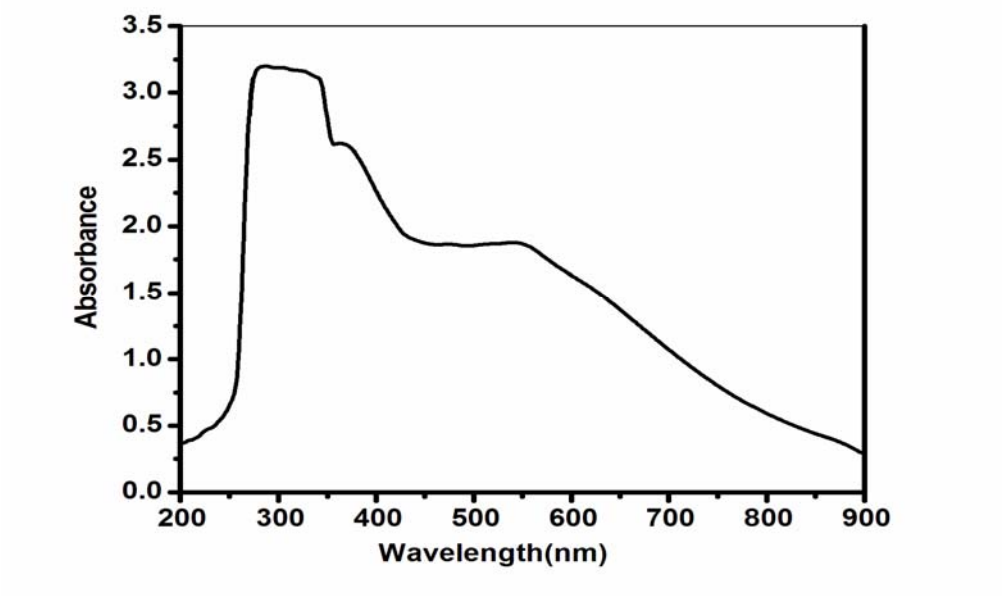

Figure 5.15. The UV-Vis spectrum of [Ru(hqaqn)$Cl_3(H_2O)]\,H_2O$

5.3.5 EPR Spectra of the Complexes

The EPR spectra of all complexes in DMSO at 77K exhibit three lines with three different g values. The presence of three g values [$g_x \neq g_y \neq g_z$] is an indication of rhombic distortion in these complexes. The average value was calculated using the equation. $g^* = [1/3\, g_x^2 + 1/3\, g_y^2 + 1/3\, g_z^2]^{1/2}$. The average g values lie in the range 2.3–2.7 are close to the values reported for similar ruthenium(III) complexes [34-38].

Table 5.6. EPR spectral data of the Ru(III) complexes

Complex	g_x	g_y	g_z	g*
$[Ru(qc5in)Cl_3H_2O]H_2O$	2.6	2.4	2.1	2.4
$[Ru(qc6in)Cl_3H_2O]H_2O$	2.5	2.3	1.9	2.2
$[Ru(hqc5in)Cl_3(H_2O)]\,H_2O$	2.5	2.4	2.2	2.4
$[Ru(hqc6in)Cl_3(H_2O)]\,H_2O$	2.6	2.4	2.1	2.4
$Ru(hqaqn)Cl_3(H_2O)]\,H_2O$	2.7	2.3	2.0	2.3

$g^* = [1/3\, g_x^2 + 1/3\, g_y^2 + 1/3\, g_z^2]^{1/2}$.

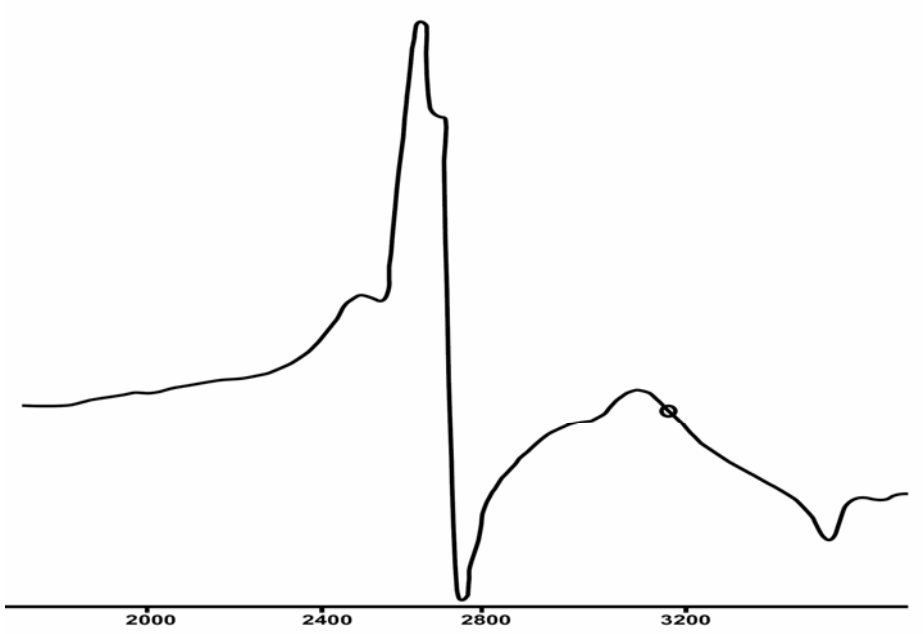

Figure 5.16. EPR spectrum of [Ru(qc5in)Cl_3H_2O]. H_2O

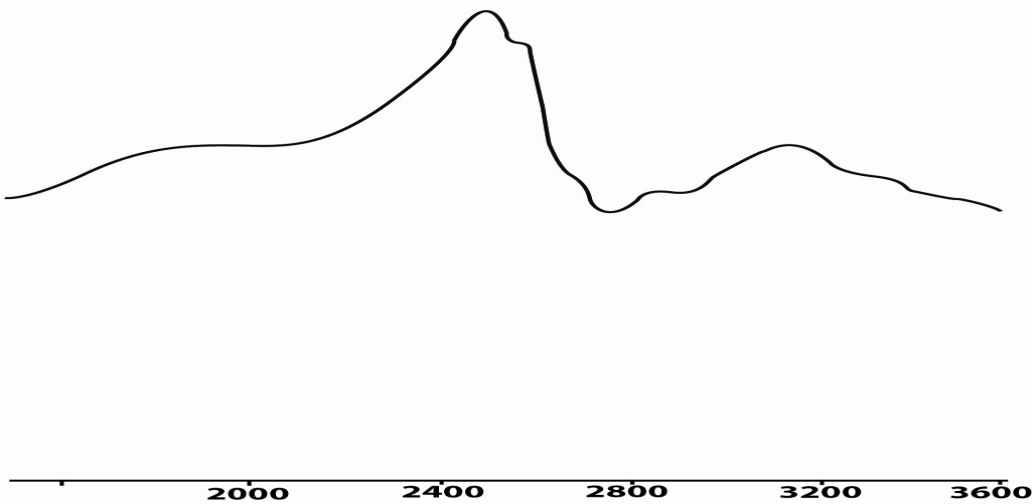

Figure 5.17. EPR spectrum of [Ru(qc6in)Cl_3H_2O] H_2O

Figure 5.18. EPR spectrum of $[Ru(hqc5in)Cl_3(H_2O)]H_2O$

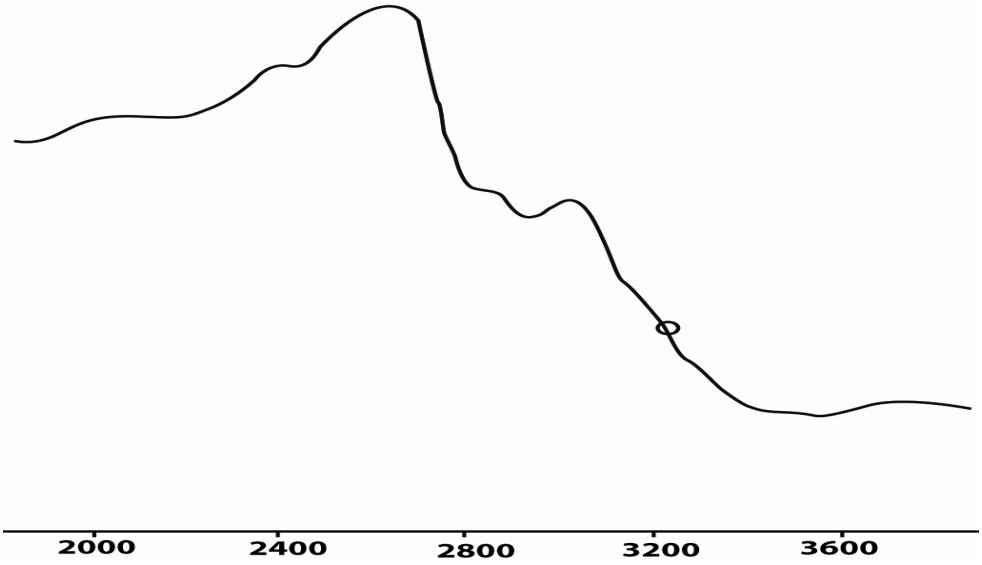

Figure 5.19. EPR spectrum of $[Ru(hqc6in)Cl_3(H_2O)]H_2O$

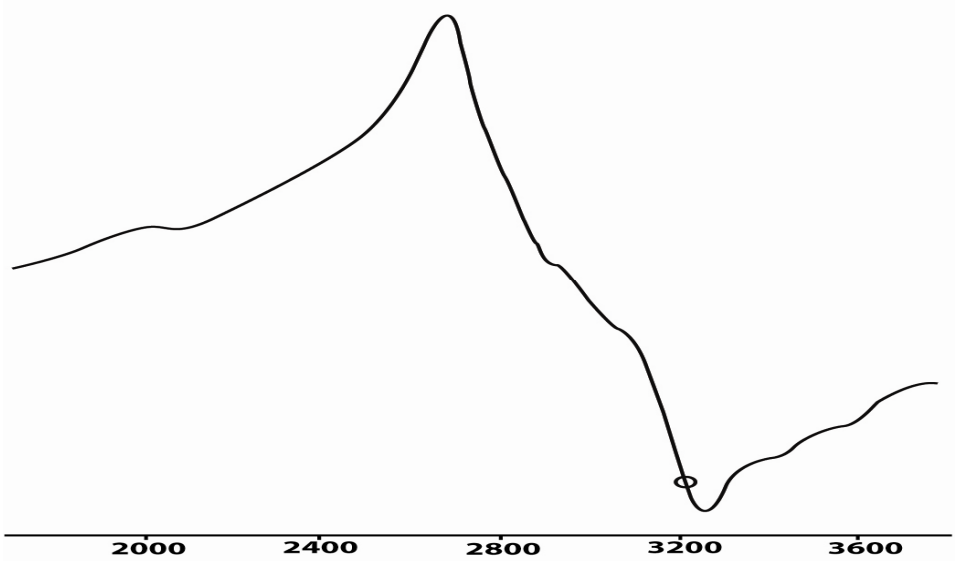

Figure 5.20. EPR spectrum of $[Ru(hqaqn)Cl_3(H_2O)]H_2O$

5.3.6 Cyclic voltammetry

The electrochemical activity of the ruthenium complexes was studied in DMSO (10^{-3} mol l^{-1}) at a scan rate of 0.100 V in the potential range +1.5 to -1.5 V by cyclic voltammetry. The cyclic voltammograms of the ruthenium complexes are shown in Figures 5.21-5.25 and the voltammetric data are summarized in Table 5.5. In all the ruthenium(II) complexes the ratio, I_{pc}/I_{pa}, falls in the range 1.08- 1.50, clearly confirming one electron transfer for redox processes, All the complexes showed only a reversible reduction wave in the -0.47 to -0.99 V range. The peak-to-peak separation (ΔE_pvalue) ranging from 164 to 170 mV reveals that this process is quasi reversible (39). This is attributed to slow electron transfer and adsorption of the complexes on the electrode surface (40). The ruthenium(III) to ruthenium(II) redox processes are influenced by the coordination number, stereochemistry and the hard or soft character of the ligands (41). Patterson and Holm have shown that softer ligands tend to produce more positive $E_{1/2}$ values, while hard ligands give rise to negative $E_{1/2}$ values (42). The observed $E_{1/2}$ values for these complexes

indicate considerable hard base character, which is likely to be due to an azomethine nitrogen donor atom involved in the coordination. Similar behaviour has been reported for mononuclear ruthenium(III) complexes (43).

Table 5.5. Cyclic voltammetric data of Ru(III) complexes

Complex	E_{pc} (V)	E_{pa} (V)	$(E_{1/2})$ (V)	ΔEp (mV)	I_{pc} (μA)	I_{pa} (μA)	I_{pc}/I_{pa}
$[Ru(qc5in)Cl_3H_2O]H_2O$	-0.768	-0.599	-0.683	170	4.81	3.87	1.24
$[Ru(qc6in)Cl_3H_2O]H_2O$	-0.986	-0.468	-0.727	518	5.00	5.43	1.09
$[Ru(hqc5in)Cl_3(H_2O)]H_2O$	-0.789	-0.598	-0.693	191	7.62	6.80	1.12
$[Ru(hqc6in)Cl_3(H_2O)]H_2O$	-0.782	-0.618	-0.700	164	7.94	6.55	1.22
$Ru(hqaqn)Cl_3(H_2O)]H_2O$	-0.986	-0.550	-0.768	436	6.32	5.84	1.08

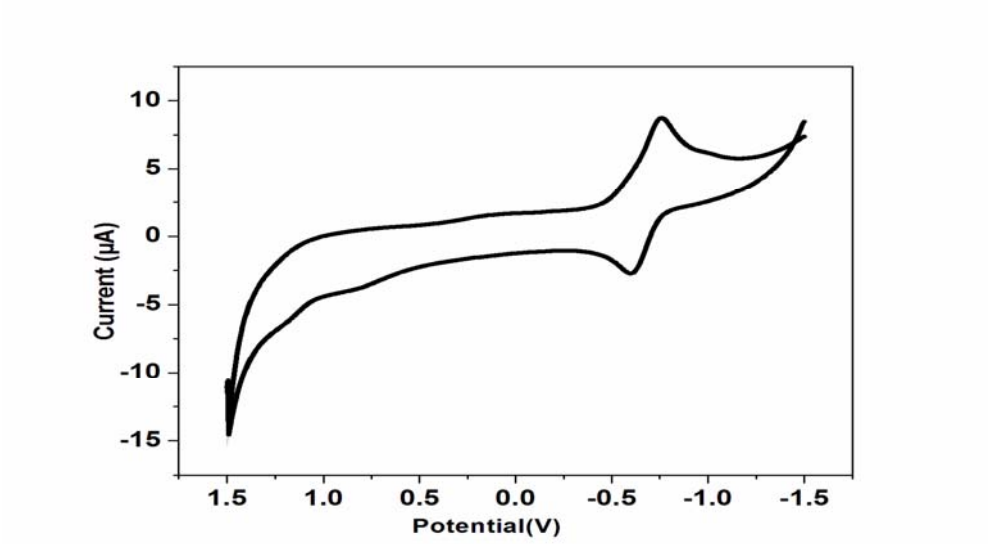

Figure 5.21. Cyclic voltammogram of $[Ru(qc5in)Cl_3H_2O].H_2O$

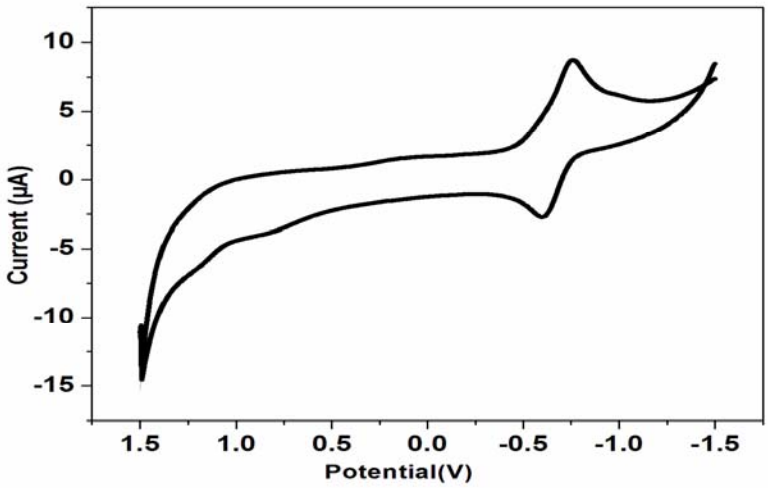

Figure 5.22. Cyclic voltammogram of Ru(qc6in)Cl_3H_2O]. H_2O

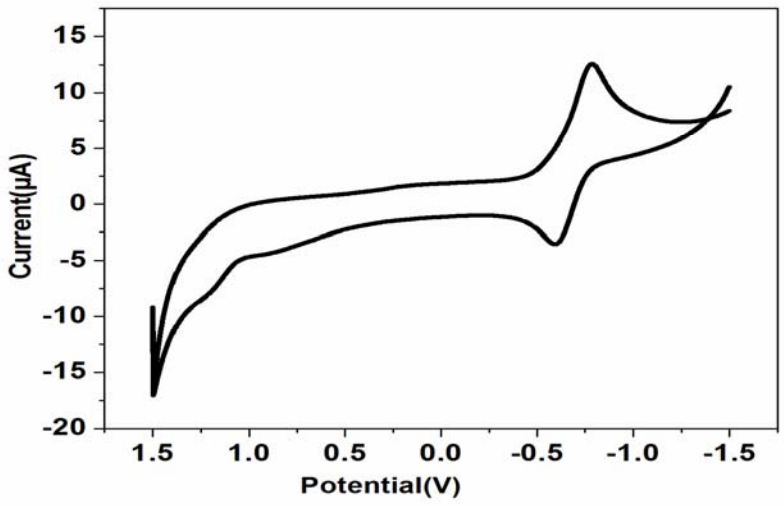

Figure 5.23. Cyclic voltammogram of [Ru(hqc5in)$Cl_3(H_2O)$]. H_2O

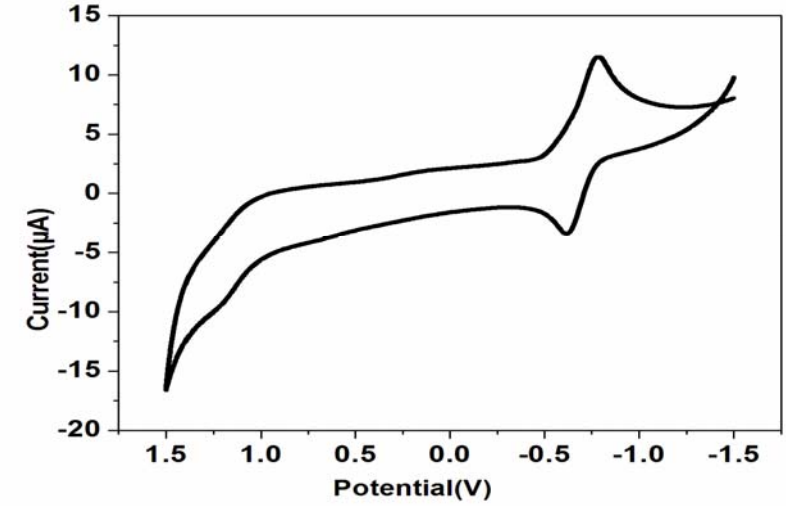

Figure 5. 24. Cyclic voltammogram of [Ru(hqc6in)$Cl_3(H_2O)$].H_2O

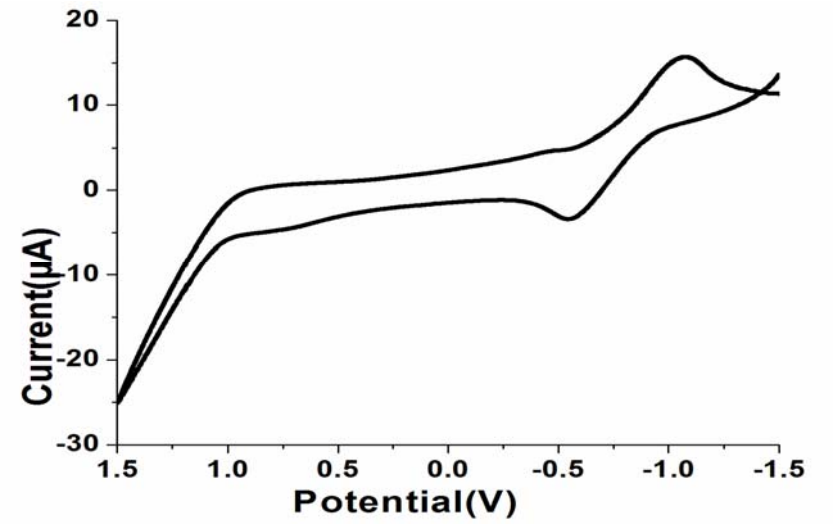

Figure 5.25. Cyclic voltammogram of [Ru(hqaqn)$Cl_3(H_2O)$].H_2O

5.3.7 Geometry of the complexes

Based on the above discussion, an octahedral structure has been assigned for the complexes and tentative structures are shown in Figure 5.27.

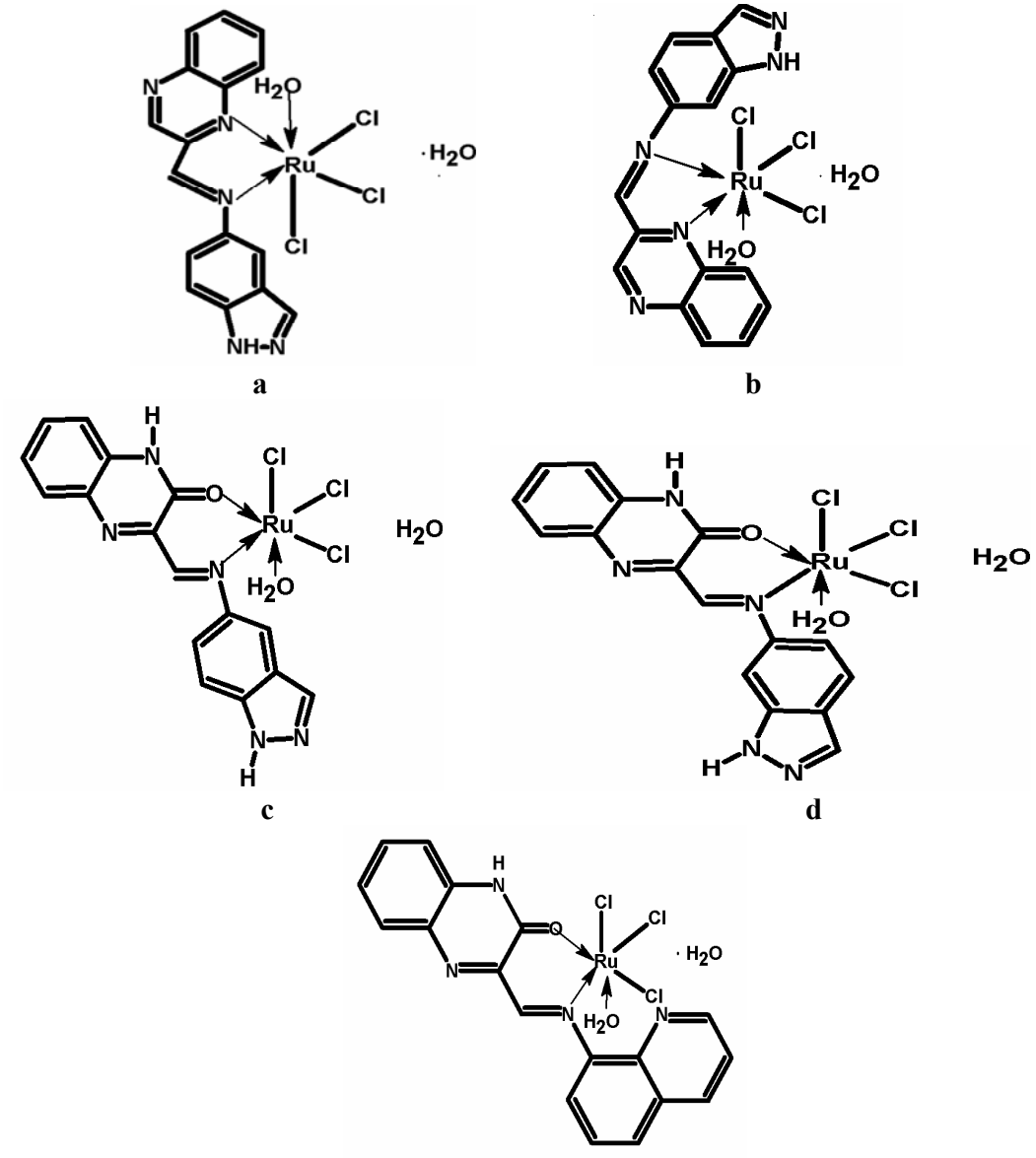

Figure 5.27. The Proposed geometry of Ru(III) complexes where

a = [Ru(qc5in)Cl_3H_2O]. H_2O, b=[Ru(qc6in)Cl_3H_2O]. H_2O

c = [Ru(hqc5in)$Cl_3(H_2O)$].H_2O, d=[Ru(hqc5in)$Cl_3(H_2O)$].H_2O

e = [Ru(hqaqn)$Cl_3(H_2O)$].H_2O

5.4 Cleavage of pUC18 DNA by Ru(III) complexes

The ability of the Ru(III) complexes to perform complexes to perform DNA cleavage was monitored by agarose gel electrophoresis using pUC18 plasmid DNA (Figure 5.26). Three clear bands were observed (lane 1 and 2) for pUC18 DNA corresponding to the conformations of the plasmid *viz*, open circular, supercoiled, and linear forms. After the addition of $[Ru(qc5in)Cl_3H_2O].H_2O$, $[Ru(qc6in)Cl_3H_2O].H_2O$ only 2 bands are visible (Lane 3 ,4 and 5). Thus the binding of the metal complexes results in the complete degradation of the open circular form of DNA. The complexes $[Ru(hqc5in)Cl_3(H_2O)]\,H_2O$ and $[Ru(hqc6in)Cl_3(H_2O)].H_2O$ failed to show a significant DNA cleavage activity (lane 6 and 7). But $[Ru(hqaqn)\,Cl_3(H_2O)]H_2O$ completely degrades three forms of pUC18 plasmid DNA (lane 8). All the results indicate that complexes $[Ru(qc5in)Cl_3H_2O].H_2O$, $[Ru(qc5in)Cl_3H_2O].H_2O$ and $Ru(hqaqn)Cl_3(H_2O)].H_2O$ shows efficient DNA-cleavage activity.

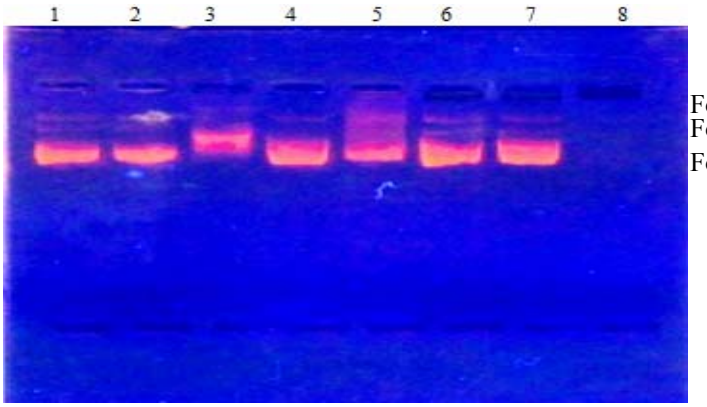

Lane 1 : pUC18 DNA
Lane 2 : pUC18DNA
Lane 3 : pUC18DNA +[Ru(qc5in)Cl_3H_2O] H_2O
Lane 4 : pUC18DNA + [Ru(qc5in)Cl_3H_2O] H_2O
Lane 5 : pUC18DNA + [Ru(qc6in)$Cl_3(H_2O)_2$]H_2O
Lane 6 : pUC18DNA + [Ru(hqc5in)$Cl_3(H_2O)$]H_2O
Lane 7 : pUC18DNA + [Ru(hqc6in)$Cl_3(H_2O)$]H_2O
Lane 8 : pUC18DNA +[Ru(hqaqn)$C1_3(H_2O)$] H_2O

Figure 5.26. Gel electrophoresis diagram of Ru(III) complexes

5.5 Conclusion

The elemental analyses suggest the molecular formulae of the complexes $[Ru(qc5in)Cl_3H_2O].H_2O$, $[Ru(qc6in)Cl_3H_2O].H_2O$, $[Ru(hqc5in)Cl_3(H_2O)].H_2O$, $[Ru(hqc6in)\ Cl_3(H_2O)].H_2O$, $[Ru(hqaqn)Cl_3(H_2O)]H_2O$. The coordinated/ lattice water present in the complexes is evidenced by weight loss in TG and presence of characteristic stretching bands in the IR spectrum. The IR spectra reveal that the bonding of qc5in and qc6in to ruthenium is through azomethine nitrogen and quinoxaline ring nitrogen where as the bonding of hqc5in, hqc6in and hqaqn is through coordination of the azomethine nitrogen and through keto oxygen. The electronic spectral data suggests an octahedral geometry for the complexes. The cleavage studies show that the hqaqn complex was highly efficient in degrading three forms of pUC18 plasmid DNA.

5.6 References

[1] R .I. Kureshy, N.H. Khan, S.H.R. Abdi, S.T. Patel, P. Iyer, *J. Mol. Catalysis* 150 (1999) 175.

[2] M. Sivagamasundari, R. Ramesh, *Spectrochimica Acta Part A.* 66 (2007) 427.

[3] D. Sukanya, R. Prabhakaran, K.Natarajan, *Polyhedron* 25 (2006) 2223.

[4] V. Mahalingam, R. Karavembu, V. Chinnusamy, K. Natarajan, *Spectrochimica Acta Part A.* 64 (2006) 886.

[5] R. Karvembu, K. Natarajan, *Polyhedron* 21 (2002) 219.

[6] R. Karvembu, K. Natarajan, *Polyhedron* 21 (2002) 1721.

[7] V. Arun, N. Sridevi, P.P. Robinson, S. Manju, K.K.M. Yusuff, *J. Mol. Catal. A: Chem*. 304 (2009)191.

[8] T. Ohkuma, H. Ooka, M. Yamakawa, T. Ikariya, R. Noyori, *J. Org.Chem.* 61 (1996) 4872.

[9] P . Sengupta, S. Ghosh, T.C.W. Mak, *Polyhedron* 20 (2001) 975.

[10] G. Venkatachalam, R. Ramesh, *Spectrochimica Acta Part A.* 61 (2005) 2081.

[11] P.M.T. Piggot, L.A. Hall, A.J.P. White, D.J. Williams, *Inorg. Chim.Acta* 357 (2004) 207.

[12] R. Ramesh, S. Maheswaran , *Journal of Inorganic Biochemistry* 96 (2003) 457.

[13] S. Kannan, R. Ramesh, Polyhedron. 25 (2006) 3095.

[14] R. Prabhakaran, A. Geetha, M. Thilagavathi, R. Karvembu, V.Krishnan, H. Bertagnolli, K. Natarajan, *J. Inorg. Biochem*. 98 (2004) 2131.

[15] Saxena, J.K. Koacher, J.P. Tandon, *J. Antibact. Antifung. Agents* 9 (1981) 435.

[16] K. Karidi, A. Garoufis, A. Tsipis, N. Hadjiliadis, H. Dulk, J.Reedijk, *J. Chem. Soc, Dalton Trans.* (2005) 1176.

[17] O. Novakova, J. Kasparkova, O. Vrana, P.M. Vanvliet, J. Reedijk, V. Brabec, *Biochemistry* 34 (1995) 12369.

[18] J. Reedijk, *Curr. Opin. Chem*. Biol. 3 (1999) 236.

[19] R. Karvembu, K. Natarajan, *Polyhedron* 21 (2002) 1721.

[20] R. Noyori, S. Hashiguchi, *Acc. Chem. Res*. 30 (1997) 97.

[21] S.I. Murahashi, H. Takaya, *Acc. Chem. Res*. 33 (2000) 225.

[22] A. Dijksman, M. Gonzalez, A.M.I. Payeras, I.W.C.E. Arends, R.A. Sheldon, *J. Am. Chem. Soc.* 123 (2001) 6826.

[23] R.A. Sheldon, J. Am W.J. Geary. *Coordination Chemistry Reviews*, 7 (1971) 81.

[24] M.M. Taqui Khan, N.H. Khan, R.I. Kureshy, A.B. Boricha, Z.A. Shaikh. *Inorganica Chimica Acta,* 170 (1990) 213.

[25] S.A. Sallam. *Transition Metal Chemistry* 30 (2005) 341.

[26] K. Nakamoto, Infrared and Raman Spectra of Inorganic and Coordination Compounds, 4th Edn, John Wiely and Sons, Inc.: New York, (1986).

[27] R. Ramesh, S. Maheswaran, *J. Inorg Biochem* 96 (2003) 457.

[28] M.M.T. Khan, D. Srinivas, R.I. Kureshy, N.H. Khan, *Inorg.Chem.,* 29 (1990) 2320.

[29] N. Jayakumar, K. Natarajan, *Synth. React. Inorg. Met.org.Chem.* 22 (1992) 349.

[30] T.D. Thangadurai, K. Natarajan *Transition Metal Chemistry* 25: (2000) 347.

[31] R. Prabhakaran, A. Geetha, M.Thilagavathi, R. Karvembu, V. Krishna, H. Bertagnolli, K. Natarajan, *J . Inorg Biochem* 98 (2004) 2131.

[32] P. S. Chittilappilly, K.K.M. Yusuff, *Indian Journal of Chemistry* 47 (2008) 848.

[33] B.N. Figgis, Introduction to Ligand Field Theory, Interscience Publishers Inc., New York, (1966).

[34] N. Jayakumar, K. Natarajan, *Synth. React. Inorg. Met.org.Chem.* 22 (1992) 349.

[35] M.M.T. Khan, R.I. Kureshy, N.H. Khan, *Polyhedron* 1 (1991) 2559.

[36] V. Chinnusamy, K. Natarajan, *Synth. React. Inorg. Met.Chem.* 24 (1994) 533.

[37] T. D. Thangadurai, K. Natarajan, *Transition Metal Chemistry* 25 (2000) 347.

[38] G. Venkatachalam, R. Ramesh, *Inorganic Chemistry Communications* 9 (2006) 703–70 7.

[39] J. Heinze. Angew. *Chem. Int. Edn;* 23 (1984) 831.

[40] A.W. Wallce, J. Murphy, J.D. Peterson, *Inorg. Chim. Acta.* 166 (1989) 47.

[41] B.J. Hathaway, *Comprehensive Coordination Chemistry*, Pergaman Press: Oxford (1987) 5.

[42] G.S. Patterson, R.H. Holm, *J. Biol. Inorg. Chem* 4 (1975) 1257.

[43] S. Priyarega, R. Prabhakaran, K. R. Aranganayagam, R. Karvembu, K. Natarajan, *Appl. Organometal. Chem. 21 (*2007) 788.

.....ooo.....

Chapter 6

Synthesis, characterisation and DNA cleavage of copper(II) complexes

Contents

6.1 Introduction

Designing of metal complexes for cleaving DNA is important for chemical as well as biological point of view. In this regard copper complexes, which possess biologically accessible redox potentials and demonstrate high nucleobase affinity, are potential reagents for cleavage of DNA (1-16). In view of these we have synthesised new copper(II) complexes by the reaction of the Schiff base ligands, quinoxaline-2-carboxalidene-5-aminoindazole (qc5in), quinoxaline-2-carboxalidene-6-aminoindazole (qc6in), 3-hydroxyquinoxaline-2-carboxalidene-5-aminoindazole (hqc5in), 3-hydroxyquinoxaline-2-carboxalidene-6-aminoindazole (hqc6in), 3-hyodroxyquinoxaline-2-carboxalidene-8-aminquinoline (hqaqn) with Cu(II) chloride. The complexes have been characterised and their DNA cleavage ability has been studied. The results of the studies are presented in this chapter.

6.2 Experimental

6.2.1 Materials

The details of materials used for the synthesis of the Schiff base ligands and their copper complexes are given in chapter 2.

6.2.2 Synthesis of Schiff base ligands

The procedure for the synthesis of the Schiff base ligands are given in Chapter 2

6.2.3 Synthesis of complexes

All the copper(II) complexes were prepared by mixing an ethanolic solution (20 mL) of $CuCl_2.2H_2O$ (0.85 g, 5 mmol,) and an ethanolic solution of the ligand, qc5in (1.37 g, 5 mmol,), qc6in (1.36 g, 5mmol), hqc5in (5 mmol, 1.4 g), hqc6in (1.4 g, 5 mmol) or hqaqn (1.5 g, 5 mmol) in ethanol (100 mL) with a ligand to metal molar ratio 1:1 and refluxing for 3hrs. The complex separated out was collected, washed with ethanol and then with petroleum ether and dried over anhydrous calcium chloride in a desiccators.

6.3 Results and discussion

All the complexes are black and non-hygroscopic. They are soluble in DMF, DMSO and insoluble in ethanol, methanol, chloroform and benzene.

6.3.1 Elemental analyses

Analytical data and conductance data are given in Table 6.1. The data suggest that all the complexes are mononuclear in nature and metal to Schiff base ratio is 1:1. The molar conductance values of the complexes in DMSO (10^{-3} mol) indicate non-electrolytic nature (17, 18). Based on the analytical and molar conductance data the complexes have been assigned the molecular formula, $[Cu(qc5in)Cl_2]$, $[Cu(qc6in)Cl_2]$, $[Cu(hqc5in)Cl_2]$, $[Cu(hqc6in)Cl_2]$ and $[Cu(hqaqn)Cl_2]$

Table 6.1. Analytical data and conductance data of copper(II) complexes

Complexes of	C (%)	H (%)	N (%)	Cl (%)	Cu (%)	Molar conductance (ohm^{-1} cm^2 mol^{-1})
qc5in	47.02 (47.13)	2.60 (2.72)	16.98 (17.18)	17.86 (17.39)	15.48 (15.58)	5.6
qc6in	47.22 (47.13)	2.98 (2.72)	17.02 (17.18)	17.18 (17.39)	15.50 (15.58)	6.0
hqc5in	45.02 (45.35)	2.58 (2.62)	16.48 (16.53)	16.62 (16.73)	14.68 (15.00)	5.4
hqc6in	46.42 (45.35)	2.60 (2.62	15.38 (15.53)	15.86 (16.73)	15.48 (15.00)	5.8
hqaqn	49.62 (49.73)	2.62 (2.78)	12.76 (12.89)	16.00 (16.31)	14.08 (14.62)	6.2

6.3.2 Infrared spectra

The IR spectra of the complexes are given in Figures 6.2-6.6 and IR spectral data given in Table 6.2. The strong broad absorption band centred at 3342 cm^{-1} for $[Cu(qc5in)Cl_2]$ and that at 3271 cm^{-1} for $[Cu(qc6in)Cl_2]$ may be due to ν(NH). A strong broad absorption band is seen at 3264 cm^{-1} for $[Cu(hqc5in)Cl_2]$, 3400 cm^{-1} for $[Cu(hqc6in)Cl_2)]$ and 3439 cm^{-1} for $[Cu(hqaqn)Cl_2]$ may be due to hydrogen bonded ν(OH) in the iminol tautomer or ν(NH) in the amide tautomer. The bands centred at 1633 cm^{-1} for qc5in, at 1630 cm^{-1} for qc6in, at 1626 cm^{-1} for hqc5in, at 1612 cm^{-1} for hqc6in and hqaqn decreases to 1612 cm^{-1}, 1605 cm^{-1}, 1602 cm^{-1}, 1600 cm^{-1} and 1602 cm^{-1} for their metal complexes suggesting the coordination of azomethine nitrogen to the metal (19-21). The ν(C=N) of the quinoxaline ring in the spectra of qc5in and qc6in undergoes a decrease in stretching frequency on complexation suggesting the coordination of the ring nitrogen to the metal in their complexes. But for $[Cu(hqc5in)Cl_2]$, $[Cu(hqc6in)Cl_2)]$ and $[Cu(hqaqn)Cl_2)]$ the nitrogen of the quinoxaline ring is not involved in coordination as the IR stretching frequency due to ν(C=N) of quinoxaline ring not altered on complexation. The bands in the range 400-420 cm^{-1} in the case of all complexes is assigned to ν(Cu-N) (22). The

stretching frequency at 471 cm^{-1} for [Cu(hqc5in)Cl_2], 485 cm^{-1} for [Cu(hqc6in)Cl_2] and 478 cm^{-1} for [Cu(hqaqn)Cl_2] may be due to ν(Cu-O) (23). The bands at 1670 cm^{-1} for hqc5in and hqc6in, 1675 cm^{-1} for hqaqn get shifted to 1652 cm^{-1}, 1654 cm^{-1} and 1658 cm^{-1} respectively indicating the involvement of keto group in coordination.

Table 6.2. The IR spectral data of Cu(II) complexes

Compound	ν(O—H)[a]	ν(C=N)[b]	ν(C=N)[c]	ν(C=O)	ν(M-O)	ν(M-N)
qc5in	3208	1633	1489	-	-	-
[Cu(qc5in)Cl_2]	3342	1612	1480	-	-	406
qc6in	3211	1633	1532	-	-	-
[Cu(qc6in)Cl_2]	3271	1605	1502	-	-	420
hqc5in	3372	1626	1497	1670	-	-
[Cu(hqc5in)Cl_2]	3264	1598	1497	1652	471	411
hqc6in	3376	1612	1493	1670	-----	-----
[Cu(hqc6in)Cl_2]	3400	1602	1492	1654	485	409
hqaqn	3378	1612	1511	1675	-	-
[Cu(hqaqn)Cl_2]	3439	1591	1511	1658	478	409

[a] **ν(N−H)/ ν(O−H) of the free Schiff base**

[b] **−CH=N of azomethine group;** [c] **(C=N) of quinoxaline**

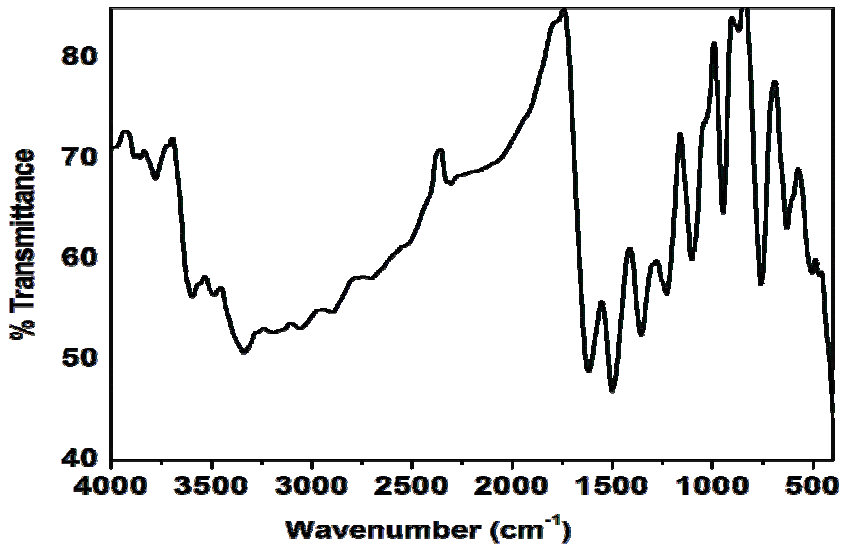

Figure 6.2. FTIR spectrum of [Cu(qc5in)Cl_2]

Figure 6.3. FTIR spectrum of [Cu(qc6in)Cl_2]

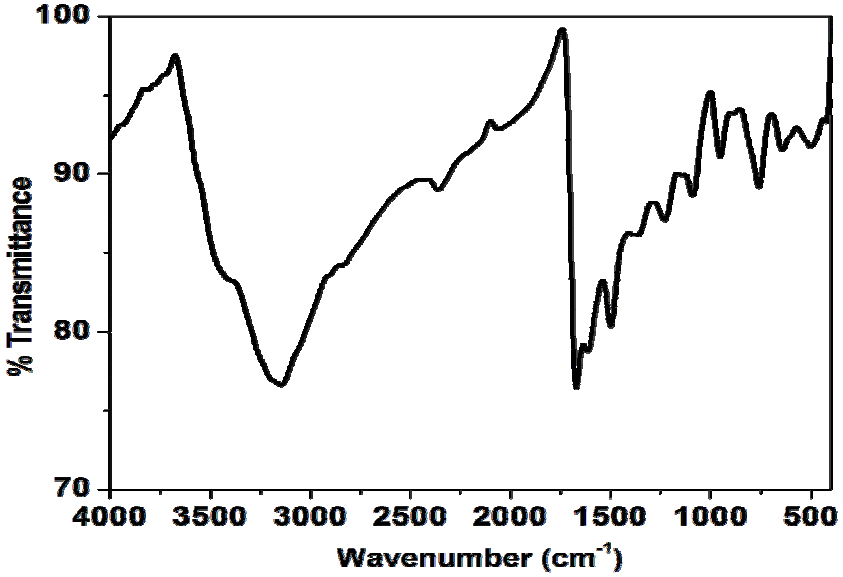

Figure 6.4. FTIR spectrum of [Cu(hqc5in)Cl_2]

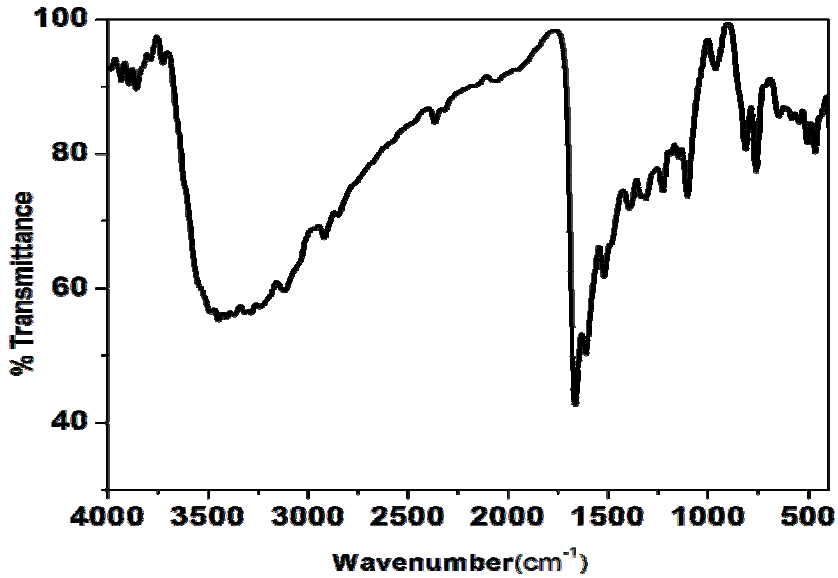

Figure 6.5. FTIR spectrum of [Cu(hqc6in)Cl_2]

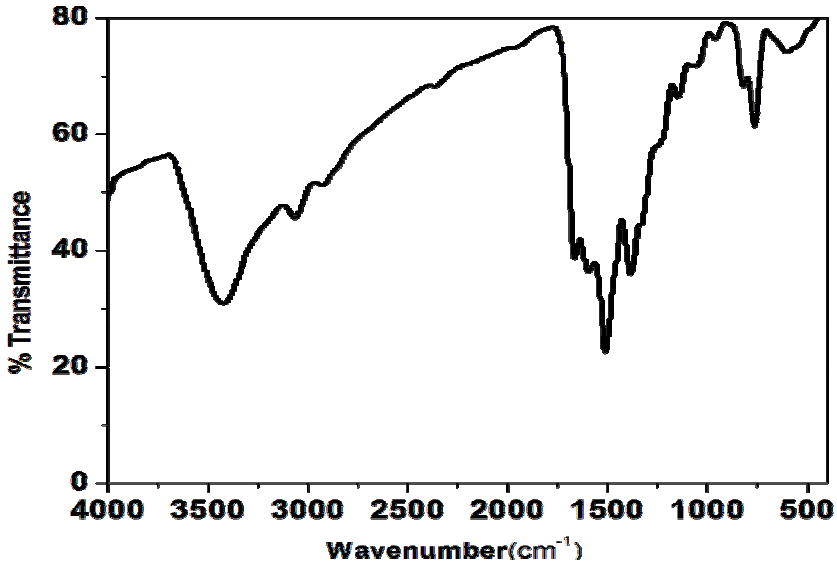

Figure 6.6. FTIR spectrum of [Cu(hqaqn)Cl_2]

6.3.3 Electronic spectra and magnetic moment data

The electronic spectra of all the complexes were recorded in DMSO solution. The Electronic spectral data of the complexes are given in Table 6.3 and in Figures 6.7-6.11. For square planar complexes with $d_{x^2-y^2}$ ground state, three spin allowed transitions are possible viz., $^2B_{1g} \rightarrow {}^2A_{1g}$ ($d_{x^2-y^2} \rightarrow d_{z^2}$), $^2B_{1g} \rightarrow {}^2B_{2g}$ ($d_{x^2-y^2} \rightarrow d_{xy}$) and $^2B_{1g} \rightarrow {}^2Eg$ ($d_{x^2-y^2} \rightarrow d_{xz}, d_{yz}$) (24) but it is often difficult to observe all the three bands since the four lower orbitals are so close together in energy. These transitions are observed as a broad shoulder band in the range 500-580 nm. Similar type of spectra has been reported for copper(II) square planar complexes (25, 26).

The magnetic moment of all the complexes lie in the range of 1.70-1.90 B.M. indicating the presence of one unpaired electron and monomeric nature of the complexes.

Table 6.3. Electronic spectral and magnetic moment data of Cu(II) complexes

Complex	Electronic spectral bands:nm(cm^{-1})	Assignments	μ_{eff} (BM)
$[Cu(qc5in)Cl_2]$	265 (37,740) 435 (22,990) 580 (17,240)	Intraligand transitions $^2B_{1g} \rightarrow {}^2E_g$ ($d_{x^2-y^2} \rightarrow d_{xz}, d_{yz}$) $^2B_{1g} \rightarrow {}^2B_{2g}$ ($d_{x^2-y^2} \rightarrow d_{xy}$)	1.76
$[Cu(qc6in)Cl_2]$	304 (33,900) 470 (21,280) 530 (18,870)	CT $^2B_{1g} \rightarrow {}^2E_g$ ($d_{x^2-y^2} \rightarrow d_{xz}, d_{yz}$ $^2B_{1g} \rightarrow {}^2B_{2g}$ ($d_{x^2-y^2} \rightarrow d_{xy}$)	1.70
$[Cu(hqc5in)Cl_2]$	265 (37,740) 330(30,300) 430 (23,260) 592 (16,890)	CT $^2B_{1g} \rightarrow {}^2A_{1g}$ ($d_{x^2-y^2} \rightarrow d_{z^2}$) $^2B_{1g} \rightarrow {}^2E_g$ ($d_{x^2-y^2} \rightarrow d_{xz}, d_{yz}$) $^2B_{1g} \rightarrow {}^2B_{2g}$ ($d_{x^2-y^2} \rightarrow d_{xy}$)	1.90
$[Cu(hqc6in)Cl_2)]$	265 (37,740) 432 (23,150) 586 (17,070)	CT $^2B_{1g} \rightarrow {}^2E_g$($d_{x^2-y^2} \rightarrow d_{xz}, d_{yz}$) $^2B_{1g} \rightarrow {}^2B_{2g}$ ($d_{x^2-y^2} \rightarrow d_{xy}$)	1.82
$[Cu(hqaqn)Cl_2]$	304 (32,900) 410 (24,390) 544 (18,380)	CT $^2B_{1g} \rightarrow {}^2E_g$($d_{x^2-y^2} \rightarrow d_{xz}, d_{yz}$) $^2B_{1g} \rightarrow {}^2B_{2g}$ ($d_{x^2-y^2} \rightarrow d_{xy}$	1.70

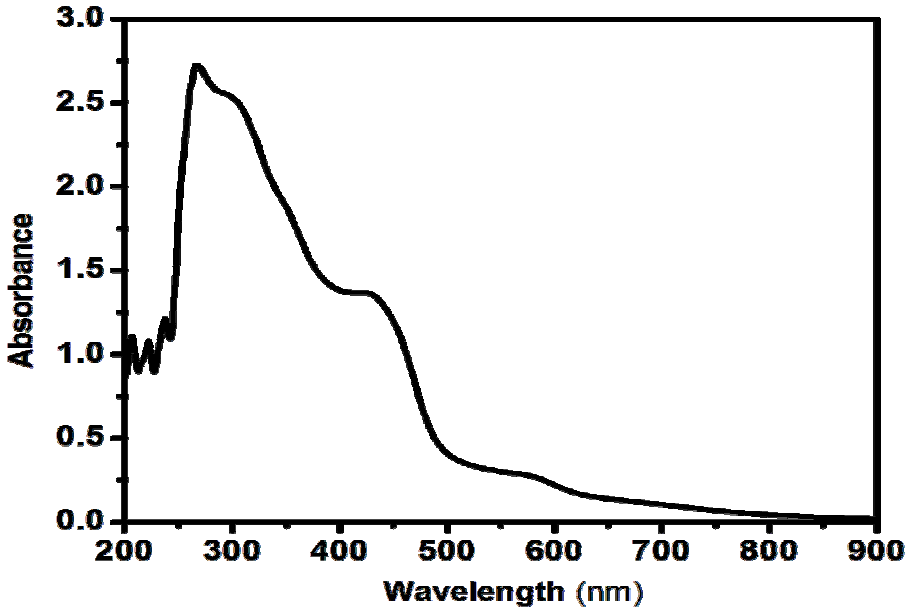

Figure 6.7. The UV-Vis spectrum of [Cu(qc5in)Cl_2]

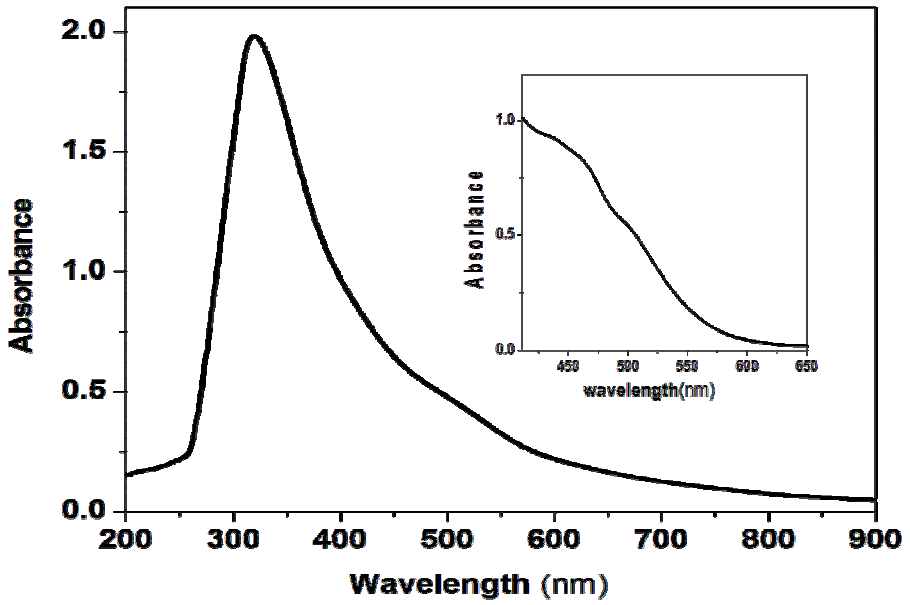

Figure 6.8. The UV-Vis spectrum of Cu(qc6in)Cl_2

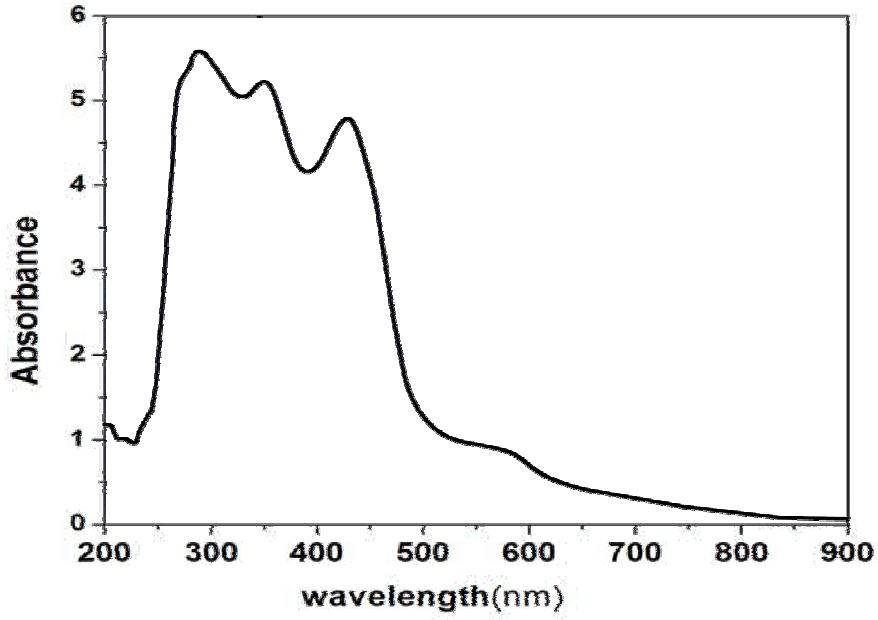

Figure 6.9. The UV-Vis spectrum of [Cu(hqc5in)Cl_2]

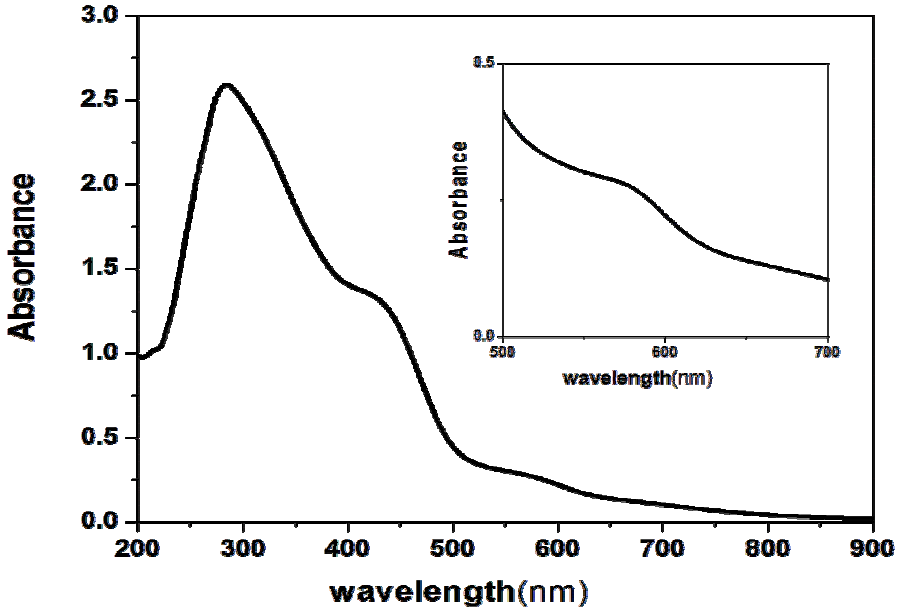

Figure 6.10. The UV-Vis spectrum of [Cu(hqc6in)Cl_2)]

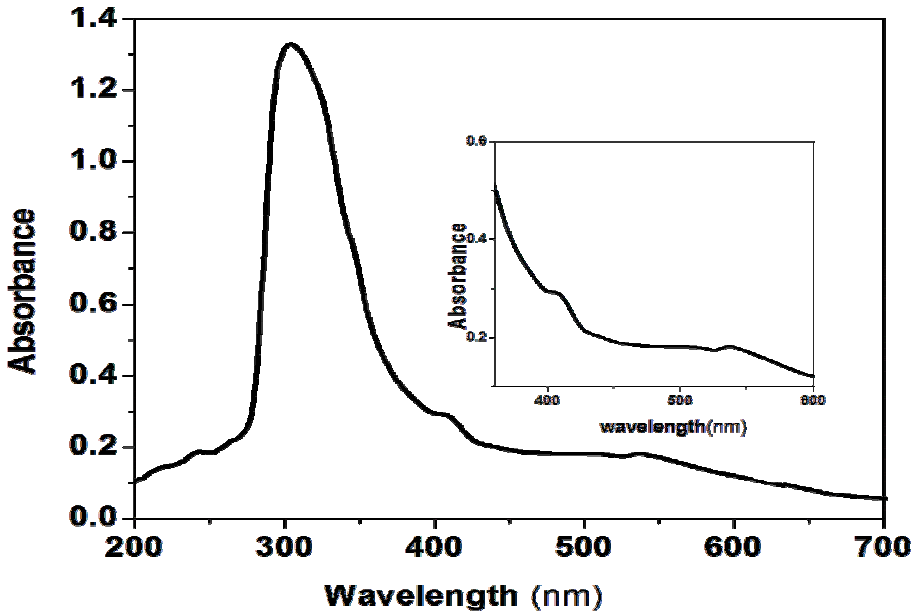

Figure 6.11. The UV-Vis spectrum of [Cu(hqaqn)Cl_2]

6.3.4 EPR spectra

The EPR spectra of the complexes in DMSO (77 K) show only one broad signal and are given in figures 6.12-6.16. The spectral parameters are presented in Table 6.4. The spectra are axial in nature and the g values are in the order: $g_{\parallel} > g_{\perp} > g_e$ (g_e is the g value of free electron, 2.0023) suggesting B_{1g} as the ground state. Furthermore, the spectra indicate a square planar geometry for the Cu(II) complexes (27, 28).

Table 6.4. EPR spectral parameters of the Cu(II) complexes

Complex	$g_{\parallel}$	$g_{\perp}$
[Cu(qc5in)Cl_2]	2.23	2.13
[Cu(qc6in)Cl_2]	2.21	2.07
[Cu(hqc5in)Cl_2]	2.10	2.01
[Cu(hqc6in)Cl_2)]	2.09	2.01
[Cu(hqaqn)Cl_2]	2.24	2.07

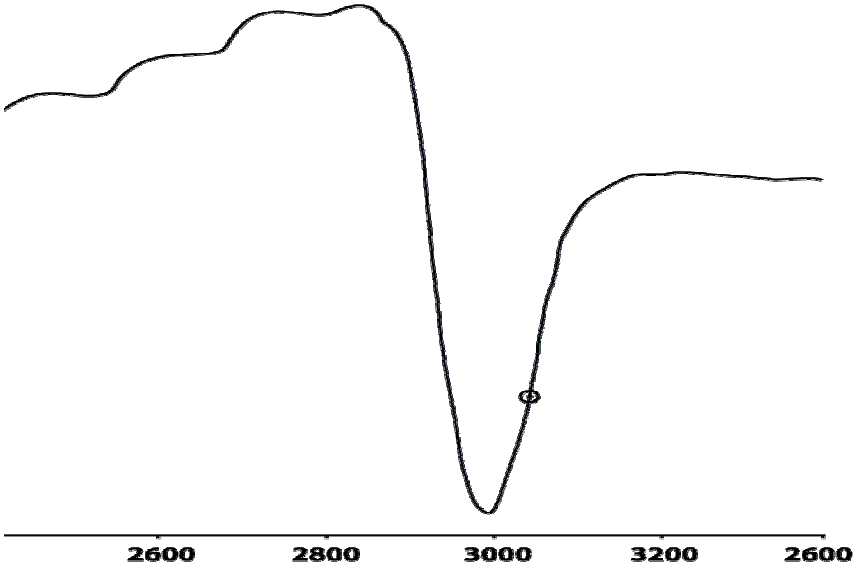

Figure 6.12. EPR spectrum of [Cu(qc5in)Cl_2]

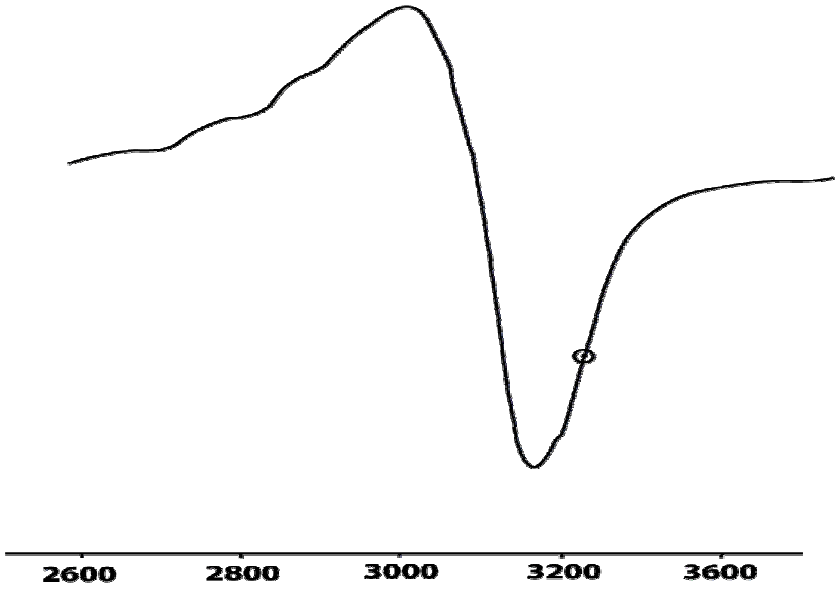

Figure 6.13. EPR spectrum of [Cu(qc6in)Cl_2]

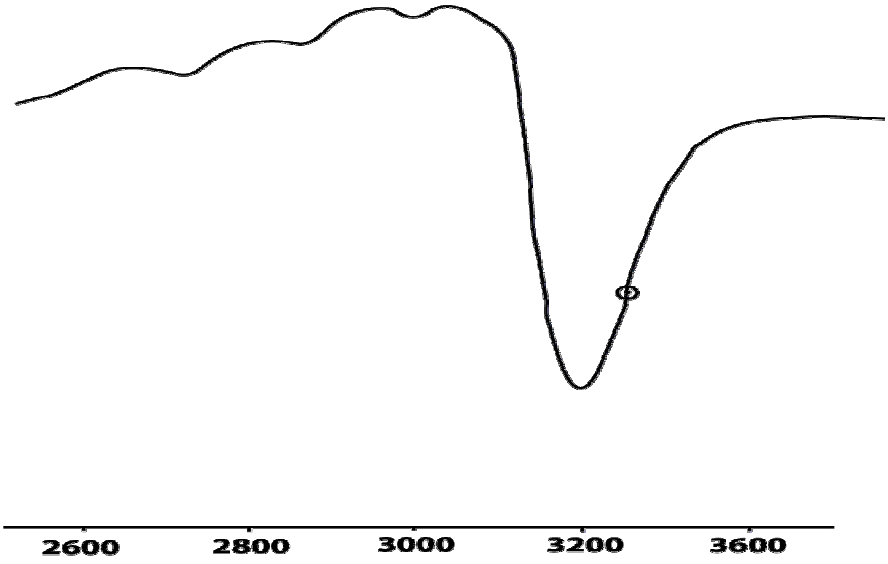

Figure 6.14. EPR spectrum of [Cu(hqc5in)Cl_2]

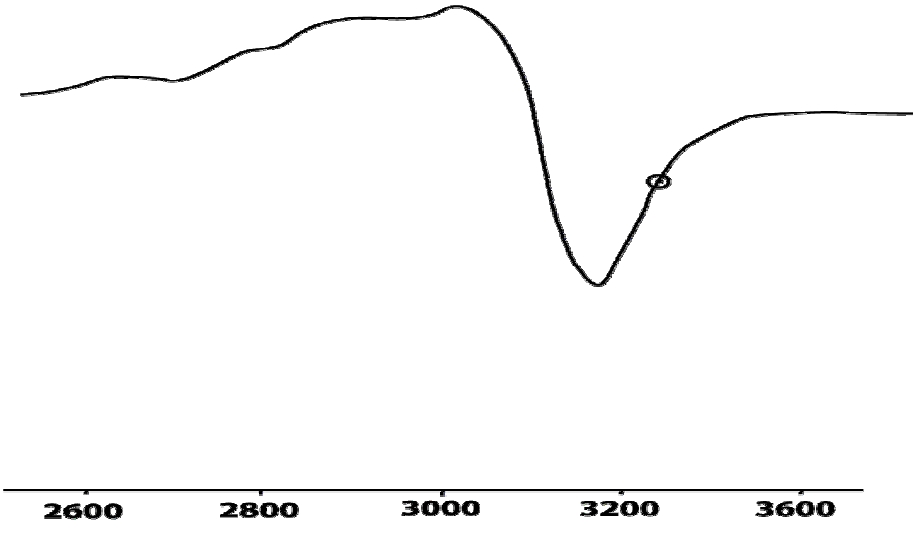

Figure 6.15. EPR spectrum of [Cu(hqc6in)Cl_2)(H_2O)$_2$]

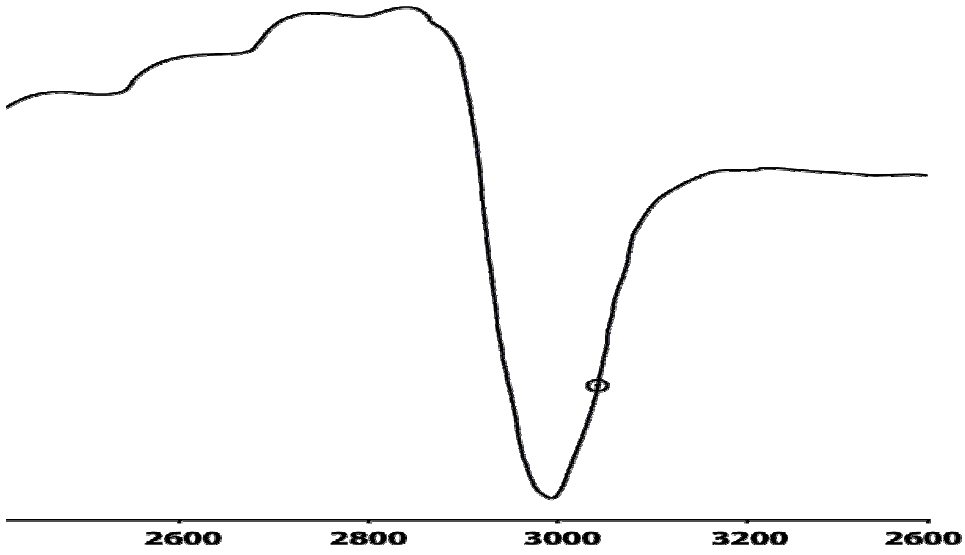

Figure 6.16. EPR spectra of [Cu(hqaqn)Cl_2]

6.3.5 Electrochemistry

The voltammograms are given in Figures 6.17-6.21 and the data are given in Table 6.5. Since the ligands used in this work are not reversibly reduced or oxidized in the applied potential range, the redox processes are assigned to the metal centers only. For these complexes the ratio of I_{pa}/I_{pc} is approximately equal to unity confirming one electron process. The peak to peak separations (ΔE_p) lie in the range of 0.70-0.11 V suggesting a quasi-reversible Cu(III)/Cu(II) redox process. The $E_{1/2}$ value falls in the range -0.37 to -0.86 V. It has been shown that the softer ligands tend to favor more positive $E_{1/2}$ values while hard ligands give rise to more negative values (30).

Table 6.5. Cyclic voltammetric data of Cu(II) complexes

Complex	E_{pc} (V)	E_{pa} (V)	$(E_{1/2})$ (V)	I_{pc} (μA)	I_{pa} (μA)	I_{pc}/I_{pa}
$[Cu(qc5in)Cl_2]$	-0.927	-0.649	-0.788	10.02	8.14	1.2
$[Cu(qc6in)Cl_2]$	-0.126	-0.648	-0.371	4.02	3.00	1.3
$[Cu(hqc5in)Cl_2]$	-0.895	-0.598	-0.746	8.40	6.98	1. 2
$[Cu(hqc6in)Cl_2)]$	-1.14	-0.564	-0.852	5.36	4.26	1.2
$[Cu(hqaqn)Cl_2]$	-1.15	-0.560	-0.855	4.10	3.00	1.3

E_{pa} = anodic peak potential, E_{pc} = cathodic peak potential, I_{pa} = anodic peak current; I_{pc} = cathodic peak current; I_{pc}/I_{pa} = number of electrons; $E^1_{1/2}/ E^2_{1/2} = 0.5 \times (E_{pa} + E_{pc})$; scan rate 100 mV

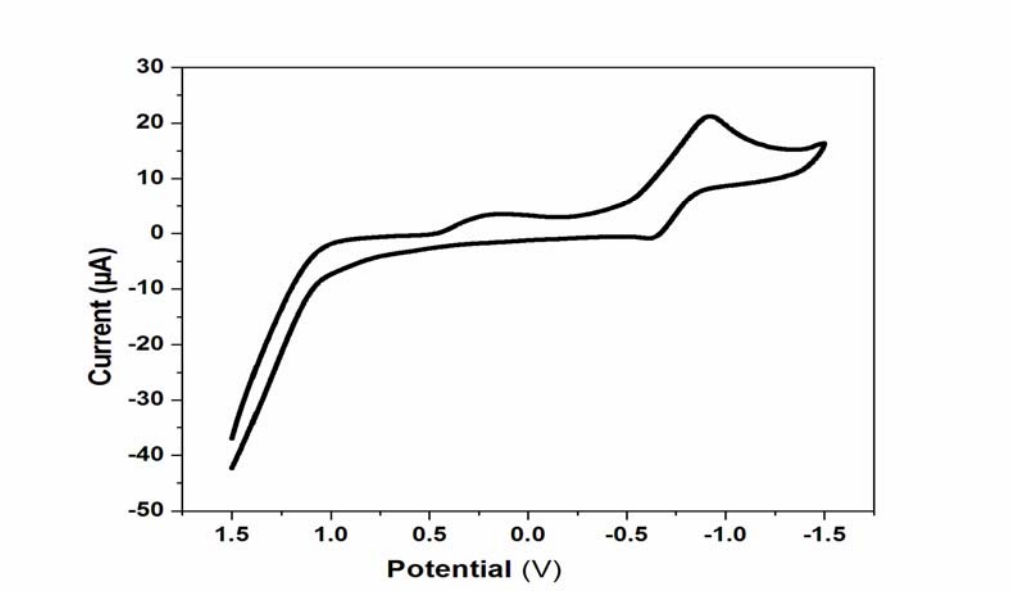

Figure 6.17. Cyclic voltammogram of $[Cu(qc5in)Cl_2]$

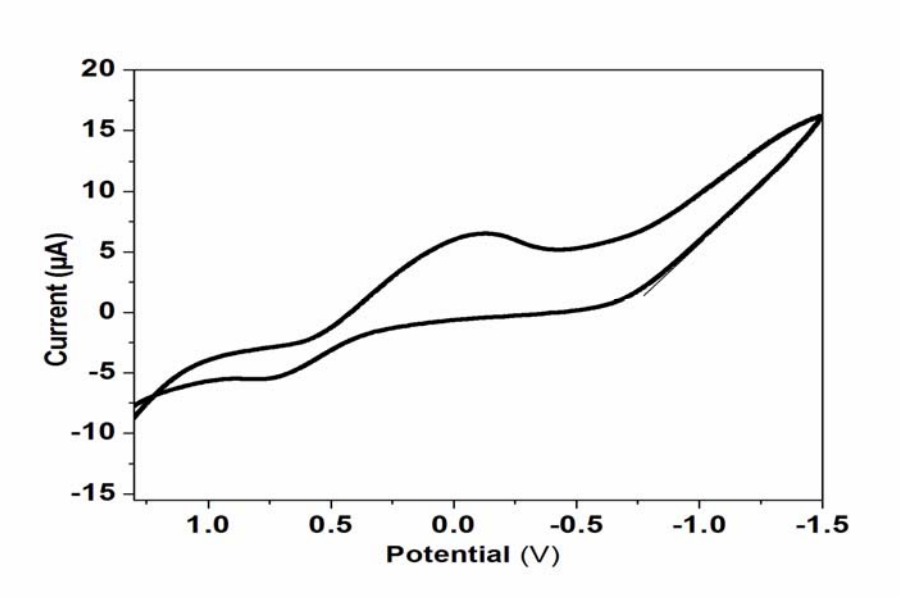

Figure 6.18. Cyclic voltammogram of [Cu(qc6in)Cl_2]

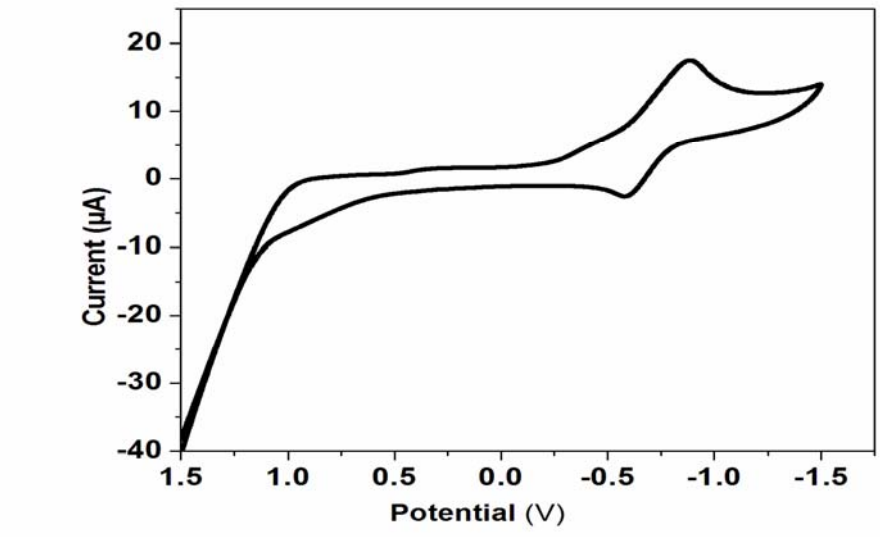

Figure 6.19. Cyclic voltammogram of [Cu(hqc5in)Cl_2]

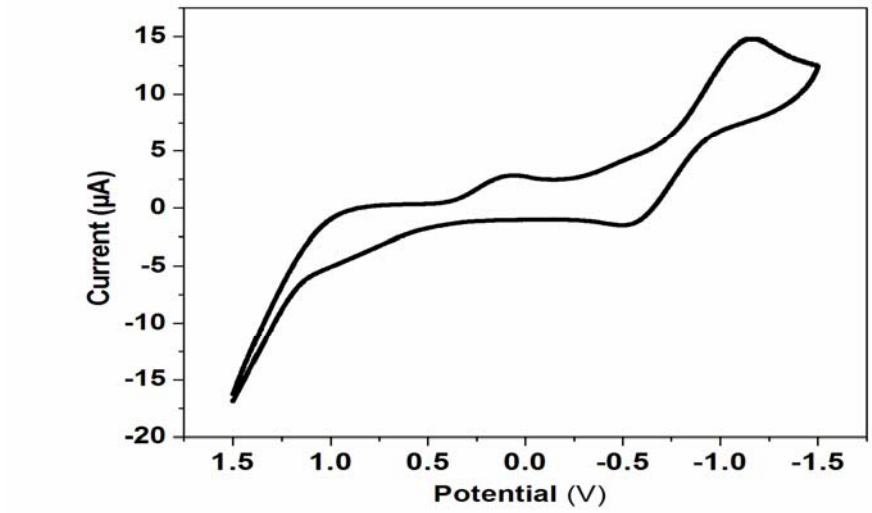

Figure 6.2 Cyclic voltammogram of [Cu(hqc6in)Cl_2]

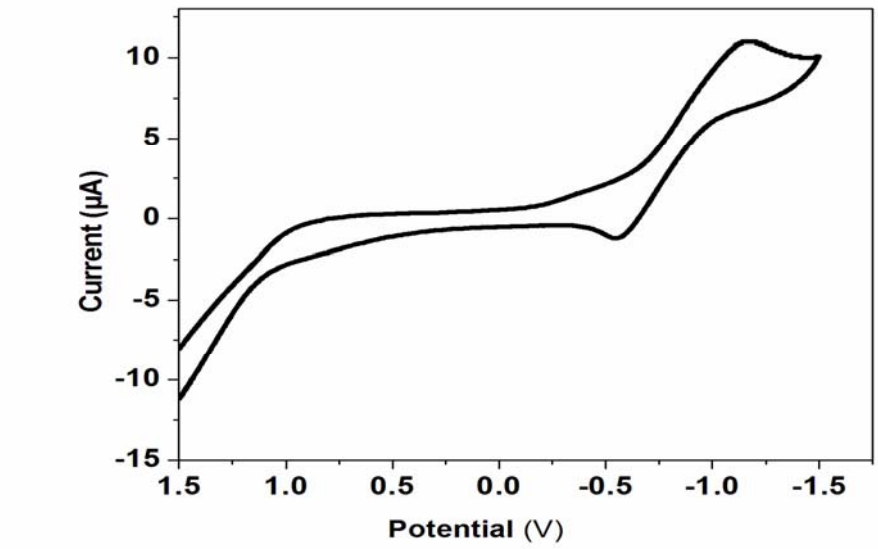

Figure 6.21 Cyclic voltammogram of [Cu(hqaqn)Cl_2]

6.3.6 Geometry of the complexes

Based on the above studies a square planar structure (Figure 6.22) has been assigned for the complexes.

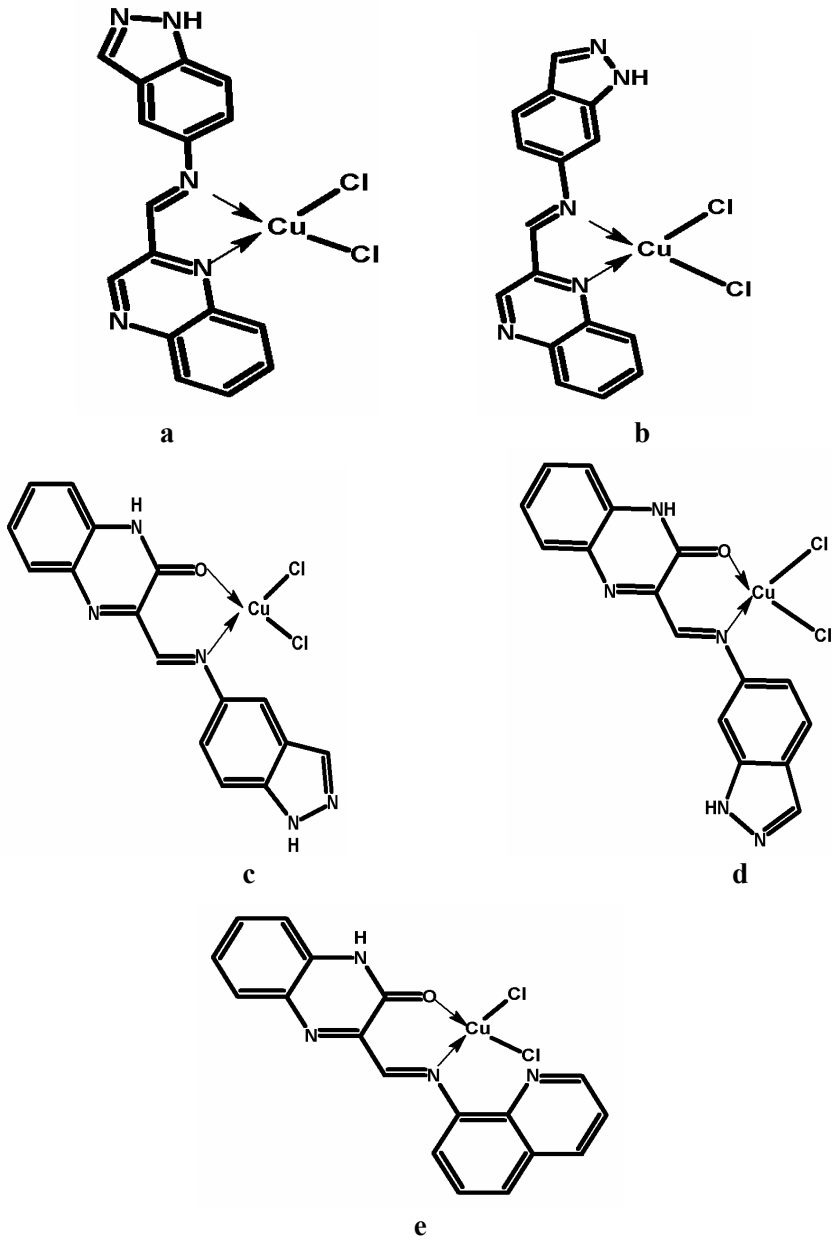

Figure 6.22. Proposed geometry of the Cu(II) complexes
Where a=Cu(qc5in)Cl_2], b= [Cu(qc6in)Cl_2], c= [Cu(hqc5in)Cl_2], d= [Cu(hqc65in)Cl_2],e=[Cu(hqaqn)Cl_2],

6.4 Cleavage of pUC18 DNA by Cu(II) complexes

The ability of complexes to perform DNA cleavage is generally monitored by agarose gel electrophoresis. Agarose gel electrophoresis using pUC18 plasmid DNA with all copper complexes was carried out and the diagram is shown in Figure 6.8. Two clear bands were observed (lane 1) for pUC18 DNA corresponding to the conformations of the plasmid *viz*, open circular, supercoiled forms.

After the addition of copper complexes only one form (supercoiled form) was visible and intensity diminishes for the complexes [Cu(qc5in)Cl_2] (Lane 3), [Cu(qc6in)Cl_2] (Lane 4) and [Cu(hqc5in)Cl_2] (Lane 5). Thus it was clear that binding of the copper complexes results in the complete degradation of the open circular form of DNA (31, 32). The complex [Cu(hqaqn)Cl_2] completely degrades two forms of pUC18 plasmid DNA (lane 6). All the results indicate that complexes [Cu(qc5in)Cl_2], [Cu(qc6in)Cl_2], [Cu(hqc5in)Cl_2] and [Cu(hqaqn)Cl_2] shows efficient DNA-cleavage activity.

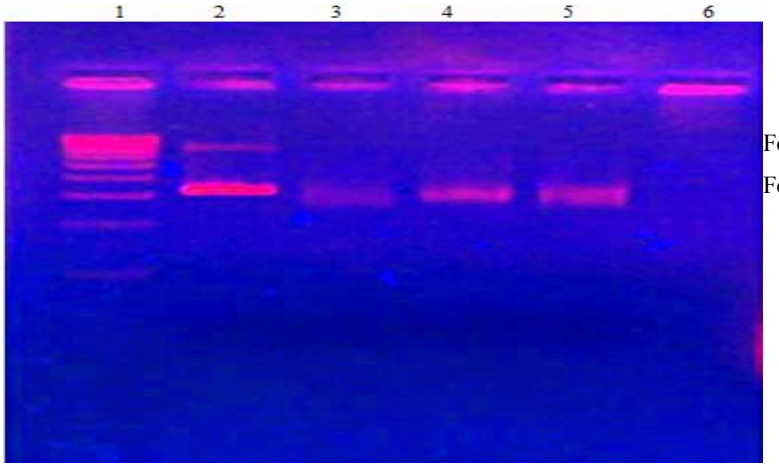

Lane 1: 500 bp DNA marker
Lane 2: pUC 18 DNA
Lane 3: pUC 18 DNA + [Cu (qc5in)$C1_2$]
Lane 4: pUC 18 DNA + [Cu (qc6in)$C1_2$]
Lane 5: pUC 18 DNA ++ [Cu (hqc5in)$C1_2$]
Lane 6: pUC 18 DNA + +[Cu (hqaqn)$C1_2$]

Figure 6.23. Gel electrophoresis diagram showing the cleavage of pUC18 plasmid DNA by Cu(II) complexes

6.5 Conclusions

The molecular formulae of the complexes were calculated from the elemental analyses data and found to be $[Cu(qc5in)Cl_2]$, $[Cu(qc6in)Cl_2]$, $[Cu(hqc5in)Cl_2]$, $[Cu(hqc6in)Cl_2]$, $[Cu(hqaqn)Cl_2]$. The normal magnetic moment values and cyclic voltammetric datas substantiate a mononuclear structure for all these complexes and electronic spectral data suggest square-planar geometry. The maximum DNA cleavage activity is shown by $[Cu(hqaqn)Cl_2]$.

6.6 References

[1] G. Albertin, E. Bordignon, *Inorg.Chem.*14 (1975) 1411.

[2] E.L. Hegg, J.N. Burstyn, *Coord. Chem. Re*V. *173* (1998) 133.

[3] F. Mancin, P. Scrimin, P. Tecilla, U. Tonellato, Chem. *Commun. (*2005) 2540.

[4] Y. An, S.D. Liu, S.Y. Deng, L.N. Ji, Z.W Mao, *J. Inorg. Biochem.* 100 *(*2006) 1586.

[5] J.L.G. Giménez, M.G. Álvarez, M.L. González, B. Macías, J. Borrás, G. Alzuet, *J. Inorg. Biochem*. 103 (2009) 923.

[6] N. Saglam, A. Colak, K. Serbest, S. Dülger, S. Guner, S. Karaböcek, A.O. Beldüz, *BioMetals* 15 (2002) 357.

[7] D.S. Sigman, *Acc. Chem. Res*, *19* (1986) 180.

[8] W.K. Pogozelski, T.D. Tullius, *Chem. ReV. 98 (*1998) 1089.

[9] S. Zhang, Y. Zhu, C. Tu, H. Wei, Z. Yang, L. Lin, J. Ding, J. Zhang, Z. Guo, *J. Inorg. Biochem,* 98 (2004) 2099.

[10] R.R. Joshi, K.N. Ganesh, *Biochem. Biophys. Res. Commun.* 182 (1992) 588.

[11] S. Ramakrishnan, S.M. Palaniandavar, *J. Chem. Soc., Dalton Trans*. 29 (2008) 3866.

[12] F. Arjmand, M. Aziz, *Eur. J. Med. Chem*. 44 (2009) 834.

[13] M.E. Katsarou, E.K. Efthimiadou, G. Psomas, A. Karaliota, D. Vourloumis, *J. Med. Chem*. 51 (2008) 470.

[14] D.S. Sigman, T.W. Bruce, C.L. Sutton, *Acc. Chem. Res. 26(*1993) 98.

[15] R.S. Kumar, S. Arunachalam, *Eur. J. Med. Chem*. 44 (2009) 1878.

[16] J. H. Gil, L. Perelló, R. Ortiz, G. Alzuet, M. G. Álvarez, M. L. González, *Polyhedron* 28 (2009) 138

[17] J. Manonmani, M. Kandaswamy, V. Narayanan, R. Thirumurugan, S. Shanmuga Sundara Raj, G. Shnamugam, M.N. Ponnusamy, H.K. Fun *Polyhedron.* 20 (2001) 3039.

[18] W.J. Geary. *Coordination Chemistry Reviews* 7 (1971) 81-122

[19] C. Jayabalakrishnan, R. Karvembu, R. Natarajan. *Trans. Met. Chem*. 27 (2002) 631.

[20] S.A. Ali, A.A. Soliman, M.M. Aboaly, R.M. Ramadan *J. Coord. Chem*. 55 (2002) 790.

[21] P. Viswanathamurthi , N. Dharmaraj, Natarajan. *Synth. React. Inorg. Met.Org. Chem.* 30 (2000) 1273.

[22] R.C. Maurya, P. Patel, S. Rajput. *Synth. React. Inorg. Met.Org. Chem*. 23 (2003) 817.

[23] K. Nakamoto *Infrared and Raman spectra of Inorganic and coordination compounds*, Wiley-Inter Science, New York. (1971)

[24] V.T. Kasumov, F. Koksal , Y. Zeren . *Spectrochimica Acta Part A.* 63(2006) 330

[25] P. Bindu, M.R.P. Kurup, *Trans. Met. Chem*. 22 (1997) 578.

[26] P. Bindu, M.R.P. Kurup, T.R. Sathyakeerty, *Polyhedron* 18(1999**)** 321.

[27] R.N. Patel, V.L.N. Gundla, D.K. patel, *Indian J. Chem. Sec. A.* 47 (2008) 353.

[28] S. Mayadevi, P.G. Prasad, K.K.M. Yusuff, *Synth. React. Inorg. Met. Org. Chem. 3*3 (2003) 481

[29] C. J. Dhanaraj, M. Sivasankaran Nair, *Mycobiology* 36 (2008) 260.

[30] G.S. Patterson, R.H. Holm *J. Bioinorg. Chem*. 4 (1975) 1257.

[31] B. Dede, I. Ozmen, F. Karipcin, *Polyhedron* 28 (2009) 3967.

[32] N. Raman, T. Baskaran, A. Selvan, R. Jeyamurugan, *J. Iran. Chem. Res.* 1 (2008) 129.

.....ꕥ.....

Chapter 7

Catalytic activity studies

Contents

7A. Hydrogenation of benzene catalysed by Ir(III complexes

A wide variety of transition metal complexes are extensively studied as reagents or catalysts for organic synthesis. The catalytic activity of transition metal Schiff base complexes is highly dependent on the environment about the metal centre and their conformational flexibility (1). Small changes in the ligand frame work enhance the steric and electronic effects of homogeneous metal complexes (2). The generally accepted order of catalyst activities for the elements of the transition series and their compounds is 2^{nd} row > 1^{st} row> 3^{rd} row.

The catalytic activities of newly synthesised iridium(III) and ruthenium(III) Schiff base complexes are studied in this chapter. This chapter is broadly divided into two sections: Part A which provides the details of hydrogenation of benzene catalysed by Ir(III) complexes and Part B which gives oxidation of 2-ethyl-1-hexanol catalysed by ruthenium (III) complexes.

7A.1 Introduction

Iridium complexes have received much attention as efficient hydrogenation catalysts. Crabtree reported that iridium complex is a highly

active catalyst for hydrogenation of highly hindered alkenes such as 2, 3-dimethyl-2-butene (3). Iridium complex-catalyzed hydrosilylations have also been reported (5-10). The activity of some common metals towards the hydrogenation of benzene and alkyl benzene decreases in the order of Rh > Ru > Ir > Pt > Ni > Pd >Co [11]. The complex $Ru(II)(L)(Cl)(H_2O)_2]\cdot H_2O$ containing 3-hydroxyquinoxaline-2-carboxalidene-4-aminoantipyrine as the Schiff base were found to be effective catalysts for the hydrogenation of benzene (12).

Cleavage of the dihydrogen molecule is the important step in the hydrogenation reaction. Presence of an electron-rich atmosphere around the metal centre facilitates breaking of the H–H bond by the interaction of the filled metal d orbital with the empty sigma antibonding molecular orbital of H_2 [13]. An increase in the N-basicity of the Schiff base ligand is found to increase the catalytic performance towards the metal catalyzed hydrogenation through such an interaction [14].

Therefore increased interactions are expected in the case of Schiff bases derived from 3-hydroxyquinoxaline-2-carboxaldehyde, which have more basic donor nitrogen atoms. The presence of quinoxaline ring provide electronic environment in the immediate coordination sphere of the metal thus allowing fine tuning of various catalytic properties of its complexes. These iridium(III) complexes derived from quinoxaline-2-carboxaldehyde exhibit excellent catalytic activity towards hydrogenation of benzene. In this chapter, the result of our studies on the catalytic activity of these complexes towards hydrogenation of benzene are presented.

7A.2 Experimental

7A.2.1 Materials

The details of the materials used for the synthesis and characterisation of Ir(III) Schiff base complexes are given in Chapter 2.

7A.2.2 Methods

The syntheses of the Schiff base ligands and their Iridium(III) complexes are given in Chapters 2 and 4.

7A.2.3 Catalytic activity measurements

The hydrogenation reactions were carried out in a 100 mL bench top mini-reactor made of stainless steel 316 (Autoclave Engineers, Division of Snap-tite, Inc. Pennsylvania). The reactor was charged with known quantities of the catalyst and benzene. Air was flushed out of the reactor with low-pressure of hydrogen, after which the inlet valve was closed and heating commenced with stirring at 600 rpm. When the designated temperature was reached, hydrogen was fed to the reactor at a predetermined pressure (time zero), which was maintained throughout the reaction with the help of a mass flow meter. During the run, samples (about 0.5 mL each) were withdrawn periodically and analyzed using a Chemito 8510 Gas Chromatograph using the column carbowax (15 %) and the products of the reaction were identified by using Varian 1200 L Single Quadrupole GC-MS.

7A.3 Results and discussion

The iridium complexes **[**Ir(qc5in)Cl_3H_2O], [Ir(qc6in)Cl_3H_2O], [Ir(hqc5in) $Cl_3(H_2O)$], [Ir(hqc6in)$Cl_3(H_2O)$] and [Ir(hqaqn)$Cl_3(H_2O)$] were tested for its activity towards the hydrogenation of benzene. The reactions were carried out under solvent free conditions with 0.34 mol benzene, 30 bar dihydrogen pressure at a temperature of 80 °C, stirring speed of 600 rpm with 6.66×10^{-6} mols of catalyst. The percentage conversion of benzene was noted after two hours of reaction (shown in Figure 7.1) and their turnover frequencies (TOF is the mol of benzene transformed per mole of the catalyst per hour) are given in Table 7. 1. Generally reduction of benzene and alkyl benzenes results in the formation of fully hydrogenated cyclohexanes. In our study hydrogenation of benzene takes place to give cyclohexane and the partially hydrogenated product cyclohexene.

Table 7.1. TOF of Ir(III) complexes in the hydrogenation of benzene

Catalyst	TOF (h^{-1})
[Ir(qc5in)Cl_3H_2O]	1654
[Ir(qc6in)Cl_3H_2O]	1481
[Ir(hqc5in)$Cl_3(H_2O)$]	692
[Ir(hqc6in)$Cl_3(H_2O)$]	1803
[Ir(hqaqn)$Cl_3(H_2O)$]	2705

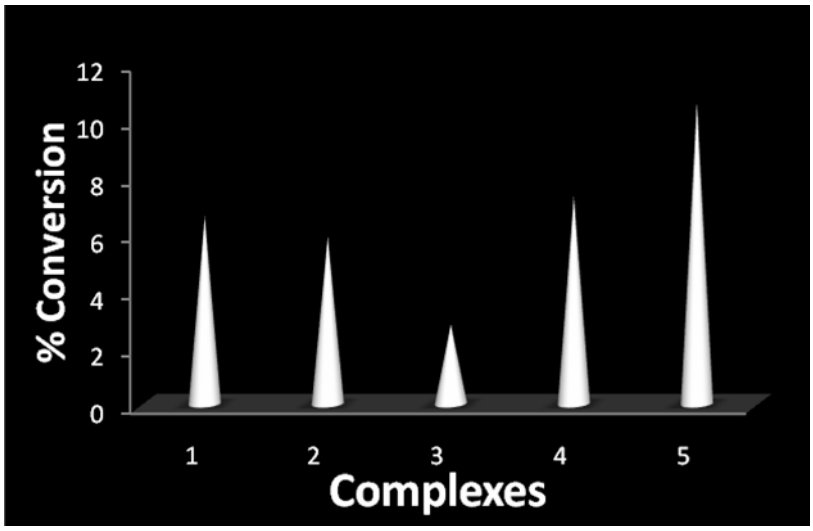

Figure 7.1. Percentage conversion of Ir(III) complexes in the hydrogenation reaction

Among these complexes, [Ir(hqaqn)$Cl_3(H_2O)$] was found to be most active. Hence a detailed study was carried out on the activity of this complex towards the hydrogenation of benzene. The reactions were performed under solvent free conditions by variation of catalyst and substrate concentrations, dihydrogen pressure, reaction time and temperature of reaction mixtures. At 80 °C, and 30 bar hydrogen pressure, turnover frequencies 2705 h^{-1} have been found for the hydrogenation of benzene. This value is much higher than that reported for some of the mononuclear iridium-based catalysts in the homogeneous hydrogenation of arenes. This higher turnover frequency may be due to the presence of electron rich nitrogen atoms in the heterocyclic Schiff base which tends to make the central

Ir(III) cations more electron rich and thus promote the overlap of the filled metal d orbital and the empty sigma antibonding molecular orbital of the hydrogen.

7A.3.1 Effect of catalyst concentration

To study the influence of catalyst concentration on the reduction of benzene quantity of the catalyst was varied in the range (5.01-10.00) × 10^{-6} mol, while the substrate concentration (0.34 mol benzene, dihydrogen pressure (30 bars) and the temperature (80 ºC) were kept constant (Table7. 2). In both cases an increase in catalyst concentration was found to raise the percentage conversion. However, with increase in catalyst concentration, change in the product distribution was observed. At lower concentrations of the catalyst, the fully hydrogenated product predominates but at increased catalyst concentrations partially hydrogenated product predominates. This would be due to the increase in catalytic active iridium sites with increase of catalyst concentration.

Table 7.2. Effect of the [Ir(hqaqn)Cl_3(H_2O)]in the hydrogenation of benzene

[catalyst] (10^{-6}mol)	[benzene] (mol)	H_2pressure (bar)	Temperature (ºC)	Conversion (%)	Selectivity (%) [b]	
					CA	CE
5.01	0.34	30	80	5.8	73	27
6.66	0.34	30	80	10.6	81	19
8.32	0.34	30	80	11.8	84	16
10.00	0.34	30	80	13.0	83	17

[b] **CA = cyclohexane, CE = cyclohexene and the product selectivity is CA (or CE) / (CA + CE)**

7A.3.2 Effect of dihydrogen pressure

To analyse the dependence of dihydrogen pressure on the reduction of benzene, a series of experiments were carried out by varying the pressure over the range of 20 to 50 bar at 80 ºC keeping both substrate concentration (0.34 mol benzene) and the catalyst loading (6.66 × 10^{-6} mol) constant. A favourable effect of conversion is observed with an increase of hydrogen pressure from 20 to 50 bars. The results of these studies are given in Table 7.3.

Table 7.3. Effect of dihydrogen pressure in the hydrogenation of benzene[a].

[catalyst] 10^{-6} mol	H_2pressure (bar)	Temperature (°C)	Conversion (%)	Selectivity (%) [b]	
				CA	CE
6.66	20	80	6.6	70	30
6.66	30	80	10.6	81	19
6.66	40	80	11.8	85	15
6.66	50	80	13.6	86	14

[b] CA = cyclohexane, CE = cyclohexene and the product selectivity is CA (or CE) / (CA + CE)

7A.3.3 Effect of temperature

The effects of temperature on the hydrogenation of benzene investigated in the range 40-100 °C keeping all other parameters constant (Table 7.4) Percentage conversion and selectivity were seen to increase with increase of temperature.

Table 7.4. Effect of temperature in the hydrogenation of benzene

[catalyst] 10^{-6} mol	H_2pressure (bar)	Temperature (°C)	Conversion (%)	Selectivity (%) [b]	
				CA	CE
6.66	30	40	5.5	72	28
6.66	30	60	7.4	80	20
6.66	30	80	10.6	81	19
6.66	30	100	12.8	86	14

7B Oxidation of 2-ethyl-1-hexanol catalysed by ruthenium(III) complexes

7B.1 Introduction

Selective oxidation of primary alcohols to aldehydes is a long standing problem of organic chemistry. The oxidation of alcohols by many ruthenium Schiff base complexes has been reported (15-21).

Ruthenium complexes act as catalysts due to their reversible and accessible oxidation states. Ruthenium complexes are known to mediate alcohol oxidation using variety of oxidants such as PhIO (22), NMO (23), BrO_3^- (24), $S_2O_8^-$ (25), *t*-BuOOH (26) and O_2 or air (27). The results of our studies on the oxidation of 2-ethyl-1-hexanol using Ru(III) complexes are presented in this chapter.

7B.2 Experimental

7B.2.1 Materials

The details of the materials used for the synthesis and characterisation of Ru Schiff base complexes are given in Chapter 2.

7B.2.2 Methods

The details of the syntheses of Schiff bases and their Ru complexes are given in Chapters 2 and 5.

7B.2.3 Catalytic activity measurements

Catalytic oxidation was carried out in a two-necked RB flask. Hydrogen peroxide (30%) was added through the septum to the magnetically stirred solution containing 2-ethyl-1-hexanol and the Ru(III) complexes. The reaction mixture was stirred and heated in a magnetic stirrer. The course of the reaction was monitored by periodically withdrawing small samples (about 0.4 mL each) which were analyzed by gas chromatography fitted with carbowax (15 %)

7B.3 Results and discussion

Oxidation of 2-ethyl-1-hexanol, a lipophilic alcohol, generally yields 2-ethyl-1-hexanal and 2-ethylhexanoic acid. Hydrogen peroxide was chosen as oxidant because it is inexpensive and liberates water as by product. The reaction is as follows (Scheme 7.1).

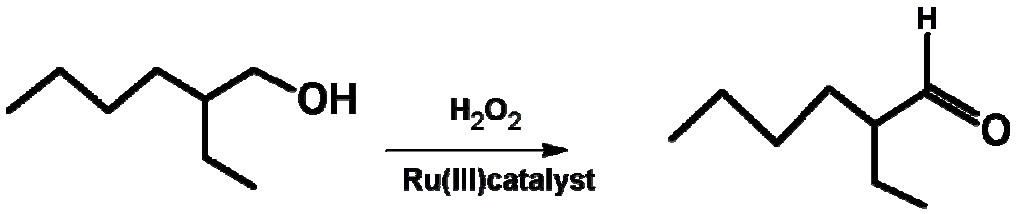

Scheme 7.1. Conversion of 2-ethyl-1-hexanol to 2-ethyl-1-hexanal

All the Ru(III) complexes were screened for their activity towards this oxidation. The results of this studies are given in the Table. Among these complexes, $[Ru(hqaqn)Cl_3(H_2O)].H_2O$ was found to be the most active catalysts with 48% conversion. We carried out a blank experiment without the catalyst under identical conditions and no oxidation products were observed. To study suitable reaction conditions for maximum transformation detailed study was carried out on the activity of the complex, $[Ru(hqaqn)Cl_3(H_2O)]H_2O$ by varying the reaction conditions: effect of the amount the catalyst, effect of temperature, effect of H_2O_2 and effect of time.

Table 7.5. Percentage conversion and turnover frequency of Ru(III) complexes

Catalyst	% of conversion	TOF(h^{-1})
$[Ru(qc5in)Cl_3H_2O]\ H_2O$	48	7905
$[Ru(qc6in)Cl_3H_2O]\ H_2O$	26	4285
$[Ru(hqc5in)Cl_3(H_2O)]\ H_2O$	4	660
$[Ru(hqc6in)Cl_3(H_2O)]H_2O$	12	1978
$[Ru(hqaqn)\ Cl_3(H_2O)]H_2O$	18	3017

Reaction conditions Reaction time-30 mts, Reaction temperature-313 K, 2-ethyl hexanol-- .20 mol, H_2O_2 - 9.7 mmol, Catalyst weight-6 mg

7B.3.1 Effect of amount of the catalyst

The reaction which carried out in the absence of catalyst did not yield any products. The influence of catalyst on the oxidation of 2-ethyl-1-hexanol was studied at 40°C by varying the amount of catalyst from 4.01×10^{-3} mol to 12.03×10^{-3} mol

keeping the amount of oxidant and substrate constant. The results of our studies are shown in the Figure 7.2.

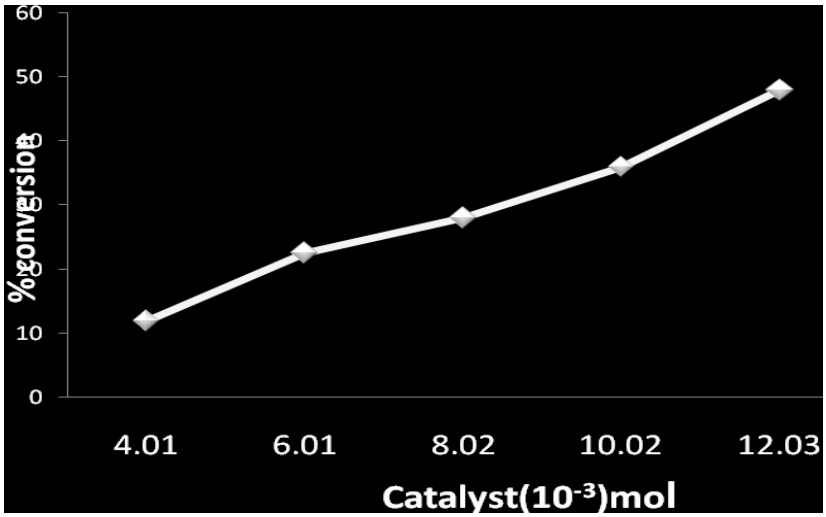

Figure 7.2. The influence of the amount of the catalyst

From the graph it is clear that percentage conversion increases with increase in the amount of catalyst.

7B.3.2 Influence of reaction temperature

The reaction was studied over a wide range of temperature in 30 ml substate from 273 K to 313 K keeping the amount of catalyst and oxidant constant. Selection of this particular temperature range is due to the reason that at higher temperatures the decomposition of H_2O_2 takes place. The results of our studies are shown in Figure 7.3. At room temperature the percentage conversion was very poor. As the temperature increased, the conversion was found to increase but if the temperature is more than 313 K one more product was also formed it might be 2-ethylhexanoic acid. The optimum temperature for carrying out the reaction is 313 K. After this temperature there is a slight decrease in conversion which may be due to the accelerated decomposition of H_2O_2.

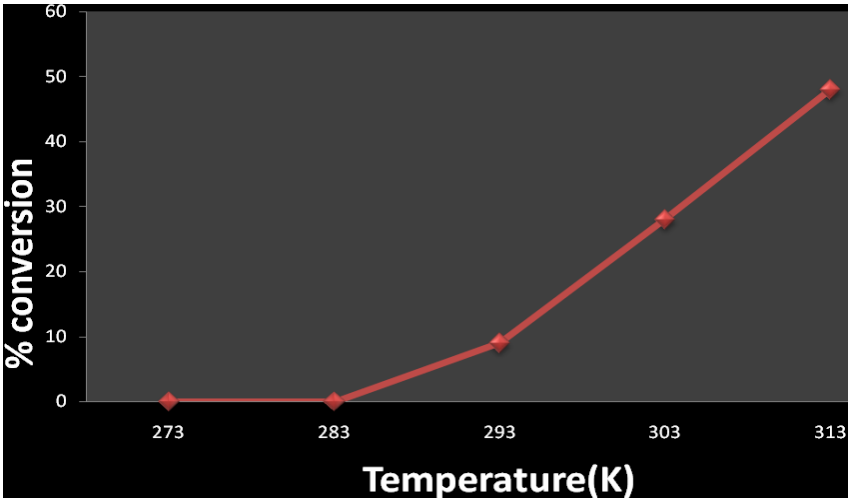

Figure 7.3 The influence of the amount of temperature

7B.3.3 Influence of reaction time

The influence of reaction time on the oxidation of 2-ethyl-1-hexanol was probed by carrying out the reaction with 6mg catalyst in. 20 mol of ethyl- hexanol and 9.7 mmol of H_2O_2 at 30 minutes. The % of conversion increases with increase of time and acquires steady value after 30 minutes. The results of our studies are shown in the Figure 7.4.

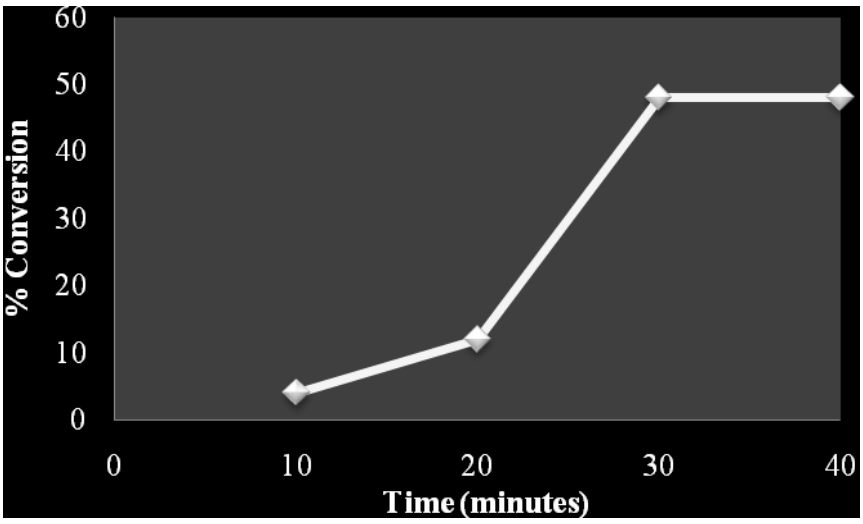

Figure 7.4 The influence of the amount of temperature

7C Conclusions of catalytic activity studies

[Ir(hqaqn)$Cl_3(H_2O)$] exhibited maximum catalytic activity for the hydrogenation of benzene**.** Turnover frequencies of 2705h^{-1} have been found for the reduction of benzene (0.34 mol) at 80 ºC with 6.66 × 10^{-6} mol catalyst and at a hydrogen pressure of 30 bar in 600 rpm stirring speed. These values are much higher than that of some of the reported iridium complex catalysts for the homogeneous aromatic hydrogenation reactions.

Complete oxidation of 2-ethyl-1-hexanol occurs in 30 minutes at the temperature of 313 K in presence of H_2O_2 (9.7 mmol) as oxidant with high selectivity to the 2-ethylhexanal. [Ru(qc5in)Cl_3H_2O].H_2O shows high turnover frequency 7905 h^{-1} in this oxidation reaction.

References

[1] N.S. Venkataramanan, G. Kuppuraj, S. Rajagopal, *Coordination Chemistry Reviews* 249 (2005) 1249.

[2] V. Dragutan, I. Dragutan, L. Delaude, A. Demonceau, *Coordination Chemistry Reviews* 251 (2007) 765.

[3] R.H. Crabtree, *Acc. Chem. Res*. 12 (1979) 331.

[4] R.H. Crabtree, H. Felkin, G.E. Morris, *Journal of Organometallic Chemistry* 111 (1977) 205.

[5] P. Schnider, G. Koch, R. Pretot, G. Wang, F.M. Bohnen, C. Kruger, A. Pfaltz, *Chem.Eur. J*. 3 (1997) 887.

[6] R.B. Bedford, S. Castillon, P.A. Chaloner, C. Claver, E. Fernandez, P.B. Hitchcock, A. Ruiz, *Organometallics.* 15 (1996) 3990.

[7] R.H. Crabtree, P.C. Demou, D. Eden, J.M. Mihelcic, C.A. Parnell, J.M. Quirk, G.E. Morris, *J. Am. Chem. Soc*. 104 (1982**)** 6994.

[8] F. Spindler, B. Pugin, H.U. Blaser, *Angew. Chem., Int. Ed. Engl. 29* (1990) 558.

[9] K. Mashima, T. Akutagawa, X. Zhang, H. Takaya, *J.Organomet. Chem*. 213 (1992) 428.

[10] X. Zhang, T. Taketomi, T. Yoshizumi, H. Kumobayashi, S. Akutagawa, K. Mashima, H. Takaya, *J. Am. Chem. Soc*. 115(1993) 3318.

[11] G. C. Bond, *'Catalysis by Metals'*, Academic Press, New York, (1962).

[12] V. Arun, N. Sridevi, P.P. Robinson, S. Manju, K.K.M. Yusuff, *J. Mol. Catal. A Chem.* 304 **(**2009**)** 191.

[13] E.A. Cagnola, M.E. Quiroga, D.A. Liprandi, P.C. Largentiere, *Applied Catalysis A*: General, 274 (2004) 205.

[14] A. Boettcher, H. Elias, E.G. Jaeger, H. Langfelderova, M. Mazur, L. Muller, H. Paulus, P.Pelikan, M. Rudolph, M. Valko, *Inorganic Chemistry*. 32 (1993) 4131.

[15] G. Csjernvik, A.H. Eu, L. Fadini, B. Pugin, J.E. Backvall, *J. Org.Chem*. 67 (2002) 165

[16] V. Mahalingam, R. Karvembu, V. Chinnusamy, K. Natarajan, *Spectrochimica Acta Part A.* 64 (2006) 886.

[17] D. Sukanya, R. Prabhakaran, K. Natarajan *Polyhedron* 25 (2006) 2223.

[18] S. Priyarega, R. Prabhakaran, K. R. Aranganayagam, R. Karvembu, K. Natarajan, *Appl. Organometal. Chem. 21 (*2007) 788.

[19] G. Venkatachalam, R. Ramesh, *Spectrochimica Acta Part A.* 61 (2005) 2081.

[20] R. Ramesh, *Inorganic Chemistry Communications* 7 (2004) 274.

[21] S. Kannan, R. Ramesh, *Polyhedron* 25 (2006) 3095.

[22] M. Sivagamasundari, R. Ramesh, *Spectrochimica Acta Part A.* 66 (2007)427

[23] P. Muller, J. Godoy, *Tetrahedron Lett. 22 (*1981) 2361

[24] M.G. Bhowon, W.H. Li Kam, R. Narain, *Polyhedron 17 (*1998) 341.

[25] W.P. Griffith, *Coord. Chem. Rev*. 21 *(*1992) 179.

[26] A.J. Bailey, L.D. Cother, W.P. Griffith, D.M. Hankin, *Transition Met.Chem.* 20 *(*1995) 590.

[27] A.M. E. Hendawy, A.H. A. Kubaisi, H.A. A. Madfa, *Polyhedron* 16 *(*1997) 3039.

[28] A. Wolfson, S. Wuyts, D.E. De Vos, I.F.J. Vankelecom, P.A. Jacobs *Tetrahedron Lett.* 43 *(*2002) 8107.

.....ooo.....

Chapter 8

Anticancer and antibacterial studies

Contents

8.1 Introduction

Transition metals possess an important role in the field of medicinal biochemistry. Transition metals exhibit different oxidation states and can interact with number of negatively charged molecules. This activity of transition metals has started the development of metal complex based drugs with promising pharmacological application and may offer unique therapeutic opportunities. Metal complexes of platinum, ruthenium, iridium, palladium and osmium with active organic molecules have been reported to exhibit antimicrobial and anticancer activities (details given in the chapter 1). Due to their unique applications researchers are still aiming towards the discovery of an effective and safe therapeutic regimen for the treatment of bacterial infections and cancers.

Cancer chemotherapy was initiated in the early stage of 1950s and the only treatment was by using mustine due to its inhibiting capability against the cancer cells (1). The involvement of inorganic metal based compounds was very limited, until the discovery of potent anti-cancer activity in certain platinum co-ordination compounds by Rosenberg and Van Camp (2). The first platinum based drug, cisplatin, was found to have anti-tumour activity and it is useful for the treatment

against several tumours. In December 1978, this compound, cis-[$PtCl_2(NH_3)_2$], received Food and Drug Authority (FDA) approval as an anti-cancer drug for testicular and ovarian cancers. The attempts to study mechanisms of resistance and thereby broaden the clinical utility of this class of agents have resulted in the discovery of oxaliplatin which is active in patients with colorectal cancer, satraplatin which shows promise in patients with prostate cancer, and picoplatin which is currently in phase III trials against small-cell lung cancer, prostate cancer, and colorectal cancer. The major classes of metal-based anticancer drugs include platinum(II), ruthenium(III), copper(II) and Pd(II) compounds.

Transition metal Schiff base complexes containing quinoxaline derivatives possess interesting biological properties, such as antibacterial and antitumour activity [3-5]. Graslund *et al*. have studied the derivatives 2,3-dimethyl-6-(2-dimethyl-aminoethyl)6*H*-indolo[2,3-*b*]quinoxaline and 6-(2-dimethylaminoethyl) 6*H*-indolo[2,3-*b*] quinoxaline for their interaction with oligodeoxynucleotide duplexes and reported that these compounds were intercalated in a non-specific fashion by an AT-specific interaction (6). Sauvain *et al*. reported that 3-(4'-chloro) phenylquinoxaline-2-carbonitrile-1,4-di-*N*-oxide had potent antimalarial activity particularly against a chloroquine- resistant strain of *Plasmodium falciparum* (7). Moarbess *et al* examined imidazo[1,2-*a*]quinoxaline, imidazo[1,5-*a*] quinoxaline and pyrazolo[1,5-*a*] quinoxaline derivatives for their *in vitro* and *in vivo* anti-tumoral activities (8). Quinoxaline-carbohydrate hybrids act as selective photo-induced DNA cleaving and cytotoxic agents (9). Some quinoxalin-2-ones have shown antifungal activity (10-11) whereas quinoxalin- 1-oxides have antibacterial activity (12). 6-aralkyl-9-substituted-6*H*-indolo[2,3-*b*]quinoxalines synthesised from 2, 3-dioxo-2,3-dihydroindole and orthophenylene diamine, shows cytostatic activity against human Molt 4/C8 and CEM T-lymphocytes as well as for murine L1210 leukemia cells (13).

Transition metal complexes containing quinoline skeleton is often used for the design of many synthetic compounds with diverse pharmacological properties. The 8-(diethylaminohexylamino)-6-methoxy-4-methylquinoline is highly effective against the protozoan parasite *Trypanosoma cruzy*, which is the agent of Chagas' disease (14). The centipede, *Scolopendra Subspines mutilalns* L. which is found to contain 3,8-dihydroxyquinoline known as *Jineol* has been prescribed for tetanus, childhood convulsions and acute heart attack (15). Cryptolepine (5-methyl-5H-indolo[3,2-b]quinoline) displays plenty of pharmacological effects, such as antimuscarinic, noradrenergic receptor antagonistic, antihypertensive, vasodilative, antithrombotic, antipyretic and anti-inflammatory properties (16-18). Quinoline containing drugs particularly 4-aminoquinolines, have a long and successful history as antimalarials (19).

In the view of the antitumour and antibacterial activities of the quinoxaline and quinoline derivatives, and in view of the DNA binding and cleavage properties of the present complexes (see chapter 3 and 4) it was thought worthwhile to study the cytoxicity and antibacterial properties of these compleses. The results of these studies are presented in this chapter.

8.2 Materials

All the materials were purchased from Sigma Aldrich unless otherwise stated. All chemicals used were of analytical grade. The cell line DU145 was purchased from National Chemical Laboratory **(**NCL**),** Pune.

Pathogenic microoganisms *Bacillus cereus* NCIM 2155, *Bacillus coagulans* NCIM 2030, *Bacillus macerans* NCIM 2131, *Bacillus circulans* NCIM 2107, *Staphylococcus aureus* NCIM 2127, *Escherichia coli* NCIM 2343 *and Proteus vulgaris* NCIM 2027 were used for the present study.

8.3 Methods/Experimental

8.3.1 Screening of metal complexes for cytotoxicity studies using tryphan blue exclusion test

The dye exclusion test is used to determine the number of viable cells present in a cell suspension. It is based on the principle that live cells possess intact cell membranes that exclude certain dyes, such as trypan blue, eosin, or propidium, whereas dead cells do not. In this test, a cell suspension is simply mixed with dye and then visually examined to determine whether cells take up or exclude dye.

The DLA cells were aspirated from the peritoneal cavity of tumour bearing mice and washed thrice using phosphate buffered saline. To 1×10^7 viable cells 1 mmol of metal complexes and ligands were added separately. The final volume of the assay mixture was made up to 1mL using phosphate buffer saline (PBS) and incubated at 37 °C for 3 hr. One mL Tryphan blue was added after incubation and the number of dead cells was counted using a haemocytometer.

8.3.2 Cytotoxicity Assays

Cytoxicity assays are widely used in *in-vitro* toxicology studies. The LDH (lactate dehydrogenase), MTT (3-(4,5-dimethylthiazol-2-yl)-2, 5-diphenyltetrazolium bromide) and neutral red assays are the most commonly employed assays for the detection of cytotoxicity of compounds. Reliability, speed and simple evaluation are some of the characteristics of this assay (20). It has been employed as an indicator of cytotoxicity in HepG2 cells following exposure to cadmium chloride as well as in toxicity studies using rat renal proximal tubular cells (21, 22). The loss of intracellular LDH and its release into the culture medium is an indicator of irreversible cell death due to cell membrane damage.

MTT assay is another cytotoxicity assay oftenly used to determine the toxicity of compounds. MTT is a water soluble tetrazolium salt, which is

converted to an insoluble purple formazan by cleavage of the tetrazolium ring by succinate dehydrogenase within the mitochondria. The formazan product is impermeable to the cell membranes and therefore it accumulates in healthy cells.

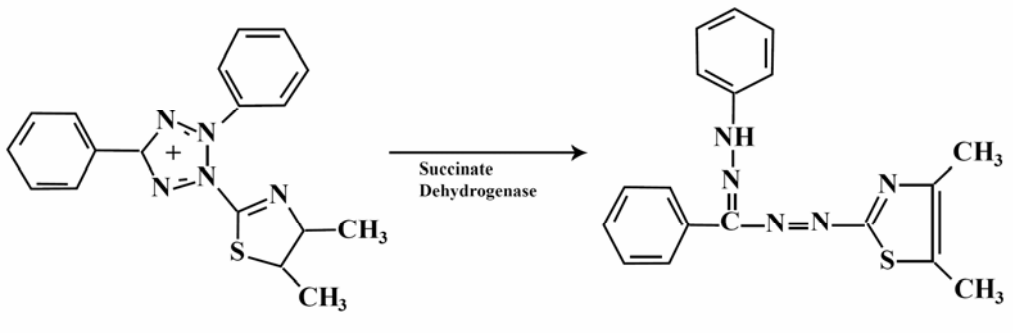

MTT **Formazan**

The MTT assay was tested for its validity in various cell lines by Mossmann (23). It has been used in HepG2 cells and in rat lung epithelial cells after expo-sure to cadmium chloride as well as in oligodendrocytes to assess cell viability (24-26).

The neutral red assay is also used to measure cytotoxicity of compounds. It has been used as an indicator of cytotoxicity in cultures of primary hepatocytes and other cell lines (27, 28). Living cells take up the neutral red, which is concentrated within the lysosomes of cells. Finally, the protein assay is indirect measurement of cell viability since it measures the protein content of viable cells that are left after washing of the treated plate. The mitocondrial activity of U_2OS cells after exposure to the metal complexes of a heptadentate N_5S_2 donor Schiff-base ligand was determined by colorimetric assay, which detects the conversion of 3-(4,5-dimethyl-thiazolyl-2)-2, 5-diphenyltetrazolium bromide (MTT) to formazon. In the present, we evaluated the cytotoxic efficacy of prepared metal complex using MTT assay.

8.3.2.1 MTT assay

DU145 cell line (prostate cancer) was seeded at a density of 5000 cells/well (100µl each) in the microplate containing Dulbecco's Modified Eagle

Medium (DMEM) medium and incubated at 37ºC in 5% carbon-dioxide incubator for 24 hr. Different concentrations of the metal complexes (5, 10, 50, 100, 200 and 400 µg) dissolved in dimethyl sulfoxide (DMSO) were added while the control wells were added with DMSO alone to the wells containing DU145 cells and incubated at 37 ºC for 24 hr. After incubation, 200 µl of cell free supernatant were aspirated and to this 100µl of MTT (1mg/ml) was added and incubated in dark for 2 hr at 37 ºC in CO_2 incubator. Lysis buffer (100µl) was added to dissolve the formazan crystals and was incubated in dark for another 4 hr. Read the plate on ELIZA reader at a wavelength of 570 nm. The signals generated directly proportional to the number of viable (metabolically active) cells in the wells. The values of the blank wells were subtracted from each well of treated and control cells, and the % viability was determined according to Kumi-Diaka (29) as given below.

$$\%\ \text{viable cells} = \frac{(\text{the absorbance of the treated cells}) - (\text{the absorbance of the blank})}{(\text{the absorbance of the control}) - (\text{the absorbance of the blank})} \times 100$$

Percentage of cytotoxicity = 100- percentage of viability

8.3.3 Antibacterial studies

8.3.3.1 Disc diffusion method

Antibacterial activity was performed using disc diffusion method (30). All the bacterial strains were swabbed on the plate containing 5mm Mueller Hinton agar. Filter paper (6 mm) discs were sterilised, placed on the agar plate surface and 1mmol of each complexes as well as ligands was dispensed separately on it. The plates were incubated at 37 °C for 24-48 hours and observed for the zone of inhibition around the disc. Antibacterial activity of the free Schiff base ligands and all complexes were screened against pathogenic microrganims such as *Bacillus cereus, Bacillus coagulans, Bacillus macerans, Bacillus circulans, Staphylococcus aureus, Escherichia coli and Proteus vulgaris.* A comparison of the antibacterial activities of the free Schiff base ligands and all the complexes with conventional bacteriocides like *ampicillin, rifampicin, vancomycin and nalidixic acid* was made.

8.4 Result and Discussion

8.4.1 Screening study using tryphan blue exclusion test

The data for the Screening study of the ligands, palladium and iridium complexes are given in Table 8.1 and 8.2. The order of the activity of the ligands is in the following order hqaqn > hqc6in> qc5in> hqc5in> qc6in. The activity was found to be higher for $[Pd(hqaqn)Cl_2]$ compared to other complexes and the activity of the complexes is in the order $[Pd(hqaqn)Cl_2]$ > $Ir(hqaqn)Cl_3(H_2O)$ > $Pd(qc5in)Cl_2$ = $Ir(hqc6in)Cl_3(H_2O)$ > $Pd(hqc5in)Cl_2$ > $Pd(hqc6in)Cl_2$ = $Pd(qc6in)Cl_2$ = $Ir(hqc5in)Cl_3(H_2O)$ > $Pd(qc6in)Cl_2$ > $Ir(qc5in)\ Cl_3H_2O]H_2O$ > $[Ir(qc6in)Cl_3H_2O]\ H_2O$

Table 8.1. The data for the screening study of the ligands and palladium complexes using tryphan blue exclusion test

Ligands	% of dead cells	Complexes	% of dead cells
qc5in	45	$[Pd(qc5in)Cl_2$	72
qc6in	38	$Pd(qc6in)Cl_2$	68
hqc5in	40	$Pd(hqc5in)Cl_2$	70
hqc6in	52	$Pd(hqc6in)Cl_2$	68
hqaqn	64	$Pd(hqaqn)Cl_2$	80

Table 8.2. The data for the screening study of the ligands and iridium complexes using tryphan blue exclusion test:

Ligands	% of dead cells	Complexes	% of dead cells
qc5in	45	62	62
qc6in	38	58	58
hqc5in	40	68	68
hqc6in	52	72	72
hqaqn	64	78	78

8.4.2 Cytotoxicity study using MTT (3-(4,5-dimethylthiazol-2-yl)-2, 5-diphenyltetrazolium bromide).

The complexes $Pd(qc5in)Cl_2$, $Pd(hqaqn)Cl_2$ and $Ir(hqaqn)Cl_3(H_2O)$ were selected for further studies due to their higher efficacy in screening study.

Percentage of cytotoxicity exhibited in the these complexes is given in Table 8.2 and in Figures 8.1-8.2.

No cytotoxicity was observed for $[Pd(qc5in)Cl_2]$. In the case of complexes, $[Pd(hqaqn)Cl_2]$, $[Ir(hqaqn)Cl_3(H_2O)]$ cytotoxicity was found to be increased with increase of concentration of complexes. When the concentration was increased to 400 µg/ml $[Pd(hqaqn)Cl_2]$ exhibited cytotoxicity of 24.57 % and $[Ir(hqaqn)\ Cl_3(H_2O)]$ exhibited 38.62 %.

Table 8.3. Percentage of cytotoxicity of $[Pd(hqaqn)Cl_2]$ and $[Ir(hqaqn)Cl_3(H_2O)]$

Working conc. of Drug (µg/ml)	% of cytotoxicity of $[Pd(hqaqn)Cl_2]$	% of cytotoxicity of $[Ir(hqaqn)Cl_3(H_2O)]$
0 (control)	0	0
5	2.29	10.00
10	9.71	15.64
50	10.86	20.12
100	16.57	28.62
200	19.40	32.71
400	24.57	38.62

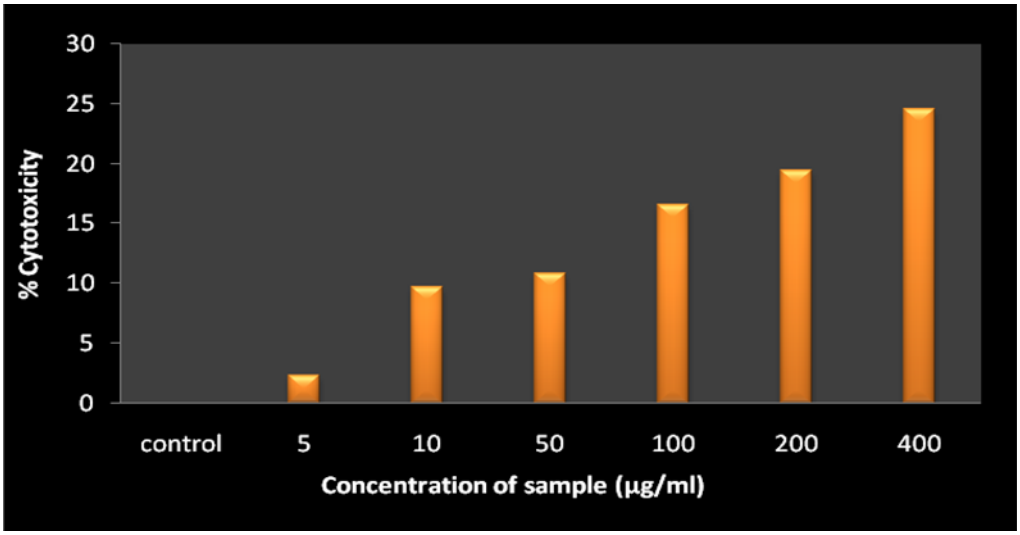

Figure 8.1. Percentage of cytotoxicity of $[Pd(hqaqn)Cl_2]$

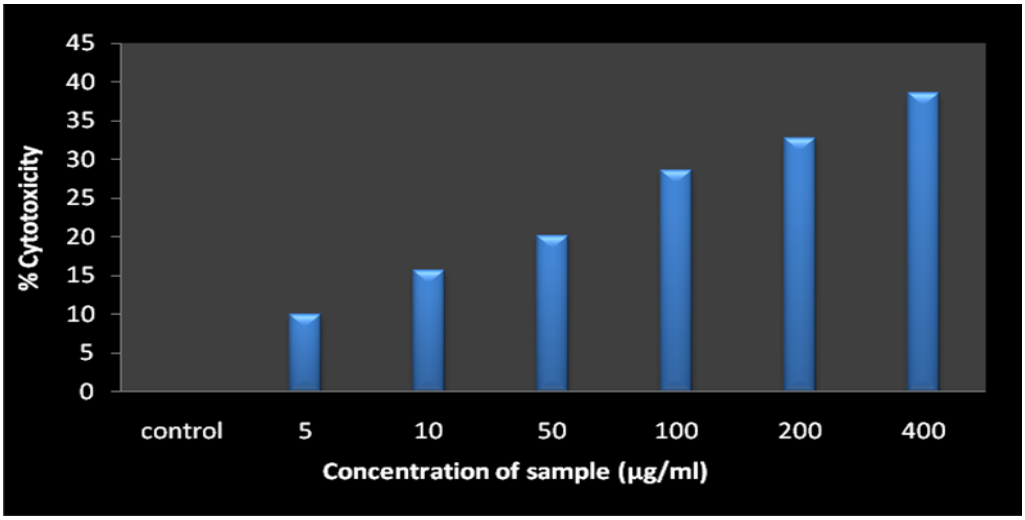

Figure 8.2. Percentage of cytotoxicity of Ir(hqaqn)$Cl_3(H_2O)$]

8.4.3 Antibacterial studies

The Schiff base ligands have been screened for their antibacterial activities against various pathogenic bacterias, *Bacillus cereus, Bacillus coagulans, Bacillus macerans, Bacillus circulans, Staphylococcus aureus, Escherichia coli, Proteus vulgaris.* The results are given in Table 8.4. As the ligand qc5in exhibits zone of inhibition with diameter of 8 mm for *Bacillus cereus* and *Bacillus coagulans,* it is active against these organisms. The ligand qc6in is found to be inactive against all the microorganisms. The only compound which exhibit activity against *E.coli.* is hqc5in.

Antibacterial activity of the palladium complexes were tested against pathogenic bacterias, *Bacillus cereus, Bacillus coagulans, Bacillus macerans, Bacillus circulans, Staphylococcus aureus, Escherichia coli, Proteus vulgaris.* Zone of inhibition is illutrated in figure 8.4 and the diameter of the zone is given in Table 8.5. Eventhough the ligand qc6in didnot show any activity its palladium complexes exhibit activity against *Bacillus cereus, Bacillus coagulans* and *Staphylococcus aureus.* [Pd(hqaqn)Cl_2] shows good activity against all the microorganisms. [Pd(hqc5in)Cl_2] and [Pd(hqaqn)Cl_2] active against *E. coli.*

Antibacterial activity of the Ir(III)) complexes were screened against pathogenic bacterias and zone of inhibition is illutrated in figure 8.5 and the diameter of the zone is given in Table 8.6. [Ir(hqaqn)$Cl_3(H_2O)$] shows good activity against all the microorganisms. All the Ir(III) complexes are active against *P. vulgaris.* Antibacterial activity of the Ru(III)) complexes were screened against pathogenic bacterias and zone of inhibition is illutrated in figure 8.6 and the diameter of the zone is given in Table 8.7.

A comparative study of the growth inhibition zone values of schiff base and its complexes indicate that metal complexes exhibit higher anti bacterial activity than the free ligand and this is probably due the greater lipophilic nature of the complexes. Such increased activity of the metal chelates can be explained on the basis of Overtone's concept (31) and Tweedy's chelation theory (32). According to Overtone's concept of cell permeability, the lipid membrane that surrounds the cell favours the passage of only lipid soluble materials due to which liposolubility is considered to be an important factor that controls the anti microbial activity. On chelation, the polarity of the metal ion will be reduced to a greater extent due to the overlap of the ligand orbital and partial sharing of positive charge of metal ion with donor groups (33) Further, it increases the delocalization of the π electrons over the whole chelate ring and enhances the lipophilicity of the complex. This increased lipophilicity enhances the penetration of the complexes into lipid membrane and thus blocks the metal binding sites of microorganisms (34). These metal complexes also disturb the respiration process of the cell and thus block the synthesis of proteins, which restricts further growth of the organism (35). The variation in the activity of different complexes against different organisms depend either on the impermeability of the cells of the microbes or difference in ribosomes of microbial cells.

Antimicrobial activity of the prepared complexes has been compared with the widely used antibiotics such as ampicillin, rifampicein, vancomycin and nalidixic acid. The activity of ampicillin against *B. cereus* is 8 mm. All the complexes except $[Ir(qc6in)Cl_3H_2O]$, $[Pd(hqc6in)Cl_2$, $Pd(qc6in)Cl_2$ shows higher activity towards *B. cereus* than the antibiotic ampicillin.

Table 8.4. Antibacterial activity data of Ligands

Synthesized ligands (40μg)	Diameter of zone of inhibition (mm)						
	B. cereus	***B. coagulans***	***B. macerans***	***B. circulans***	***S. aureus***	***E. coli***	***P. vulgaris***
qc5in	8	8	-------	-------	-------	-------	-------
qc6in	-------	-------	-------	-------	-------	-------	-------
hqc5in	8		7			10	8
hqc6in	-------	-------	7	-------	-------	-------	10
hqaqn	9	-------	-------	-------	-------	-------	7

Table 8.5. Antibacterial activity data of Pd(II) complexes

Synthesized Complexes (40μg)	Diameter of zone of inhibition (mm)						
	B. cereus	***B .coagulans***	***B. macerans***	***B .circulans***	***S. aureus***	***E. coli***	***P. vulgaris***
$[Pd(qc5in)Cl_2]$	8	9	6	-------	8	--------	7
$[Pd(qc6in)Cl_2]$	9	9	------	------	8	-------	9
$[Pd(hqc5in)Cl_2]$	8	----	7	------	-----	12	8
$Pd(hqc6in)Cl_2]$	-----	------	8	-------	-------	-------	12
$[Pd(hqaqn)Cl_2]$	11	10	11	10	9	8	9

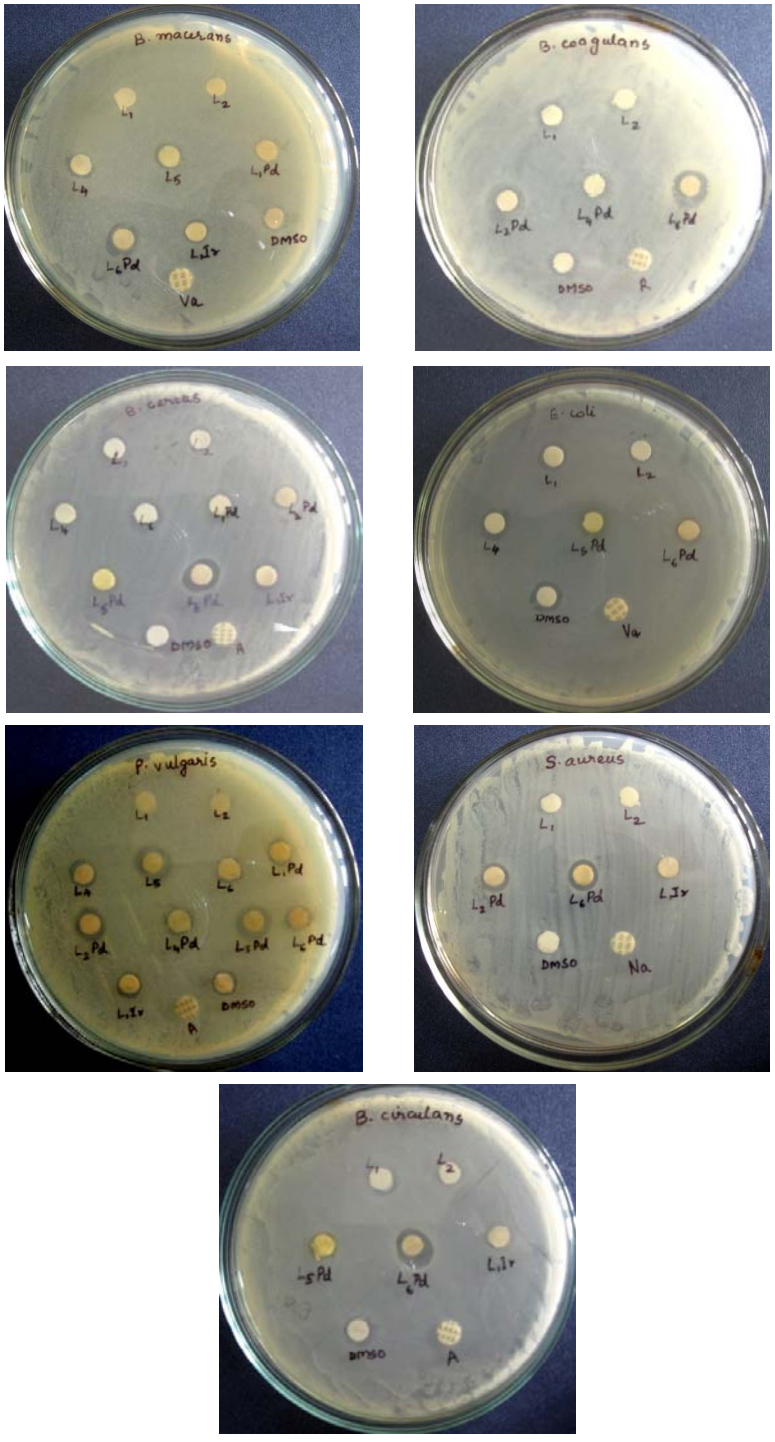

Figure 8.3. Antibiogram of Pd(II) complexes Where L_1=qc5in, L_2=qc6in, L4=hqc5in,L5=hqc6in, L6=hqaqn, L1-Pd= [Pd(qc5in)Cl_2], L2-Pd=[Pd(qc6in)Cl_2], L4-Pd=[Pd(hqc5in)Cl_2], L5-Pd= [Pd(hqc6in)Cl_2], L6-Pd= [Pd(hqaqn)Cl_2]

Table 8.6. Antibacterial activity data of Ir(III) complexes

Synthesized Complexes (40µg)	Diameter of zone of inhibition (mm)						
	B. cereus	***B. coagulans***	***B. macerans***	***B. circulans***	***S. aureus***	***E. coli***	***P. vulgaris***
$[Ir(qc5in)Cl_3H_2O]\ H_2O$	8	8		-------	--------	--------	4
$[Ir(qc6in)Cl_3H_2O]\ H_2O$	-------	9	------	------	---------	------	9
$[Ir(hqc5in)Cl_3(H_2O)]$	8	------	7	--------	---------	12	7
$[Ir(hqc6in)Cl_3(H_2O)]$	--------	-----	8	---------	------	--------	12
$[Ir(hqaqn)Cl_3(H_2O)]$	11	10	11	10	9	8	9

Table 8.7. Antibacterial data of Antibiotics

Antibiotic	Diameter of zone of inhibition (mm) for						
	B. cereus	***B. coagulase***	***B. macerans***	***B. circulans***	***S. aureus***	***E. coli***	***P. vulgaris***
ampicillin	8	-	-	7	-	-	9
rifampicein	-	7	-	-	-	-	-
vancomycin	-	-	8	-	-	9	-
nalidixic acid	-	-	-	-	8	-	-

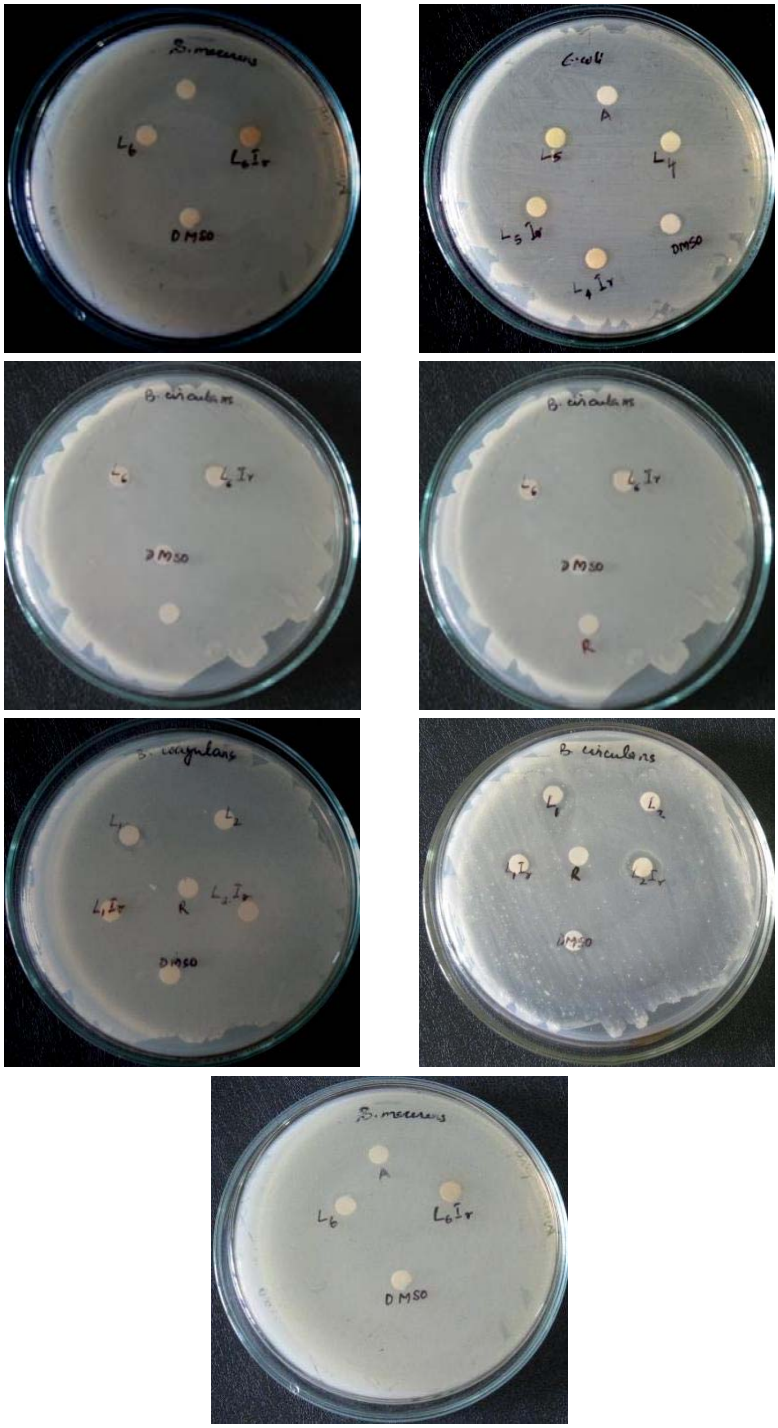

Figure 8.5. Antibiogram of Ir(III) complexes where L_1=qc5in, L_2=qc6in, L4=hqc5in,L5=hqc6in, L6=hqaqn L1-Ir= [Pd(qc5in)Cl_2], L2-Ir =[Pd(qc6in)Cl_2], L4-Ir=[Pd(hqc5in)Cl_2] L5-Pd= [Pd(hqc6in)Cl_2], L6-Pd= [Pd(hqaqn)Cl_2

Table 8.8. Antibacterial activity data of ruthenium complexes

Synthesized complexes (40μg)	Diameter of zone of inhibition (mm)				
	B. cereus	*B. coagulans*	*B. macerans*	*B. circulans*	*P.v ulgaris*
[Ru(qc5in)Cl_3H_2O]. H_2O	12	9	6	11	8
[Ru(qc6in)Cl_3H_2O]. H_2O	12	9	------	------	9
Ru(hqc5in)$Cl_3(H_2O).H_2O$	12		10	--------	------
Ru(hqc6in)$Cl_3(H_2O].H_2O$	----	------	10	-------	12
Ru(hqaqn)$Cl_3(H_2O].H_2O$	11	11	9	11	10

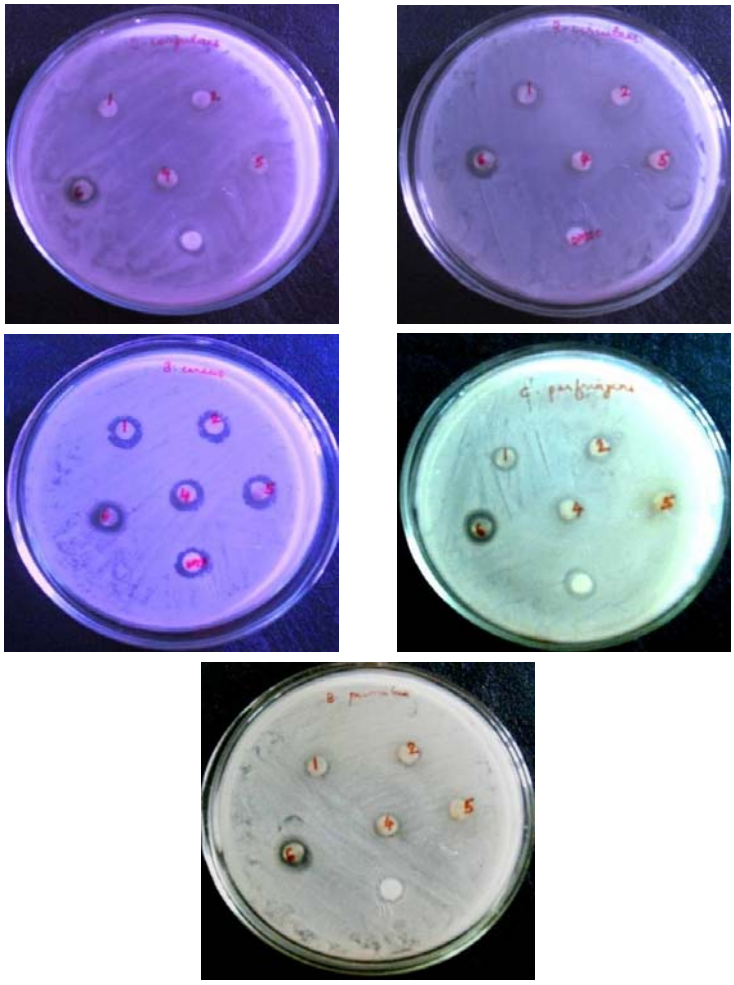

Figure.8.6. Antibiogram of Ru(III) complexes where 1=[Ru(qc5in)Cl_3H_2O].H_2O, 2=[Ru(qc6in)Cl_3H_2O].H_2O, 4=[Ru(hqc5in)$Cl_3(H_2O)$].H_2O, 5=[Ru(hqc6in)$Cl_3(H_2O)$].H_2O, 6= [Ru(hqaqn) $Cl_3(H_2O)$.H_2O

8.5 Conclusion

The newly synthesised complexes exhibited enhanced antibacterial activity over corresponding ligands. [Ir(hqaqn)$Cl_3(H_2O)$] and [Pd(hqaqn)Cl_2] exhibit anti-cancer property. The complexes of hqaqn show higher antibacterial activity and cytotoxicity.

8.6 References

[1] Eve Wiltshaw *Platinum Metals Rev,* 23(1979) 90.

[2] B. Rosenberg, L. Van Camp, *Cancer Res.*30 (1970) I799.

[3] D. J. Brown (Ed.), *Quinoxalines,* Wiley, New York (2004)

[4] G. W. H. Cheeseman, R. F. Cookson (Eds.), *Condensed Pyrazines*, Wiley, New York (1979)

[5] A. Carta, P. Corona, M. Loriga, *Curr. Med. Chem.* 12 (2005) 2259.

[6] N. Patel, J. Bergman, A. Graslund, *Nucleot. Nucl.* 10 (1991) 699.

[7] B. Zarranz, A. Jaso, I. Aldana, A. Monge, S. Maurel, E. Deharo, V. Jullian and M. Sauvain, *Arzneim. Forsch.* 55 (2005) 754.

[8] G. Moarbess, C. D. Masquefa, V. Bonnard, S. G. Paniagua, J. Vidal, F. Bressolle, F. Pinguet, B. P. Antoine, *Bioorg. Med. Chem.*16 (2008) 6601.

[9] K. Toshima, T. Ozawa, T. Kimura, S. Matsumura, Bioorg. *Med. Chem. Lett.* 14 (2004) 2777.

[10] G. A. Carter, T. Clark, C. S. James, R. S. T. Loeffler, *Pestic. Sci.* 14 (1983) 135.

[11] P. Sanna, A. Carta, M. Loriga, S. Zanetti and L. Sechi,, *Farmaco* 54 (1999) 169.

[12] J. P. Dirlam, J. E. Presslitz and B. J. Williams, *J. Med. Chem.* 26 (1983) 1122.

[13] S. S. Karki, R. Hazare, S. Kumar, V. S. Bhadauria, J. Balzarini, E.D. Clercq**,** *Acta Pharm.* 59 (2009) 431.

[14] E.Chiari, A.B. Oliveira, M.A.F Prado, R.J. Alves, L.M Galvno and F.G. Araujo, *Antimicrob Agents Chemother, 40* (1996) 613.

[15] K. Kim, H. Kim, K. Park, K.Cho, *J.Korean Chem.Soc*. 42 (1998) 227.

[16] T.H. Jonckers,S.V. Miert, K. Cimanga, C. Bailly, P. Colson, M.C. Gillet, D. Pauw, *J.Med.Chem.,* 45 (2002) 3497.

[17] L. Dassonneville, A. Lansiaux, A. Wattelet, N. Wattez, C. Mahievu, S.V. Miert, Eur.J.Pharmacol, 409 (2000) 9.

[18] J. Godlewska, K. Badowoska, J. Ramza, L. Kaczmarek, P.Czoch, A. Opolski, *Radiol Oncol.,* 38 (2004)137.

[19] P.M. O'Neill, P.G. Bray, S.R. Hawley, S.A. Ward, B.K. Park *Pharmacol.Ther,* 77 *(*1998) 29.

[20] T. Decker, M.J. Lohmann-Matthes, *Immunol. Meth*. 15 (1988) 61.

[21] W. Dong, P.P. Simeonova, R. Gallucci, J. Matheson, L. Flood, S. Wang, A. Hubbs, I.M. Luster, *Toxicol. Appl. Pharmacol*. 1551 (1998) 359.

[22] M. Fukumoto, T. Kujiraoka, M. Hara, T. Shibasaki, H. Tatsuo, M. Yoshida, *Life Sci.* 69 (2000) 247.

[23] T.J. Mossmann, *J. Immunol. Meth*. 65 (1983) 55.

[24] G. Fotakis, J.A. Timbrell, *Toxicology Letters* 160 (2006) 171.

[25] A.B. Hart, H.C. Lee, S.G. Shukla, A. Shukla, M. Osier, D.J. Eneman, J. Chiu, *Toxicology.* 133(1999) 43.

[26] G. Almazan, H. Liu, A. Khorchid, S. Sundararajan, K.A. Martinez-Bermudez, S. Chemtob, *Free Radic. Biol. Med.* 29 (2000) 858.

[27] R. Fautz, B. Husein, C. Hechenberger, *Mutat. Res*. 253 (1991)173.

[28] D.C. Morgan, C.K. Mills, L.D. Lefkowitz, S.S. Lefkowitz, *J. Immunol. Meth.* 145 (1991) 259.

[29] J. Kumi-Diaka, *Biology of the Cell.* 94 (2002) 37.

[30] A.W. Bauer, W.M.M. Kirby, J.C. Sherries, M. Tuck, *J. Am. clin. Pathol.* 45 (1966) 493.

[31] H. M. Parekh, P. B. Pansuriya, M. N. Patel, *Polish J. Che.* 79 (2005) 1843.

[32] B. G. Tweedy, *Phyto Pathology* 55 (1964) 910.

[33] J. Parekh, P. Inamdhar, R. Nair, S. Baluja, and S. Chanda, *J. Serb. Chem. Soc*. 70 (2005) 1155.

[34] Y. Vaghasia, R. Nair, M. Soni, S. Baluja, and S Chanda, *J. Serb. Chem.* Soc. 69 (2004) 991.

[35] Raman, Res. *J. Chem. Environ.* 9 (2005)13.

.....ꕥ.....

Summary and Conclusion

The interaction of transition metal complexes with DNA can cause DNA damage in cancer cells, block the division of cancer cells and result in cell death. The present thesis deals with the studies on the synthesis, characterization, catalytic applications and DNA interaction of some new transition metal complexes of the Schiff bases derived from quinoxaline-2-carboxaldehyde and 3-hydroxyquinoxaline-2-carboxaldehyde. The thesis is divided into eight chapters. Contents of the various chapters are briefly described as follows:

Chapter 1

This chapter involves a general introduction to Schiff bases and a brief discussion of their biological and catalytic applications in various processes. Various applications of quinoxalines are also discussed in this chapter as Schiff base ligands used in the present investigation contain quinoxaline ring. A brief description about the structure of DNA and its different binding modes like intercalation, groove binding, electrostatic binding, has been included. Furthermore a brief discussion on DNA cleavage is also included. The scope of the present work is also given in this chapter.

Chapter 2

Chapter 2 deals with the details on various experimental and characterization techniques employed in the present study. Information about the synthesis and characterization of the five new Schiff bases, quinoxaline-2-carboxalidine-5-aminoindazole (qc5in), quinoxaline-2-carboxalidine-6-aminoindazole (qc6in), 3-hydroxyquinoxaline-2-carboxalidene-5-aminoindazole (hqc5in), 3-hydroxyquinoxaline-2-carboxalidene-6-aminoindazole (hqc6in), and 3-hydroxyquinoxaline-2-carboxalidine-8-aminoquinoline (hqaqn) is included in

this chapter. These Schiff bases formed via the condensation of quinoxaline-2-carboxaldehyde, 3-hydroxy-quinoxaline-2-carboxaldehyde with the amines such as 5-aminoindazole, 6-aminoindazole and 8-aminoquinoline were characterized using elemental analysis and spectroscopic techniques such as FT-IR, UV-visible spectroscopy and NMR. For the DNA binding studies UV-Vis absorption spectra, cyclic voltammetry, differential pulse voltammetry and circular dichroism spectra were used. Gel electrophoresis experiments were also performed to investigate the DNA cleavage of these complexes. Details regarding these instruments are presented in this chapter.

Chapter 3

New palladium complexes [Pd(qc5in)Cl_2], [Pd(qc6in)Cl_2], [Pd(hqc5in)Cl_2] [Pd(hqc6in)Cl_2], [Pd(hqaqn)Cl_2] were synthesised and characterised by elemental analysis, FT-IR, UV-Vis and atomic absorption spectroscopy, conductance and magnetic susceptibility measurements. The electronic spectra of all these complexes exhibit d-d bands characteristic of square planar Pd(II) complexes. The complexes are found to be diamagnetic. The molar conductance values suggest non electrolytic nature of these complexes and coordination of the chloride ion to the metal. A decrease in the azomethine stretching frequency of the ligand was observed in the IR spectra of all the complexes suggesting complex formation. Electrochemical studies of the complexes were carried out using cyclic voltammetry in DMSO solution using platinum disc working electrode and Pt wire counter electrode. All the potentials were referenced to Ag/AgCl reference electrode. All the complexes exhibit quasi reversible oxidation and reduction. The I_{pc}/I_{pa} ratio indicates one electron transfer in this redox process.

The DNA binding behaviour of these complexes was studied by UV-Vis spectra, CV, DPV and CD spectral studies. Upon electronic absorption

spectral titration, qc5in, qc6in and hqaqn complexes show hyperchromism with slight red shift and hqc5in and hqc6in complexes show hyperchromism without any shift. The intrinsic binding constant K_b was calculated. The K_b values were found to be 4.9×10^5 M^{-1}, 3.1×10^5 M^{-1}, 2.1×10^3 M^{-1}, 3.2×10^3 M^{-1}, 5.5×10^5 M^{-1} respectively. The slight red shift and increase of the absorption intensity with the increase of concentration of DNA observed for complexes suggest a strong binding involving the aromatic group and the base pairs of DNA. The obivious shift of peak potentials for all the complexes indicates the strong association of these complexes with DNA through groove binding. Negative shift of $E_{1/2}$ in the case of hqc5in and hqc6in complexes may be attributed to electrostatic binding mode. Additional evidences in favour of the interactions of DNA were obtained by CD measurements. The observed circular dichroism spectrum of herring sperm DNA in Tris-HCl buffer consist of a positive band at 276 nm due to base stacking and a negative band at 245 nm due to helicity with zero-cross over at 260 nm is characteristic of right-handed B-form DNA. Thus simple groove binding and electrostatic interaction of small molecules with DNA shows less or no perturbations on the base stacking and helicity bands. The small increase in the molar ellipticity of the positive band and negative band of the CD spectrum of DNA observed for $[Pd(qc5in)Cl_2]$, $[Pd(qc6in)Cl_2]$ and $[Pd(hqaqn)Cl_2]$ indicate that the interaction between the metal complexes and DNA is through groove binding. In the case of hqc5in and hqc6in complexes the intensity of the negative ellipticity band decreases almost similar to that for the positive ellipticity. This suggests that the DNA binding of the complexes do not affect the conformations of DNA. Agarose gel electrophoresis assay suggest that these complexes are able to cleave the pUC18 plasmid DNA. Thus the studies clearly reveal that binding of DNA with the complexes $[Pd(qc5in)Cl_2]$, $[Pd(qc6in)Cl_2]$ and

[Pd(hqaqn)Cl_2] is through groove binding and that with the complexes [Pd(hqc5in)Cl_2] and [Pd(hqc6in)Cl_2] is electrostatic in nature.

Chapter 4

New iridium complexes [Ir(qc5in)Cl_3H_2O]), [Ir(qc6in)Cl_3H_2O]), [Ir(hqc5in)$Cl_3(H_2O)$], [Ir(hqc6in)$Cl_3(H_2O)$] and [Ir(hqaqn)$Cl_3(H_2O)$] were synthesised and characterisd by elemental analysis, FT-IR, UV-Vis and atomic absorption spectroscopy, conductance and magnetic susceptibility measurements. The electronic spectra of all these complexes show d-d bands characteristic of octahedral Ir(III) complexes. All the complexes are diamagnetic. The molar conductance values suggest non electrolytic nature of these complexes. All complexes show quasi reversible oxidation and reduction. The I_{pc}/I_{pa} ratio for the complexes indicates one electron transfer in this redox process.

The DNA binding behaviour of these complexes was studied by UV-Vis spectra, CV, DPV and CD spectral techniques. Upon electronic absorption titration all the complexes exhibit hyperchromism with blue shift. The Kb values for [Ir(qc5in)Cl_3H_2O].H_2O, [Ir(qc6in)Cl_3H_2O].H_2O, [Ir(hqc5in)$Cl_3(H_2O$], [Ir(hqc6in)$Cl_3(H_2O$] and [Ir(hqaqn)$Cl_3(H_2O$] were found to be 3.1×10^5 M^{-1}, 2.3×10^5 M^{-1}, 2.0×10^5 M^{-1}, 1.2×10^5 M^{-1}, 4.5×10^6 M^{-1} respectively. The shift of peak potentials for all the complexes indicates the strong association of these complexes and DNA by intercalation and groove binding. On the addition of complexes, [Ir(qc5in)Cl_3H_2O]H_2O, [Ir(qc6in)Cl_3H_2O]H_2O, [Ir(hqc5in)Cl_3H_2O] and [Ir(hqc6in)Cl_3H_2O] to the DNA solution, the positive band at 275 nm shows a slight red shift (1-3 nm) and an increase in the molar ellipticity suggesting that there exist interaction between aromatic rings of the complex and base pairs of DNA. But on the addition of [Ir(hqaqn)Cl_3H_2O], to the DNA solution, both bands show a slight red shift(1-3 nm) and a large

increase in the molar ellipticity suggesting intercalative mode of binding. All the results clearly reveal that binding of DNA with the complexes, $[Ir(qc5in)Cl_3H_2O]H_2O$, $[Ir(qc6in)Cl_3H_2O]H_2O$, $[Ir(hqc5in)Cl_3H_2O]$ and $[Ir(hqc6in)Cl_3H_2O]$ through groove binding and that $[Ir(hqaqn)Cl_3H_2O]$ intercalatively bind with DNA. Agarose gel electrophoresis assay indicated the ability of these complexes to cleave the pUC18 plasmid DNA.

Chapter 5

Chapter 5 deals with the synthesis and characterization of the ruthenium(III) complexes, $[Ru(qc5in)Cl_3H_2O].H_2O$, $[Ru(qc6in)Cl_3H_2O].H_2O$, $[Ru(hqc5in)Cl_3(H_2O)_2].H_2O$, $[Ru(hqc6in)Cl_3(H_2O)].H_2O$ and $[Ru(hqaqn)Cl_3(H_2O)].H_2O$. The presence of coordinated and lattice water molecules in the complexes could be confirmed from the TG and IR studies. All these complexes exhibit magnetic moment values which lie in the range 1.72-1.86 B.M indicating the presence of one unpaired electron and +3 oxidation state. The EPR spectra of all complexes in DMSO at 77K exhibit three different g values indicating the presence of magnetic anisotropy and rhombic distortion in these complexes. The electronic spectra of all the complexes exhibit bands in the region 502-580nm. These bands have been attributed to d-d transitions [$^2T_{2g}\rightarrow{}^2A_{2g}$, $^2T_{1g}$, $^2T_{2g}\rightarrow{}^2T_{1g}$, and $^2T_{2g}\rightarrow{}^2A_{2g}$]. The redox properties of all the complexes were investigated in DMSO solution by cyclic voltammetry. Cyclic voltammogram of each complex exhibits a reversible oxidation and reduction peaks at the scan rate $100mVs^{-1}$. The redox processes are quasi reversible with high peak-to-peak separation values. The I_{pc}/I_{pa} ratio suggests one electron transfer in this redox process. Gel electrophoresis assay indicate that the complexes are able to cleave the pUC18 plasmid DNA. One of ruthenium complexes $[Ru(hqaqn)Cl_3(H_2O)]H_2O$ completely degrades both the forms of pUC18 plasmid DNA.

Chapter 6

In this chapter, studies on the synthesis, characterization and DNA cleavage of copper(II) complexes, [Cu(qc5in)Cl_2], [Cu(qc6in)Cl_2], [Cu(hqc5in)Cl_2], [Cu(hqc6in)Cl_2] and [Cu(hqaqn)Cl_2] are presented. The magnetic moment of all the Cu(II) Schiff base complexes at room temperature lie in the range of 1.70-1.90 B.M indicating the presence of one unpaired electron and monomeric nature of the complexes. FT-IR spectra reveal that the azomethine stretching decreases for all the complexes suggesting bonding of azomethine nitrogen to the metal. The complexes exhibit a peak in the range 582–680 nm indicating square planar nature for the complexes. EPR spectra of the complexes recorded at LNT (77 K) also suggest square planar geometry. All these complexes show one well defined redox couple corresponding to Cu^{II}/Cu^{I} as expected. The redox processes are quasi reversible with high peak-to-peak separation values. The I_{pc}/I_{pa} ratio suggests one electron transfer in this redox process. Gel electrophoresis studies reveal the ability of these complexes to cleave the pUC18 plasmid DNA. One of the complexes, [Cu(hqaqn)Cl_2], completely degrade the open circular form and supercoiled form.

Chapter 7

This chapter deals with the application of the iridium(III) complexes and ruthenium(III) complexes. The iridium(III) complexes were found to act as catalysts for the hydrogenation of benzene. Catalytic experiments were carried out in a 100 mL bench top mini-reactor and products were analysed by CHEMITO 8510 GC. Both partial and complete reduction products were obtained during the hydrogenation. A detailed study was carried out with [Ir(hqaqn)$Cl_3(H_2O)$], as it exhibited maximum catalytic activity in the screening study. Influence of various parameters on the rate of reaction was investigated. Turnover frequencies of 2705 h^{-1} have been found for the

reduction of benzene (0.34 mol) at 80 ºC with 6.66×10^{-6} mol catalyst and at a hydrogen pressure of 30 bar in 600 rpm stirring speed. These values are much higher than that of some of the reported iridium complex catalysts for the homogeneous aromatic hydrogenation reactions.

Selective oxidation of primary alcohols to aldehydes is a long standing problem of organic chemistry. A study was conducted to examine the oxidation of an industrially important lipophilic alcohol, 2-ethyl-1-hexanol, to 2-ethyl-1-hexanal using the ruthenium(III) complexes as catalysts. Complete oxidation of 2-ethyl-1-hexanol occurs in 30 minutes at 313 K, in presence of H_2O_2 (9.7 mmol) as oxidant. $[Ru(qc5in)Cl_3H_2O].H_2O$ shows high turnover frequency of 7905 h^{-1} in this oxidation reaction.

Chapter 8

The potential utility of the Pd and Ir complexes as anticarcinogenic agents was also investigated. For the screening studies cytotoxicity was tested on DLA cells by tryphan-blue exclusion method. The drug at toxic concentration damages the cell and makes pores on the membrane through which tryphan-blue enters. The damaged cells were stained blue by tryphan-blue stain and could be distinguished from viable cells. All the complexes exibit higher cytotoxicity compared to that of the ligands. Among the complexes, $[Pd(hqaqn)Cl_2]$, $[Pd(qc5in)Cl_2]$and $[Ir(hqaqn)Cl_3H_2O]$ exhibit higher activity (80% cytotoxicity)

Cytotoxic effects of the complexes $[(Pd(hqaqn)Cl_2]$ $[Ir(hqaqn)Cl_3H_2O]$ and $[Pd(qc5in)Cl_2]$ on prostate cell line (DU145) were tested using MTT assay. A gradual decrease of viable cell was observed on increasing Conc. from 5µg/ml to 400µg/ml. $[Ir(hqaqn)Cl_3(H_2O)]$ shows more cytotoxicity (38.62%) compared to $[Pd(hqaqn)Cl_2]$ (24.57%). $[Pd(qc5in)Cl_2]$ have no cytotoxic effect.

Antibacterial activity studies of Pd(II), Ir(III), Ru(III),and Cu(II) complexes were carried out by disc diffusion method. Mueller Hinton agar plate of about 5mm thickness was prepared for this study. The test organism *Bacillus cereus, Bacillus coagulans, Bacillus macerans, Bacillus circulans, Staphylococcus aureus, Escherichia coli or Proteus vulgaris* was swabbed on the agar plate. Sterile filter paper discs were placed on the agar surface and 10µl solution of each of the complex and the ligand was poured on it. The plate was incubated at 37°C for 24-48 hours and observed for the activity. The results reveal that the cytotoxicity was found to be higher for the complexes than that for the ligands under identical experimental conditions. Furthermore when compared to standard bacteriocides, like ampicillin, rifampicin, vancomycin and nalidixic acid all the prepared complexes showed a higher inhibitory action.

.....ooo.....

List of Research Publications

- **P. Leeju**, V. Arun, M. Sebastian, G. Varsha, Digna Varghese, K. K. M. Yusuff, "N-[(E)-Quinoxalin-2-ylmethylidene]-1Hindazol-5-amine" *Acta Cryst*. (2009). E65, o1981
- V. Arun, P.P. Robinson, S. Manju, **P. Leeju**, G. Varsha, V. Digna, K.K.M. Yusuff, "A novel fluorescent bisazomethine dye derived from 3- hydroxyquinoxaline-2-carboxaldehyde and 2,3- diaminomaleonitrile" Dyes and Pigments 82(3) (2009) 268-275
- G. Varsha, V. Arun, P. P. Robinson, Manju Sebastian, Digna Varghese, **P. Leeju,** V. P. Jayachandran, K. K. M. Yusuff, "Two new fluorescent heterocyclic perimidines: first syntheses, crystal structure, and spectral characterization" *Tetrahedron Letters* 51 (2010) 2174–2177.
- Manju Sebastian, V. Arun, P.P. Robinson, **P. Leeju**, Digna Varghese, G. Varsha and K.K.M. Yusuff, "Synthesis, characterization and the crystal structure of a new Cobalt(II) Schiff base complex with quinoxaline-2-carboxalidine-2-Amino-5-methylphenol" *Journal of Coordination Chemistry*. 63 (2010) 307-314.
- Manju Sebastian, V. Arun, P.P. Robinson, **P. Leeju**, Digna Varghese, G. Varsha and K.K.M. Yusuff, "Template synthesis and spectral characterization of some Schiff base complexes derived from quinoxaline-2-carboxaldehyde and L-histidine" *Journal of Coordination Chemistry*, 2010
- D. Varghese, V. Arun, M. Sebastian, **P. Leeju**, G. Varsha, K.K.M. Yusuff, "N,N'-Bis[(E)-quinoxalin-2-ylmethylidene]ethane-1,2-diamine" Acta Cryst. E65 (2009) o435.
- G. Varsha, V. Arun, M. Sebastian, **P. Leeju**, D. Varghese, K.K.M. Yusuff, "(Z)-2-Amino-3-[(E)-benzylideneamino]-but-2-enedinitrile" Acta Cryst. E65 (2009) o919.

Not related to the work presented in this thesis

.....ഇ.....